THE BINDING AND ACTIVATION OF THE GLUCAGON-LIKE PEPTIDE-1 RECEPTOR BY EXENDIN-4

Nasr Elsayed Mohammed Nasr

Submitted in accordance with the requirements for the degree of

Doctor of Philosophy

The University of Leeds
Faculty of Biological sciences

November, 2010

Acknowledgements

It would not have been possible to write this doctoral thesis without the help and support of the kind people around me, to only some of whom it is possible to give particular mention here.

This thesis would not have been possible without the good advice, unparalleled support, supreme patience and friendship of my supervisor, Dr Daniel Donnelly, not to mention his advice and knowledge of the field of study. Really, Dr Daniel Donnelly has done more than supervision.

I am most grateful to my group members Ros Mann, Philip Miller, Clare Wishart and Richard Weaver for their support and assistance since the start of my postgraduate work. I would like to thank Clara Redondo for her kindness and support, together with the other members of Findlay group Renske, Jimmy, Lindsey, Mari and Girish. A special word of thanks also goes to Jeff Keen and Nat for their help and support. I would like to acknowledge the financial, academic and technical support of the University of Leeds, IMSB and LIGHT staff, particularly the necessary support for this research.

I am also indebted to my professors at the University of Kafr Elsheikh (Egypt) with special word of thanks to biochemistry department, FVM, Prof Ibrahim Fattouh, Prof Khalid Kahilo, Prof Azza Elkattawy as well as Prof Shawky Abdelhady, Dr Samir Elshazly and Dr Tarek Abouzaid for their support and encouragement. I am very grateful for the Egyptian government and people for providing my scholarship.

Many other people in my life were not directly involved in the science but were nonetheless important to me during my PhD. I would like to thank my wife Noha for her personal support and great patience at all times. My parents, brother Sabry Nasr and sisters have given me their unequivocal support throughout, as always, for which my mere expression of thanks likewise does not suffice. Special word of thanks also goes to my son Mohammed and my princess Sarah.

Last, but by no means least, I thank my friends in Egypt, Great Britain and elsewhere for their support and encouragement throughout.

For any errors or inadequacies that may remain in this work, of course, the responsibility is entirely my own.

Abstract

Background and purpose

Exendin-4 (EX4) has the same physiological properties as glucagon-like peptide-1 (7-36)amide (GLP-1). EX4 has 50% identity with GLP-1, with an extra nine amino acids at its C-terminus. The two peptides mediate their functions through coupling to the glucagon like peptide-1 receptor (GLP-1R) with similar affinity and potency. Unlike N-terminally truncated GLP-1, (GLP-1(15-36)amide), the equivalently truncated EX4(9-39) binds GLP-1R without significant loss of affinity; furthermore, GLP-1(15-36) is a partial agonist while EX4(9-39) is an antagonist. Previous binding analysis of either N or C-terminally truncated EX4 at rGLP-1R suggested that the residues responsible for its extra affinity are at its C-terminus, EX4 residues 31-39. Crystal structures supported by mutagenesis showed similar interactions of both GLP-1 and EX4 at the isolated N-terminal domain of human GLP-1R (hGLP-1R-NTD) apart from a subtle hydrogen bond between Ser32 in EX4 and Glu68 in hGLP-1R-NTD.

Experimental approach

The affinities and activities of GLP-1, EX4 and various analogues were measured at human and rat GLP-1R (hGLP-1R and rGLP-1R, respectively) and various receptor variants. Computer models, molecular dynamics coupled with *in silico* mutagenesis, were used to model and interpret the data.

Key results

The membrane-tethered NTDs of hGLP-1R displayed similar affinity for GLP-1 and EX4 in contrast to previous studies using the soluble isolated domain. The selective high affinity at rGLP-1R and the rGLP-1R-like mutant hGLP-1R-Glu68Asp for EX4(9–39) over EX4(9–30) was due to Ser32 in the ligand. This selectivity was not observed with hGLP-1R and the hGLP-1R-like mutant rGLP-1R-Asp68Glu. Gly16-EX4(9–30) was an agonist for rGLP-1R and hGLP-1R-

Glu68Asp but was an antagonist for hGLP-1R and rGLP-1R-Asp68Glu. Glu22-GLP-1(15-36) was a partial agonist for all tested receptors. Insertion of (EEEAVRL) of EX4 instead of their equivalent sequence in GLP-1(15-36) prevented its activity and did not enhance its affinity. Substitution of Ser32 in EX4 by similar hydrogen bond donor amino acids did not enhance EX4 affinity or potency.

Conclusions and implications

GLP-1 and EX4 bind to the NTD of hGLP-1R with similar affinity. A hydrogen bond between Ser32 of EX4 and Asp68 of rGLP-1R is responsible for the improved affinity of EX4 and can play a role in the antagonist/agonist switch of Gly16-EX4(9–30) at the rat receptor. The discovery of the novel antagonist/agonist switch suggests a new mechanism of activation by GLP-1 which does not require its extreme N-terminal residues.

Contents

List of Abbreviations

cAMP cyclic adenosine mono-phosphate

AKT The serine/threonine protein kinase or PKB protein kinase B, which plays a key role in cellular processes such as glucose metabolism, cell proliferation, apoptosis, transcription and cell migration.

Bcl-2 Apoptosis controlling gene discovered in B-cell lymphoma 2

Bcl-xL Apoptosis controling gene discovered in B-cell lymphoma

CREB cAMP response element-binding

CRFR-2β CRF receptor type 2β

CRF Corticotropin-releasing factor

DM Diabetes mellitus

DMEM Dulbecco's Modified Eagle's Medium

DPP-IV dipeptidyl peptidase IV

EC_{50} half maximal effective concentration

ED_{50} Pharmacologically, effective dose is the amount of drug that produces a therapeutic response in 50% of the people taking it

EDTA Ethylenediamine tetraacetic acid

EGF Epidermal growth factor

Epac Exchange protein directly activated by cAMP

ERK Extra-cellular signal-regulated kinase

EX4 Exendin-4

GIP glucose-dependent insulin releasing polypeptide

GLP-1 Glucagon-like peptide-1

GPCR G protein-coupled receptor

GR Glucagon receptor

GRF Growth hormone releasing factor

HBB HEPES binding buffer

HEK-293 Human embryonic kidney-293

HEPES 4-(2-hydroxyethyl)-1-piperazineethanesulfonic acid

IC_{50} log of half maximal inhibitory concentration

i.v. Intravenous

IBMX Iso-butyl-methyl-xanthine

ICL1 Intracellular loop1

IRS-2 insulin receptor substrate 2

LB Luria-Bertani

MEK Mitogen-activated protein kinase (MAPK) kinase

NIDDM Non-insulin-dependent diabetes mellitus

NTD N-terminal domain

OD optical density

PTH1R Parathyroid hormone 1 receptor

PBS Phosphate buffered saline

PDX Pancreatic duodenal homeobox-1

PI 3-K phosphoinositide-3 kinase

pIC_{50} –log of IC_{50}

PKA protein kinase A

RT-PCR Reverse transcriptase- polymerase chain reaction

SEM Standard error of the mean

7TM Seven trans-membrane

TAE Tris-acetate-EDTA

TFB1 Transformation buffer 1

TFB2 Transformation buffer 2

VPAC Vasoactive intestinal polypeptide receptor

WT Wild type

Amino Acid Abbreviations

	Amino Acid	Three letter code	One letter code
Non-Polar	Alanine	Ala	A
	Cysteine	Cys	C
	Glycine	Gly	G
	Isoleucine	Iso	I
	Leucine	Leu	L
	Methionine	Met	M
	Phenylalanine	Phe	F
	Proline	Pro	P
	Tryptophan	Trp	W
	Valine	Val	V
Polar	Asparagine	Asn	N
	Glutamine	Gln	Q
	Serine	Ser	S
	Threonine	Thr	T
	Tyrosine	Tyr	Y
Positively Charged	Arginine	Arg	R
	Histidine	His	H
	Lysine	Lys	K
Negatively Charged	Aspartic Acid	Asp	D
	Glutamic Acid	Glu	E

List of Figures

List of Tables

1 - General introduction

1.1 Non-insulin-dependent diabetes mellitus (NIDDM)

Diabetes mellitus (DM) is a world wide socio-economic wasting syndrome that leads to severe and chronic morbidity such as cardiovascular disease or loss of function such as renal failure, blindness and limb amputation (Hogan et al., 2003). Although huge advances have been achieved in diabetic care, DM is still out of complete control and prevalence of the disease is expected to be doubled (Saydah et al., 2004), which reveals a high demand for discovering new therapies.

In the healthy body, the basal glucose level is maintained within a narrow range (4 to 8 mmol/l) by a continuous low level of insulin supply through the portal circulation, which controls the rate of the hepatic glucogenesis during the inter-meal periods: while, in the postprandial stage, the blood glucose is determined by the difference between the amount of glucose entering the circulation after rapid absorption through the intestine and the amount of glucose leaving the blood by tissue uptake (Cherrington, 1999). Therefore, insulin secretion increases in response to high levels of blood glucose, which up-regulates glucose uptake by liver, muscle and kidney, as well as down-regulates hepatic and renal gluconeogenesis (Meyer et al., 2004).

The physiological response of pancreatic β-cells, the unique insulin producers, to elevated blood glucose is biphasic; the first phase is insulin release (10-15 min) which is the main control of postprandial glucose level and the second phase is longer lasting (30-60 min) (Hermans et al., 1995). The loss of the first phase is the main characteristic of NIDDM and impaired glucose tolerance. Even well dietary-controlled diabetic patients have impaired insulin

secretion in the first half hour after a meal with consequent hyperglycemia (Pfeifer et al., 1981, Rendell et al., 1981).

The consequent hyperglycemia not only leads to fatigue of β-cells but also leads to progressive oxidative stress on β-cells (Brownlee, 2003, Poitout and Robertson, 2002) accompanied by inadequate insulin secretion and gradual depletion of insulin stores. The low insulin production results from the negative effect of hyperglycemia on insulin gene expression by β-cells and their apoptosis as well, a condition known as glucotoxicity (Jovanovic and Gondos, 1999, Kaiser et al., 2003).

Although insulin secretion increases in response to blood glucose, the blood glucose is not the only stimulant of insulin secretion, a fact that has been demonstrated by recording higher insulin secretion just after the ingestion of a glucose rich meal than in response to i.v. glucose infusion, which is defined by the 'incretin' concept (Yalow et al., 1988, Creutzfeldt, 1979).

1.1.1 Incretin concept

Bayliss and Starling, (1902) predicted that a pancreatic stimulant might be produced by gut in response to nutrient ingestion and affect metabolism of carbohydrates. Later, Moore, (1906) assumed that the duodenum releases 'chemical excitant' for pancreatic secretion and tried to treat diabetes by injection of gut extracts. By the same manner, Zunz and Labarre, (1929) used secretin-free gut extract that succeeded in curing hypoglycemia in dogs. La Barre and Still, (1930) used the term 'incretin' to define the phenomenon.

Unger and Eisentraut, (1969) described the relationship between the intestine and the pancreatic islets 'enteroinsular axis'. This axis was suggested to include nutrient, neural and hormonal signals from the intestine to the cells secreting insulin, glucagon and somatostatin (Creutzfeldt, 1979). In addition,

the hormonal part, incretin, should fulfil two criteria: 1) it must be released by nutrients, particularly carbohydrates, and 2) it should have an glucose dependent insulinotropic effect (Creutzfeldt, 1979).

At that time, only one hormone had been found to fit those requirements, which was glucose-dependent insulinotropic polypeptide (GIP). GIP is produced by K-cells that mainly present in the midzone of the duodenal villi and, to a lesser extent, in the jejunum (Polak and Bloom, 1982). Interestingly, GIP was firstly isolated as 'enterogastrone', which inhibits gastric secretion in response to presence of fat or its digestive products in the intestinal lumen. Later, high levels of GIP were detected shortly after ingestion of a meal containing either fat or carbohydrate (Brown, 1974, Cleator and Gourlay, 1975, Ross and Dupre, 1978).

However, immuno-neutralization of endogenous GIP indicated that intestinal hormone rather than GIP could fulfill the incretin description (Ebert et al., 1979, Ebert and Creutzfeldt, 1982). These observations were supported by reported insulinotropic activity remained in gut extract after removal of GIP by immuno-adsorption (Ebert et al., 1983). Moreover, a big contribution to the incretin effect from the lower intestine was reported in studies of patients with varying degrees of resection of the small intestine. Despite equal increase in plasma GIP, patients with preserved ileal residues had higher incretin effects than patients without ileal residues (Lauritsen et al., 1980). Taken together, another incretin hormone should be present that works along with GIP. Later, the second incretin hormone was isolated and named as glucagon-like peptide-1 (GLP-1).

1.2 Glucagon-like peptide-1 (GLP-1)

1.2.1 Discovery

The missing incretin hormone remained undiscovered until the late 1970s when the era of recombinant DNA technology started providing the tools essential for its identification. In the early 1980s, the cloning of cDNA encoding preproglucagon from the pancreas of the anglerfish was completed. The gene was found to encode glucagon and glucagon related peptide (GRP) (Lund et al., 1982, Lund et al., 1983). The presence of GRP proximal to the sequence of glucagon, with high homology to the sequence of GIP, led to the suggestion that GRP would be an incretin hormone (Lund et al., 1982). Shortly after that, similar mammalian (including human) cDNAs were cloned (Heinrich et al., 1984, Bell et al., 1984, Bell et al., 1983, Lopez et al., 1983). In the same manner, mRNAs were cloned (Lund et al., 1981, Drucker and Brubaker, 1989) and it has became clear that GRP-1 is a homologue of GLP-1 and it was proven to be an insulinotropic incretin. However, the bioactive form of GLP-1 is debatable and will be reviewed below (section 1.2.2)

1.2.2 Structure function relationship

GLP-1 results from a post-translational cleavage of the product of the glucagon gene by the prohormone convertase PC1/3 (Dhanvantari et al., 2001). The cleavage site for PC requires two adjacent amino acids: arginine and lysine. Accordingly, GLP-1 would be 36 or 37 amino acids in length. Consequently, synthetic GLP-1 (1-36) and GLP-1 (1-37) were tested for biological activity (Ghiglione et al., 1984). The reported results were frustrating with none of the previously reported biological observations being repeatable, even when a hyper dose (25 nM) of GLP-1 was used; therefore, a big question was addressed 'How glucagon-like is glucagon-like peptide?' (Ghiglione et al.,

1984). Later, it was suggested that the bioactive GLP-1 could be N-terminally truncated. The prediction was based on the alignment of the sequence of GLP-1 with the other members of the glucagon family when the best alignment was with the histidine at position 7, and not position 1 of GLP-1 (Schmidt et al., 1985). This prediction became real when it was discovered that GLP-1 was actually further N-terminally truncated by post-translational processing in the intestinal L-cells (Drucker et al., 1986, Mojsov et al., 1986). Furthermore, the discovered truncated GLP-1(7-37) and GLP-1(7-36)amide were found to be potent insulinotropic hormones in the isolated perfused pancreas of rats (Mojsov et al., 1987), pigs (Holst et al., 1987), and in humans (Kreymann et al., 1987).

Accordingly, bioactive GLP-1(7-36) became a member of the glucagon superfamily of peptide hormones. Classification of this family is based on their considerable sequence homology, having anywhere from 21% to 48% amino acid identity with glucagon. The family includes GLP-1(7-37) and GLP-1(7-36)amide, GIP, exendin-3 and -4, secretin, peptide histidine-methionine amide (PHM), GLP-2, helospectin-1 and -2, helodermin, pituitary adenyl cyclase-activating polypeptides (PACAP)-38, and -27, PACAP-related peptide (PRP), GH-releasing factor (GRF), and vasoactive intestinal peptide (VIP). In addition to the sequence homology, many of the peptides share other characteristics like being produced from the gut; most of them are agonists and/or neurotransmitters. Furthermore, most of them are co-encoded within the same precursor, such as the peptide hormones derived from the cleavage of preproglucagon. However, some members differ significantly in the physiological processes that they regulate. For example, the major function of glucagon is to maintain blood glucose levels during fasting, whereas GLP-1

functions primarily during feeding to stimulate insulin release and to lower blood glucose levels. In total, the common characteristics of the family could help as study of one member could be applied to other members.

Focusing on GLP-1, in this text, GLP-1 is written instead of GLP-1(7-36)amide and each amino acid in its sequence is marked by (*) next to it, for example His7*, in order to clearly distinguish it from the receptor numbers. The sequence of GLP-1 is highly conserved in all animal species. The conservation of GLP-1 reflects both its physiological importance and the fact that the entire amino acid sequence of GLP-1 is required for full biological activity. Removal of the N-terminal histidine (to yield GLP-1 (8-37)) results in a 90% loss of receptor binding and insulinotropic activity (Suzuki et al., 1989, Gefel et al., 1990, Ohneda et al., 1991, Mojsov, 1992). The positive charge of the imidazole side chain of the histidine residue appears to be crucial for GLP-1 actions (Hareter et al., 1997). However, histidine substitution by tyrosine, as in GIP and GRF, has a lesser effect suggesting the importance of an aromatic ring at that position (Parker et al., 1998). An N-terminal truncation of GLP-1 by two residues reduces binding affinity to approximately 1% that of full-length peptide (Montrose-Rafizadeh et al., 1997, Knudsen and Pridal, 1996). Furthermore, 60-fold reduction in GLP-1 binding activity has been observed by a further N-terminal truncation of GLP-1 of eight residues (Lopez de Maturana and Donnelly, 2002). Also, addition of an amino acid to the N-terminus of GLP-1(6-37) reduces its biological activity by 90% (Suzuki et al., 1989, Ohneda et al., 1991). Truncation at the C-terminus also reduced the biological activity of GLP-1 considerably (Suzuki et al., 1989, Gefel et al., 1990, Mojsov, 1992, Knudsen and Pridal, 1996). Substitution in the N-terminal part of the GLP-1 molecule, with the corresponding glucagon residues, reduced the affinity for the GLP-1R

only moderately whereas exchanges in the C-terminal portion of GLP-1 reduced the affinity for the GLP-1R more than 100-fold (Hjorth et al., 1994). In contrast, the binding affinity of GLP-1 to its receptor is more sensitive to GIP-like changes in the N-terminal region than to changes in the C-terminal region (Gallwitz et al., 1994). Unfortunately, attempts to generate smaller active fragments of GLP-1 that retain potent insulinotropic activity have failed (Ohneda et al., 1991, Watanabe et al., 1994, Gallwitz et al., 1990).

By another approach using peptide analogues in which individual amino acids are substituted, the studies reported that the residues in positions His7, Gly10*, Phe12*, Thr13*, Asp15*, Phe28*, and Ile29* are important for the binding affinity and biological activity of GLP-1 (Adelhorst et al., 1994, Gallwitz et al., 1994, Watanabe et al., 1994). Replacement of these amino acids with alanine increased IC_{50} of native GLP-1 (0.27nM) to 59, 36, 36, 11, 35 and 25 nM respectively. Likewise, these substitutions increased the EC_{50} from 2.6 nM to $>10^4$, 33, 65, $>10^4$, 2600 and 70 nM respectively (Adelhorst et al., 1994).

Two-dimensional nuclear magnetic resonance (NMR) spectroscopy of GLP-1 in a membrane-like environment (a dodecylphosphocholine micelle) revealed that GLP-1 consists of an N-terminal random coil segment (residues 1-7), two helical segments (7-14 and 18-29), and a linker region (15-17) a structure similar to that observed for glucagon (Thornton and Gorenstein, 1994). However, in the receptor-peptide interaction, the N-terminal segment formed a helix. This observation points out that the receptor-bound conformation of GLP-1 can be different from its conformation in solution (Murage et al., 2008).

The importance of the central kink or the linker region, particularly Gly22* of GLP-1 in its receptor interaction is controversial. It was reported that the presence of a flexible, helix-destabilizing, Gly22* in GLP-1 has an important role for membrane and receptor binding because of high flexibility of the peptide (Thornton and Gorenstein, 1994, Murage et al., 2008). Gly22* removal reduced GLP-1 binding affinity (Parker et al., 1998). In contrast, a Gly22Ala substitution has no detectable effect on either GLP-1 binding affinity or biological activity (Gallwitz et al., 1994). Furthermore, it was proposed that the linker region weakens GLP-1 binding affinity compared to EX4 as Gly22* destabilizes the helix of GLP-1 (Neidigh et al., 2001, Runge et al., 2007).

1.2.3 GLP-1 Secretion, metabolism and clearance

GLP-1 is produced by certain types of cell located in the distal jejunum and ileum of the small intestine (Mojsov et al., 1990, Orskov et al., 1994). These cells are known as L-cells, which are clearly different from pancreatic glucagon producing cells (Grimelius et al., 1976). L-cells are flask shaped open type cells with microvilli that reach the intestinal lumen to be in direct contact with the digested nutrients. Also, L-cells have a domain rich in endocrine granules located near the basal lamina along with its blood supply (Eissele et al., 1992). Hence, L-cells have an ideal morphology and position to contact their nutrient stimulant and deliver its response. Although L-cells are well known as a main source of circulating GLP-1, a small amount of locally produced immunoreactive GLP-1 could be detected as in the pancreas (Orskov et al., 1994) and different regions of nervous tissue (Dorn et al., 1983, Larsen et al., 1997).

GLP-1 is secreted mainly in response to ingestion of carbohydrate rich meal (Brubaker, 2006). As introduced before, oral, but not intravenous glucose administration is a GLP-1 stimulant in humans (Unger et al., 1968, Hermans et al., 1995). However, GLP-1 can be secreted in response to a mixed meal of sugars, fat, protein and fibers (Takahashi et al., 1991, Elliott et al., 1993). In fact, after a meal, GLP-1 is released into the blood in a biphasic pattern: an early relatively short first phase (within 10 -15 min) then followed by a longer (30 - 60 min) second phase (Hermans et al., 1995).

Obviously, it is likely that the first phase can not be stimulated by direct contact with the nutrients in the intestinal lumen because the main populations of L-cells are located in the distal part of the intestine. Nevertheless, the first phase can be stimulated by direct contact between nutrients and small populations of L-cells, which are scattered in the more proximal parts of the small intestine (Theodorakis et al., 2006). Alternatively, this phase could be controlled by other stimuli that include the autonomic nervous system (Rocca and Brubaker, 1999, Balks et al., 1997), the neurotransmitter acetylcholine (Anini et al., 2002, Anini and Brubaker, 2003), gastrin-releasing peptide (GRP) (McDonald et al., 1983) and the calcitonin gene related peptide (Herrmann-Rinke et al., 2000). GIP stimulated GLP-1 release has been reported in canines and rodents but not in humans (Nuck et al., 1993).

Unlike the first phase, it is clear that the second or later phase of GLP-1 secretion is stimulated by direct contact between the digested nutrients and intestinal L-cells (Roberge and Brubaker, 1991). At the molecular level, GLP-1 secretion is stimulated via glucose metabolism by a group of intracellular signals, such as PKA, PKC, calcium and MAPK (Reimann and Gribble, 2002). Compared to factors contributing to GLP-1 stimulation, few studies have been

carried out to investigate the inhibition of GLP-1 secretion. These studies reported that insulin, somatostatin (Wider et al., 1976), and the neuropeptide galanin (Saifia et al., 1998) can inhibit GLP-1 secretion.

Once the bioactive form of GLP-1 is released into the blood stream it survives for less than two minutes. This short half-life is due to rapid inactivation by a widely distributed proteolytic enzyme called dipeptidyl peptidase-IV (DPP-IV) (Deacon et al., 1995). DPP-IV, also known as CD26, is a serine protease that specifically cleaves dipeptides from the amino terminus of oligopeptides or proteins if they contain alanine or proline residue in position two. Accordingly, bioactive GLP-1 (7-36) is a typical substrate, to be rapidly broken down by DPP-IV cleavage to the poorly active or inactive product GLP-1(9-37) or GLP-1(9-36)NH_2 (Kieffer et al., 1995). Intriguingly, DPP-IV can be found wherever GLP-1 is; DPP-IV is expressed in the endothelial cells lining blood vessels that drain the intestinal mucosa including GLP-1 secretory cells (Hansen et al., 1999). Moreover, DPP-IV is detected as a soluble protein in the circulation (Mentlein, 1999). Consequently, more than half of synthesized GLP-1 enters circulation as an inactive form (Marguet et al., 2000). In addition, neutral endopeptidase 24.11 (NEP-24.11), a membrane–bound zinc metallopeptidase, has been reported to have activity on GLP-1 with up to half of the circulating GLP-1 undergoing C-terminal cleavage by NEP-24.11 (Plamboeck et al., 2005). The half-life of GLP-1 metabolites is 5 min, which is controlled by renal clearance and hence the kidney is the major route for elimination of GLP-1 through both glomerular filtration and tubular uptake. The kidney involvement is indicated by the high levels of GLP-1 metabolites in patients with renal insufficiency, while the level of intact GLP-1 remains as normal (Meier et al., 2004).

Between release by L-cells and clearance by the kidney, fasting plasma levels of bioactive GLP-1 are maintained at 5 -10 pmol/L in humans with a 2-3 fold increase after a meal depending on the size and composition of the meal (Elliott et al., 1993). Interestingly, postprandial levels of bioactive GLP-1 are reduced in NIDDM patients (Vaag et al., 1996). Since the breakdown and clearance rate of GLP-1 is similar in healthy, NIDDM and obese persons, the reduction in postprandial GLP-1 in obese and NIDDM patients could be due to reduction in GLP-1 secretion (Vilsboll et al., 2003). While the reason for GLP-1 reduction is not known in NIDDM individuals, the cause in obese people could be related to leptin resistance (Anini and Brubaker, 2003).

1.2.4 Physiological action of GLP-1

GLP-1 has a non-redundant glucose homeostatic effect mediated by controlling several interactive functions in more than one organ (Figure 1-1). In the pancreas, GLP-1 works with glucose to stimulate insulin synthesis by pancreatic β-cells (Kreymann et al., 1987, Mojsov et al., 1987) in different synergistic ways, including increasing cyclic adenosine monophosphate (cAMP) with its downstream action, replenishing β-cells insulin stores by promoting insulin gene transcription (Drucker et al., 1987), as well as by restoring glucose sensitivity in glucose resistant β-cells (Holz et al., 1993). Also, GLP-1 increases β-cell mass by stimulating β-cell proliferation and by inhibiting β-cell apoptosis (Buteau et al., 2004, Farilla et al., 2003, Yusta et al., 2006). In addition, GLP-1 up-regulates somatostatin secretion by pancreatic δ-cells (Fehmann and Habener, 1991). In contrast, GLP-1 inhibits glucagon secretion by pancreatic α-cells (Heller et al., 1997). It is worth noting that GLP-1's physiological action on the pancreas is mediated through a glucose-dependant mechanism, which will be described in detail by introducing the GLP-1 signaling cascade.

The systemic action of GLP-1 contributes to the normalization of blood glucose by delaying the movement of food from the stomach to the intestine. Deceleration of gastric emptying antagonizes the meal-related increase in postprandial blood glucose levels (Willms et al., 1996). Surprisingly, although the reduction in postprandial glucose level in diabetic patients has been found to be accompanied by a reduction in insulin secretion (Nauck et al., 1997), it has been reported that the delay in food emptying is better for normalizing blood glucose than the GLP-1 incretin effect (Meier and Nauck, 2005).

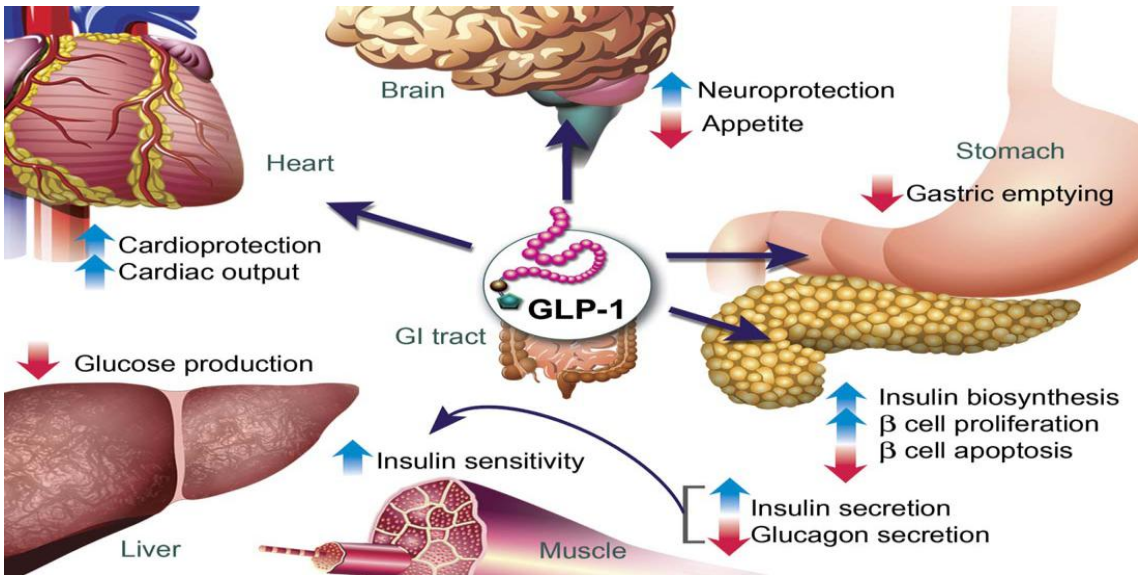

Figure 1-1: Physiological actions of GLP-1.

GLP-1 mediates glucoregulatory effect through acting directly on the endocrine pancreas, heart, stomach, and brain, whereas actions on liver and muscle are indirect. GLP-1 actions include upregulation of some functions (blue arrows) and down regulation of others (red arrows) (Drucker, 2006).

Moreover, GLP-1 works peripherally and/or centrally on the nervous tissues mediating gluco-regulatory action. GLP-1R has been detected in the areas that regulate feeding behaviour (Turton et al., 1996) and gastric motility (Nagell et al., 2006). Animal studies revealed that central or peripheral administration of GLP-1R agonists reduced food and water intake with a

consequent loss in body weight (Turton et al., 1996). The rapid inactivation of more than 50% of secreted GLP-1 locally by DPP-IV and the availability of only low levels of bioactive GLP-1 result in the proposal of a neural mechanism to mediate GLP-1R agonist- dependent insulin secretion (Deacon et al., 1996, Balkan and Li, 2000). In experimentally hyperglycaemic mice, GLP-1 stimulated neural pathways that inhibit muscle glucose uptake, increase insulin secretion and inhibit hepatic glycolysis (Knauf et al., 2005). GLP-1 not only recruits neuronal cells but also protects them from apoptosis, as well as improving their memory and learning functions (During et al., 2003).

The beneficial effect of GLP-1 extends to include the cardiovascular system. Three days treatment with GLP-1 in patients with acute myocardial infarction and angioplasty improved regional and global left ventricular function and was accompanied by a reduced death rate and short duration of hospitalization (Nikolaidis et al., 2004). However, it is not known whether GLP-1 has a direct positive effect on the cardiac tissue in humans or whether its effects are due to improving metabolism and related blood parameters (Nikolaidis et al., 2004). However, it has been reported that GLP-1 has a direct protective effect on isolated heart preparation (Zhao et al., 2006). Additionally, GLP-1 action has been related to improved endothelial function in NIDDM patients (Nystrom et al., 2004). Furthermore, the improved endothelial function was associated with a protective role of GLP-1 in the kidneys, as well as increased water and salt excretion (Yu et al., 2003, Gutzwiller et al., 2004). GLP-1 has been suggested to increase hepatic glucose disposal and to inhibit hepatic glucose production (Prigeon et al., 2003). Also, GLP-1 promotes lypolysis in both human and rat adipocytes (Ruiz-Grande et al., 1992, Villanueva-Penacarrillo et al., 2001).

1.2.5 GLP-1 intracellular signal transduction pathways

G protein-coupled receptors (GPCRs) have been found to be involved in the mechanism by which L-cells can sense and respond to the nutrient composition in the lumen of the gut (Fredriksson et al., 2003). L-cells are present in the distal ileum and colon with their apical side in contact with the gut lumen, which can detect free fatty acids (FFAs), glucose and carbohydrates. FFAs have been shown to stimulate G protein-coupled receptor 120 (GPR120), which is present in L-cells and provides strong evidence for its role in GLP-1 release (Hirasawa et al., 2005). Glucose stimulates secretion of GLP-1 by ATP closure of ATP-sensitive potassium channels (K_{ATP}) (Reimann and Gribble, 2002) while other non-metabolizable sugars enhance GLP-1 secretion through a sodium–glucose cotransporter-dependent mechanism (Gribble et al., 2003). As a result of these stimuli, L-cells release GLP-1 by exocytosis into the blood stream.

In fact, the most relevant action is the promotion of glucose stimulated insulin secretion from β-cells. When the intact GLP-1 reaches the pancreatic β-cells in the islets of Langerhans, it binds to the GLP-1R present on the cell surface and activates this receptor (Goke and Conlon, 1988). Once GLP-1R is in an active conformation it can couple with heterotrimeric G-proteins (demonstrated in Figure 1-2), of the stimulatory G protein (G_s) type, on the intracellular face of the receptor. Consequently, G_s in turn activates the enzyme adenylyl cyclase, which raises intracellular levels of the second messenger cAMP (Hoosein and Gurd, 1984). However, the subunits are also believed to activate phospholipase Cβ (PLC-β) pathways (Kristiansen, 2004).

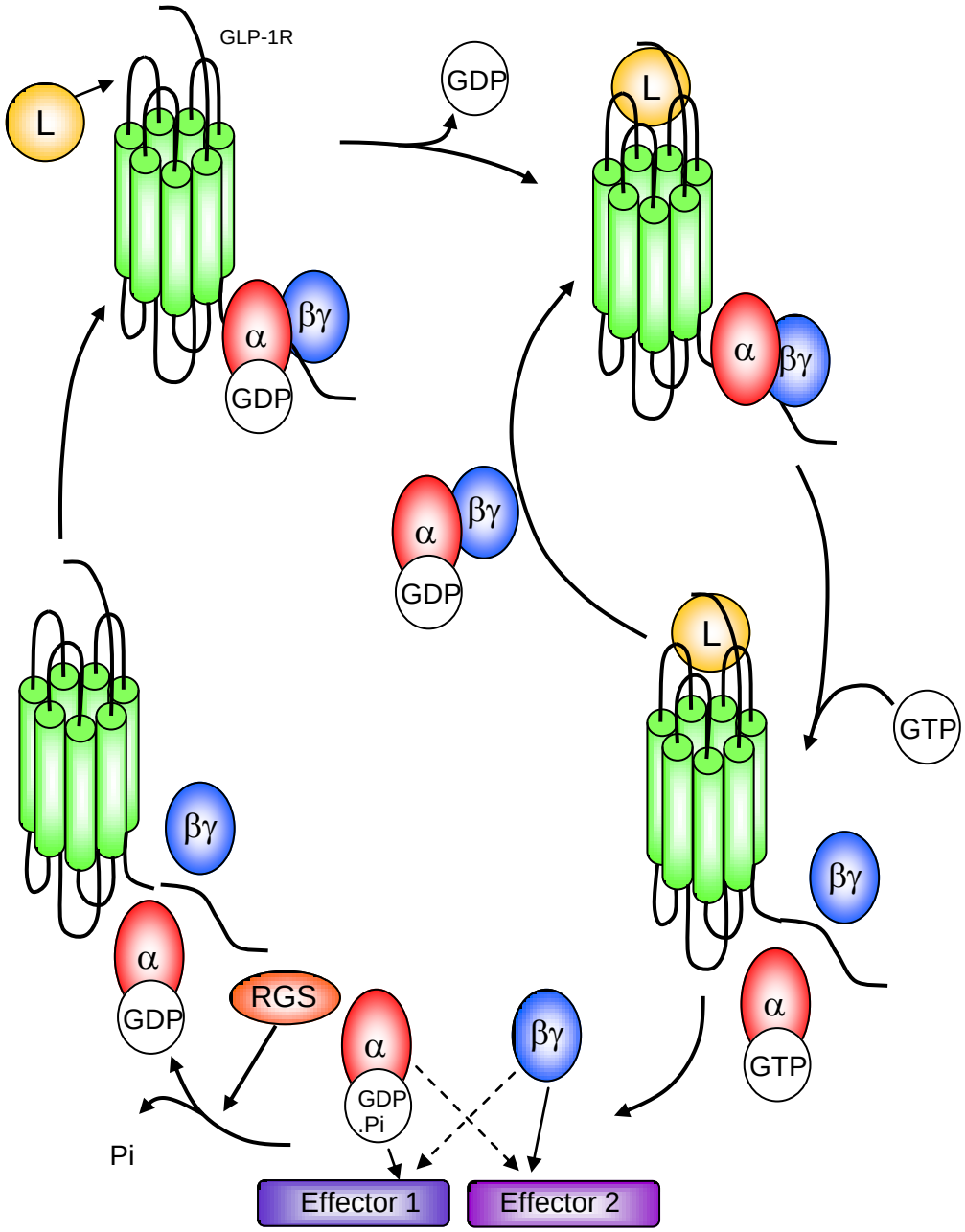

Figure 1-2: The GTPase cycle.

The binding of a ligand (L) to the GPCR-G-protein complex triggers the release of GDP from G_α. The empty state of G_α has low affinity to the ligand-bound GPCR and permits the binding of GTP. GTP-bound G_α subsequently dissociates from $G_{\beta\gamma}$ and both components stimulate various effectors. Intrinsic GTP hydrolysis, which can be accelerated by the binding of a regulator of G protein signalling (RGS), eventually turns off the G_α via release of a phosphate (Pi). Finally the GDP-bound G_α combines with the G_β and the ligand-free GPCR returns to its resting phase. Taken from (Ho and Wong, 2002).

The fact that insulin secretion from β-cells takes place in the absence of GLP-1 signalling (Dupre and Beck, 1966) makes the exact mechanism by which the GLP-1 signalling cascade leads to increased insulin secretion difficult to fully understood. However, it has been suggested that GLP-1 reduces K_{ATP} channel activity by elevating the sensitivity of K_{ATP} channels to ATP, along with supporting calcium-dependent exocytosis leading to exocytosis of insulin via membrane depolarisation (Figure 1-3) (Suga et al., 2000, Gromada et al., 1998).

Pancreatic β-cells sense the levels of circulating glucose in the blood by glucose uptake via the GLUT2 glucose transporter present in the cell membrane. GLUT2 has low affinity for glucose and, accordingly, the rate of glucose transport changes with fluctuations in blood glucose concentration (Saltiel, 2001). Once inside the cell, glucose is phosphorylated to glucose-6-phosphate by glucokinase. The Michaelis constant (KM) of glucokinase for glucose is 100 times higher than that of other hexokinases; therefore, glukokinase has a lower affinity for glucose than other hexokinases. This lower affinity makes glukokinase a rate-limiting enzyme that acts as the 'glucose sensor' linking extra-cellular glucose concentrations to insulin secretion (Matschinsky, 2002). Intracellular ATP levels increase as a result of the breakdown of glucose-6-phosphate by glycolysis, which yields increased levels of intracellular cAMP (Saltiel, 2001).

Hence, GLP-1 leads to the inhibition of K_{ATP} through increasing its sensitivity to ATP. K_{ATP} channel inhibition depolarizes the membrane and causes the opening of voltage-dependant calcium channels, leading to an influx of calcium ions (Ca^{2+}) into the β-cell. The increase in the intracellular Ca^{2+} concentration is the trigger for secretion by exocytosis of insulin stored

in vesicles, but only in the presence of the amplifying messenger molecules diacylglycerol (DAG), non-esterified arachidonic acid and 1S-hydroxyeicosatetraenoic acid (12-S-HETE) (Turk et al., 1993). Insulin secretion leads to the excess glucose present in the bloodstream being sequestered and stored in various forms for later use and balances the opposing actions of glucagon, which causes the release of glucose stored in liver and muscle (Saltiel, 2001).

Additionally, GLP-1 sustains β-cell insulin stores through stimulation of proinsulin gene expression (Drucker et al., 1987). GLP-1 increases proinsulin gene transcription and mRNA stability through cyclic AMP-dependent PKA-independent mechanisms (Wang et al., 2005). Additionaly, GLP-1 increases the expression of pancreatic and duodenal homeobox-1 (Pdx-1), by increasing Pdx-1 gene transcription and by enhancing Pdx-1 binding to the insulin gene promoter (Figure 1.3) (Wang et al., 1999, Wang et al., 2005).

Moreover, increased Pdx-1 gene expression is associated with increased β-cell mass (Stoffers et al., 2000). Also, GLP-1 supports survival and proliferation of β-cells via inhibition of apoptotic pathways. GLP-1 does this by reducing caspase-3 expression (Wang and Brubaker, 2002), as well as up-regulating Bcl-2 and down-regulating Bax expression (Farilla et al., 2003). Furthermore, GLP-1 extends β-cell mass by promoting β-cell proliferation through both transactivation of the epidermal growth factor receptor (EGFR) and down-regulation of the transcriptional regulator Foxo1 via phosphorylation-dependent nuclear exclusion in an EGFR-dependent manner (Buteau et al., 2003). GLP-1 also enhances the proliferation of β-cells by reducing the expression of two negative intracellular regulators CREMα, an inhibitor of the cAMP/PKA/CREB pathway, and DUSP14, an inhibitor of the MAPK/ERK1/2

pathway (Klinger et al., 2008). In conclusion, it could be said that GLP-1 comprehensively directs all β-cell processes toward optimum insulin production.

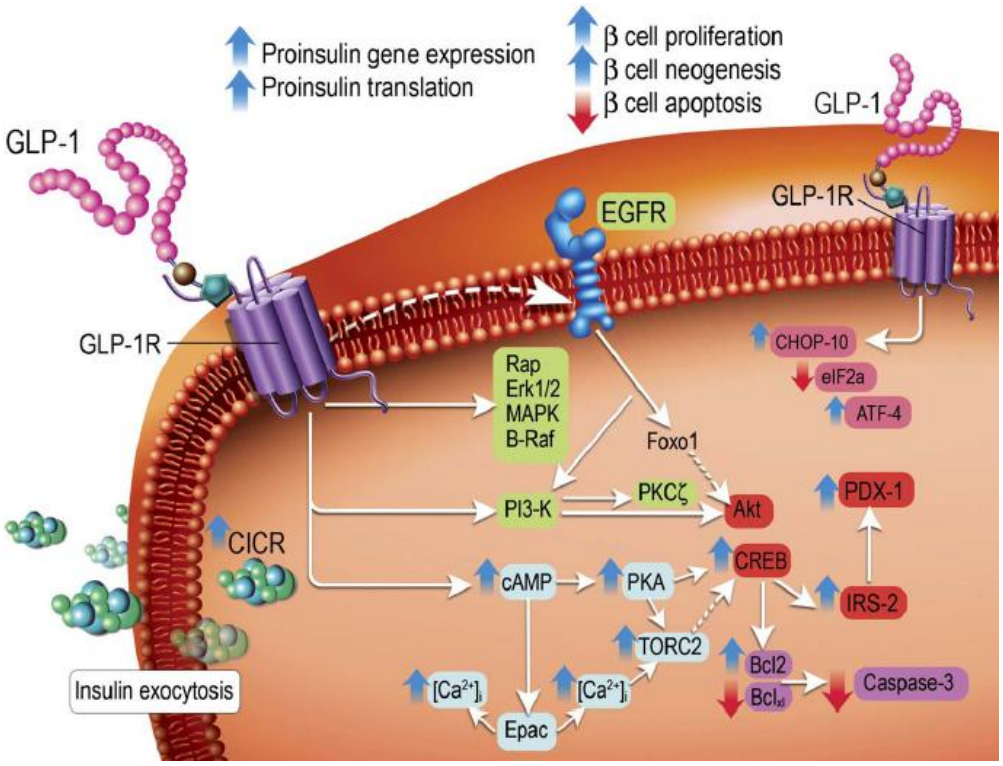

Figure 1-3: GLP-1 signal transduction pathways in the pancreatic β-cell.

GLP-1 receptor interaction not only leads to insulin depletion by exocytosis but also stimulates insulin repletion via enhancement of some intracellular and extracellular mechanisms (blue arrows) and inhibition of others (red arrows) (Drucker, 2006).

1.2.6 GLP-1 as potential anti-diabetic therapy

The continuous increase in the number of diabetic patients, particularly those with NIDDM, raises the need for the discovery of new antidiabetic drugs. The most commonly used sulfonylurea-derived oral hypoglycaemic agents act by binding to the sulfonylurea receptor subunit of the K_{ATP} channel of pancreatic β-cells leading to insulin exocytosis (Babenko et al., 1998). However, the same channels are present in cardiac and vascular smooth muscle (Yokoshiki et al., 1998). As a result, closure of the K_{ATP} channel by sulfonylureas interferes with ischemic preconditioning, which could contribute to cardiac ischemia and infarction (Brady and Terzic, 1998). Furthermore, the effects of sulfonylurea

insulin secretgogues are not glucose-dependent giving rise to an additional potential side effect, hypoglycaemia (Veneman et al., 1998). While sulphonylureas enhance insulin secretion they do not replenish the evacuated insulin stores.

In contrast, GLP-1 stimulates insulin synthesis and secretion in interactive processes that sustain a convenient insulin supply. Additionally, GLP-1 mediates other interactive physiological functions that support normalized glucose homeostasis. The failure of sulfonylureas and the success of GLP-1 suggested that GLP-1 might be a good candidate to enhance β-cell function in diabetic patients, without increasing the risk of hypoglycemia that accompanies sulfonylurea treatment. However, the suggestion is challenged by the short half life of GLP-1 due to rapid breakdown by DPP-IV and rapid renal clearance. Consequently, several alternate strategies for utilizing the beneficial effect of GLP-1 for diabetes therapy are under investigation.

The strategies include modifying different positions within the N-terminus of GLP-1 in order to resist breakdown by DPP-IV. The most successful analogues have D-amino acid substitutions at position 2 of GLP-1, with at least ten-fold increases in DPP-IV resistance, as well as maintaining most of the biological activity of native GLP-1 (Siegel et al., 1999). Likewise, other modifications have been created, including, N-terminal modification at His1* and Ala2* and chimeric derivatives created by replacing the N-terminus of GLP-1 with the corresponding region of its related peptides (e.g., glucagon, GIP, PACAP, secretin, VIP) (Xiao et al., 2001).

Another strategy was applied to produce long acting GLP-1 by acylation at its C-terminus, which protects GLP-1 from enzymatic break down and delays its renal excretion. The analogue has been known as Liraglutide and was

approved as a commercial drug in the EU in 2009 (Vilsboll, 2009). Liraglutide retains the physiological properties of GLP-1 (Kendall, 2005, Garber et al., 2009). Another long acting GLP-1 is being developed by conjugating GLP-1 with albumin derivatives which could increase GLP-1 plasma half-life (Baggio et al., 2008).

To maintain naturally-produced intact GLP-1, an alternate strategy was adopted to develop orally available DPP-IV inhibitors such as sitagliptin and vildagliptin. These inhibitors showed 80%-90% inhibition of DPP-IV and an approximately two-fold increase in circulating bioactive GLP-1 in humans (Herman et al., 2006, He et al., 2007). However, the inhibition of DPP-IV affected the level of many other substrates of DPP-IV, including chemokines, hormones and neuropeptides (Drucker, 2007).

The ease of oral administration of DPP-IV inhibitors prompted research to develop non-peptide, orally available GLP-1R agonists (Su et al., 2008) or pulmonary delivery of GLP-1R agonists (Qian et al., 2009). Another promising approach has been targeting enhancement of L-cells via stimulation of their GPCRs. For example, oral treatment with G protein-coupled receptor 119 (GPR119) agonists enhanced GLP-1 secretion in WT rats (Shah, 2009).

Overall, it would be the best if a naturally modified GLP-1 was discovered, and indeed this was the case with the discovery of EX4, a peptide derived from lizard venom. The natural substitution of Ala for Gly at position two protects EX4 from rapid degradation by DPP-IV, while it nevertheless retains all the normal physiological functions of GLP-1 (Eng et al., 1992). The synthetic form of EX4, exenatide (Byetta®) is the first GLP-1 mimetic to receive FDA approval in 2005 (Gedulin et al., 2005).

1.3 Exendins

1.3.1 Discovery of exendins

Exendins (EXs) are a family of peptides originally isolated from saliva of the Gila monster lizard *Heloderma suspectum* that includes helospectin (EX1), helodermin (EX2), EX3 and EX4. Although EXs are not found in mammals, exogenous EXs have endocrine function in regulation of the mammalian pancreatic secretion, the first example of an exocrine secretion that has an endocrine function (Eng et al., 1990, Eng et al., 1992). In the Gila monster, EXs are released to the circulation directly after a prey ingestion without any certain role in the energy homeostasis of the lizard i.e EXs are not the GLP-1 equivalent in the lizard (Young, 2002). Initial purification and characterization studies of EXs reported that they had an amino-terminal histidine (His1) revealing close relationship with the peptides of the glucagon superfamily, especially GLP-1 (Eng et al., 1990). Furthermore, functional investigation of the exendins showed that they are pancreatic secretagogue peptides that stimulate amylase production through activation of VIP receptors, the exceptions to this being EX3 and EX4, which interact exclusively with GLP-1R receptor to enhance pancreatic acinar cAMP levels (Eng et al., 1992, Raufman et al., 1991). This exception has caused EX3 and EX4 to receive special attention as a research subject over the other EXs as the presence of a mammalian analogue would be expected. Consistent with the title of this thesis, this work is focusing primarily upon EX4 and each amino acid of its sequence is marked by (**) for example His1**.

1.3.2 Physiological action

Based on laboratory and clinical studies, EX4 mediates similar physiological properties in glucose homeostasis to the native GLP-1 such as the delay of gastric emptying (Kolterman et al., 2003) and the reduction of food intake (Szayna et al., 2000). In addition, EX4 stimulates glucose-dependent insulin secretion (Egan et al., 2002, Parkes et al., 2001) and supports β-cell function and proliferation, as well as islet neogenesis from the precursor cells both *in vitro* and *in vivo* (Tourrel et al., 2002, Xu et al., 1999). EX4 not only shares GLP-1's gluco-regulatory action but also mediates its actions through coupling to GLP-1R as a more potent agonist than GLP-1 (Thorens et al., 1993, Goke et al., 1993).

1.3.3 Structure function relationship

All the above appears consistent with the high identity in primary structure between EX4 and GLP-1. EX4 is a 39 amino acid peptide with 53% identity with GLP-1, and an overall 80% identity in the N-terminus (Figure 1-4), which highlights the importance of this region in GLP-1R activation (Kieffer and Habener, 1999). The most prominent variation in the N-terminus (surrounded by a rectangle in Figure 1-4) between EX4 and GLP-1 is the substitution of Ala8* in GLP-1 by Gly2** in EX4 (Figure 1-4), the feature that protects EX4 from rapid degradation in plasma by DPP-IV (Goke et al., 1993). As a result, unlike GLP-1, EX4 has a long half-life with a consequent potent action. Moreover, while GLP-1 affinity is highly sensitive to N-terminal cleavage, EX4 can be truncated by up to eight residues without a significant loss of affinity but with a change to antagonistic function (Thorens et al., 1993).

Furthermore, Montrose-Rafizadeh et al., 1997 investigated the successive removal of residues from the N-terminus of EX4 and assessed the receptor interaction for each truncated form. Removal of the first amino acid attenuates EX4 agonistic activity while the successive removal of amino acids (from 2^{nd} to 9^{th}) leads to the loss of the receptor activation with an antagonistic effect. The deletion of these amino acids does not significantly affect the affinity of the truncated EX4 for the receptor.

The central region of EX4, residues 10-30 (displayed as 'H' in Figure 1-4), shares eight identical residues with equivalent region of GLP-1 (Figure 1-4) and has been shown by NMR analysis to be a highly stabilized helical structure (Neidigh et al., 2001). The eight identical amino acids in both EX4 and GLP-1 would lie on the same face of an ideal α-helix of their sequence (Figure 1-5), indicating the face of the helix that is likely to mediate the critical contact with the receptor (Lopez de Maturana and Donnelly, 2002). Binding analysis of truncated EX4 (9 – 30) and its equivalent GLP-1(15-36) that exclude the effect of the N-termini of both ligands and the C-terminus of EX4, showed that EX4(9-30) had slightly higher affinity than GLP-1(15-36) (pIC_{50} (–log of half maximal inhibitory concentration) are 6.7 and 6.4 respectively) for rGLP-1R. Therefore, the retention of receptor affinity by truncated EX4 suggests that, relative to GLP-1, both the central region and C-terminus of EX4 play a vital role in receptor binding, which is termed 'N-independent affinity' (Al-Sabah and Donnelly, 2003a).

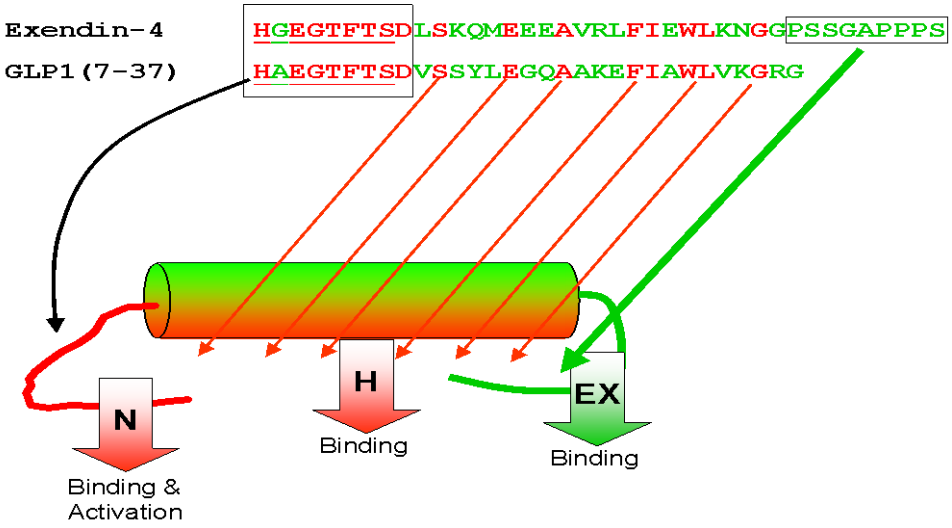

Figure 1-4: The sequence of both GLP-1 and EX4, and schematic diagram of EX4. The conserved amino acids are in red colour. The N-termini are underlined and surrounded by a rectangle. The characteristic extra C-terminal 9 amino acids of EX4 are also surrounded by a rectangle. The proposed structure is demonstrated by a schematic diagram of EX4 showing its three interactions: N, H, and EX.

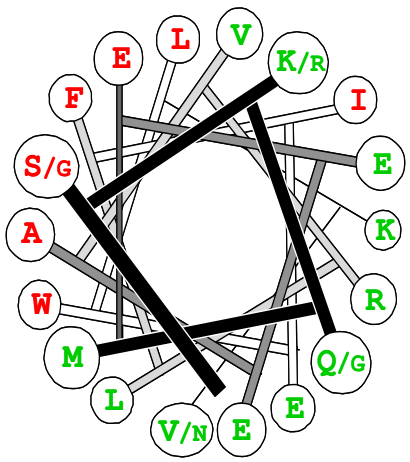

Figure 1-5: The helical wheel representation of EX4.

Residues that are conserved with GLP-1 are showed in red. Other EX4 residues are shown in green.

Despite the above, the higher helicity of the central part of EX4 over the corresponding area of GLP-1 cannot be overlooked. NMR spectroscopy of EX4 and GLP-1 has revealed that the helix in EX4 is more regular than that in GLP-1 (Neidigh et al., 2001), perhaps due to the presence of a helix-stabilising Glu16**: Arg20** interaction in EX4 compared with a helix destabilising Gly22* in GLP-1. However, for that reason, comparison of the binding data for EX4(9–30) and Gly16-EX4(9–30) demonstrated that the disruption of the putative helical structure did not result in a loss of affinity since pIC_{50} values for EX4(9–30) and Gly16-EX4(9–30) are not significantly different (P>1) (Al-Sabah and Donnelly, 2003a)

Replacement of the destabilising segment in GLP-1 (EGQAAKE) with its counterpart in EX4 (EEEAVRL) did not change GLP-1(15-36) affinity (Al-Sabah and Donnelly, 2003a). This suggests that the small difference in affinity between GLP-1(15–36) and EX4(9–30) is due to some other factors. However, a later study using both biophysical and pharmacological analysis of EX4 and its truncated analogues bound to isolated hGLP-1R-NTD suggested that the superaffinity of EX4 is due to its stable helical structure (Runge et al., 2007).

Collectively, (Lopez de Maturana et al., 2003) proposed two defined interactions, common to EX4 or GLP-1, according to their contribution to receptor-ligand interaction (Figure 1-6). These regions are firstly ‘N’ for the interaction between N-terminus of the peptide and GLP-1R core domain and secondly is ‘H’ for the interaction between the central helical regions of the peptide, particularly the face of the helix composed of the conserved residues, and rGLP-1R-NTD. In addition to ‘N’ and ‘H’, it was proposed that EX4 has an ‘EX’ interaction unique to EX4 and its N-terminally truncated analogue EX4(9-

39), which enables its N-independent affinity by enhancing its affinity to the rGLP-1R- NTD.

A complementary study by the same laboratory proposed that the 'EX' interaction is formed between the NTD of the receptor and the extended C-terminal region of EX4 (Al-Sabah and Donnelly, 2003a). Despite establishing a guidance model for the ligand receptor interaction based on the percentage of binding energy with either EX4 or GLP-1, the investigation did not characterize the exact residues of the receptor NTD involved in this interaction. However, the result of the study appears consistent with models for peptide-receptor binding at other Family B GPCRs (Bergwitz et al., 1996, Runge et al., 2003).

Taken together, while the N-termini in both EX4 and GLP-1 have nearly the same amino acid sequence, as well as similar 'H' interaction, EX4 has 9 amino acids more in its C-terminus. The additional 9 residues have been shown, by NMR, to form a 'trp cage' in hydrophobic conditions, such as trifluoroethanol (TFE) (Neidigh et al., 2001). Creating a chimera between this region and the less stable form of GLP-1, GLP-1 Gly8 EX4(31-39), improved its biological stability and receptor affinity (Doyle et al., 2003). Interestingly, truncated EX4(9-39) retains a high affinity for the isolated rGLP-1R-NTD (Lopez de Maturana et al., 2003), which confirms the independence of this affinity from both the N-terminus of EX4 (Montrose-Rafizadeh et al., 1997) and the loop regions of the receptors (Lopez de Maturana and Donnelly, 2002). Like the N-terminus of EX4, deletion of the characteristic nine amino acid C-terminus of EX4(9-39) reduced affinity for rGLP-1R (Al-Sabah and Donnelly, 2003a) suggesting that C-terminus of EX4 could confer its superaffinity for rGLP-1R-NTD.

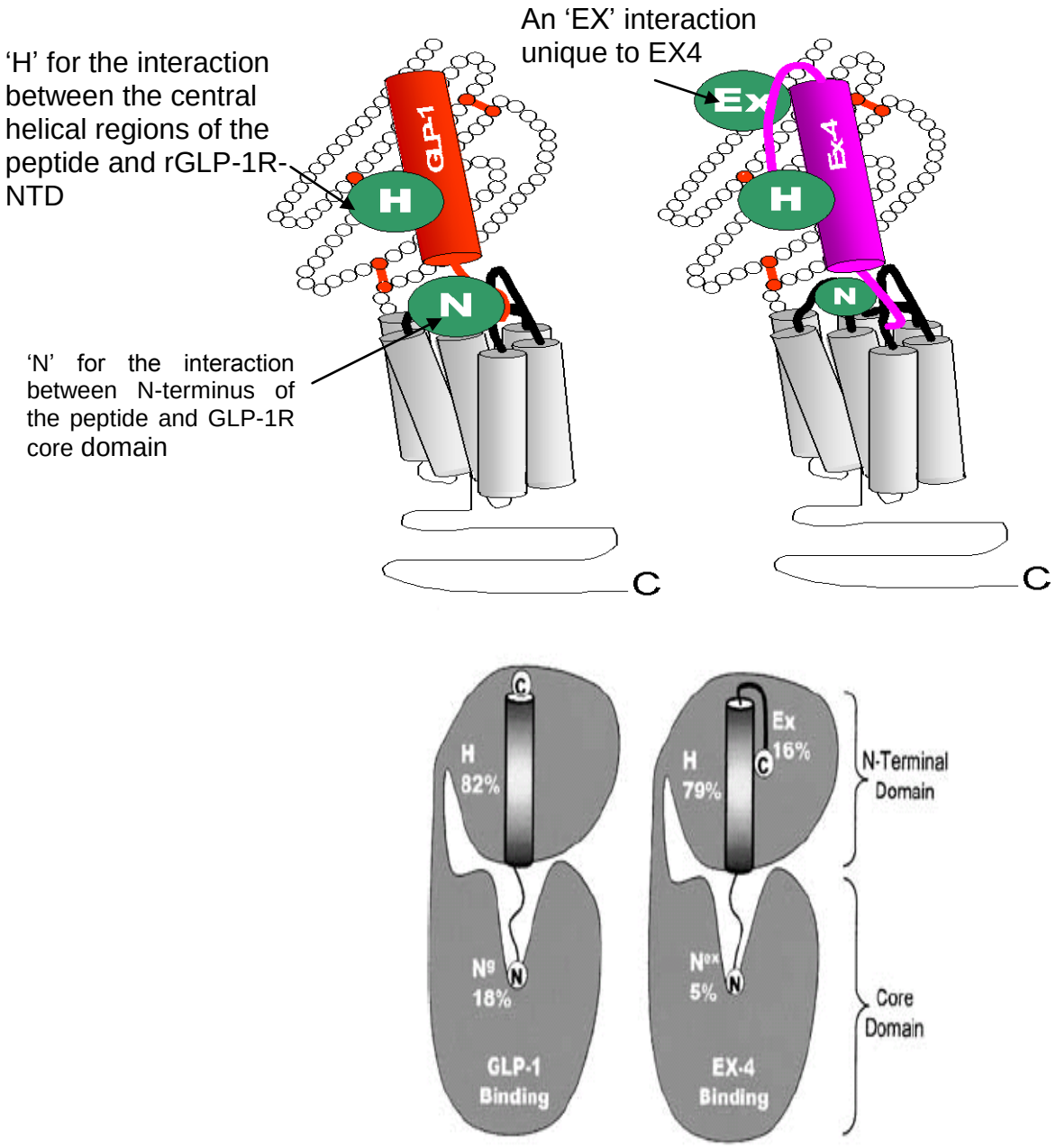

Figure 1-6 : Three dimensional cartoons of the receptor peptide complex of either GLP-1 or EX4.
Top: GLP-1 (left) or EX4 (right), GLP-1 has 'H' and 'N' interactions only while EX4 has 'H' and 'N', as well as 'EX' interactions. **Bottom:** Energy of binding, the proportional energy contributed to each region is shown during the binding of the peptides, either GLP-1 or EX4, with rGLP-1R. The energy of binding was calculated using the equation $\Delta G = -RTInK$ (where R is the universal gas constant, T is the temperature of the binding assay in degrees Kelvin and K is the affinity constant approximated by IC_{50}) for each truncated peptide as a percentage of its full-length counterpart, giving the relative contribution to binding of each region (adapted from Al-Sabah and Donnelly, 2003a).

1.3.4 EX4 metabolism and clearance

EX4 has a half-life of 26 min in humans' blood (Edwards et al., 2001). EX4 is not degraded significantly by DPP-IV (Thum et al., 2002) and it is a poor substrate for other enzymes like NEP-24.11 (Hupe-Sodmann et al., 1995). EX4 is cleared exclusively by the kidneys (Simonsen et al., 2006).

1.4 The superfamily of G protein-coupled receptors

1.4.1 Definition and classification

GPCRs include receptors for diverse endogenous ligands such as amines, peptides, amino acids, glycoproteins, prostanoids, phospholipids, fatty acids, nucleosides, nucleotides, Ca^{2+} ions, and sensory receptors for various exogenous ligands such as odorants, bitter and sweet tastants, pheromones, and photons of light. Moreover, about 80% of known hormones and neuro-transmitters activate cellular signal transduction mechanisms by activating GPCRs (Birnbaumer et al., 1990). Accordingly, dysfunctions of GPCRs cause human diseases. Therefore, GPCRs are targets for 30 - 45% of current drugs under development (Drews, 2000, Hopkins et al., 2000) and, due to their excellent potential for drug design, GPCR targets represent up to 30% of the portfolio of many pharmaceutical companies (Klabunde and Hessler, 2002).

The availability of advanced biological techniques such as protein engineering, molecular modelling, and genetic approaches to study GPCRs has provided a huge amount of information about their structure and function. In general, GPCRs are a group of receptors that share a common membrane topology of seven trans-membrane (7TM) helices connected by alternative ECLs and ICLs, with an extra-cellular N-terminus and a cytoplasmic C-terminus (Ballesteros and Weinstein, 1992). Furthermore, GPCRs mediate most of their intracellular actions through coupling and activation of G proteins, the pathway

from which the receptors derive their name (Gether et al., 2002). G-proteins transmit the signal to an effector protein, such as an enzymes or ion channel, resulting in rapid changes in the concentration of the intracellular signalling molecules such as cAMP or inositol phosphates (Cabrera-Vera et al., 2003).

However, not all receptors that activate G-proteins are members of GPCRs; other receptors such as the receptor for epidermal growth factor g can activate G-proteins (Iismaa, 1995) and interestingly some GPCRs may use both heterotrimeric G proteins and other cytoplasmic non-G protein transducers. Therefore, alternative names like 7TM receptors or serpentine-like receptors are preferred by some authors (Pierce et al., 2002). On the other hand, other heptahelical receptors or serpentine-like receptors like bacteriorhodopsin are not related to GPCRs in function or evolution.

In order to overcome that confusion, members of the superfamily of GPCRs have been identified and classified by their native ligands, by phylogenetic analysis of their amino acid sequences, by analysis of clustering of genes in the human genome, and by analysis of globular domains and motifs in the N-terminus (Fredriksson et al., 2003). (Fredriksson et al., 2003) classified GPCRs into five main families that they termed glutamate (G, with 15 members), rhodopsin (R, 701), adhesion (A, 24), frizzled/taste2 (F, 24) and secretin (S, 15), to which they applied the acronym GRAFS (Figure 1- 7). However, the A-F system is the most commonly used (Attwood and Findlay, 1994, Kolakowski, 1994). According to the A-F system GPCRs include the receptors related to the 'light receptor' rhodopsin and the β_2-adrenergic receptor (family A), the receptors related to the secretin receptor (family B), and the receptors related to the metabotropic neurotransmitter receptors (family C), STE2 receptors (family D), and STE3 receptors (family E). The principal

differences between the GRAFS system and A-F system are the division of Family B GPCRs into secretin and adhesion families and the incorporation of the recently discovered Frizzled and Taste2 receptors. The common structural elements of the major families according to A-C system are shown in Figure 1-8

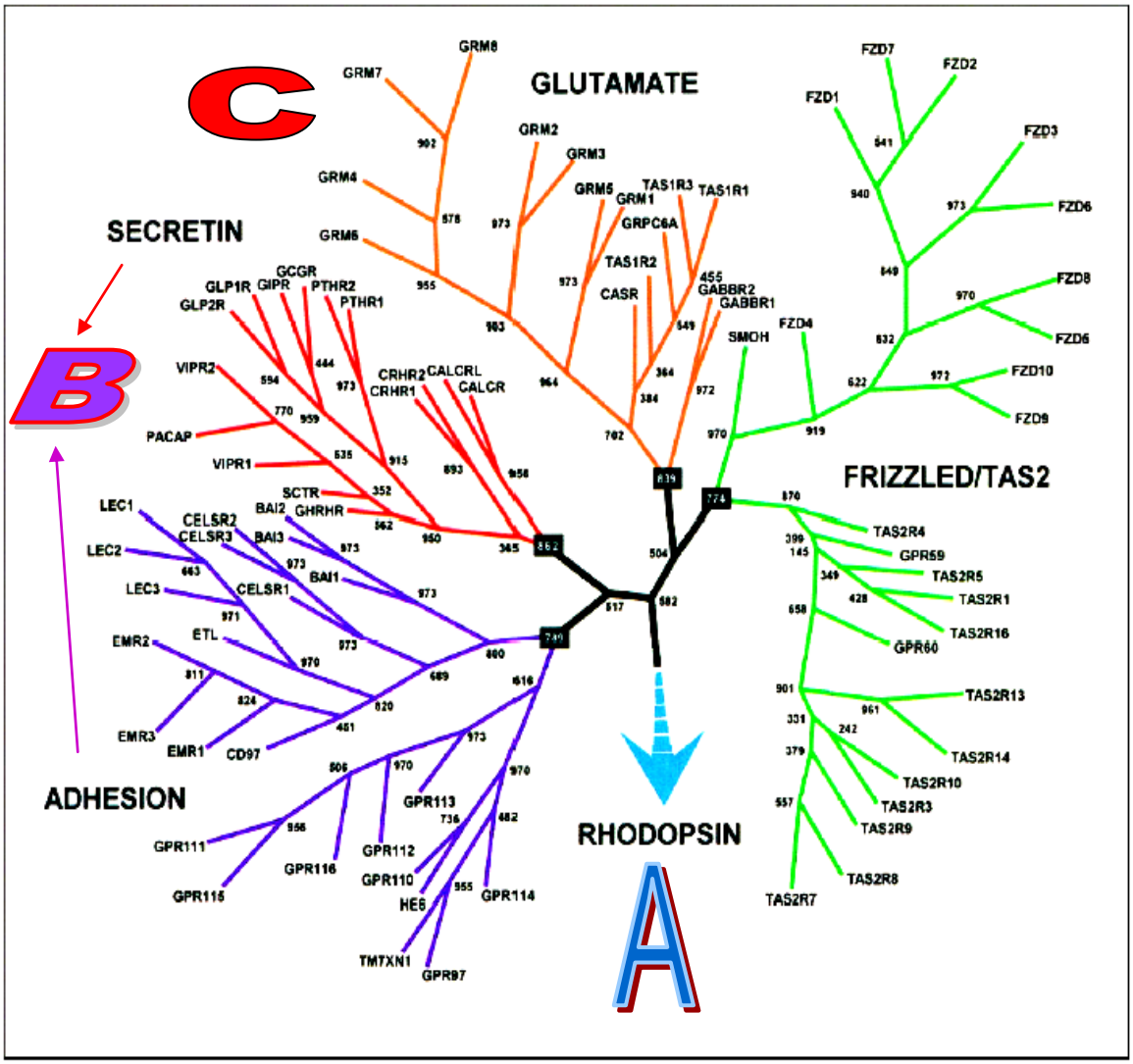

Figure 1-7: Phylogenetic tree of the GPCRs.
GRAFS classified GPCRs based on the human genome into five main families that termed glutamate (G, with 15 members), rhodopsin (R, 701), adhesion (A, 24), frizzled/taste2 (F, 24) and secretin (S, 15). The big letters A, B and C refer to the position of this families in the A-C system. These branches of rhodopsin family were removed from figure and replaced by an arrow toward the rhodopsin family for simplification (Fredriksson et al., 2003).

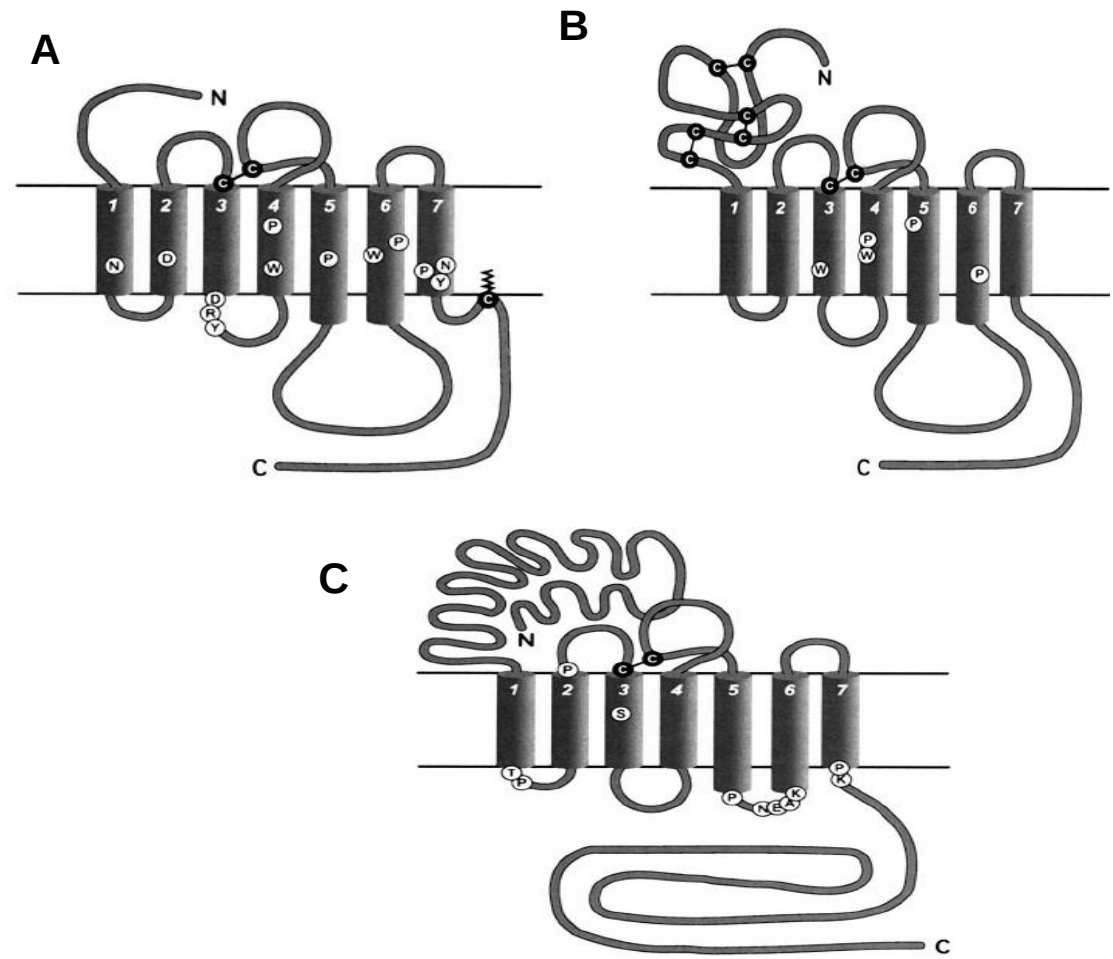

Figure 1-8: Common structural elements of the three major subfamilies GPCRs.

In general, the three major subfamilies GPCRs are characterized by a series of highly conserved key residues (black letter in white circles) and a disulphide bridge connecting ECL2 and ECL3 (white letters in black circles). **A:** Family A receptors are specifically characterized by DRY motif at the bottom of TM 3 and a palmitoylated cysteine in thecarboxy-terminal tail causing formation of a putative fourth intracellular loop. **B:** Family B receptors are specifically characterized by a long NTD containing several cysteines forming disulphide bridges. Unlike the A receptors, the palmitoylation site and DRY motif are missing. Moreover, the conserved prolines are different. **C:** Family C receptors are specifically characterized by a unique, very short and highly conserved third intracellular loop. The NTD is very long (about 600 amino acids) and thought to contain the ligand-binding site. The C receptors do not have any of the key features characterizing A and B receptors. (Adapted from (Gether, 2000).

1.4.2 Structure

The pharmacological importance of GPCRs has raised the interest in investigating their structure to understand how they bind their ligands and transduce their signals. At first, crystallization of membrane protein was difficult resulting from difficulties in preparing samples suitable for crystallographic studies. At that time, the bacteriorhodopsin structure was determined by using electron cryo-microscopy (Henderson et al., 1990). Although bacteriorhodopsin does not activate G proteins it was considered a bacterial homologue of mammalian rhodopsin because of its trans-membrane structure and similar chromophore.

One decade later, the crystal structure of rhodopsin was determined at 2.8 Å resolution (Palczewski et al., 2000). The structure displayed seven helices that are arranged counter-clockwise when viewed from the intra-discal side, with helices 1, 2, 3 and 5 tilted and helices 5 and 7 distorted at Pro residues. Helix 2 also has a kink due to the flexibility of the Gly-Gly sequence in the middle of the helix. The helices are connected by a network of hydrogen bonds and hydrophobic interactions that constrain the receptor in an inactive conformation (Figures 1-9 and 1-10; Palcewski et al., 2000).

Although the individual families within the GPCR superfamily have no detectable sequence identity, the entire receptors share the characteristic structure of 7TM helices connected by alternating ICLs and ECLs. The N-terminus is extra-cellular and variable in length. The binding domains vary depending on the family of receptor, type of ligand (small molecule or peptide; agonist or antagonist; Figure 1-11). In general, small ligands are thought to bind in the central cavity formed by the TM helices, while larger and peptide ligands interact with the extra-cellular regions of the receptors. The C-terminus is

located in the cytoplasm and, along with the ICLs, interacts with an intracellular heterotrimeric G protein to initiate signal transduction and mediate its effect. These cytoplasmic domains are targets of post-translational modifications such as phosphorylation, dephosphorylation, palmitoylation and ubiquitination.

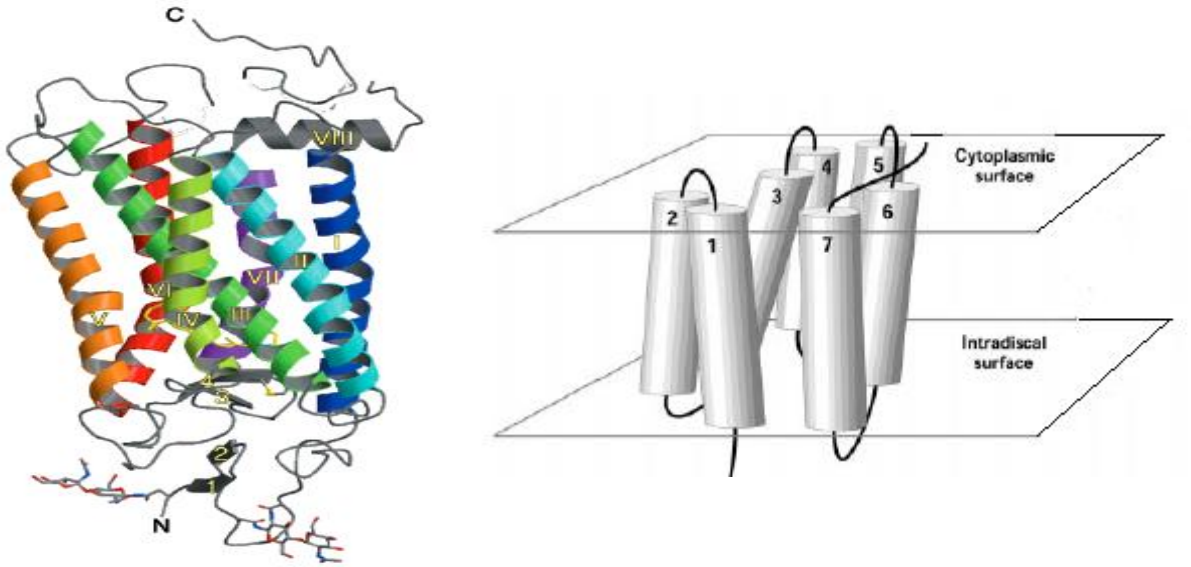

Figure 1-9: The crystal structure of rhodopsin.
Left: ribbon drawing of the crystal structure of rhodopsin. The figure is shown as parallel to the plane of the membrane. The transmembrane helices are numbered in latin numbers while antiparallel β sheets are numbered in Arabic numbers (from Paleczewski et al., 2000). **Right:** cartoon representation, the intradiscal surface are toward the bottom and cytoplasmic surface is toward the top of the figure (modified from (Marin et al., 2000)

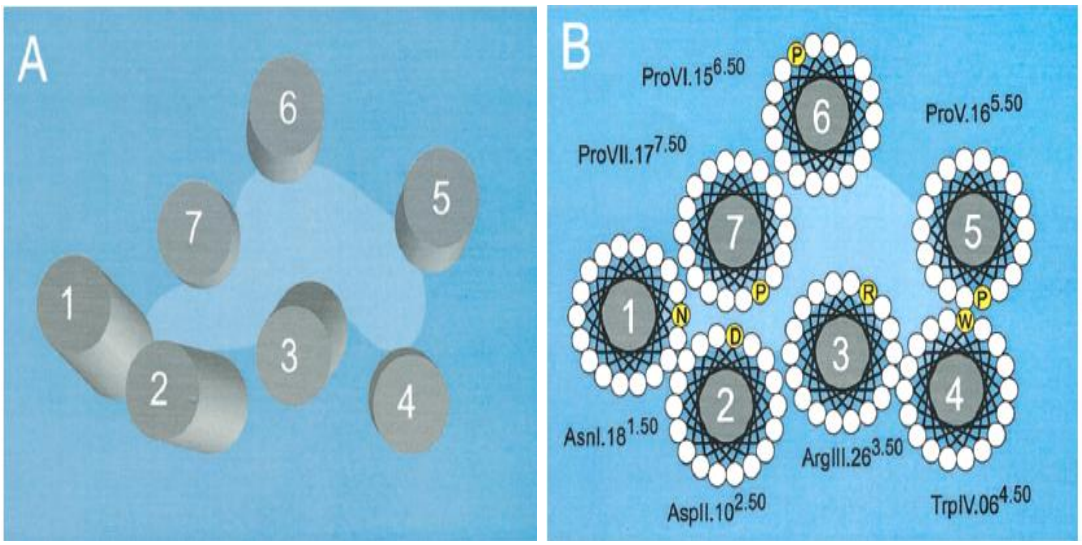

Figure 1-10: The predicted structure of rhodopsin-like GPCRs.

A: Diagram of a rhodopsin-like GPCR as seen from the extra-cellular side with each helix represented by a cylinder. The helices are organized in a counter clockwise pattern. **B:** 'Helical wheel' diagram of helices showed in A. The conserved fingerprint residues are shown in yellow. Based on the Schwartz numbering scheme, the number is given according to its predicted relative position in the helix (Schwartz et al., 1995). For example, ProV.16 indicates residue number 16 in TM 5. In the Ballesteros-Weinstein numbering scheme the most conserved residue in each helix has been given the number 50 (Baldwin et al., 1997). The residues are indicated according to the Schwartz scheme followed by the Ballesteros-Weinstein number in superscript (Gether, 2000).

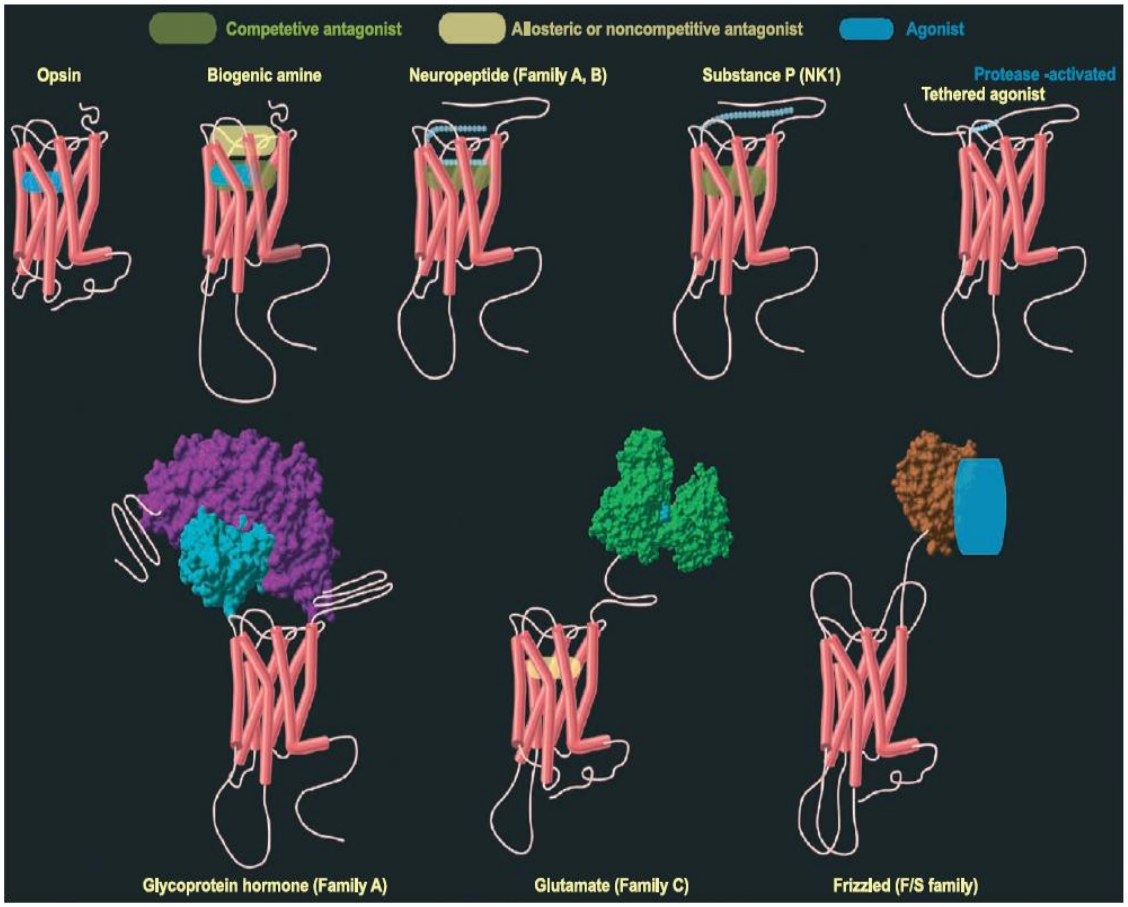

Figure 1-11: Schematic models of ligand- GPCRs complexes.
The binding sites are located in different regions of the receptor according to the type of the ligand. The binding sites for all small molecule ligands in Family A receptors are embedded deeply between the 7 TM helices. Competitive antagonists and agonists interact with partially overlapping binding sites in biogenic amine receptors. in muscarinic receptors, the binding sites for allosteric antagonists have been identified localized extra-cellular of primary binding sites. In many peptide receptors (e.g., NPY, angiotensin II, and GnRH receptors), the binding sites for the native peptides include residues from both extracellular domain (NTD and ECLs) and core domain. The binding sites for substance P in the NK1 neurokinin receptor involve only extracellular domains. Leucine-rich repeat (LRR) region in the N-termini and ECLs include the binding sites of the receptors interacting with glycoprotein hormones (LH, TSH, and FSH) and relaxin peptides. Thrombin and serine proteases activate PAR1–4 by cleavage of the N-terminus. Thereafter, the remained part activates the receptor as a tethered agonist by interacting with ECL2 (except PAR3). PAR3 is probably activated by a tethered agonist from another membrane protein. The binding sites of Family C involve a large Venus flytrap module (VFM). The closed state conformation of the VFM is started by binding and trapping of the agonist, whereas the open state conformation is maintained by a competitive antagonist. In mGlu receptors, the binding sites for non-competitive antagonists are buried between the 7 TM helices. In Frizzled receptors, the binding sites involve N-terminal cysteine-rich domain (CRD) (Kristiansen, 2004).

1.4.3 Family B GPCRs

It was in 1991 when the receptor for the gut hormone secretin was cloned (Ishihara et al., 1991) and classified as a GPCR, which is different from those in the rhodopsin family and later referred to as Family B. Family B GPCRs have the superfamily characteristic 7TM topology with their specific characteristic conserved amino acid sequence and the ability to regulate intracellular cAMP and its downstream system (Kolakowski, 1994).

Family B GPCRs are characterised by their amino terminal signal peptide, as well as a long NTD, which is essential for ligand binding (Figure 1.8). This NTD contains six conserved cysteine residues, as well as two conserved tryptophans and an aspartate, which could support the importance of this domain in the hormone receptors (Harmar, 2001). In addition, Family B GPCRs have conserved cysteine residues within the extra-cellular loops ECL1 and ECL2 which may form a disulphide bridge analogous to that in Family A GPCRs (Mann et al., 2010a).

Investigation of the trans-membrane helices and associated loops revealed that they may be important for specific ligand interaction (Harmar, 2001). ICL3 contains the major determinants required for a specific G protein-coupling, a splice variation in this region can give rise to receptors that vary in their ability to couple to different G-proteins (Pisegna and Wank, 1996). Furthermore, the alternative splicing in ICL1 of the CRF1 (Nabhan et al., 1995) and calcitonin receptors (Nussenzveig et al., 1994) exhibited an effect on G-protein-coupling. In the alternative GPCRs classification system (GRAFS), Family B is called ‘the secretin, S, receptors’. Subfamily Secretin ‘S’ group basically corresponds to Family B of the A-F system and its name is related to the fact that the secretin receptor was the first one to be cloned in this family

(Fredriksson et al., 2003). Subfamily 'S' in the GRAFS system (Figure 1-7) includes the classical hormone receptors that have ligands that are polypeptide hormones of length 27-141 amino acid residues. The receptors, and sometimes their ligands, are homologous to each other which has led to their classification into one group. The members of the group are named after their ligand such as receptors for glucagon, glucagon-like peptide-1 and glucagon-like peptide-2 (Harmar, 2001).

1.4.3.1 N-terminal domain (NTD) of Family B GPCRs

In general, Family B GPCRs share 30-50% amino acid identity; however they do not have any significant homolgy with other GPCRs families. Family B GPCRs have a family characteristic long extra-cellular domain, or 'NTD', of 100-150 amino acids (Segre and Goldring, 1993), and an integral membrane 'core domain', or 'J domain', consisting of the 7TM helices with their interconnecting loops either intracellular or extra-cellular. The NTD has six conserved cysteine residues connected by the disulphide bonds, which are vital for the correct folding of the domain (Grauschopf et al., 2000, Bazarsuren et al., 2002).

Initially, a 3D NMR structure of most of the mouse corticotropin-releasing factor receptor 2β NTD (CRFR2β-NTD) was determined (Grace et al., 2004). The structure showed that the NTD represents an example of a short consensus repeat (scr) fold (or Sushi domain) and the most essential features stabilising this fold are conserved across the entire Family B GPCR (e.g. three disulphide bonds supported two anti-parallel β-sheets regions surrounding a central core of a buried salt bridge between Asp65 and Arg101 flanked by two buried aromatic rings of Trp71 and Trp109) (Figure 1-12).

The disulphide bonds are the highly conserved post-transtional modification in Family B as they have been described in isolated N-terminal fragments of both GLP-1R and PTH-1R (Lee et al., 1994, Gaudin et al., 1995, Wilmen et al., 1996, Knudsen et al., 2000, Vilardaga et al., 1997, Grauschopf et al., 2000). Mutation of any of these six cysteines in the full receptors of GLP-1, secretin, Vasoactive intestinal polypeptide receptor (VPAC), and Parathyroid hormone 1 receptor (PTH1R) disabled binding function of those receptors. Grace's et al, published a second structure with ligand bound (Grace et al., 2007) which showed two disordered loops: loop 1 seems to be flexible and contains high sequence variability within CRFR family. Loop 2 appeared to contain some highly conserved residues and become structured upon antagonist (astressin) binding.

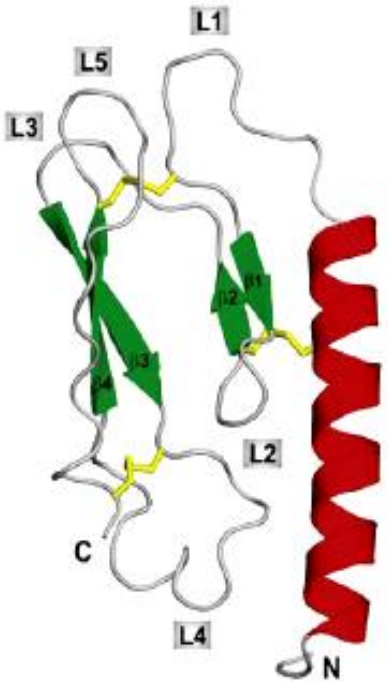

Figure 1-12: Common structural elements of Family B GPCR NTDs.

Family B GPCR NTDs have a common stracture characters that include an N-terminal α-helix (red), two β-sheets composed of strands β1 to β4 (green), with loop regions L1 to L5 (grey). The domains are stabilized by three conserved disulphide bridges (yellow sticks) (Parthier et al., 2009).

The role of a disulphide bond between ECL1 and ECL2 in Family B receptors is controversial. Studies of the human VIP receptor have shown a disulphide bond is present between two conserved cysteines at positions 215 and 285 in the ECLs, which are critical for binding and activation (Knudsen et al., 2000). An investigation into the role of the cysteine residues 281, ECL1, and 351, ECL2, in the PTH receptor showed a marked decrease in receptor function and expression following their mutation to serine. However, the double mutation of both slightly improved ligand binding affinity (Lee et al., 1994). In contrast, in the human VIP 1 receptor, mutation of either Cys208 or Cyc215 in ECL1 to glycine had affinity comparable to wild type (WT). However, when this mutation was applied to Cys288 in ECL2, no binding of VIP could be detected. Additionally, although the Cys208 and Cys215 double mutant bound VIP, it had a 10 times higher dissociation constant than the WT receptor (Gaudin et al., 1995). Similarly, in secretin receptors, the mutation of either Cys193 in ECL1 or Cys263 in ECL2 to serine, as well as their double mutation to serine, resulted in non-detectable ligand binding, although these receptors could still be activated (Vilardaga et al., 1997). In rGLP-1R, mutation of Cys226 in ECL1 to alanine reduced GLP-1 potency as a result of presence of a free thiol group on the other Cys296 in ECL2 that interferes with the optimum activation by GLP-1. Consequently, the GLP-1 potency was restored by a double alanine mutation of both Cys226 in ECL1 and Cys296 in ECL2 that indicates a disulphide bond (Mann et al., 2010a).

Following the first NMR structure of a family B NTD, nine representative NTDs have been solved by X-ray crystallography or NMR spectroscopy in complex with bound ligands: murine CRFR2β-NTD bound to the synthetic antagonist astressin (Grace et al., 2007), PACAP receptor type 1(PAC1R) in

complex with the antagonist PACAP(6–38) (Sun et al., 2007), GIPR-NTD bound to its natural peptide hormone GIP(1–42) (Parthier et al., 2007), hGLP-1R-NTD in complex with the antagonist EX4(9–39) (Runge et al., 2008), PTH1R-NTD bound to the truncated ligand PTH(15–34) (Pioszak and Xu, 2008), two structures of CRFR1 in complex with the truncated ligands CRF(22–41) and CRF(27–41) (Pioszak et al., 2008), hGLP-1R-NTD in complex with GLP-1 (Underwood et al., 2010), CRFR1-NTD in complex with its high affinity agonist αhcCRF (Grace et al.), Calcitonin receptor-like receptor (CLR) and the receptor activity modifying protein 1 (RAMP1), CLR/RAMP1-NTD (ter Haar et al., 2010). Collectively, the structures provide a common picture for the interaction of Family B GPCRs with their cognate peptide hormones and first indications of the origins of ligand selectivity. Although no experimentally determined full-length Family B receptor structure has been determined to date, the structure elucidation of individual Family B GPCR NTDs with their respective ligands represents a considerable step towards a molecular understanding of their action.

Although the NTDs share the 'secretin recognition fold' (Parthier et al., 2007), individual loops (in particular loops 1 and 4) deviate significantly, a finding that is evident from both the NMR structure ensembles and the high B-factors in the crystal structures. The exceptionally long loop1 of PTH1R-NTD is disordered in the crystals (Pioszak and Xu, 2008), whereas the conformation of loop 4 of CRFR1-NTD and CRFR2β-NTD seems to adapt to ligand binding (Grace et al., 2007, Pioszak et al., 2008). Intriguingly, the solution structure of PAC1R-NTD in complex with PACAP(6–38) (Sun et al., 2007) exhibits an apparent difference in loop 4 topology (Figure 1-13). Although the overall structure of PAC1R-NTD is similar to the other NTDs, loop 4 proceeds to β-

strand 4 'above' the terminal disulphide bond; in all other NTD structures, this loop proceeds 'below' this disulphide, resulting in an inverse direction of loop 4 compared with the other NTDs. The same exceptional topology was also present in the CRFR2β-NTD NMR structure ensemble (Grace et al., 2004) but, later, was revised in a refined structure of the domain (Grace et al., 2007).

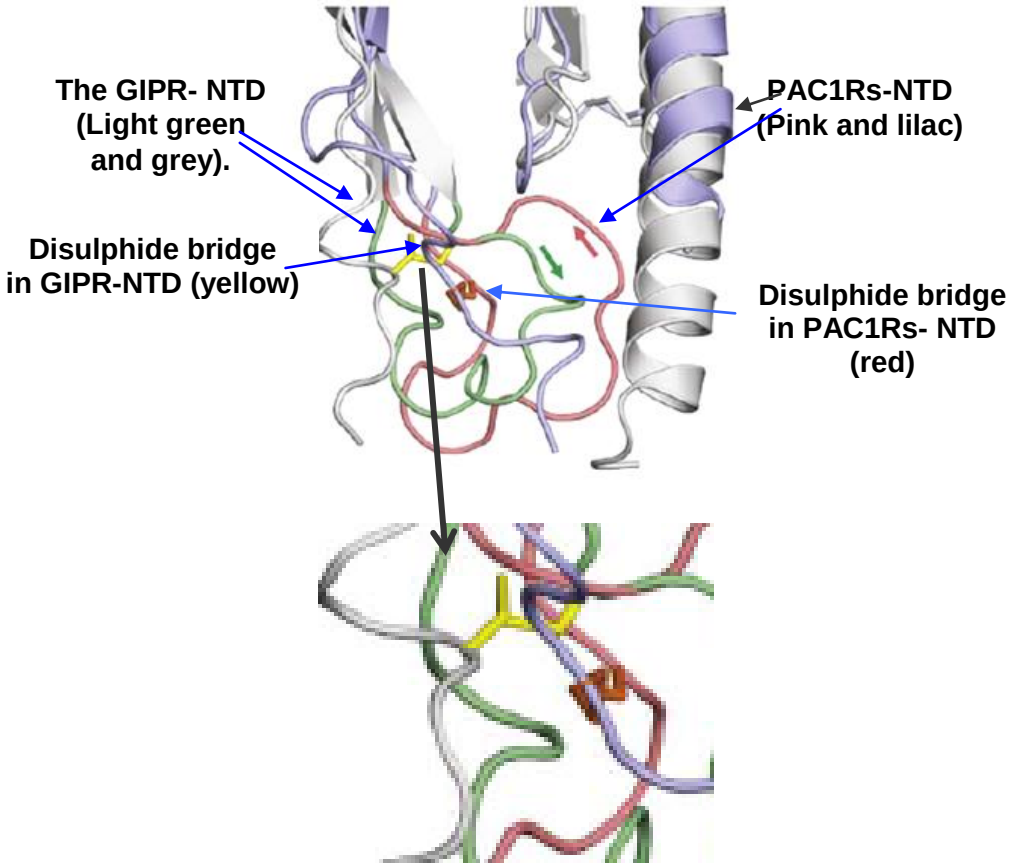

Figure 1-13: The odd topology of loop 4 in PAC1Rs-NTD.

The direction of the main chain of loop 4 (indicated by arrows) in PAC1Rs-NTD (pink and lilac) is opposite to that in GIPR- NTD (light green and grey) and the other Family B NTDs. The position of the disulphide bridge , which in PAC1Rs-NTD (red) lies 'below' the loop, whereas in GIPR-NTD (yellow) it is 'above' the loop (look at the maximized view in the bottom of the figure) (Parthier et al., 2009).

Glycosylation is important for correct receptor function of many Family A GPCRs, enhancing folding, intracellular trafficking, ligand binding and signal transduction (Zhang et al., 1995, Davis et al., 1995, Russo et al., 1991). Incontrast, glycosylation has an indefinite role in Family B GPCRs, although all member of the Family B have N-linked glycosylation sites within the NTD. Studies on the secretin receptor showed that glycosylation is important for ligand binding but not for receptor trafficking (Pang et al., 1999). On the other hand, glycosylation appeared unnecessary for PTH1R (Zhou et al., 2000). Likewise, mutation of glycosylation sites of the CRLR did not affect function except for Asn123 where glycosylation of which would be essential for a functional adrenomedullin receptor, perhaps due to changes in the tertiary structure of the domain (Kamitani and Sakata, 2001).

1.4.3.2 Two domain model of Family B GPCRs-ligand interaction

The NTD contributes to the majority of the ligand binding determinants. This contribution could be clearly proved by binding the isolated NTD of the PTH1R (Grauschopf et al., 2000) and GLP-1R (Bazarsuren et al., 2002, Lopez de Maturana et al., 2003) to their respective ligands, albeit with lower affinity than with the native receptor. However, studies of chimeric full-length receptor constructs with their native ligands revealed the same conclusion. For example: PTH1R and calcitonin hybrid ligands (N-CT/PTH-C and N-PTH/CT-C) which could not activate WT receptors, could nevertheless activate chimeric CT/PTH and PTH/CT receptors respectively (Bergwitz et al., 1996). Likewise, the similar results were recorded for GIPR and GLP-1R (Gelling et al., 1997), calcitonin/glucagon receptors (Stroop et al., 1995) and VIP/secretin receptors (Holtmann et al., 1995).

Furthermore, using truncated and full-length ligands with their relevant receptors confirmed the hypothesis (Al-Sabah and Donnelly, 2003a). Additionally, a C-terminal fragment PTH (14-34) binds to PTH1R but does not activate it (Caulfield et al., 1990), while in contrast, an N-terminal fragment of the same peptide PTH(1-14) can induce a weak cAMP response, albeit with low affinity (Luck et al., 1999).

The two domain model for Family B ligand-receptor interaction could be summarized in the tethering of the C-terminal end of the ligand by the NTD leaving the ligand N-terminus to interact with the 'J domain' of the receptor,i.e. the ECLs and trans-membrane α-helices (Hoare, 2005). In each structure, the ligand adopts an α-helical conformation sandwiched between the two β-sheets of the NTD with the ligand C-terminus fixed by intermolecular hydrogen bonds to NTD side chains (Figure 1-14 and15). Residues of the ligand interacting with the NTD form an amphipathic α-helix, with at least three hydrophobic residues occupying a complementary ligand binding groove on the surface of the NTD. In return, the ligand binding groove is lined by hydrophobic residues from loop 2 and loop 4 and from the NTD C-terminus (Figure 1-15 A and B). In the mean time, the involvement of those hydrophobic residues was confirmed by mutagenic analysis (Grace et al., 2007, Parthier et al., 2007, Sun et al., 2007, Pioszak et al., 2008).

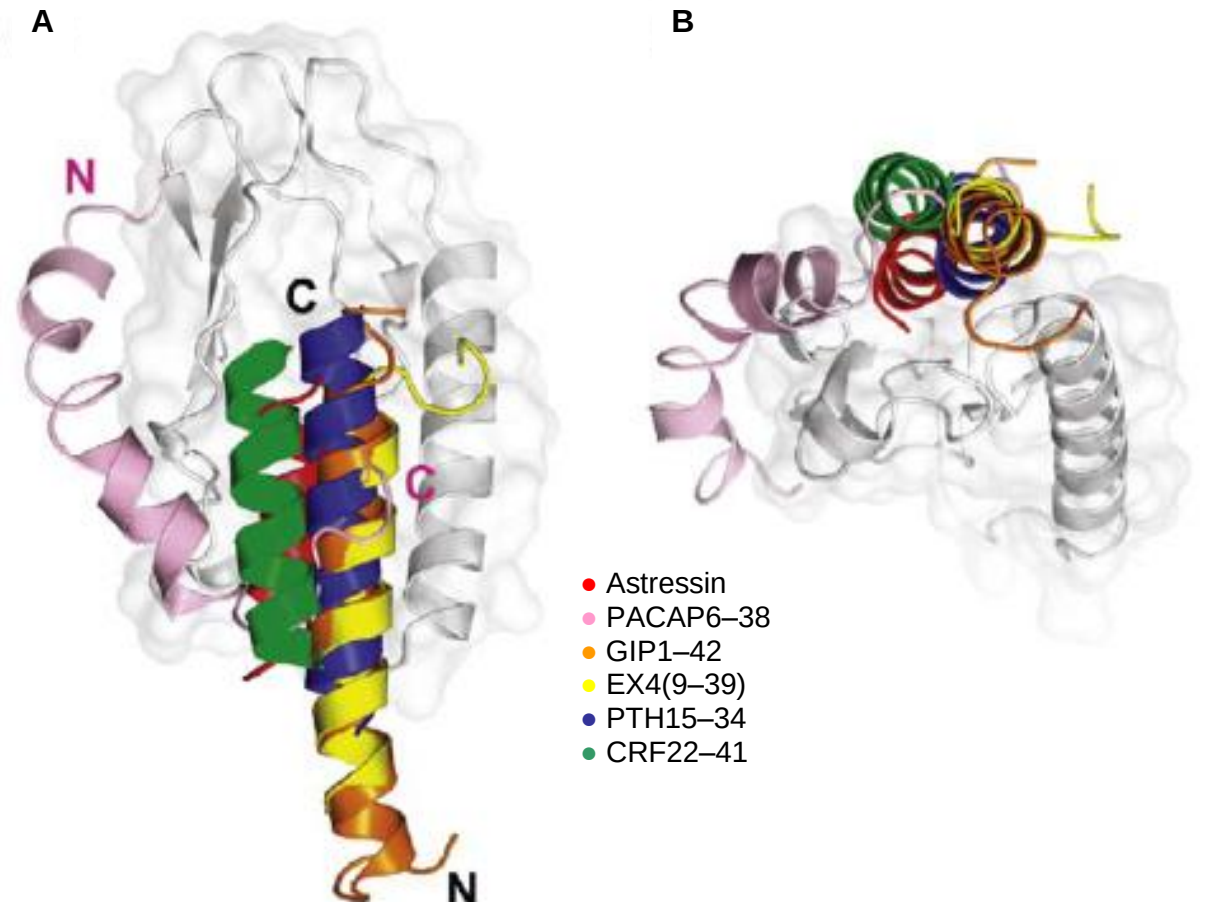

Figure 1-14: Structures of Family B GPCR ligands bound to the NTDs.

A: Superposition of the NTD-ligand complexes. NTD is shown as grey cartoon with surface representation. The bound ligands are keyed and labelled in the figure. The binding mode of NTD-bound PACAP6–38 is aberrant to those of the other ligands (N and C-termini are labelled in pink letters). **B:** View rotated about a horizontal axis by 90°. All peptides exhibit an α-helical conformation with only their C-termini while their N-termini are free to interact other parts of the receptors. N-terminal residues of GIP, exendin and CRF do not contact the NTD (Parthier et al., 2009).

Despite high similarity between members of Family B, some differences and exceptions were observed. The conformations of loops 2, 4 and part of loops of CFR1-NTD and CRFR2β-NTD differ in the ligand-free and ligand-bound states (Grace et al., 2007, Pioszak et al., 2008, Grace et al.) (Figure 1-16c). Exceptionally, PACAP C-terminus interacts with the NTD binding groove while the peptide wraps around the NTD where the PACAP N-terminus interacts via the outer face of β-strands β3 and β4 with a kink in the centre of the ligand orientated towards the ligand-binding groove (Figure 1-14). The kink seems to divide PACAP into two α-helical segments (Sun et al., 2007).

Differences in ligand binding modes have also ben noticed. These differences would suggest sub-classification of Family B NTD into CRF-like and glucagon-like. The CRF ligand group that includes CRF(22-41) and astressin showed much longer N-terminal ends, which could be related to the much shorter N-terminal helices of CFR1R-NTD and CRFR2β-NTD (Figures 1-14 and 1-15b). Other restrictions are due to additional glycine residue in the loop 2 of CRF receptors. In contrast, the glucagon ligand group (GIP, EX4, GLP-1 and PTH) has a shorter N-terminus because of extensive hydrophobic interactions with the longer N-terminal helices of their respective receptors NTDs as shown in Figures 1-14 and1-15a (Parthier et al., 2009).

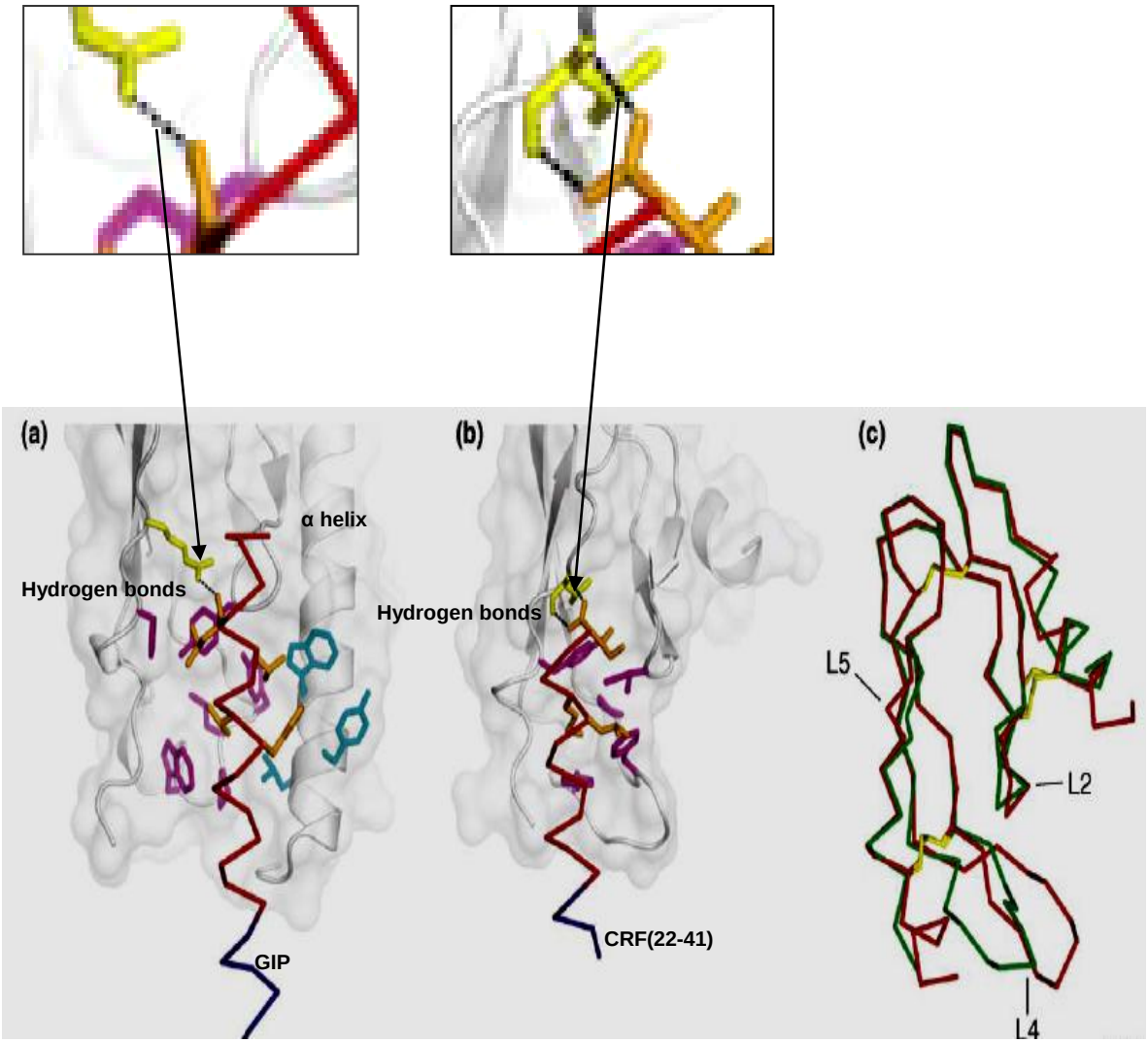

Figure 1-15: Binding of Family B GPCR ligands to the NTDs.

(a) The binding mode of GIP (shown as Cα trace, red and blue) to GIPR-NTD (grey). Hydrophobic residues in the NTD core from loop 2, loop 4 and the C-terminus (magenta) and from the N-terminal helix (cyan) interact with corresponding residues (orange sticks) from the C-terminal region of the ligand (Cα trace, red). The C-terminal end of the ligand is stabilized by an intermolecular hydrogen bond (black dots, see boxed panels for close up views) between the ligand backbone and a polar NTD residue in loop 5 (yellow sticks). N-terminal residues of the ligand not in contact with the NTD are depicted as a blue Cα trace. **(b)** CRF(22–41)/CRFR1-NTD complex (same colour code of GIP/ GIPR-NTD complex). Hydrophobic interactions between the NTD and the ligand are similar, but they lack contributions from the residual N-terminal α-helix of the NTD. The CRF C-terminal amide group is involved in two intermolecular hydrogen bonds to the NTD. **(c)** The CRFR1-NTD undergoes a conformational change upon ligand binding (Pioszak et al., 2008). Backbone superposition of ligand-free (red) and ligand-bound (green) CRFR1-NTD (for simplicity, the ligand, CRF(22–41), is not shown). Disulphide bonds are shown as yellow sticks. Structural differences are observed in loop 2 (L2), loop 4 (L4) and at the end of loop 5 (L5) (Parthier et al., 2009).

.

1.4.3.3 GLP-1 Receptor

1.4.3.3.1 Discovery and genetics

The advent of the discovery GLP-1 with its challengers to the field of diabetes control has raised interest in the receptor through which GLP-1 mediates its biological function. High-affinity binding sites (51 nM) for GLP-1 and activation of cAMP signal transduction in insulinoma cell lines were found, suggesting that the hormone acts through specific receptors located on the surface of pancreatic β-cells that are coupled to the stimulatory G protein (G_s) (Drucker et al., 1987, Goke and Conlon, 1988). Further studies identified the receptor in rodent insulinoma cell lines, rat and human pancreatic β-cells and somatostatin secreting cells (Fehmann and Habener, 1991, Gros et al., 1992).

A cDNA for the rGLP-1R was eventually isolated by transient expression of a rat pancreatic islet cDNA library in COS cells which was then screened by binding of radiolabeled GLP-1 (Thorens, 1992). Subsequently, a pancreatic hGLP-1R that shares approximately 90% sequence identity with the rGLP-1R was cloned (Dillon et al., 1993, Thorens et al., 1993, Graziano et al., 1993). The gene for the hGLP-1R is localized to chromosome 6p21 while the rat gene is localized to chromosome 20p12 (Stoffel et al., 1993) http://www.ncbi.nlm.nih.gov/gene?term=rat%20glp-1r). GLP-1R is a 64-kDa protein (Widmann et al., 1995) and although alternate splicing results in 2 different transcripts for both the rat and the human GLP-1R, there has been only one functionally distinct GLP-1R described (Thorens, 1992, Dillon et al., 1993). Although various polymorphisms have been associated with the hGLP-1R human gene locus (Stoffel et al., 1993), linkage analysis eliminates an association with the majority of NIDDM cases based on the populations studied (Tanizawa et al., 1994, Zhang et al., 1994, Yagi et al., 1996, Tokuyama et al.,

2004). One patient diagnosed with NIDDM from a Japanese study (Tokuyama et al., 2004) demonstrated impairment of insulin secretion, insulin sensitivity, and glucose tolerance and had a missense mutation resulting in substitution of threonine 149 with methionine (T149M). The similar mutated receptor showed a reduced affinity *in vitro* for GLP-1 and EX4 (Beinborn et al., 2005).

1.4.3.3.2 Structure/function studies

As introduced above, the identified receptor is a member of the 7TM family B GPCRs including receptors for glucagon, VIP, secretin, GIP, PACAP, GHF, calcitonin, and PTH. The identity of the amino acid sequence between these receptor proteins ranges between 27% and 49%, while the sequence identity to receptors of other subfamilies of GPCRs is less than 10%. The GLP-1R consists of 463 amino acids containing eight hydrophobic segments. The N-terminal hydrophobic segment is probably a signal sequence, whereas the others are trans-membrane-spanning hydrophobic motifs.

As mentioned above, rat and human GLP-1R are 90% identical (Thorens, 1992, Thorens et al., 1993), differing at 42 amino acid positions (Tibaduiza et al., 2001). Accordingly, the difference between the two types rarely took the attention of research groups. However, a previous study has found that the non-peptidic antagonist T-0632 binds with almost 100-fold greater affinity to the hGLP-1R than to the rat receptor homolog and the species selectivity of T-0632 is reversed by exchange of a single NTD residue (Trp33Ser) between the human and rat GLP-1R respectively (Tibaduiza et al., 2001).

The crystal structure of hGLP-1R-NTD in complex with EX4(9-39) has been solved (Runge et al., 2008). The structure revealed that the core structure of hGLP-1R-NTD is similar to those of other published structures of Family B members (introduced above as SCR) showing the six conserved cysteine residues with their disulphide bonds, two regions of anti-parallel β-sheets (β-strands 1–5), and centrally positioned conserved residues Asp67, Trp72, Pro86, Arg102, Gly108, and Trp110 of GLP-1R-NTD (Figure 1-16, A and B). In more specific detail, hGLP-1R-NTD contains an α-helix and the tertiary structure is stabilized by the disulphide bonds and by multiple intra-molecular interactions between the secondary structure elements. The α-helix is defined by residues Leu32-Glu52 and includes Cys46, which forms a disulphide bridge with Cys71 on the β2 sheet. The α-helix is terminated by three successive Pro residues (Pro54-Pro56, in rat type Pro54, Leu55 and Leu56) positioned at the beginning of loop1 (Pro54-Phe61) (Runge et al., 2008).

The residues Cys62-Asp67 (β1 sheet) and Ala70-Gly75 (β2 sheet) constitute the first anti-parallel β-sheet. β1 and β2 are separated by a short turn (turn 1, Glu68 and Tyr69). The side chain of Arg64 of β1 interacts with the dipole of the α-helix through hydrogen bonds with the backbone of Leu50 and Asp53. The positioning of the Arg64 side chain is further guided by a hydrogen bond with the backbone carbonyl of Pro54 of loop1 and by an ionic interaction with Asp74 of β2. The residues Gly78-Ser84 (β3), His99-Thr105 (β4), Leu109-Leu111 (β5), and Asp122 (β-bridge with β4) form the second region of anti-parallel β-sheets. β3 and β4 are separated by a long well-defined loop (loop 2, Pro86-Gly98) that is important for ligand binding as previously introduced. The disulphide bridge between Cys62 and Cys104 connects the beginning of β1 and the end of β4. Cys85 is positioned at the end of β3 and forms a disulphide

bridge with Cys126 in the C-terminal part of GLP-1R-NTD. The segment from Leu109-Asp122 resembles a β-strand with an insertion of a flexible loop (loop 3, Gln112-Leu118) (Runge et al., 2008).

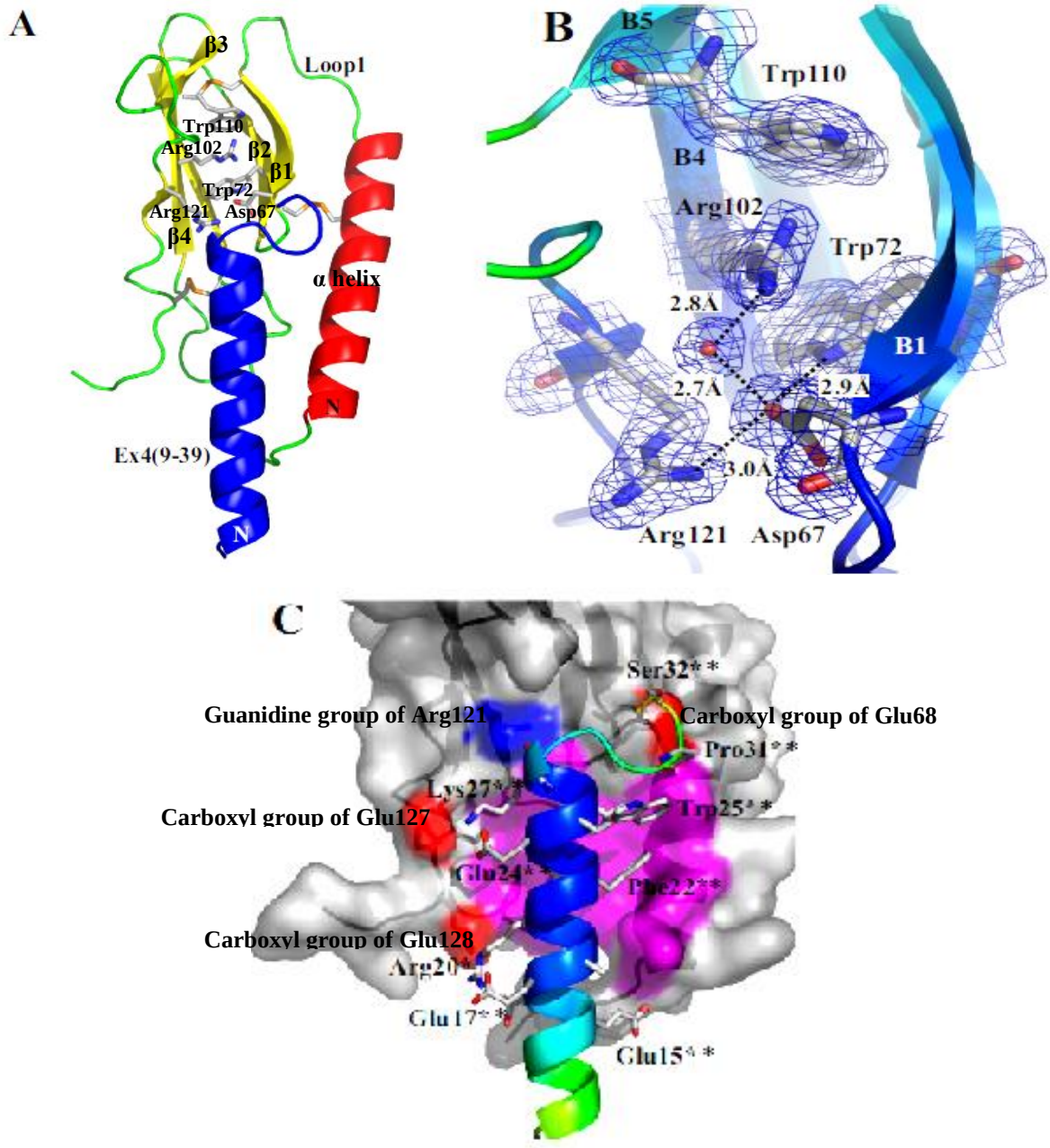

Figure 1-16: The structure of hGLP-1R-NTD in complex with EX4(9 –39).
A: Ribbon diagram illustrating the structure of hGLP-1R-NTD with EX4(9 –39) shown in blue. The disulphide bridges and the residues Asp67, Trp72, Arg102, Trp110, and Arg121 are shown in sticks coloured by atoms. **B:** the same set of residues of hGLP-1R-NTD and the coordinated water molecule. **C:** surface representation of hGLP-1R-NTD in gray, highlighting the carboxyl group of Glu68, Glu127, and Glu128 in red, the Guanidine group of Arg121 in blue, and the hydrophobic binding surface in magenta. The secondary structure representation of EX4(9–39) is coloured according to B-factors (blue=20–25 and green-yellow=45–60). The interacting amino acids of EX4(9 –39) are marked by (**) and are shown by sticks (Runge et al., 2008).

Residues Arg24-Gln27 and Gly132-Tyr145 were not resolved in the crystal structure. The conserved Asp67 of hGLP-1R-NTD is centrally positioned, forming intra-molecular interactions, as also observed for CRFR2β-NTD, PAC1R-NTD, and GIPR-NTD. The side chain of Asp67 interacts indirectly through a water molecule with the side chain of Arg102 and directly via hydrogen bonds with the side chain of Trp72 and Arg121 (Figure 1-16B). In addition, the side chain and backbone of Asp67 interact with Tyr69 and Ala70, stabilizing the turn between β1 and β2. Gly108 has a structural function stabilizing the turn after β4 that allows the positioning of the Trp110 side chain below the Cys62-Cys104 disulphide bridge and above Arg102. Arg102 is thereby sandwiched between the side chains of Trp72 and Trp110 in a manner similar to CRFR2β-NTD. Pro86 at the beginning of loop 2 plays a structurally important role for the formation of the ligand binding site. The side chain of Pro86 fills out a hydrophobic cavity formed by Tyr42 of the α-helix, Tyr69 of turn 1, Ala70 of β2, Val83 of β3, Val100 of β4, the Cys85-Cys126 disulphide bridge, and two residues of loop 2 itself, Tyr88 and Leu89 (Runge et al., 2008).

Regarding ligand Interactions with hGLP-1R-NTD, the structure exhibited by EX4(9–39) is a well defined α-helix from Leu10** to Asn28**, and the residues that interact with hGLP-1R-NTD lie between Glu15** and Ser32** (Figure 1-16C). Glu15** is conserved in EX4 and GLP-1, and it interacts with the dipole of the α-helix of hGLP-1R-NTD by a hydrogen bond with the backbone amide of Leu32, the first residue in the α-helix of hGLP-1R-NTD (Runge et al., 2008).

The amphipathic nature of the Glu16**-Lys27** segment (see Figure 1-15) enables hydrophobic interactions with hGLP-1R-NTD through one face of the α-helix and hydrophilic interactions with the other face. The hydrophilic face is constituted by Glu16**, Glu17**, Arg20**, Glu24**, and Lys27**, of which only Arg20** and Lys27** interact directly with hGLP-1R-NTD (Figure 1-16A). The side chain of Arg20** binds to the side chain of Glu128 of hGLP-1R-NTD. Also, Arg20** is positioned by Glu16** and Glu17** in an arrangement that could stabilize the α-helical conformation of EX4(9–39) itself. In a similar arrangement, the side chain of Lys27** appears to interact with both the side chain of Glu127 of hGLP-1R-NTD and the side chain of Glu24**. In addition, the backbone carbonyl of Lys27** at the end of the α-helix forms a hydrogen bond with the side chain of Arg121 in hGLP-1R-NTD (Runge et al., 2008).

The hydrophobic face of EX4(9–39) is constituted by residues Ala18**, Val19**, Phe22**, Ile23**, Trp25**, Leu26**, and Pro31** (Figure 1-17B). Of these, Val19**, Phe22**, Ile23**, and Leu26** are buried by the hydrophobic interaction with hGLP-1R-NTD. Phe22** is uniquely conserved in the glucagon subfamily and it interacts directly with Leu32, Thr35, Val36, and Trp39 on the α-helix of hGLP-1R-NTD. Surprisingly, the structure displayed a minor effect of residues EX4(31-39) of EX4 on the interaction with hGLP-1R-NTD represented by a suggested hydrogen bond between EX4 Ser32** and Glu68 with a potential weak effect on the affinity of EX4 (Runge et al., 2008).

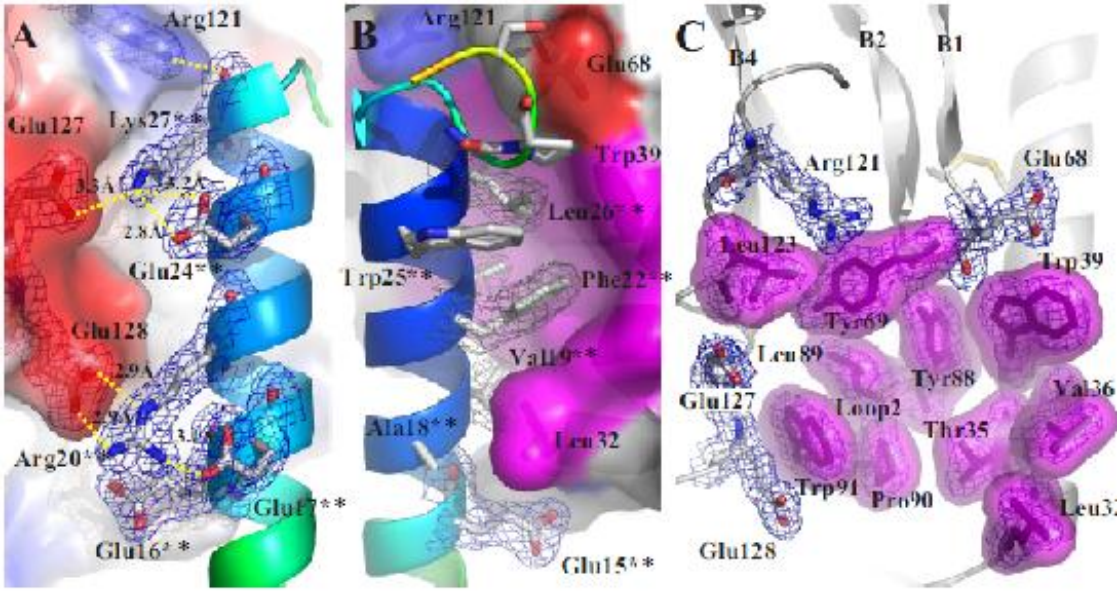

Figure 1-17: Hydrophilic and hydrophobic interactions between EX4(9–39) and hGLP-1R-NTD.
The colour code system of Figure 1-17 is applied. **A:** The hydrophilic interactions, the EX4(9-39) residues Glu16**, Glu17**, Arg20**, Glu24**, and Lys27** are illustrated as sticks, and the electron density is shown in blue. The residues Arg121, Glu127, and Glu128 of NTD are illustrated with the same colour code **B:** The hydrophobic interactions, the side chains of Glu15**, Ala18**, Val19**, Phe22**, Ile23**, Trp25**, Leu26**, Pro31**, and Ser32** are illustrated as sticks. The electron density is shown of Glu15** in blue and of Val19**, Phe22**, and Leu26** in grey. The surface of the hydrophobic binding cavity of NTD is illustrated in magenta. The surface of Glu68 and Arg121 is illustrated in red and blue, respectively. **C:** all the residues of NTD directly involved in binding of EX4(9 –39) are illustrated as sticks with electron density. The hydrophobic residues are highlighted by a magenta surface representation. Leu32, T35, Val36, and Trp39 belong to the α-helix and Tyr88, Leu89, Pro90, and Trp91 belong to loop 2. The β-strands are labelled β1-β5 (Runge et al., 2008).

More recently, the crystal structure of hGLP-1R-NTD in complex with GLP-1 was solved in the same laboratory (Figure 1-18) (Underwood et al., 2010). The GLP-1-bound structure (resolution 2.1Å) revealed nearly the same main features of the former EX4(9-39)-bound structure (resolution 2.2Å) with little differences specific for GLP-1. However, the authors' suggest that, unlike EX4 Lys27**, in GLP-1, the equivalent Val33* is unable to interact with Glu127 causing Glu127 to change rotamer conformation and point its side chain away from GLP-1. The side chain of Leu123 is flipped towards Arg121, which again is

flipped towards Pro119, closing the water accessible cavity observed in the EX4(9-39)-bound structure (Figure1-19A).

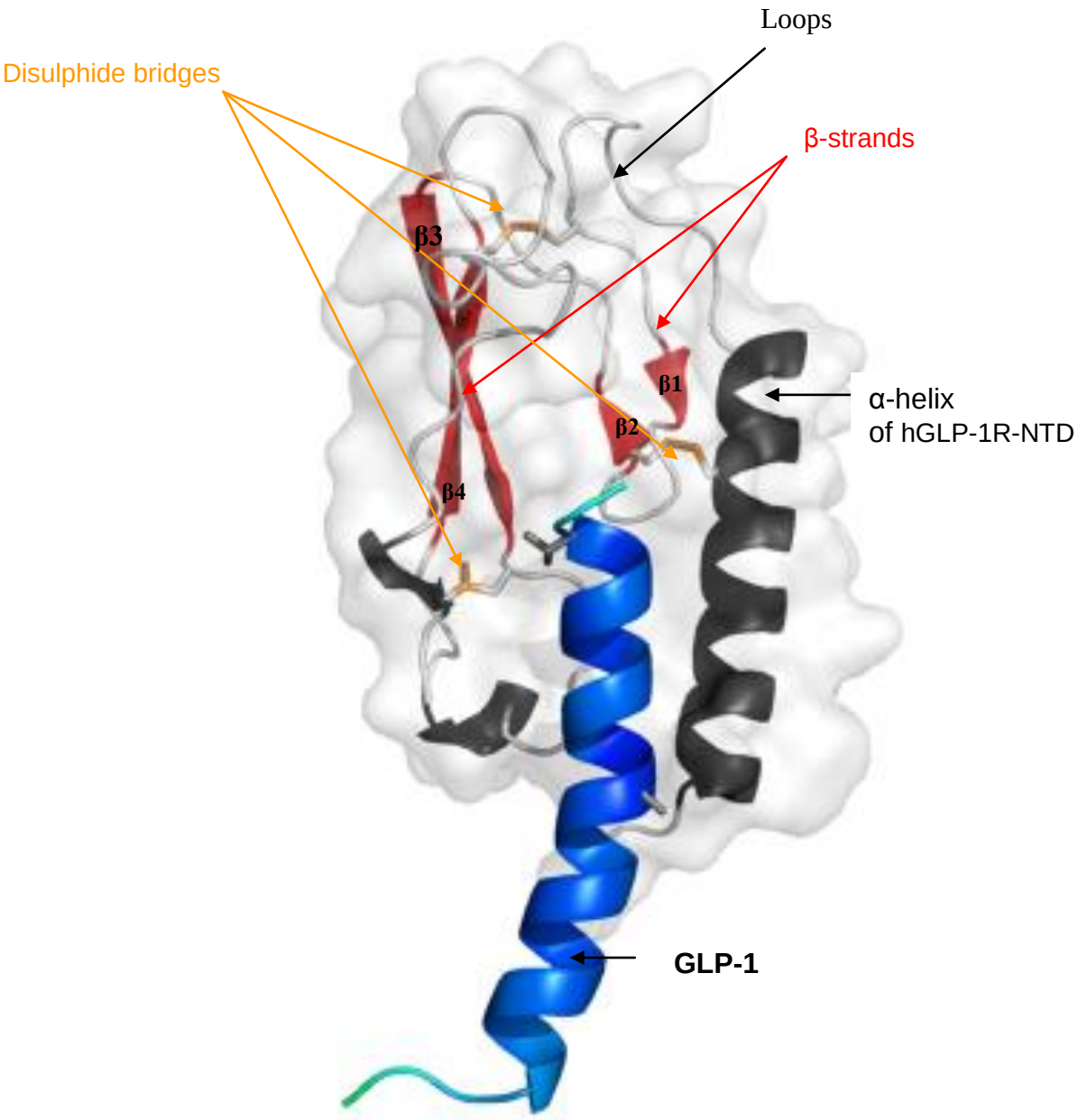

Figure 1-18: Structure of the GLP-1-bound to hGLP-1R-NTD.
GLP-1 (blue helix) bound to hGLP-1R-NTD (α-helix in black, β-strands in red and loops in gray and disulphide bridges are shown as orange sticks) (reproduced from Underwood et al., 2010).

The apparent GLP-1-specific conformations affect the conserved core of the NTD by rotating the guanidine group of Arg102 and by decreasing the distance between Asp67 and Arg102 compared to the EX4(9-39)-bound structure, without affecting the relative position and conformation of Trp72 and Trp110 (Figure 1-19B). This enables a direct interaction through a hydrogen bond between Asp67 and Arg102 unlike what was observed in the EX4(9-39)-bound structure, where a water molecule mediated the interaction between Asp67 and Arg102 (Figure 1-19B).

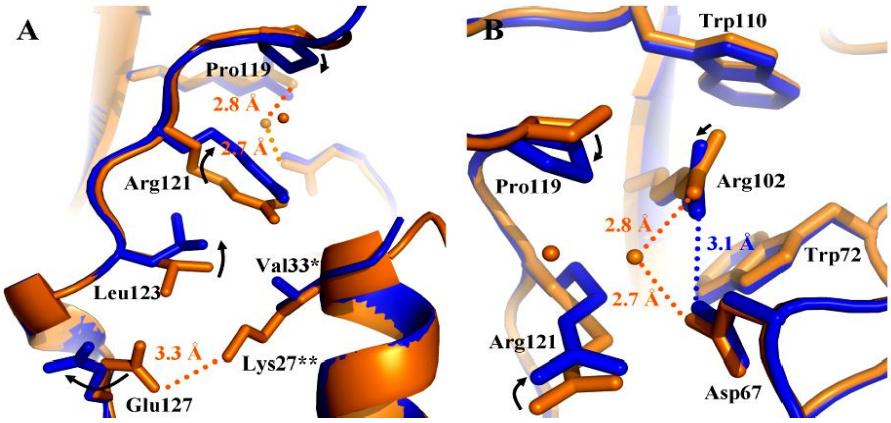

Figure 1-19: Differences between the GLP-1- and EX4(9-39)-bound structure of hGLP-1R-NTD.

Ribbon diagrams showing significant differences in side chain conformations between the GLP-1- bound structure in blue and the EX4(9-39)-bound structure in orange of hGLP-1R- NTD. Water molecules in orange are present only in the EX4(9-39)-bound structure. **A:** One diverging residue, Val33* of GLP-1 and Lys27** of EX4(9-39), causes a shift in the conformations of four residues namely Glu127, Leu123, Arg121 and Pro119 (note the directions of the black arrows) **B:** The GLP-1 specific conformations affect the conserved core of the NTD by rotating the guanidine group of Arg102 and by decreasing the distance between Asp67 and Arg102 compared to the EX4(9-39)-bound structure without affecting the relative position of Trp72 and Trp110 reflected by absence of arrows around them (taken from Underwood et al., 2010).

The GLP-1-bound structure described GLP-1 as two regular α-helical segments separated by a kink around Gly22*. The structure of His7*-Gly10* was not resolved probably due to the inherent flexibility in this part of GLP-1 and other peptide ligands for Family B receptors (Neidigh et al., 2001). The first α-helix segment Thr13*-Glu21* does not interact with hGLP-1R-NTD. The C-terminal segment (Ala24*-Val33*) interacts with NTD.

The interacting segment (Ala24*-Val33*) has an amphiphilic nature that enables hydrophilic and hydrophobic interactions through opposite faces of the α-helix (Figures 1-14 and 1-15). The hydrophilic face is mapped by residues Gln23*, Lys26*, Glu27* and Lys34*. Lys26* is the only residue which may interact directly with the NTD (Figure 1-20A). The hydrophobic face of GLP-1, which interacts with the NTD is defined by Ala24*, Ala25*, Phe28*, Ile29*, Leu32* and Val33* (Figure 1-20B). The importance of Phe28*, Ile29* and Leu32* in GLP-1 binding has previously been demonstrated by Ala-scanning of GLP-1 (Adelhorst et al., 1994). However, the functional consequences of the ligand-specific conformational differences are not known (Underwood et al., 2010).

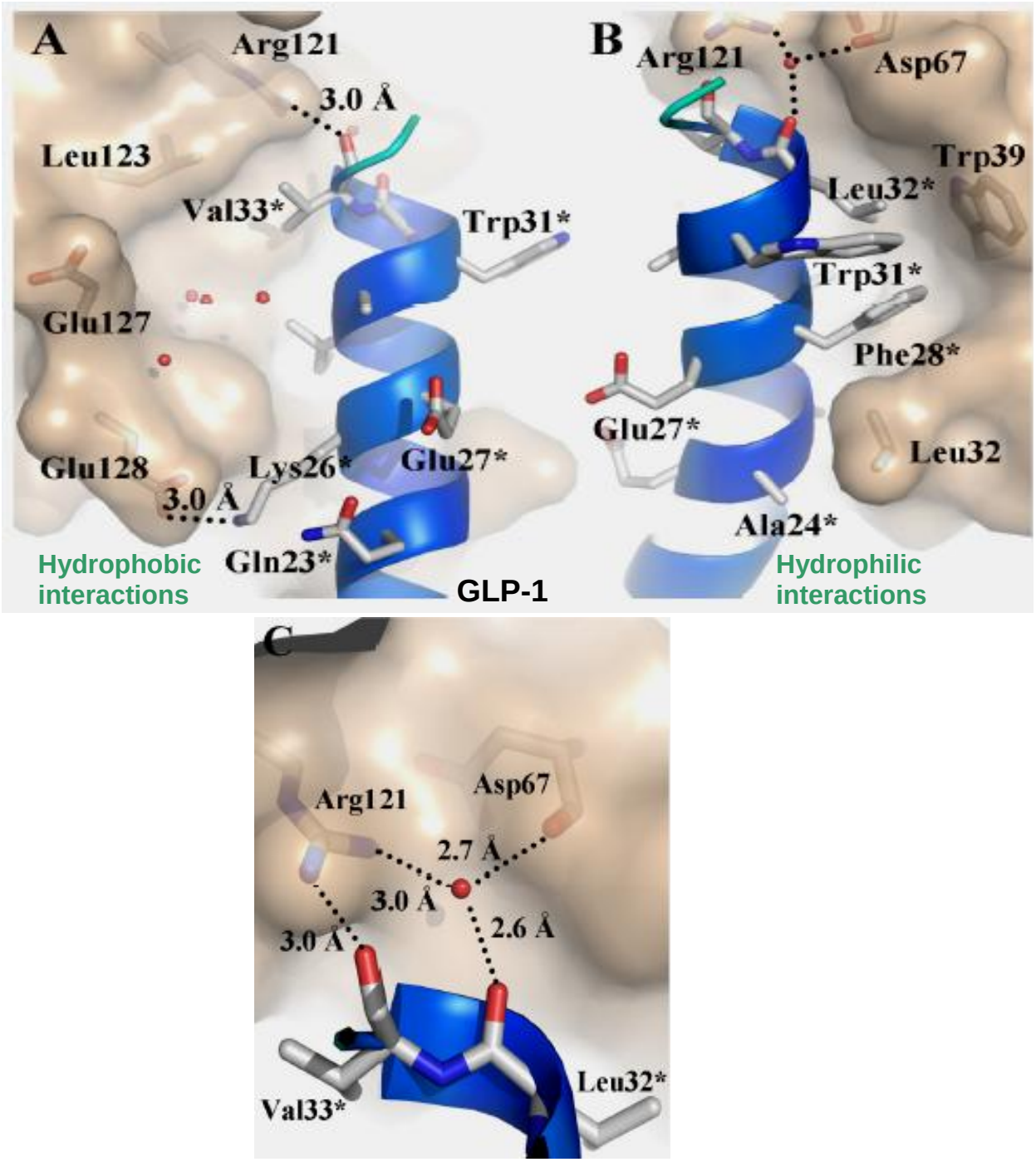

Figure 1-20: Interactions between GLP-1 and hGLP-1R-NTD.
Ribbon diagram of GLP-1 in marine with hGLP-1R-NTD, Residues of GLP-1 and NTD are illustrated as sticks. The surfaces of the binding cavities of NTD are illustrated in gray **A:** The hydrophilic interactions, GLP- residues Gln23*, Lys26*, Glu27*, Trp31* and Val33* are illustrated as sticks, and NTD receptor residues Arg121, Leu123, Glu127 and Glu128. **B:** The hydrophobic interactions, GLP-1 residues Ala24*, Glu27*, Phe28*, Trp31* and Leu32* and NTD residues Leu32, Trp39, Asp67 and Arg121. **C:** A common motif found in the hGLP-1R-NTD and in the GIPR-NTD. The side chain of Arg121 interacts with the backbone carbonyls of Asp67 and Leu32* through a water molecule (Taken from Underwood et al., 2010).

Ligand-binding analyses of the recombinant receptors expressed on the surface of β-cells or heterologous cells showed that the affinity for the binding of GLP-1 is approximately 1 nM. All of the other peptides of the glucagon superfamily bind poorly or not at all, with the exception of glucagon, which is a weak, full agonist with a binding affinity 100- to 1,000-fold lower than that of GLP-1 (Fehmann et al., 1994, Kieffer et al., 1996). EX4 is a potent agonist displaying a similar binding affinity to the GLP-1 receptor while the amino terminally truncated form EX4(9-39) is a potent antagonist of GLP-1, inhibiting GLP-1 binding and the resultant cAMP formation (Goke et al., 1993, Thorens et al., 1993).

Before publication of the crystal structure, several structure/function studies had determined which regions of the GLP-1 receptor were critical for binding specificity, signal transduction and receptor regulation/desensitization. One approach was the generation of chimeric receptors in which the substitution of as few as four residues (Thr29 to Leu32 of GLP-1R-NTD was changed to the Ala29 to Met32 of the glucagon receptor) resulting in a 50-fold decrease in selectivity of this receptor for GLP-1 over glucagon (Graziano et al., 1996). Similarly, chimeric GLP-1R/GIPR indicated that the GIPR-NTD receptor acts as a ligand-specific binding domain (Gelling et al., 1997) which is confirmed by binding the isolated, solubilized GLP-1R-NTD to GLP-1 (Wilmen et al., 1997).

Another approach for identifying binding residues has been via a number of site-directed mutagenesis analyses of GLP-1R. However, due to the large size of the NTD, targeted mutagenesis strategies of the whole region were not considered practical. The majority of these studies were carried on the rGLP-1R and Figure 1-21 highlights the mutated residues in the various regions of this

receptor. These studies have defined a picture of what regions of GLP-1R are important for binding and agonist recognition.

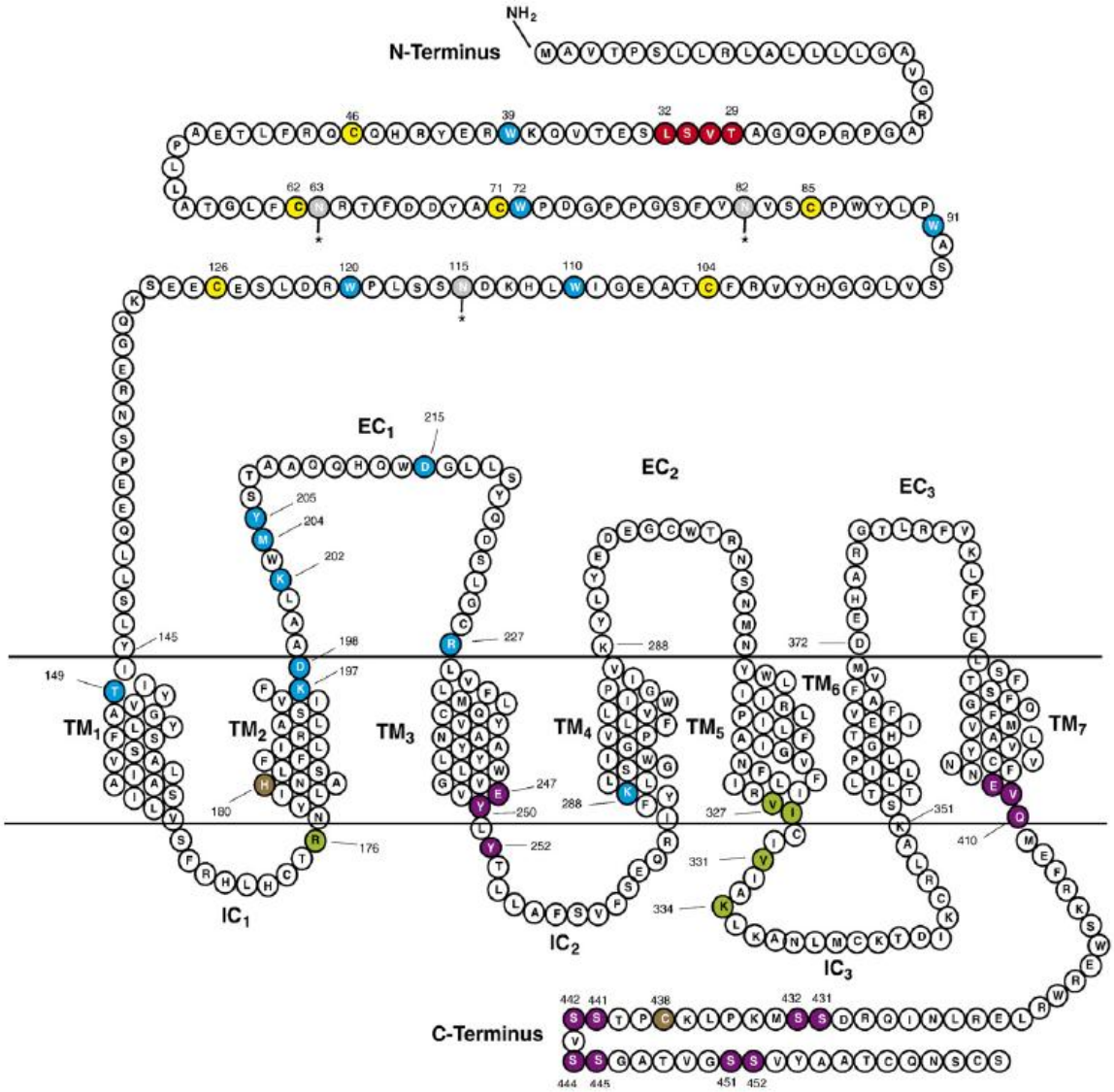

Figure 1-21: Amino acid sequence of the rGLP-1R.

The diagram is showing the predicted domains, the NTD, the 7TM helices (TM1–TM7), the 3 ECLs (ECL1, ECL2, ECL3) and the 3 intracellular loops (ICL1, ICL2, ICL3). Every group of relevant amino acids is marked by one colour as keyed and labeled in the bottom left corner of the diagram. All residues were shown with the same situation in other Family B GPCRs except red and brown ones were shown important for GLP-1 exclusively (modified from (Doyle and Egan, 2007).

Mutagenesis of single tryptophan residues at positions 39, 72, 91, 110, and 120 of rGLP-1R all prevented GLP-1 binding but this may simply be due to indirect structural effects caused by removing these large groups (Wilmen et al., 1997). Likewise, mutation of Lys38 and Arg40 has been shown to adversely affect GLP-1 binding in the GLP-1R (Wilmen et al., 1997, Van Eyll et al., 1996). Asp67 is highly conserved across Family B and investigations of this site in the glucagon, secretin and VPAC receptors have shown this residue is important (Carruthers et al., 1994, Couvineau et al., 1995, Di Paolo et al., 1999). A single nucleotide polymorphism in mice in which Asp60 changes to Gly in the growth hormone releasing hormone (GHRH) receptor causes the condition called 'little mouse' syndrome (Lin et al., 1993). NMR analysis (Grace et al., 2004) of the CRFR-NTD has shown this residue to be involved in a salt bridge with a conserved Arg/Lys residue elsewhere in the N-domain (Arg102 in GLP-1R).

Denaturation of the isolated N-terminal receptor fragment of the rat (Wilmen et al., 1996) or human (Bazarsuren et al., 2002) receptor results in complete loss of affinity for the native peptide. Deletion of portions of the rGLP-1R-NTD indicates that the negative charge at position Asp198 is not essential for affinity (Lopez de Maturana and Donnelly, 2002). In contrast, substitution with alanine at 198 results in a significant reduction in binding to GLP-1 (Xiao et al., 2000, Lopez de Maturana and Donnelly, 2002). However, N-terminally truncated EX4(9-39) and GLP-1(15-36) maintained their affinity for the receptor with the alanine mutation at 198, demonstrating that the Asp198 residue is probably important for association of rGLP-1R to the N-terminus of GLP-1 (Lopez de Maturana and Donnelly, 2002).

His180 (Heller et al., 1996) and Arg176 (Mathi et al., 1997) in ICL1/TM2 region of the rGLP-1R have been found to be of importance in cAMP production. Further charged residues concentrated at the distal TM2/ECL1 region (Lys197, Lys202, Asp215, and Arg227) have been identified as binding determinants for GLP-1 (Xiao et al., 2000). Double alanine mutation of 204Met/Tyr205 resulted in an almost 90-fold reduction in GLP-1 affinity and a complete loss of cAMP production. Further mutagenesis studies on these two residues revealed that the loss of function was due to a loss in hydrophobicity in this region (Lopez de Maturana et al., 2004).

In the TM4 of the rGLP-1R, while exchange of Lys288 with Ala or Leu greatly reduces affinity for GLP-1, substitution with Arg has very little effect, indicating that a positive charge is indispensable at this position for biological function (Al-Sabah and Donnelly, 2003). As stated above, the T149M mutation in the hGLP-1R is important in the biological activity of GLP-1 exhibiting both a reduced affinity for GLP-1 and a reduced cAMP production (Beinborn et al., 2005).

Similar to the Family A members, the ICL3 region of the Family B GPCR contains the major determinants required for specific G protein coupling. Mutation of the Lys334-Leu335-Lys336 portion in ICL3 led to significant reduction in cAMP production while still maintaining affinity for GLP-1 comparable to the WT receptor (Takhar et al., 1996). Further specific Ala point mutations of this region suggested that Lys334 was principally responsible for the attenuation in cAMP response (Takhar et al., 1996). Point mutations of residues Val327, Ile328, and Val339 in the N-terminal region of ICL3 proximal to the TM5 revealed the importance of them in cAMP stimulation (Mathi et al., 1997). Based on a comparison with a corresponding region (ICL3/TM5 junction)

in the M5 muscarinic receptor, β-cells that expressing GLP-1R that lacks either the Val331-Ala333 region of the TM5 domain or the Lys334-Leu335-Lys336 of the ICL3 domain showed an absence of GLP-1-induced increases in insulin secretion, cAMP production, and Ca^{2+} channel activation in the β-cells expressing the mutated receptor (Salapatek et al., 1999). This specified these regions as being essential for coupling to adenylyl cyclase.

1.4.3.3.3 Receptor desensitization, internalization and resensitization

The short-term and long-term attenuation or loss of cellular response to agonist over time is a common feature of signaling through GPCRs and other cell surface receptors, a phenomenon referred to as desensitization (reviewed in (Ferguson, 2001, Claing et al., 2002). Desensitization is based on an activation of a GPCR that leads to (1) activation and inhibition of specific signaling pathways in the cell, (2) short-term desensitization mediated by phosphorylation of GPCRs by G protein-coupled receptor kinases (GRKs) followed by β-arrestin binding to GPCRs that uncouple the receptor at the plasma membrane from the G-protein, and (3) endocytosis of the receptor followed by postendocytic sorting of the receptor either back (4) to the plasma membrane (receptor recycling) or (5) to lysosomes for degradation (Figure 1-22). Short-term desensitization may also involve phosphorylation of GPCRs by second messenger-dependent protein kinases, which uncouple GPCRs at the plasma membrane from G proteins. Some of the effector proteins that are activated by many GPCRs, including GRKs and second messenger-activated protein kinases, take part in feedback regulation of GPCR signaling.

Heterologous desensitization does not require agonist activation but is mediated by second messenger-dependent kinases that phosphorylate a variety of proteins, leading to generalized receptor hypo-responsiveness (Ferguson, 2001). In contrast, homologous desensitization requires agonist activation, which leads to GRK-mediated phosphorylation of the receptors (Claing et al., 2002).

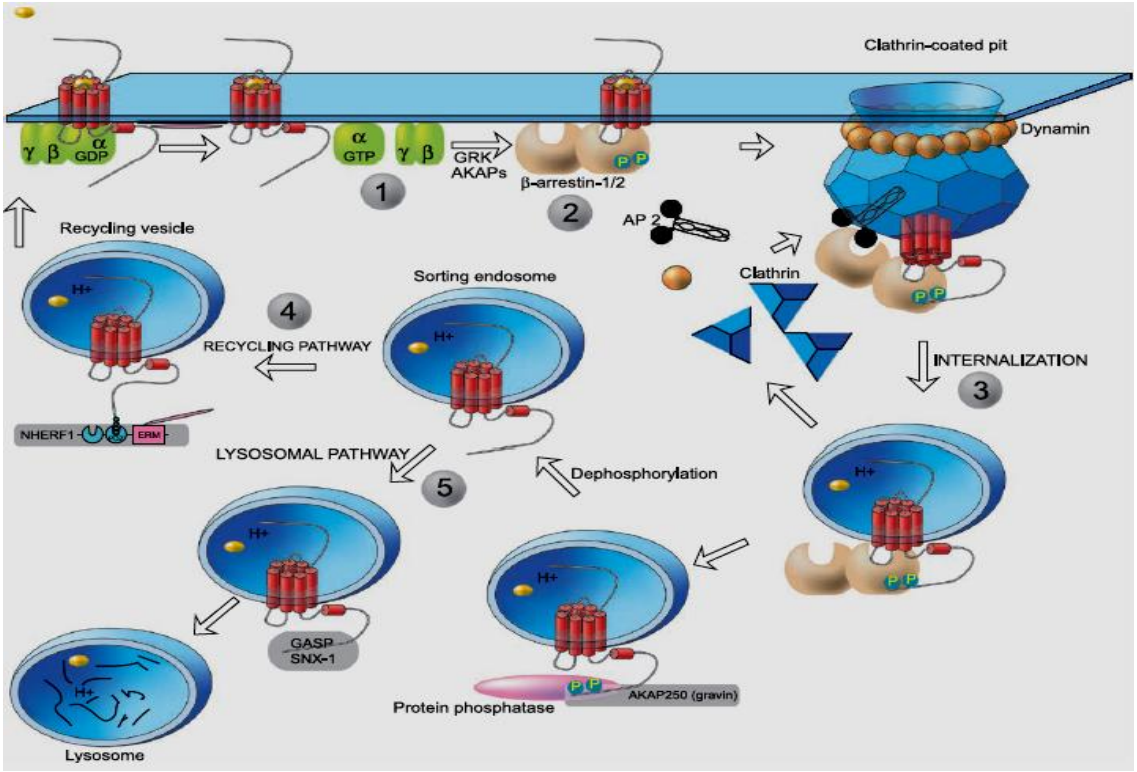

Figure 1-22: Pathways involved in desensitization and resensitization of GPCR signaling.

Activation of a GPCR leads to (1) activation and inhibition of specific signaling pathways in the cell, (2) short-term desensitization, GPCR is phosphorylated by GRKs then it binds to β-arrestin, which exhibits high affinity for agonist-occupied, phosphorylated receptors. β-Arrestin inhibits G protein coupling, thereby terminating the G protein activation. (3) endocytosis of the receptor, these interactions direct the phosphorylated receptor to punctate clathrincoated pits in the cell membrane, which are internalized by action of the GTPase dynamin or may also target the receptor to clathrin-coated pits3. Upon internalization,receptors can either be (4) recycled back to the plasma membrane or (5) degraded in lysosomes (Kristiansen, 2004).

GLP-1R internalization has a complex regulation, possibly involving both clathrin-coated pit and caveolin-dependent mechanisms. Endocytosis of GLP-1R is shown to be mediated via primarily a clathrin coated pit-dependent mechanism and, in the presence of agonist, the receptor cycles between the plasma membrane and endosomal compartments (Widmann et al., 1995). The recognition sequence for the clathrin-coated pit is located in the cytoplasmic C-terminus of the receptor and C-terminally truncated mutants showed aberrant internalization rates (Widmann et al., 1997, Vazquez et al., 2005a). Substitution of three residues (Glu408-Gln410) located proximal to TM7 with alanine led to much faster internalization (Vazquez et al., 2005a). Deletion of the last 33 amino acids in one study prevented GLP-1R internalization (Widmann et al., 1997) whereas in another study, the same deletion slowed internalization of the modified receptors by 78% (Vazquez et al., 2005a). In contrast, when the 44 C-terminal amino acids were deleted, receptor internalization was only 47% slower with the mutant versus the WT GLP-1R (Vazquez et al., 2005a). These studies indicate that the neighbouring trans-membrane domain of the carboxyl-terminal tail of the GLP-1R contains sequence elements that regulate agonist-dependent internalisation and transmembrane signalling.

Trafficking of GLP-1R to and from the cell membrane may also be caveolin-1-dependent. In one study, GLP-1 binding and activity was inhibited by over-expression of a dominant negative form of caveolin-1 (P132L-cav1). Added to that, a classical caveolin-1 binding motif has been found in the ICL2 region (247-EGVYLYTLLAFSVF-260). Consequently, Glu247Ala substitution reduced association with caveolin-1 while membranes expressing Glu247Ala and membranes expressing Tyr250/252Ala showed reduced binding affinity to GLP-1 (Syme et al., 2006).

A large GTPase, dynamin, is critical for both clathrin and caveolae mediated GPCR internalization. Expression of a dominant negative form of dynamin (Lys44Ala-dynamin) inhibited internalization of GLP-1R which was reflected by a 2.5-fold increase in the amount of GLP-1R at the cell membrane (Syme et al., 2006).

Desensitization is a common feature of GPCRs which is represented by loss of receptor sensitivity and an attenuation of signaling that occur despite the continued presence of a ligand. Desensitization has been divided into two forms: Homologous desensitization is a process whereby only the activated GPCRs are desensitized, whereas heterologous desensitization is a processe whereby the activation of one GPCR can result in the inhibition of another, heterologous GPCR to signal. Accordingly, removal of phosphorylation sites at 3 serine doublets located at positions 441/442, 444/445, and 451/452 led to a complete suppression of GLP-1R internalization. Phosphorylation of these sites also is linked with homologous desensitization of the GLP-1R expressed in cells (Widmann et al., 1996b, Widmann et al., 1996a, Widmann et al., 1997). Furthermore, heterologous desensitization occurs upon treatment with phorbol 12-myristate 13-acetate (PMA) which results in phosphorylation by protein kinase C (PKC) of four serine doublets (431/432, 441/442, 444/445, and 451/452) (Widmann et al., 1996b). An *in vitro* observations showed that EX-4 is more potent than native GLP-1 in producing GLP-1R desensitization, though chronic exposure to EX-4 in normal or transgenic mice is not associated with significant downregulation of GLP-1 receptor-dependent responses coupled to glucose homeostasis in vivo (Baggio et al., 2004).

Three N-linked glycosylation sites have been identified in the GLP-1R-NTD. The importance of glycosylation of the GLP-1R in RINm5F cells was studied using the antibiotic tunicamycin (Goke et al., 1994). Treatment resulted in reduced binding affinity and cAMP response to GLP-1 although mRNA levels of GLP-1R in treated cells did not differ, indicating that glycosylation of GLP-1R is necessary for correct insertion into the cell membrane (Goke et al., 1994). Tunicamycin inhibited glycosylation by preventing the transfer of the first N-acetylglucosamine residue to dolichol phosphate, one of the first intermediates in the synthesis of asparagine-linked glycosylation (Lehle and Schwarz, 1976). However, the significance of this effect *in vivo* has not yet been determined (Doyle and Egan, 2007).

The GLP-1R is also palmitoylated and replacing Cys438 with alanine blocked ^{3}H palmitate incorporation into GLP-1R and reduced cAMP production 3-fold but without any effect on expression of GLP-1R in the cell (Vazquez et al., 2005b). The loss GLP-1R function was partially regained by replacement of both Ser431 and Ser432 by Ala (Figure 1-21). Therefore, palmitoylation of Cys438 could regulate phosphorylation of these serine residues and could consequently regulate GLP-1R function (Vazquez et al., 2005b).

1.5 Aims and strategy

The overall aim of this study was to further understand the mechanism that underlies the binding and activation of GLP-1R by EX4, particularly its C-terminus, based on conclusions obtained from the previous work in Donnelly's laboratory.

Lopez de Maturana reported a higher affinity of EX4 over GLP-1 at the isolated rGLP-1R-NTD expressed in *E.coli* and proposed a model for the ligand-receptor interaction, suggesting two common interactions for GLP-1 and EX4, 'N' and 'H' (Figure 1-6) (Lopez de Maturana et al., 2003). Additionally, the model proposed an 'EX' interaction which was shown by Al-Sabah & Donnelly to be specific for the C-terminus of EX4 at rGLP-1R-NTD (Al-Sabah & Donnelly, 2003a). However, the specific individual amino acids responsible for the EX interaction, in either EX4 or rGLP-1R-NTD, remained to be determined and this therefore formed the basis of this PhD study.

Shortly before the start of this study (when there were no known structures for any Family B NTDs), (Kalliomaa, 2005) finished a bioinformatic study yielding computer-built models for EX4 docked in rGLP-1R-NTD. The models suggested some residues in rGLP-1R-NTD that might be involved in an interaction with the C-terminus of EX4. Therefore, the initial plan of the study started with the mutation and pharmacological analysis of 19 of the residues suggested by Kalliomaa's models. The strategy revolved around the idea that, if a residue contributed to an 'EX' interaction, it would affect EX4 binding but not that of GLP-1, since GLP-1 does not have an equivalent C-terminal sequence. However, this initial study failed to identify the 'EX' interaction but nevertheless resulted in the mapping of some residues that were important for EX4 and GLP-1 binding and activity which was consistent with the later publications of crystal

structures of the hGLP-1R-NTD bound to EX4(9-39) and GLP-1 respectively (Runge et al., 2008, Underwood et al., 2010).

The study then turned to mutagenesis of the receptor residues that were suggested by the new crystal structures to be involved in the interaction with non-identical or divergent amino acids in the helical region ('H' interaction) of EX4 and GLP-1 in order to determine whether they were responsible for the differential affinity of these peptides for GLP-1R. The strategy behind the selection of each individual residues is introduced before the relevant results in later sections.

Interestingly, Runge's crystal structure identified an interaction between Glu68 of hGLP-1R and Ser32** of EX4 (Runge et al., 2008). While this was a possible candidate for the EX interaction, the authors stated that it is a subtle interaction and would not contribute to the superior affinity of EX4. Nevertheless, this interaction was targeted in this PhD study for a more detailed analysis using truncated and full-length forms of rat and human GLP-1R, as well as full-length, truncated and modified ligands. As will be described in more detail, this phase of the study identified the EX interaction in the rGLP_1R as being derived from a hydrogen bond between Asp-68 and Ser-32**.

The final phase of the study involved the investigation of the mechanism underlying the ability of peptides to activate GLP-1R. While truncated EX4(9-30) retained no agonist properties, the equivalent GLP-1 peptide GLP-1(15-36) displayed agonism, despite both peptides having similar binding affinity. Therefore, the sequence differences between these peptides, as well as the observed structural differences, were used as a basis to explore the critical determinants of peptide efficacy.

2 - Materials and methods

2.1 Polymerase chain reaction

2.1.1 PCR primer design for plasmid constructs

The original cDNA for the rat GLP-1 receptor (NCBI accession number M97797) was a gift from Professor Bernard Thorens of the Institute of Pharmacology and Toxicology at the University of Lausanne, Switzerland and was supplied cloned as a construct in the pcDNA1 vector (Invitrogen) (Thorens, 1992). Previous members of the Donnelly laboratory sub-cloned the GLP-1R DNA sequence into the pcDNA3 vector (Invitrogen) (Lopez de Maturana and Donnelly, 2002) to create the pcDNA3-GLP-1R construct. Later, Dr Abidi added a C-terminal myc-tag (as used in Sinfield, 2005). The full-length myc-tagged receptor was used as the basis for mutagenesis studies in this thesis. Figure 2-1 shows a diagrammatic layout of plasmid pcDNA3 with myc-tagged rGLP-1R protein.

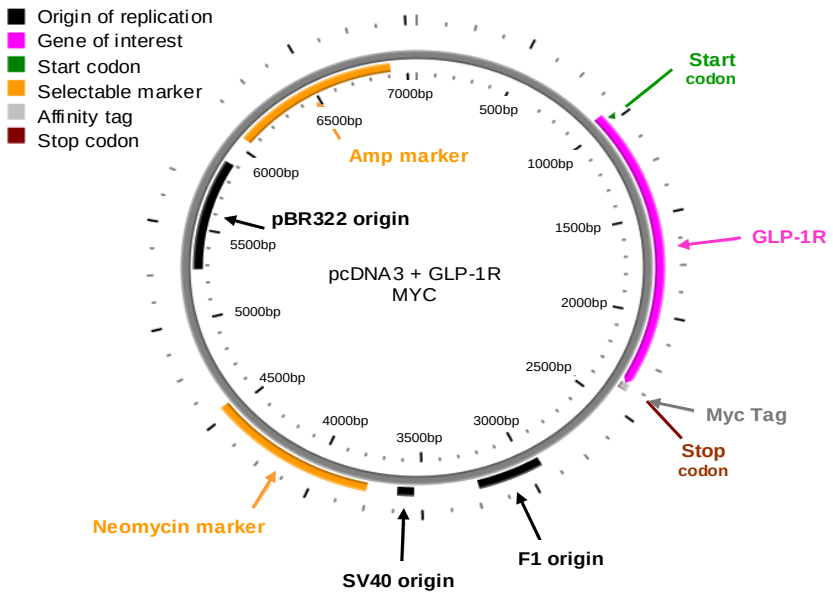

Figure 2-1: Plasmid construct of pcDNA3 with the myc-tagged rGLP-1R cDNA.

The figure displays diagrammatic representation of the plasmid construct containing the pcDNA3 vector and DNA coding sequence for the entire GLP-1 receptor including the addition of a myc tag. The important features of this construct are shown and labelled in the figure key (Sinfield, 2005).

2.1.2 QuikChange Mutagenesis

Quikchange primers were designed using the freely available software PrimerX (http://bioinformatics.org/primerx/Appendix.htm), the instructions were followed and the results page displayed a list of primers designed for introducing the mutation of choice. The primer pairs selected from the list were the shortest primers with the fewest base changes introduced (appendix 16).

DNA primers were designed to introduce the desired mutation into the DNA of interest as described previously. The rest of the procedure was carried out using the Quikchange® Site-Directed Mutagenesis kit (Stratagene catalog #200518) following the instruction manual of the manufacturer.

2.1.3 Agarose Gel Electrophoresis

Electrophoresis quality agarose 0.8 g was weighed and was made up to 100 ml (w/v), with 1X Tris-Acetate-EDTA (TAE) (appendix 7), then was heated, with swirling, until it was homogenous and all the agarose had been disolved. Once cooled, 10 μl of 1% w/v ethidium bromide was added to the solution, which was then poured into the plastic casting tray containing the comb and left to set for approximately 30min. Once set, the comb was removed revealing the wells in the gel for DNA sample loading. The casting tray was transferred to the electrophoresis cell. Sufficient 1X TAE (appendix 7) electrophoresis buffer was added to the cell to cover the gel. DNA samples, as well as a DNA marker ladder containing fragments of known quantities, were diluted with 6X gel-loading buffer to a final concentration of 1X and loaded into the wells to run in parallel. The electrophoresis cell was connected to a power supply and the gel resolved at 60 V (constant voltage) for 40 minutes. Once finished, the gel was removed from the tank and visualised by UV light with Uvidoc system. The quantity of DNA in the

sample could be roughly estimated by eye comparing the brightness of the band to be quantified with the band of the closest size in the DNA marker ladder.

2.1.4 Quantification of DNA using ultra-violet spectrophotometry

The cuvette was placed in the spectrophotometer, 980 µl dH_2O added to it and the baseline set. To this, 20 µl DNA were added producing a dilution factor of fifty. The absorbance was measured at 260 nm (A260) and 280 nm (A280) and the results were printed out. The purity of the DNA sample was assessed by dividing A260 by A280 to give a ratio where any value above 1.8 was a sample of high purity. The quantity of DNA was calculated using the formula:

A260 x Dilution Factor x 50 µg = Concentration of DNA (µg/ml)

2.1.5 Confirmation of mutations by DNA sequencing

The evaluated DNA was sequenced by dye terminator sequencing using 0.4 µg DNA and T7P primer in the Department of Biochemistry, Oxford University. The sequence received was aligned against WT rGLP-1R gene sequence (NCBI accession number M97797) using BLAST to confirm mutation.

2.2 Bacterial transformation

2.2.1 Production of agar plates for *E. coli* growth

The required volume of Luria-Bertani (LB) agar medium (appendix 1) was calculated on the basis that each 90 mm by 15 mm Petri dish needs 25 ml of LB agar medium. The bottle, with the lid loosened, was sterilised by autoclaving and allowed to cool until it could be held comfortably in a bare hand. Ampicillin 100 µg/ml was added to media, if required, and 25 ml of molten media poured into each Petri dish, their lids were slid to one-third open and left under the flame to set for 20 to 30 min. Once set the lids were replaced, the side of each Petri dish was labelled with the type of media, antibiotic and date, sealed with a strip of parafilm around the opening and the entire stack wrapped in cling film for immediate use or

stored for up to a month at 2-8°C due to the shelf life of the antibiotic they contained.

2.2.2 Making transformation quality *E. coli* of high competency

A sterile Petri dish containing solid LB agar media (appendix 1) without antibiotic was pre-warmed to 37°C for 30 min. Some frozen untransformed cells were scraped from a frozen stock. Using a metal inoculating loop, the cells were gently wiped in a zigzag motion along each side of an incomplete imaginary pentagon in the plate. The plate was incubated in a 37°C incubator overnight. The following morning a single bacterial colony was picked and placed in a sterile 250 ml flask containing 50 ml LB medium (Appendix 2) without antibiotic and incubated at 37°C/250 rpm for approximately 4 to 5 h in a heated orbital shaker. The optical density (OD) of the flask was measured every 30 to 45 min until reaching an OD_{600} of 0.25. The flask was immediately removed and placed in an ice-bath for 10 min, then centrifuged at 4000 rpm (2500 *xg*), 4°C for 10 min. The supernatant was discarded and the tube inverted on an absorbent paper towel and left inverted for 2 min. It was then placed back on the ice and the cell pellet was re-suspended in 80 ml ice-cold TFB1 buffer (appendix 13). After that, the cells were collected by spinning again at 4000 rpm (2500 *xg*) at 4°C for 5 min. The cell pellet was re-suspended in 4 ml ice-cold TFB2 buffer (Appendix 14). 500 µl aliquots were prepared in sterile microfuge tubes, frozen by snap freezing in liquid nitrogen and stored at -80˚C.

2.2.3 Transformation of competent *E. coli*

The aliquots of competent cells was removed from the -80°C freezer and placed on ice to thaw for 30 min. Once thawed the 40 µl of competent cells plus 3 µl DNA solution were pipetted into a microfuge tube and placed on ice for 30 min. After that, the incubated tube was placed in a 42°C water bath for exactly

45 s following which it was quickly returned back on ice for a further 2 min. After that, 900 µl of 2X YT media (Appendix 4) without antibiotic were added. The tube was then incubated for 1hr at 37°C with shaking followed by centrifugation at 4000 rpm (2500 *xg*) for 2 min, the supernatant discarded and the cell pellet gently re-suspended in 100 µl of a pre-warmed 2X YT media. The cell suspension was spread over the surface of the Petri dish of LB agar media containing ampicillin (appendix 1 and 3) as a selective antibiotic and incubated in a 37°C incubator overnight. Next morning, the plate was checked, wrapped in cling film and stored at 2-8°C in the fridge until the colonies were to be used, for up to a maximum of two weeks.

2.3 Mini-preparation of DNA Using *E. coli* by alkaline lysis

A single bacterial colony of the transformed cells from an agar plate was picked up and ejected into a universal tube containing LB media with ampicillin (appendix 2 and 3) then incubated in a heated orbital shaker at 37°C/250 rpm overnight. 1.5 ml of the bacterial growth was poured into a 1.5 ml microfuge tube, and centrifuged at 6000 rpm (4000 *xg*) for 2 min. The supernatant was discarded and the tube inverted for 2 min to remove any remaining supernatant. The pellet was resuspended in 200 µl of an ice-cold lysis buffer (Appendix 5) by vortexing and incubated at the room temperature for 5min. Then 400 µl of a room temperature 0.2 M NaOH and 1% SDS solution were added (appendix 6), the tubes gently inverted 5 times in the rack to mix, and then incubated for exactly 5 min at the room temperature. After that, 300 µl of an ice-cold 7.5M ammonium acetate (pH 7.8) (appendix 8) containing RNaseA (125 µg/ml) were added to the tube, inverted 5 times in the rack and incubated on ice for 10 min. Then the tube was centrifuged at 13,000 rpm (13,780 *xg*) for 15 min. After centrifugation the clear supernatant was poured into the duplicate tube containing 600 µl 100%

isopropanol, inverted twice and left at the room temperature for 10 min then was centrifuged at 13,000 rpm (13,780 *xg*) for 15 min. The supernatant was discarded, the tube inverted on a paper towel for 2 min. After that, 200 µl 70% ethanol was added to the tube without disturbing the small translucent or invisible DNA pellet. The tube was centrifuged at 13,000 rpm (13,780 *xg*) for 3 min. The supernatant was removed and the tube was incubated opened at 37°C for up to 30 min or until the odour of ethanol could not be detected. Finally, 40 µl deionised water were added and the DNA pellet dissolved by pipetting. An aliquot of the DNA solution was assessed for purity and quantity by the agarose gel electrophoresis and UV spectrophotometry and stored at -20°C.

2.4 Midi-Preps of DNA

A single bacterial colony of transformed *E. coli* XL2-Blue cells from an agar plate and ejected into the conical flask containing 50 ml LB media with ampicillin (appendix 2 and 3) and incubated overnight at 37°C/250 rpm in a heated orbital shaker. The next morning, the cell suspension was poured into a 50 ml falcon tube and spun at 4,000 rpm (2,325 *xg*) at 4°C for 30 min. The supernatant was discarded and the tubes left inverted on a paper towel for 2 min. The plasmid DNA was extracted using GenEluteTMHP plasmid mediprep kit (Sigma, NA0200) following the instruction manual of the manufacturer.

2.5 Cell culture

2.5.1 General maintenance of HEK-293 cell-lines

HEK-239 cells were grown on Nunclon treated plastics in Dulbeccos Modified Eagle's Medium (DMEM) supplemented with 10% foetal bovine serum and antibiotic to form CM-10 media (appendix 9), under conditions of 37°C, 5% CO_2 and 90-95% humidity. HEK-293 cells were grown to 70-75% confluence in a 25 cm^2 flask and passaged by discarding the growth media. Then 5 ml of

phosphate buffered saline (PBS) without Ca^{2+} or Mg^{2+} (Sigma) were used to rinse the flask and discarded. A further 5 ml of PBS without Mg^{2+} and Ca^{2+} were added and left for 5 minutes at room temperature to detach the cells. Once all the cells were detached, as indicated by giving the flask a gentle tip, 5 ml of CM-10 was added and the homogenous mixture was transferred to a universal tube and centrifuged at 2000 rpm (617 *xg*) for 2 min. The supernatant was discarded, the cells re-suspended in 5 ml of fresh CM-10, and a proportion of cell suspension transferred to a 25 cm^2 flask containing fresh CM-10 media to a final volume of 10 ml. The flask was placed in the incubator and left to grow. The health and growth of the cells were monitored daily under the microscope.

2.5.2 Freezing and storage of HEK-293 cell-line in liquid nitrogen

The HEK-293 cells to be frozen were passaged from a 70-75% confluent flask and then transferred into a universal tube and centifuged at 2000 rpm (617 *xg*) for 2 min. The supernatant was discarded and the pellet was re-suspended in 1 ml cryo-preservation media (appendix 10). The cryovial was placed in an isopropanol box at room temperature, which should ensure when sealed the contents freeze at a rate of 1°C per minute when placed in a -80°C freezer overnight. The next day the cryovials were transferred into a cryovial storage box in a rack in the liquid nitrogen vessel stored in the gase phase of a liquid nitrogen store.

2.5.3 Reviving frozen HEK-293 cell-lines

The desired vial was removed from the liquid nitrogen and placed in a container of water at 37°C to thaw. The contents of the vial were removed to a 25 cm^2 flask containing 9 ml of prewarmed CM-10 media (appendix 9). The flask was incubated for three hours when the healthy cells should have adhered to the plastic and the media should be changed to remove the residual toxic DMSO

carried over from the freezing media. The media was changed the next day and the cells were allowed to grow normally as described above.

2.5.4 Stable transfection of the HEK-293 cell-line

Untransfected HEK-293 cells with a low a passage number were grown to 40-60% confluency. The pcDNA3 vector construct (5 µg) containing full-length rGLP-1R_{myc} DNA were diluted into a total volume of 150 µl with prewarmed DMEM plus 20 µl of SuperFect® transfection reagent (Qiagen, catalogue number 301305) were used following the instruction manual of the manufacturer. The selective antibiotic Geneticin® (G418) was added to the growing CM-10 medium to a final concentration of 800 µg/ml. Every three days the media was changed. Under these selective conditions, the untransfected cells should have died and only cells successfully transfected with the Geneticin® (G418) resistance gene should have grown normally. A third of the cells from the 70-75% confluent flask were passaged into a 2 ml cryovial and frozen, as described above, as the master vial of this transfection. The cells were maintained normally without selective antibiotic.

2.5.5 Production of crude membrane preparations

Two 175 cm^2 flasks were seeded with the HEK-293 cell line expressing the desired receptor and grown to 70-75% confluence. Once ready, five 140 cm^2 Petri dishes were placed in the tissue culture hood and coated with a sterile 0.0125% solution (0.125 mg/ml) of poly-D-lysine (>300,000 MW) and left to dry without lids for 10 min. Once dried, 5 ml of cold PBS containing Mg^{2+} and Ca^{2+} were added to each dish, washed and discarded to remove excess poly-D-lysine. The dishes were covered and 35 ml of pre-warmed CM-10 growth media (appendix 9) was added to each dish. The cells were detached from the plastics as described above and the resulting cell pellet was resuspended in 20 ml of

growth media and 4 ml added to each dish. The dishes were grown for three days until they were confluent then the growth media was aspirated and discarded. For each dish, 5 ml of ice cold sterile MilliQ water were added and left for 5 min then aspirated and discarded, and 5 ml of an ice cold PBS were added, agitated gently then discarded. After that, the remains of the cells were scraped from the dishes using a sterile disposable cell scraper and transferred to a labelled 1.5 ml microfuge tube which was immediately placed on ice followed by centrifugation at 13,000 rpm (13,780 *xg*) for 30 min in a microfuge at room temperature. The supernatant was discarded and the tubes tapped on tissue paper to remove any remaining supernatant. The pellet from each dish was resuspended in 200 µl HEPES binding buffer (HBB) (appendix 11) and passed through a microneedle using a 1 ml syringe ten times and combined into one microfuge tube, from which the crude cell membrane solution was aliquoted in 100 µl volumes and stored in a -80°C freezer.

2.6 Competitive radiolabelled binding assay

2.6.1 Peptides

EX4, EX4(9–39) and GLP-1 were from Bachem (Saffron Walden,U.K.). All other truncated peptide ligandswere custom synthesised by Genosphere Biotechnologies (Paris, France). ^{125}I-EX-4(9–39), labelled via Bolton–Hunter reagent at Lys-12, was purchased from NEN-Perkin-Elmer (Boston, MA, U.S.A.). ^{125}I-GLP-1(7-36), labelled via lactoperoxidase metod and was a gift from Novo Nordisk A/S (Novo Allé, Denmark). All the peptide sequence used in this study are aligned in appendix 16. An alignment of each group of peptides will be mentioned when needed prior to the relevant chapter.

2.6.2 Ligand binding assay for crude membrane preparations

Each ligand to be investigated for binding affinity was tested in a binding competition assay consisting of 8 concentration data points, in triplicate, to enable a binding curve to be plotted. The standard ligand concentrations were tested over a log scale consisting of 1 μM, 100 nM, 10 nM, 1 nM, 100 pM, 10 pM, 1 pM and vehicle (HBB) only. The amount of non-specific binding of the iodinated ligand was determined as the amount of binding still present when the highest concentration of the competing ligand (1 μM) was used. 100 ml 1 % milk powder in 1X PBS solution was made and stirred at room temperature for 30 min, then filtered. Bacitracin was added to HBB (appendix 11) to give a final concentration of 50 μg/ml and stored on ice. The calculated amount of HBB was pipetted to a universal tube for the addition of the radioligand and kept on ice. The unlabelled ligand to be tested for binding affinity was made to the required concentrations in HBB on ice. Each 100 μl aliquot of membrane preparation was passed through a needle, using a 1 ml syringe, 10 times to give a homogenous mixture, which was then diluted in HBB to the desired protein concentration. In a 96-well polypropylene plate, ^{125}I-GLP-1 was diluted to 200 pM as calculated according to the decay factor of that day and 50 μl added to each well. A 50 μl aliquot of each unlabelled ligand to be tested was pipetted into each well, except for the total count wells where it was substituted with HBB. Universal tubes containing the membrane suspension were mixed by shaking and 100 μl was added to each well. The resulting reaction mixture in each binding well had a volume of 200 μl and a final ^{125}I-labelled ligand concentration of 50 pM. The plate was incubated for 1 hr at room temperature. From prepared ^{125}I-GLP-1, five tubes containing 50 μl were placed in a counting tray and counted in the gamma counter for 1min to check the ^{125}I-GLP-1 was close to the correct 59,532 counts per minute (predicted from

50pM radio-ligand). Meanwhile, 200 ul of milk solution was added to each well of the Multiscreen® HTS filtered plate fitted firmly on a Millipore vacuum pump and passed through its filter. The contents of each well of the polypropylene plate was transferred to its corresponding position in the filter plate and filtered. After that the filter plate was washed 3 times with washing buffer (appendix 12) to remove any unbound ^{125}I-GLP-1 from the filter leaving only the non-specifically bound ^{125}I-GLP-1. The filter bottom of each well was punched out to a counting tube. The tubes containing filters were transferred in order to the counting trays of the gamma counter and counted in sequence for 1 min and the data print out collected. The data in counts per minute (CPM) obtained from the gamma counter was analyzed using GraphPad prism 5.0 software (San Diego, CA, U.S.A.).

2.7 The LANCE™ cAMP accumulation assay

The LANCE™ cAMP accumulation assay (Perkin Elmer) is a homogenous time-resolved fluorescence resonance energy transfer (TR-FRET) immunoassay designed to measure cAMP produced upon modulation of adenyl cyclase activity by GPCRs. LANCE™ is based on the competition between a europium-labeled cAMP tracer complex and sample cAMP for binding sites on cAMP-specific antibodies labeled with the dye Alexa Fluor® 647. The europium-labeled cAMP tracer complex is formed by the interaction between Biotin-cAMP (bcAMP) and streptavidin labeled with Europium-W8044 chelate (Eu-SA). When the labelled antibodies are bound to the Eu-SA/b-cAMP tracer, a light pulse at 340 nm excites the Eu-chelate molecules of the tracer. The energy emitted by the Eu-chelate is transferred to an Alexa molecule on the antibodies, which in turn emits light at 665 nm. The fluorescence intensity measured at 665 nm will decrease in the presence

of cAMP from test samples and resulting signals will be inversely proportional to the cAMP concentration of a sample (Figure2-2)

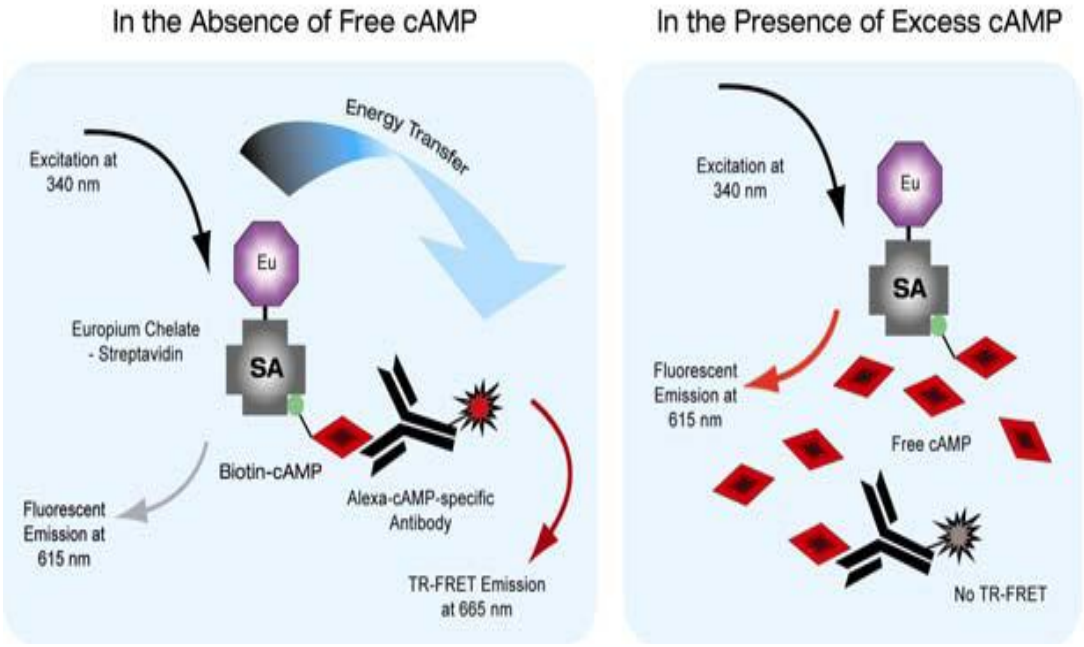

Figure 2-2 LANCE cAMP Assay Principle (taken from Perkin Elmer user's guide of LANCE™ cAMP 384 Kit).

Cell based protocol of the assay was carried out using cells expressing the receptor of interest, which were harvested and washed with stimulation buffer (Appendix 15). The cells were re-suspended in stimulation buffer at the optimised concentration. Cell numbers and 3-isobutyl-1-methylxanthine (IBMX) concentration were set based upon optimization experiments in order that raw fluorescence data fell within the linear range determined by a standard cAMP concentration curve. IBMX is competitive non-selective phosphodiesterase (PDE) inhibitor which protects the produced cAMP from breakdown by PDE. IBMX and the Alexa Fluor® 647 labelled antibodies were added to the cell suspension at a final concentration of 500 µM and 0.005 % (v/v) respectively. The standard ligand was tested at concentrations over a log scale consisting of 1 µM, 100 nM, 10 nM, 1 nM, 100 pM, 10 pM, 1 pM and vehicle (stimulation buffer) only. Triplicates of 6 µl/well of each

ligand concentration were transferred to a white 384-well low volume OptiPlate (Greiner). 6 µl of the prepared cell suspension were added to each well and the contents of the plate were mixed by gentle tip then sealed and left for stimulation for 30 min at room temperature. Meanwhile, the detection mix was prepared in a separate tube by diluting the Eu-W8044 labelled streptavidin 2250-fold in Detection buffer supplied in the kit. The Biotin-cAMP was then added to give it 750-fold dilution. This mixture was incubated for at least 15min at room temperature to allow streptavidin-biotin complex formation to occur. Once the stimulation time was finished, 12 µl of Detection mix was added to each well and incubated at room temperature for 1 hr. The acceptor fluorescence signal was then read at 665 nm using Victor^{TM} X4 2030 Multilabel Reader (Perkin Elmer). The signal is inversely proportional to the ammount of cAMP synthesized by the tested concentration of the agonist. The data output was analysed and graphed using GraphPad PRISM 5.0 software (San Diego, CA, U.S.A.)

2.8 Statistical analysis

The recorded data were analyzed and graphed into curves and tables. Dose-response curves and competition binding curves were fitted using Prism (GraphPad Software Inc., San Diego, CA, U.S.A.). The curves represent one of at least three independent experiments for which each point is the mean of triplicate values, with SEM displayed as error bars. Counts and LANCE^{TM} signals were normalised to the maximal specific binding, or maximal response, within each dataset unless otherwise stated. pIC_{50} and pEC_{50} values were derived from curve fitting using non-linear regression analysis. In tables, pIC_{50} and pEC_{50} values represent the mean ± SEM of three or more independent experiments performed in triplicates.The pEC_{50} or pIC_{50} values are compared to corresponding

values for the control receptor or ligand using the unpaired t-test. Significance was considered when $P < 0.05$ and marked by (*), whereas high significance was considered when $P < 0.01$. Fold difference is shown as (d) and calculated from the averaged pIC_{50} and pEC_{50} values for the control WT receptor or ligand and the tested mutant or ligand.

3 - Determining of 'EX' interaction using protein model-based mutants

3.1 Introduction

Using a series of full-length and truncated analogues of both GLP-1 and EX4 (as well as either mutated or truncated rGLP-1R), a receptor-peptide interaction model has been proposed (Lopez de Maturana et al., 2003). Two common interactions were proposed for both EX4 and GLP-1R-NTD: 'N' describing interaction between the N-terminus of the peptide and the rGLP-1R core domain; and 'H' describing the interaction between the central helical region of the peptide and rGLP-1R-NTD. A third interaction was also proposed: 'EX' describes the interaction unique to EX4 and its N-terminally truncated analogues, which is responsible for its N-independent affinity. Al-Sabah and Donnelly, (2003a) later proposed that the 'EX' interaction is formed between the rGLP-1R-NTD and the C-terminal region of EX4 and speculated that this may be via the 'Trp cage' formed by this region of EX4. However, the residues in rGLP-1R-NTD involved in the 'EX' interaction have not been determined and therefore the aim of this work was to identify the source of the 'EX' interaction.

Having a long sequence (153 amino acids), it would be too time consuming to scan the entire rGLP-1R- NTD residue by residue via mutagenesis. Therefore, a method to target potential sites of the 'EX' interaction had to be found. At this stage of the project there were no available crystal structure for any Family B GPCR; however, the availability of NMR structures for CRFR2β-NTD (Grace et al., 2004), a Family B GPCR member, facilitated a protein structure modelling strategy.

Kalliomaa (2005) carried out computer modelling for EX4 interacting with rGLP-1-NTD and assigned the residues of the receptor that could interact with C terminus of EX4, the potential source of the 'EX' interaction. Kallioma's work was accomplished through four main stages: building homology models for rGLP-1R-NTD, finding a representative structure for EX4, prediction of the binding site and finally docking of EX4 and rGLP-1R-NTD.

3.1.1 Homology modelling

Homology modelling is based on the idea that most sequences sharing at least 25% identity over an alignment of at least 80 residues also share the same basic structure (Westhead et al., 2002). Accordingly, one or more known protein structures can be used as templates to build a model for a chosen target protein as well as the prediction accuracy increases with the target-template identity (Eswar et al., 2003). Homology modelling is usually acompolished through four main steps: fold assignment, alignment of sequences, modelling and model evaluation (Eswar et al., 2003).

Kalliomaa, (2005) carried out the first step by assignment of the NMR structure of CRFR2β-NTD (Grace et al., 2004), which is known to be a potential template for modelling. Kallioma, (2005) searched sequence similarity against protein data bank (PDB) database by using Basic Local Alignment Search Tool (BLAST) program (Altschul et al., 1997) to confirm that there is no any other potential template structures exist. Furthermore, only residues 39 to 120 of CRFR2β-NTD structre were accepted because residues before this range was a cloning artefact and last 13 residues showed a very disordered structure (Kalliomaa, 2005).

In the second step, the sequences of CRFR2β-NTD (39-120) and GLP-1R (40-128) were aligned with ClustalW (Thompson et al., 1994) and manually checked. The results revealed fairly low identity (26%). Improvement of the alignment was very difficult because it could lead to losing the alignment of important structures like the six conserved cysteins (Kalliomaa, 2005). JPRED (Cuff et al., 1998) was used for secondary structure prediction of rGLP-1R-NTD so that the alignment of secondary structure elements could also be checked because the NMR structure of CRFR2β-NTD (Grace et al., 2004) contained 20 models with well-defined core and variable loop regions (Figure 3-1B). Additionally, the results demonstrated that the best representative models of CRFR2β-NTD were 13 and 18; However, further clustering results divided one of the two models to give final three models 13, 15 and 18 (heads of table in Figure 3-3) (Kalliomaa, 2005). Kalliomaa (2005) investigated the selected models with RasMol viewer (Sayle and Milner-White, 1995) and showed a great difference on the second variable loop. This loop turns over 180 degrees with models 18 and 15 being the most divergent and model 13 in between. This structure difference could affect potential binding sites within this region. Accordingly, the author decided to use the three models separately in the further modelling work.

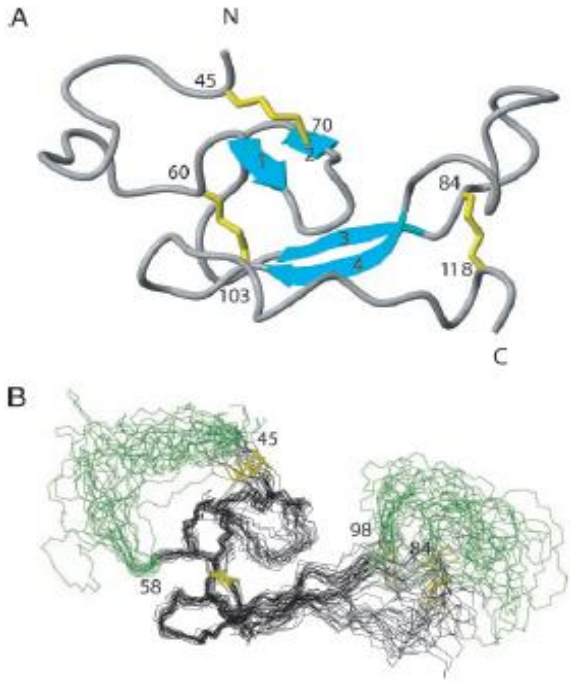

Figure 3-1: The 3D structure of CRFR2β-NTD.

A: A ribbon diagram of the CRFR2β-NTD highlighting the β-sheets in blue and the disulphide bonds in yellow. **B:** Superposition of 20 conformers representing the 3D NMR structure. Only amino acid residues 44–119 are shown (as a black core). The bundle is obtained by superimposing the backbone Cα carbons of residues 58–83 and 99–113. Green colour represents disordered loops (residues 39-58 and 84-98) (Grace et al., 2004).

The output results were utilized for crossing to the third step, building the structure model of rGLP-1R-NT using MODELLER program (Sali and Blundell, 1993). MODELLER builds models from protein sequence by using spatial restraints like restraints on distances and dihedral angles based on the structural alignment of the target (rGLP-1R-NTD) and template (CRFR2β-NTD) as well as stereochemical restraints and statistical preferences for non-bonded interatomic distances and dihedral angles derived from known protein structures (Eswar et al., 2003). MODELLER produced, in each run, ten 3D models of rGLP-1R-NTD for each of the three structures. These were named as 13A_X, 15A_X, and 18A_X where A represents the first round of model building, while X identifies which of the 10 models produced by MODELLER is being represented. MODELLER specifies

each model with molecular probability density function (pdf), which is inversely proportional to the quality of the model. Hence, the models could be ranked based on their pdf.

The large number of models for rGLP-1R-NTD released by MODELLER raised the need for the final step, evaluation of the models. Kalliomaa, (2005) used PROCHECK program (Laskowski et al., 1993) to select the highest quality model based on the stereochemical quality of the protein structure. PROCHECK produces a summary report of Ramachandran plot statistics that define phi-psi torsion angles for all residues in the target structure. The high quality model were selected for each of the three representative structures (13A_6, 15A_4, and 18A_1)

Kalliomaa, (2005) then used the chosen model in a second homology procedure as the template structure plus the CRFR2β-NTD structure to see if it would improve the model quality. The output models were called B (13B_X, 15B_X, and 18B_X) and were evaluated in the same way as the A models. Finally, six high quality submodels for each of the three main structures, three from A models and three from B models were subjected to further refinement by energy minimisation.

Energy minimisation optimises structures into the lowest energy conformation (Sali and Blundell, 1993). Energy minimisation improves the initial structure without change via the adjustment the bond lengths and angles to values near their local minimum (McCammon and Harvey, 1987). Energy minimisation was carried out with TINKER (Ponder and Richard, 1987) and AMBER7 (Pearlman et al., 1995). The best energy minimised model for each three structures were selected to represent GLP-1R. The final three homology models were named GLP-1R_13, GLP-1R_15 and GLP-1R_18

3.1.2 EX4 structure

Kalliomaa, (2005) used an NMR EX4 exprimental structure (Pdb id:JRJ) that has 36 models. The structures showed well defined helical structure with much variability between models in the N-terminus. However, the disordered N-terminus is not important in the modelling of docking because N-terminus of EX4, based on previous laboratory studies (Al-Sabah and Donnelly, 2003a), does not bind to rGLP-1R. EX4 models were aligned and clustered by using OLDERADO (Kelley and Sutcliffe, 1997). OLDERADO is an internet server combining two programs: NMRCORE for maping core residues and NMRCLUST for structural alignments of the core domains and clustering of the aligned structures. By uploading the ensemble of structures to that server, the output describes conformationally related subfamilies and the most representative structure for each family. The most representative structure of EX4 was revealed as model 21 (Kalliomaa, 2005).

3.1.3 Prediction of the Binding site

Kalliomaa, (2005) used protein-protein interface prediction program (PPI-PRED) (Bradford and Westhead, 2005) to detect the potential binding interface patches. Given a Pdb file, PPI-PRED analyses protein surfaces patches based on hydrophobicity, electrostatic potential conservation, shape and solvent accessibility. The program was guided by multiple sequence alignment (MSA) of CRFR family and glucagon family GPCRs then between the members of each subfamily using the sequence retrival system (SRS, http://srs.ebi.ac.uk) along with identification of the conserved residues using ClustalW (Thompson et al., 1994). The available binding data was also used as an assessment of the computational work. The results defined two patches of rGLP-1R-NTD binding sites: one was defined around 27-33 residues and another patch was predicted in the core

structure and extends to the beginning of the 2nd loop (residues 46-65). The two patches of residues were used in the docking procedure to select only complexes which had these regions in the binding interface. After that, NACCESS (Hubbard and Thornton, 1993) was used to analyse the pdb file to ientify core and solvent accessible residues. In the same way, the conserved residues of EX4 were predicted by alignment with other peptides interacting with the other member of Family B GPCRs (Kalliomaa, 2005).

3.1.4 Docking EX4 and rGLP-1R

In this step, Kalliomaa, (2005) applied what is known as protein-protein docking modelling. Protein-protein dockingis a two-stage process: first a set of 3D complexes is created and second they are scored to identify the most favourable conformations. Although protein conformational changes upon binding are well known, identification of of specific binding sites should be carried out before performing that computionally (Chen et al, 2003). Alternatively, Kalliomaa, (2005) used rigid body docking via Fast Fourier Transfer (FFT) methods (Russel et al., 2004) by using ZDOCK program (Chen et al, 2003). FFT keeps the protein structures unchanged and search for shape and chemical complementry between structures to rank the created protein-protein complexes. In Kalliomaa's work, ZDOCK returned 2000 top scoring complexes of EX4 (NMR model 21) and rGLP-1R-NTD (homology models 13, 15 and 18). However, this large number was reduced to less than 100 by introducing residues restraints from the previously predicted patches (27-33, 46-65) together with the peptide interface residues. After that, the complexes were cheked to confirm that the peptide binding interface was correct and the EX4 Trp-cage (C-terminus) could make some contacts with rGLP-1R-NTD particularly with chemical shift residues and conserved residues based on the previously reported results about the evident contact between Trp-cage of EX4

and rGLP-1R-NTD(Al-Sabah and Donnelly, 2003a). Kalliomaa's work is summarised in Figure 3-2.

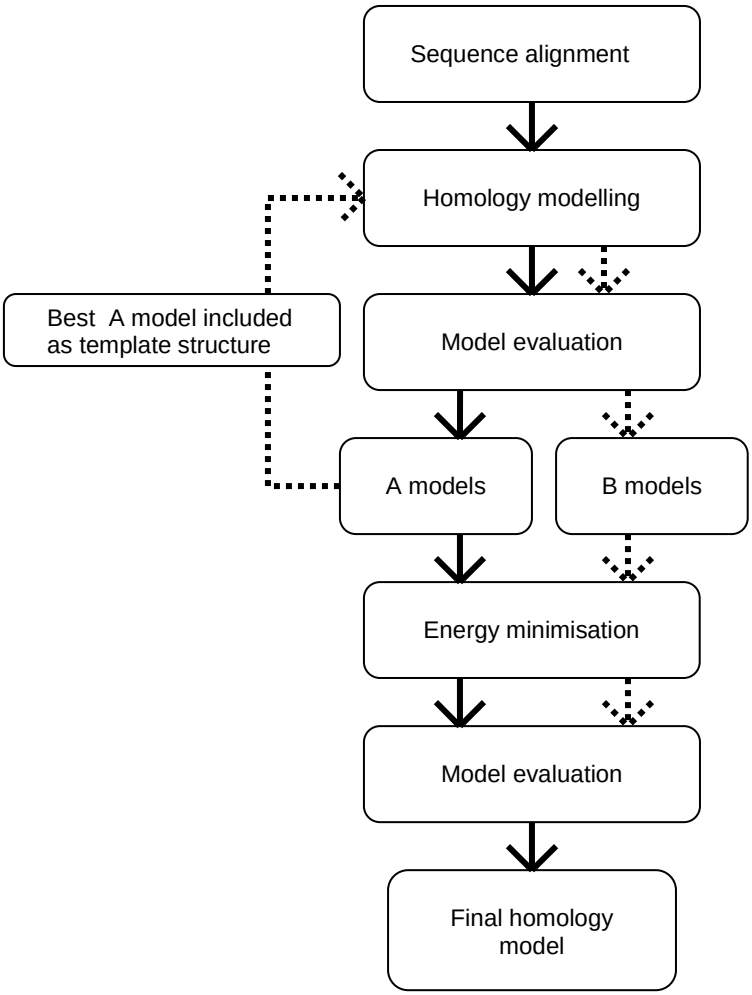

Figure 3-2 : An outline of Kalliomaa, (2005) computer based study

The steps are in descending order with crossing from one to another by downward arrow. Dotted arrows are for building the B models (taken from Kalliomaa, 2005).

3.2 Strategy

Each model suggested different residues involved in the binding of the C-terminus of EX4. A number of those models were expected to be accurate enough to determine the amino residues of rGLP-1R that would contribute to the 'EX' interaction. Consequently, site directed mutagenesis was used to modify the target residues as well as ligand binding assay was used to assess which model was correct.

Based upon this study, 19 amino acids of the GLP-1R-NTD, suggested contributing to the 'EX' interaction by Kalliomaa's models, were targeted as potential 'EX' interaction sites. Since conserved residues across species have been considered important for receptor-ligand interactions, the selected residues were checked by sequence alignment to ensure they were conserved between rat, human and mouse types of receptors. If any of the selected 19 residues was involved in the 'EX' interaction, mutation of it would be expected to affect EX4 binding but would not be expected to affect GLP-1 binding as GLP-1 does not have residues equivalent to EX4(31-39).

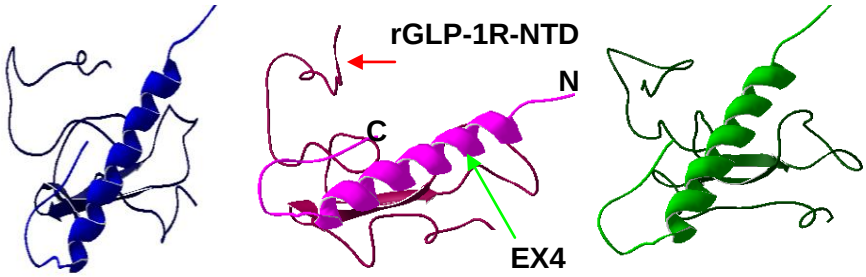

GLP-1R residues involved in peptide binding.
Residues in close proximity with EX-4 Trp-cage are highlighted in red.

ResNo	18_1	18_14	18_21	13_5	13_11	13_14	15_5	15_8	15_14	15_33	SP no
1	R	R	R	R	R	R	R	R	R	R	40
2	E	E	E	E	E	E	E	E	E	E	41
3	Y	Y	Y	Y	Y	Y	Y	Y	Y	Y	42
4	R	R	R	R	R	R	R	R	R	R	43
5	H	H	H	H	H	H	H	H	H	H	44
6	Q	Q	Q	Q	Q	Q	Q	Q	Q	Q	45
7	C	C	C	C	C	C	C	C	C	C	46
8	Q	Q	Q	Q	Q	Q	Q	Q	Q	Q	47
9	R	R	R	R	R	R	R	R	R	R	48
10	F	F	F	F	F	F	F	F	F	F	49
11	L	L	L	L	L	L	L	L	L	L	50
12	T	T	T	T	T	T	T	T	T	T	51
13	E	E	E	E	E	E	E	E	E	E	52
14	A	A	A	A	A	A	A	A	A	A	53
15	P	P	P	P	P	P	P	P	P	P	54
16	L	L	L	L	L	L	L	L	L	L	55
17	L	L	L	L	L	L	L	L	L	L	56
18	A	A	A	A	A	A	A	A	A	A	57
19	T	T	T	T	T	T	T	T	T	T	58
20	G	G	G	G	G	G	G	G	G	G	59
21	L	L	L	L	L	L	L	L	L	L	60
22	F	F	F	F	F	F	F	F	F	F	61
23	C	C	C	C	C	C	C	C	C	C	62
24	N	N	N	N	N	N	N	N	N	N	63
25	R	R	R	R	R	R	R	R	R	R	64
26	T	T	T	T	T	T	T	T	T	T	65
27	F	F	F	F	F	F	F	F	F	F	66
28	D	D	D	D	D	D	D	D	D	D	67
29	D	D	D	D	D	D	D	D	D	D	68
30	Y	Y	Y	Y	Y	Y	Y	Y	Y	Y	69
31	A	A	A	A	A	A	A	A	A	A	70
32	C	C	C	C	C	C	C	C	C	C	71
33	W	W	W	W	W	W	W	W	W	W	72
34	P	P	P	P	P	P	P	P	P	P	73
35	D	D	D	D	D	D	D	D	D	D	74
36	G	G	G	G	G	G	G	G	G	G	75
37	P	P	P	P	P	P	P	P	P	P	76
38	P	P	P	P	P	P	P	P	P	P	77
39	G	G	G	G	G	G	G	G	G	G	78
40	S	S	S	S	S	S	S	S	S	S	79
41	F	F	F	F	F	F	F	F	F	F	80
42	V	V	V	V	V	V	V	V	V	V	81
43	N	N	N	N	N	N	N	N	N	N	82
44	V	V	V	V	V	V	V	V	V	V	83
45	S	S	S	S	S	S	S	S	S	S	84

Figure 3-3: Residue-residue interactions based Kalliomaa's models of EX4 docked in rGLP-1R-NTD.

The three NTD models are shown on the top with different colors (blue=18_x, pink=13_x, green=15_x). EX4 is drawn as coiled ribbon with long curved thick tube at its C-terminus end and another short one representing its N-terminus. The matched colour in the table shows the receptor's residues involved in the peptide binding. The red colour is for residues suggested to be contributing to trp-cage receptor interaction in each complex. Numbers on the right side identify residues in the rGLP-1R sequence (Kalliomaa, 2005).

3.3 Methodological considerations

3.3.1 Preparation of mutant receptor

Two pairs of primers were designed for each desired mutation and used to generate site-directed mutations of rGLP-1R (see methods section 2.1). All the rGLP-1R mutants were expressed with a Myc tag to facilitate the detection of the receptor, by either immuno-histochemistry or western blotting, in case of undetectable binding affinity and/or activity.

Each mutant DNA product was sent for sequencing to confirm the mutation of the residue of interest. The generated sequences for mutated constructs were aligned with the GenBank accession M97797 using the Blast 2 alignment program (Tatusova and Madden, 1999) (http://www.ncbi.nlm.nih.gov/blast/bl2seq/bl2.html). All sequences were correct and were in the proper open reading frame. Once the DNA constructs were confirmed, they were amplified and purified by midiprep from transformed bacteria producing optimum DNA quality and concentration for transfection.

3.3.2 Creation of stable cell lines

Flasks (25 cm^2) of HEK-293 cells were seeded as required and were transfected individually using each mutant DNA. The successfully transfected cells were selected by growing cells on media containing antibiotic Geneticin® (G418) to produce a mixed population of stable cell lines from the surviving cells. Although it took a long time to select stable cells by this method compared to transient transfection, the stable cell lines saved time in the long run by providing an easy and consistent source on request of both live cells and/or their membrane preparation for each planned experiment, as well as a liquid nitrogen frozen stock of those cells.

3.3.3 Competitive heterologous radioligand binding assay

The stable cells were used to generate crude membrane preparations required for competitive binding analysis using radio-labelled $^{125}I^-$ GLP-1 (Chapter 2.6). In the beginning, three dilutions of original stock of each membrane fraction were prepared. Then each dilution was subjected to a total and non-specific competitive binding assay using radio-labelled $^{125}I^-$GLP-1 against unlabelled EX4. The result of this screening provided a quick idea about binding and non-binding mutants in general and about the most suitable membrane protein concentration dilution of each binding mutant that would be used to generate a full competitive binding curve. The mutated receptors showing binding activities were subjected to a full curve competition binding assay using a fixed concentration of ^{125}I-GLP-1 (50 pM) against various different log concentrations of EX4 (1μM, 100nM, 10nM, 1nM, 100pM, 10pM, 1pM) .

3.3.4 LANCE™ cAMP assay

The assay protocol was carried out as described in Chapter 2 but with the number of cells being 4000/well, and using higher concentrations of agonists (up to 100 μM), GLP-1 and EX4. The same conditions were applied to mutated and non-mutated rGLP-1R.

3.4 Results

3.4.1 Preparation of mutant receptors

Figure 3-4 shows an annotated section of the sequences of the pcDNA3 constructs that were used to confirm correctly made mutants.

Figure 3-4: Sections of the nucleotide sequence of rGLP-1R$_{myc}$ single alanine mutated receptors. Mutated codons are squared by pink squares.

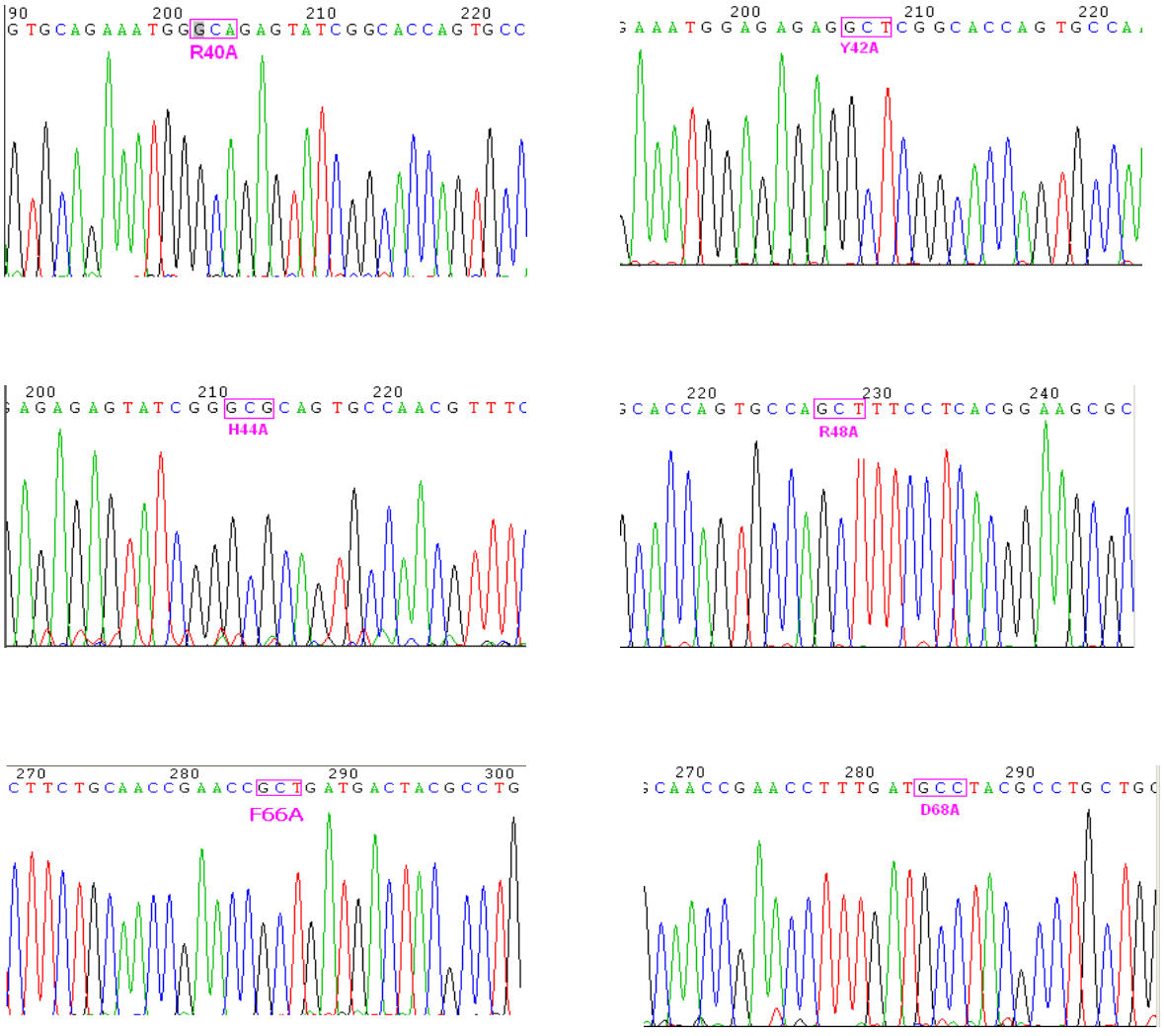

Figure 3-4 continued...

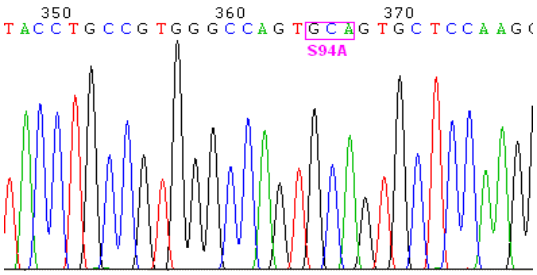

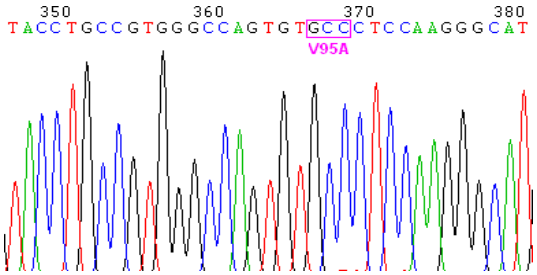

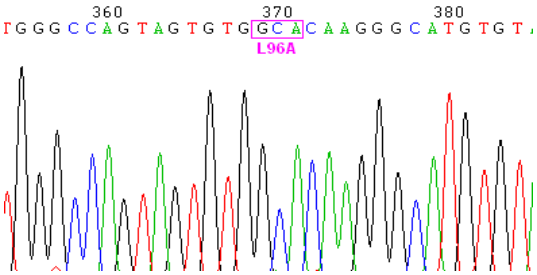

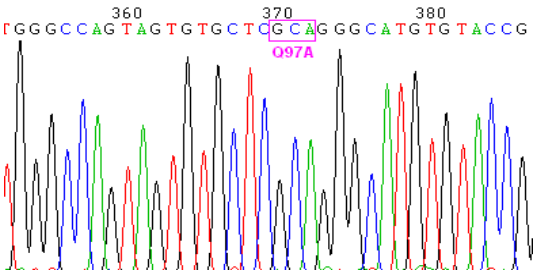

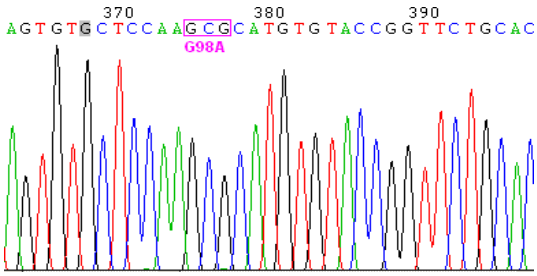

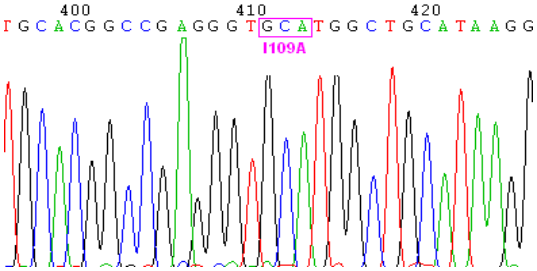

Figure 3-4continued...

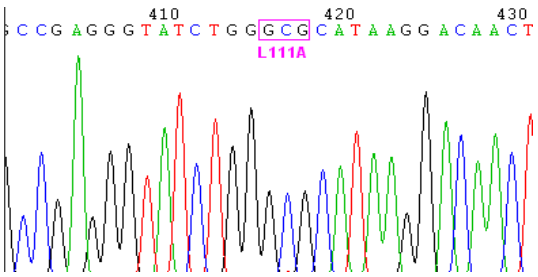

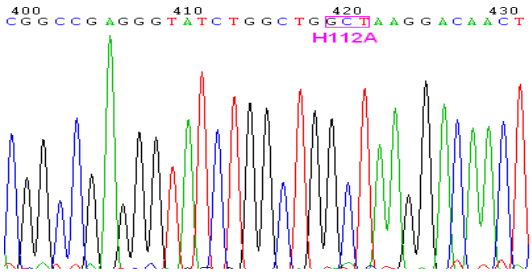

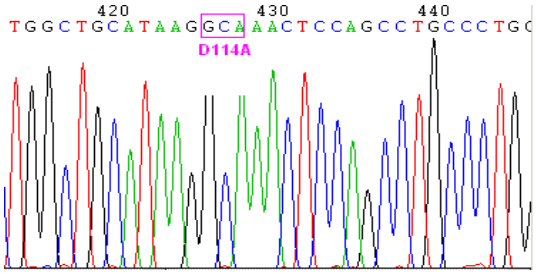

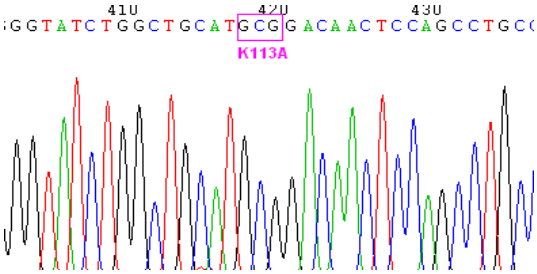

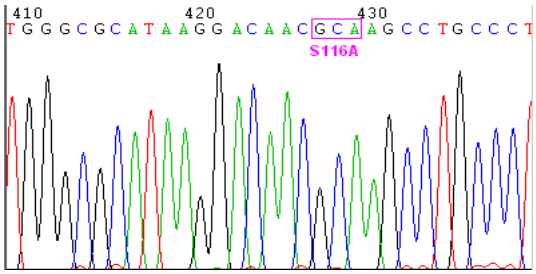

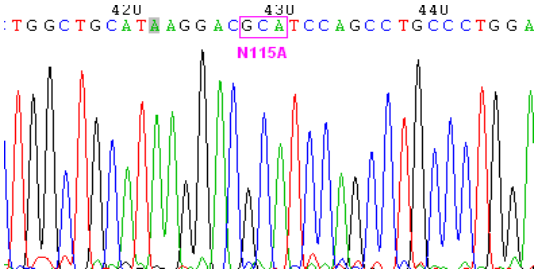

3.4.2 Radiolabeled ligand binding analysis

The data obtained from the binding analyses were graphed and interpreted by Graph Pad Prism (Figure 3-4). Binding curves in the figures represent one of at least three independent experiments for which each point is the mean of triplicate values, with s.e.m. displayed as error bars. Counts were normalised to the maximal specific binding within each dataset. As seen in Figure 3-5, compared to the non-mutated receptor, the competitive binding assay revealed binding for only fifteen mutants, while the other three mutants (rGLP-1R-Phe66Ala, rGLP-1R-Tyr42Ala and rGLP-1R-Val95Ala) failed to show any detectable binding. Further statistical analysis (see 2.8) of the receptors showing binding (Table 3-1) revealed that there were non-significant effects on the affinity for EX4 compared with WT rGLP-1R$_{myc}$ (p>0. 5).

Table 3-1: pIC$_{50}$ values of Ala mutation of rGLP-1R at potential positions to interact with C-terminus of EX4. Overview of pIC$_{50}$ values for each mutant tested by heterologous ^{125}I-GLP-1 against unlabelled EX4. d refers to fold difference, which is calculated using pIC$_{50}$ value of wild rGLP-1R$_{myc}$. ND means no detectable binding.

Receptor	pIC$_{50}$	d	Receptor	pIC$_{50}$	d
rGLP-1R$_{myc}$	9.60 ± 0.13		**rGLP-1R-Gly98Ala**	10.41± 0.25	0.13
rGLP-1R-Arg40Ala	10.03 ± 0.02	0.30	**rGLP-1R-Glu107Ala**	9.73 ± 0.09	0.60
rGLP-1R-Tyr42Ala	ND		**rGLP-1R-Ile109Ala**	9.23 ± 0.04	1.92
rGLP-1R-His44Ala	9.83 ± 0.17	0.47	**rGLP-1R-Leu111Ala**	10.10 ± 0.12	0.26
rGLP-1R-Phe66Ala	ND		**rGLP-1R-His112Ala**	9.80 ± 0.10	0.51
rGLP-1R-Asp68Ala	9.57 ± 0.17	0.86	**rGLP-1R-Lys113Ala**	9.98 ± 0.13	0.34
rGLP-1R-Ser94Ala	9.56 ± 0.13	0.88	**rGLP-1R-Asp114Ala**	9.57 ± 0.13	0.86
rGLP-1R-Val95Ala	ND		**rGLP-1R-Asn115Ala**	9.71 ± 0.16	0.64
rGLP-1R-Leu96Ala	9.20 ± 0.15	2.03	**rGLP-1R-Ser116Ala**	9.35 ± 0.06	1.44
rGLP-1R-Gln97Ala	9.85 ± 0.08	0.46			

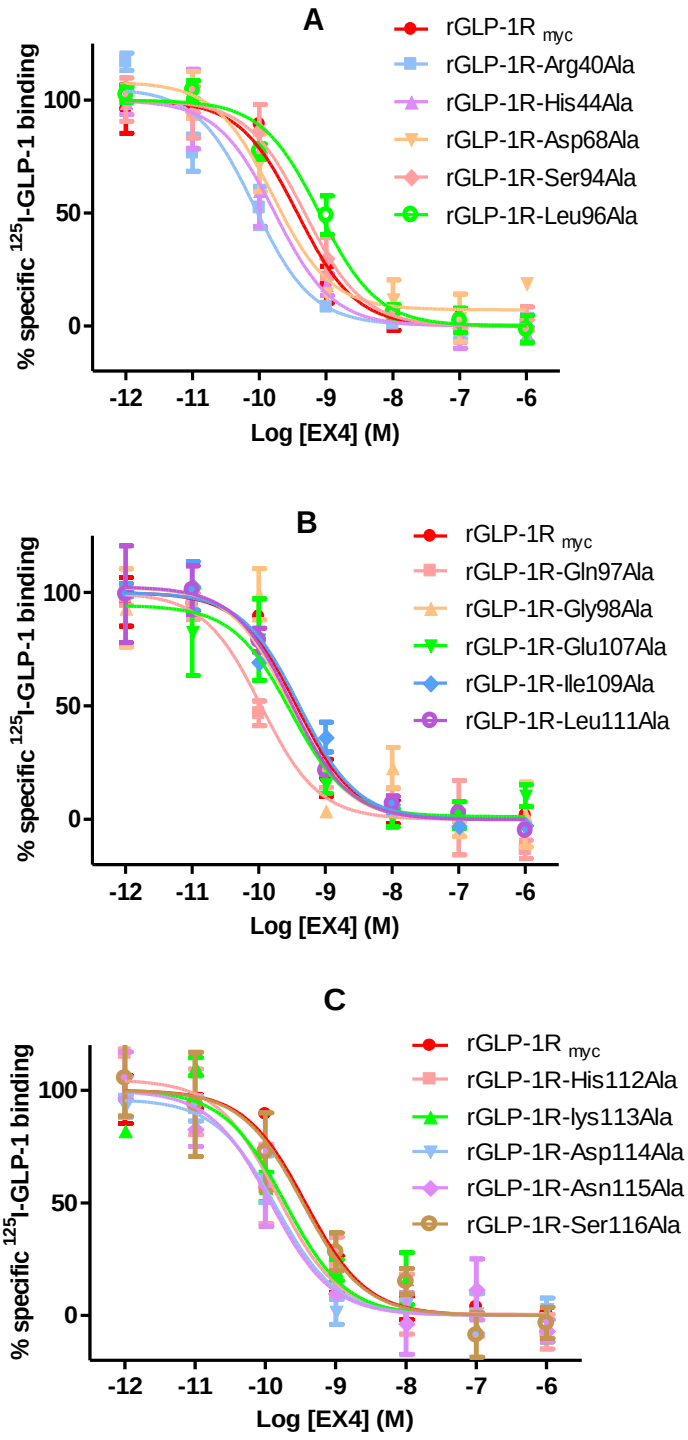

Figure 3-5: Competition-binding curves of Ala replacement mutants of rGLP-1R.

Competitive heterologous radiolabelled ligand binding assays of the fifteen rGLP-1R$_{myc}$ alanine mutants. Three subfigures A, B and C, binding in each part (A-C), five mutants are keyed and labelled and were compared with non-mutated rGLP-1R$_{myc}$. All curves show no significant (P> 0.1) affinity change in any of the mutants.

3.4.3 LANCE™ cAMP assay for non-binding mutants

The mutated receptors rGLP-1R-Phe66Ala, rGLP-1R-Tyr42Ala and rGLP-1R-Val95Ala that did not show binding activity, were subjected to further investigation via LANCE cAMP assay after stimulation by either EX4 or GLP-1. One mutant, Phe66Ala responded to stimulation by both ligands but with highly reduced potency, reflected by right shifted dose-response curves as shown in Figure 3-6 and with >225-fold difference in EC_{50} (Table 3-2).

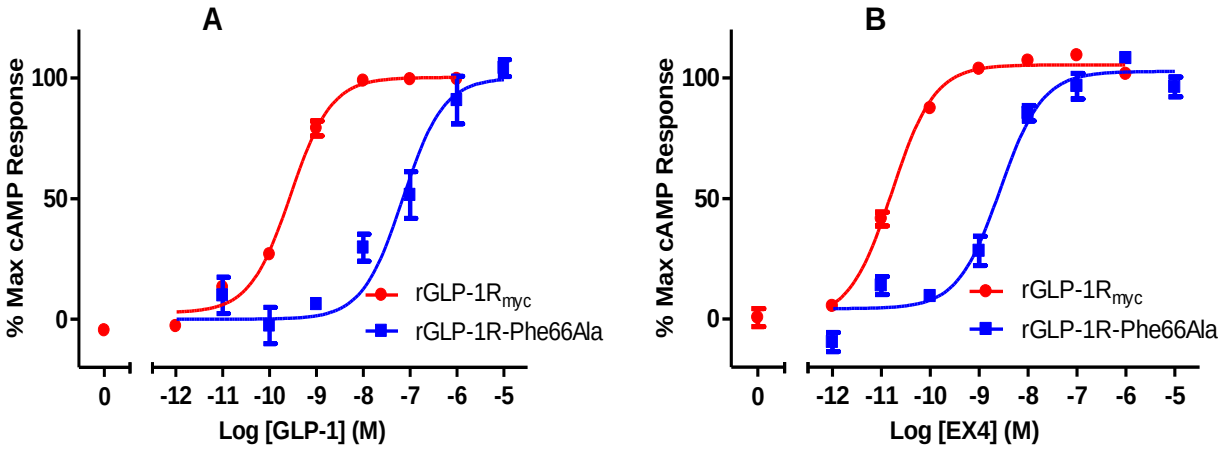

Figure 3-6: Dose response curves of rGLP-1R-Phe66Ala.

HEK-293 stably expressing rGLP-1R$_{myc}$ and rGLP-1R-Phe66Ala mutant were stimulated by either (A) GLP-1 or (B) EX4. The curve for the rGLP-1R-Phe66Ala (■) is widely shifted to right of rGLP-1R$_{myc}$ (●) indicating great reduction in potency of both GLP-1 and EX4. Values for pEC_{50} are given in Table 3-2.

Table 3-2: pEC_{50} values for the rGLP-1R-Phe66Ala stimulated by either GLP-1 or EX4.

	GLP-1		EX4	
	pEC_{50}	**d**	**pEC_{50}**	**d**
rGLP-1R$_{myc}$	9.60 ± 0.06		10.74 ± 0.08	
rGLP-1R-Phe66Ala	7.43 ± 0.13**	226.29	8.37 ± 0.15**	224.04

d is the fold difference between the pEC_{50} values of the mutant compared with WT rGLP-1R$_{myc}$. ** P<0.0001.

The mutated receptors rGLP-1R-Tyr42 and rGLP-1R-Val95 did not respond to stimulation by either GLP-1 or EX4, as shown in Figure 3-7.

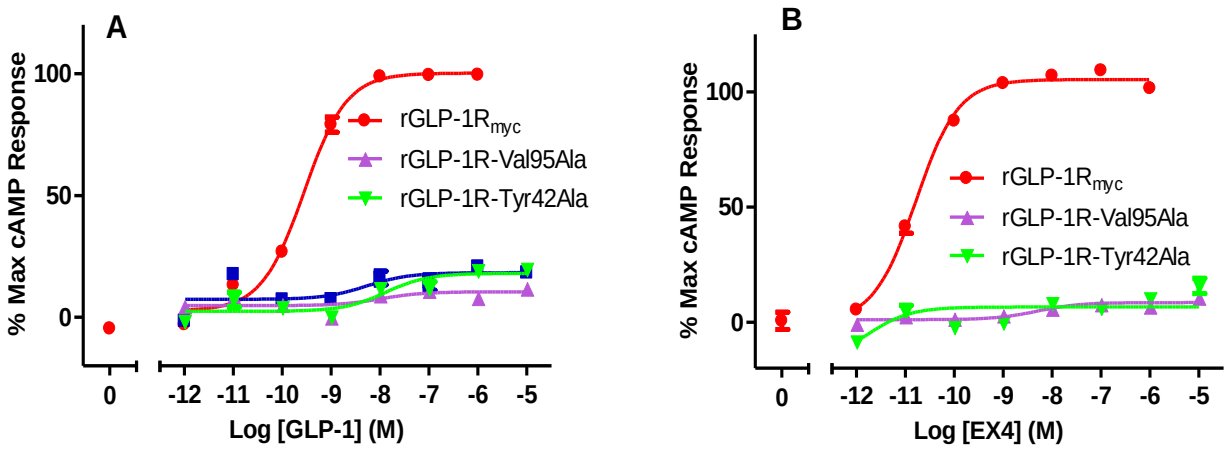

Figure 3-7: Dose response curves of rGLP-1R-Val95Ala and rGLP-1R-Tyr42Ala versus WT rGLP-1R$_{myc}$.

HEK-293 stably expressing rGLP-1R$_{myc}$ (●) , rGLP-1R-Val95Ala (▲) rGLP-1R-Tyr42Ala (▼) were stimulated by either (A) GLP-1 or (B) EX4. Both of the mutants show flat dose response curves compared to rGLP-1R$_{myc}$ demonstrating a negligible response to either GLP-1 or EX4.

The rGLP-1R-Tyr42Ala and rGLP-1R-Val95Ala either have faulty expression or else the mutated residues are highly important for the affinity and/or activity of the receptors.

3.5 Discussion

(Kalliomaa, 2005) provided a number of different models proposing possible sites of interactions between the rGLP-1R-NTD and EX4 with particular attention to the C-terminal region of EX$, assumed at that time for form a Trp-cage. Based upon those models, 19 residues that were suggested to contribute to the Trp-cage interaction in at least one model (as well as being conserved between rat, human and mice subtypes of GLP-1R) were selected for testing. Each residue was mutated to alanine in order to assess the role of each side chain in EX4 binding.

Most of the mutated receptors displayed binding characteristics not significantly different from the WT receptor, without any significant effect on the affinity of EX4 ($P>0.5$) (Table 3-1, Figure 3-5). However, three of these mutants; rGLP-1R-Tyr42Ala, rGLP-1R-Phe66Ala and rGLP-1R-Val95Ala failed to bind the radio-labelled agonist. This failure could mean either the mutants affect GLP-1 binding or that expression of the desired receptors is defective. Further investigations to explore the reason were carried out. Cell lines expressing the three mutants were subjected to cAMP accumulation assay, as cAMP is the second messenger produced in response of agonist activation.

The concentration of the agonist used in the the LANCE^{TM} cAMP assay was much higher than that of the radiolabelled ligand used in the binding assay (1µM rather than 50 pM) and hence any reduction in the affinity due to the mutation would be detected as a reduction in potency. However, compared to the control WT cell line, rGLP-1R-Phe66Ala responded with 224-fold lower potency (Figure 3-5, Table 3-2) while the others, rGLP-1R-Tyr42Ala and rGLP-1R-Val95Ala, failed to produce any cAMP in response compared to the WT receptor activation by the same concentration of GLP-1 (Figure 3-7).

Kalliomaa built the models based upon a CRFR2β-NTD structure with a very low level of sequence conservation with GLP-1R (26%) which makes the accurate alignment between the target and template very difficult and needs high manual intervention. However, it was acceptable, taking into consideration the availability of this unique template for a Family B GPCR at that time, along with other features that supported the template selection such as localization of common conserved groups within the aligned area, common phylogenetic origin of the two receptors and the binding mechanism of their relevant ligands. However, the NMR structure of CRFR2β-NTD has a missing area at the distal N-terminal region, which is known to affect the affinity of ligand binding in GLP-1 (Runge et al., 2008, Underwood et al., 2010)

At the time of planning this work, the CRFR2β-NTD NMR structure was the only available template for a Family B GPCR NTD, and the work had to use Kalliomaa's models. Later, a new model based on an NMR structure (Tan et al., 2006, Sun et al., 2007) of Family B members were published. Sun *et al.,* (2007) generated an NMR structure for the PAC1-R-NTD with the ligand PACAP bound. This structure not only displayed the conserved 'scr' structure of Family B GPCR-NTDs seen in the original version of CRFR2β-NTD but also had a more extended α-helical N-terminus. Later, (Grace et al., 2007) generated a new NMR structure for CRFR2β-NTD bound to its antagonist, astressin, providing a clearer idea about the binding pattern of this complex.

Thereafter, (Parthier et al., 2007) reported the 1.9 Å resolution crystal structure of the complex of human GIPR-NTD (residues 24–138) with its agonist, the incretin hormone GIP(1–42). This complex closelt resembles GLP-1R and its agonist GLP-1. The structure supports the existence of an 'H' interaction between the helix of the peptide, as well as its C-terminus (residues 15-30) and the NTD of

the receptors. However, the N-terminus of the GIP (1–42) peptide is free to interact with the remaining trans-membrane structure of the receptor. More recently, a GLP-1R crystal structure in complex with EX4(9-39) was released (Runge et al., 2008).

The crystal structures describe in detail the residues that contribute to the receptor/peptide interaction, which in GLP-1R are Val30, Leu32, T35, Val36, Lys38, Trp39, Tyr69, Tyr88, Leu89, Pro90, Trp91, Arg102, Gly108 and Trp110 (Figure 3-7). Based upon this description, the mutated residues described in this chapter lie far away from the residues that were later reported to contribute to the ligand interaction. This now explains why most of their mutants described in this chapter did not interfere with the ligand binding. The structure also explains why the rGLP-1R-Phe66Ala and rGLP-1R-Tyr42Ala mutations prevented binding. According to Runge's structure, rGLP-1R-Phe66 is located in the first β strand of the receptor and, along with rGLP-1R-Tyr42, rGLP-1R-Pro90 and rGLP-1R-Trp91 are exclusively conserved in what the authors identified as the 'glucagon receptor branch'. Glucagon receptor branch includes Tyr42, Phe66, Pro90 and Trp91 of GLP-1R-NTD, which are exclusively conserved in the Family B GPCR-NTDs and likely to define specificity for the ligands of the glucagon peptide subfamily (Runge et al., 2008).

Accordingly, it could be said that mutation of these residues is more likely to disturb the receptor structure. Also, rGLP-1R-Tyr42 is a part of the hydrophobic cavity formed by Tyr42 of the α-helix, Tyr69 of turn 1, Ala70 of β-strand 2, Val83 of ß-strand 3, Val100 of β-strand 4, the Cys85-Cys126 disulphide bridge and two residues of loop 2 itself (Tyr88 and Leu89). This hydrophobic cavity is filled by the side chain of Pro86 at the beginning of loop 2, which plays a structurally important

role for the formation of the ligand binding site of GLP-1R-NTD (Figure 3-8) (Runge et al., 2008).

A molecular mechanism has been proposed for the activation of the secretin receptor, whereby natural agonist ligand binding to the receptor amino-terminal domain induces a conformational change in that domain, which exposes an endogenous agonist sequence that is totally distinct from the hormonal agonist (Ding et al., 2006). Surprisingly, a peptide sequence based upon GLP-1R residues 63-70 (NRTFD), has been reported as the endogenous agonist (Dong et al., 2008). In contrast, the results observed for the rGLP-1R-Phe66Ala mutant revealed the maintained activity of the receptor unless the other residues compensate the job of rGLP-1R-Phe66 in case of its mutation.

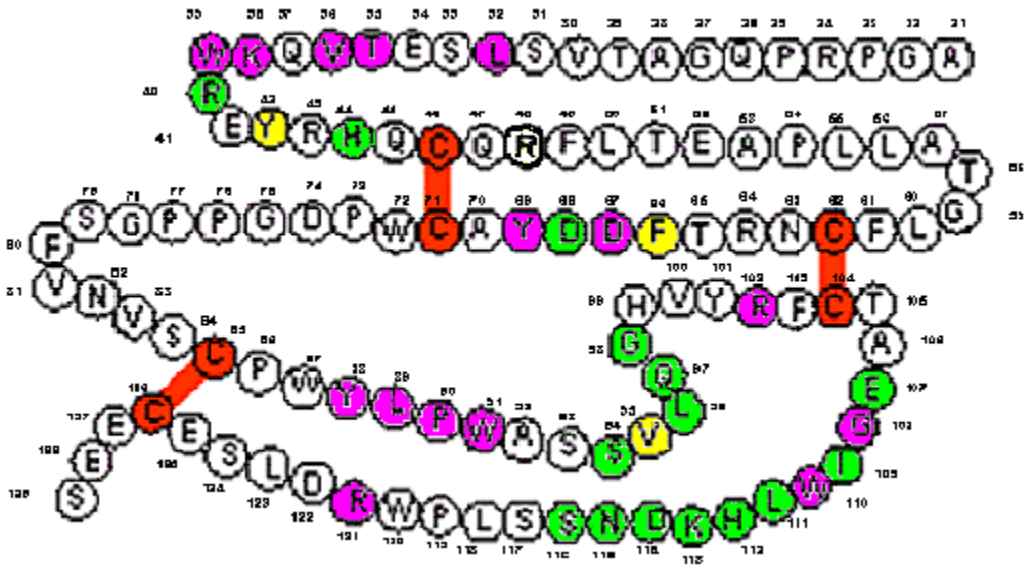

Figure 3-8: A diagram of the residues of the rGLP-1R-NTD.
According to the crystal structure, the equivalent residues contribute to the binding interface (in magenta). Model-based mutated residues bind normally as WT (green). Model based mutated residues interfered with binding of the ligand, which are also shown to be involved in the ligand binding by crystalization (yellow). The conserved cysteine residues are connected by disulphide bonds (red).

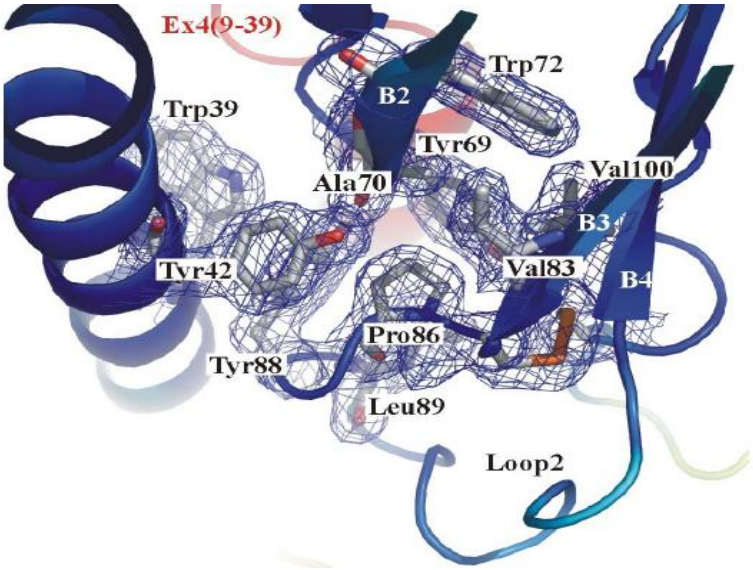

Figure 3-9: The hydrophobic binding cavity as shown by crystal structure of GLP-1R-NTD bound to EX4(9-39).

This hydrophobic cavity is formed by Tyr42 of the α-helix, Tyr69 of turn 1, Ala70 of β-strand 2, Val83 of β-strand 3, Val100 of β-strand 4, the Cys85-Cys126 disulphide bridge and two residues of loop 2 itself; Tyr88 and Leu89. This cavity is filled by the side chain of Pro86 at the beginning of loop 2 which plays a structurally important role for the formation of the ligand binding site of GLP-1R-NTD (Runge et al., 2008).

In short, although rGLP-1R-Phe66 and rGLP-1R-Tyr42 are not directly involved in the ligand binding, they could alternatively modulate the binding site of the NTD by intramolecular interactions, based upon their incorporation in the glucagon receptor branch and hydrophobic binding cavity, in order to accommodate specifically the glucagon peptide subfamily. Likewise, rGLP-1R-Val95 is located within GLP-1R loop 2 that connects between β3 and β4. Loop 2 is also important for ligand binding (Figure 3-8) (Runge et al., 2008).

After all, Kalliomaa's work was a first trial for building a rGLP-1R-NTD/peptide binding model but the limited information at that time lowered the quality of the models. It has now become clear that Kalliomaa's models are unreliable in determining EX4 binding sites in rGLP-1R-NTD, and so alternative approaches to locate the 'EX' interaction were attempted.

4 - Determining of 'EX' interaction using crystal structure-based mutants

4.1 Introduction and strategy

The mutant receptors that were built based on Kalliomaa's models failed to show differential binding between GLP-1 and EX4. After completion of that phase of work, (Parthier et al., 2007) released the 1st crystal structure of a Family B GPCR-NTD. This was the structure of the GIPR-NTD bound to GIP. Based on an alignment between GIPR and rGLP-1R on the one hand (Figure 4-1A) and between GIP, GLP-1 and EX4 on the other hand (Figure 4-1B), the residues assigned in GIPR as determinants for GIP binding were suggested to play the same role in rGLP-1R and should hence should reflect residues in either GLP-1 or EX4 that bind to GLP-1R, as described in Figure 4-2.

It was clear that Kalliomaa's models were inaccurate and this explained the inability to identify the basis for the 'EX' interaction in Chapter 3. Indeed, in 2008 Runge et al. published the structure of hGLP-1R-NTD bound to EX4(9-39) which confirmed the similarity to GLP-1R. Interestingly, all the residues contributing to NTD binding in either GLP-1 or EX4 were included in the helical region i.e forming the 'H' interaction in the previously proposed model (Lopez de Maturana et al., 2003). Interestingly, a combination of pharmacological and biophysical approaches revealed that the removal of the EX4 C-terminal region had no effect upon binding to the hGLP-1R (Runge et al., 2007). Furthermore, the crystal structure of hGLP-1R-NTD bound to EX4(9-39), showed minimal interaction with the C-terminal region of the ligand except for a hydrogen bond between EX4 Ser32** and hGLP-1R-Glu68 (Runge et al., 2008).

More recently, a crystal structure of hGLP-1R-NTD bound to GLP-1 has been published (Underwood et al., 2010), which also showed that the interacting ligand residues involved in receptor interaction were limited to its helical region. Hence, both of the structures located the residues in NTD that interact with 'H' of the ligand, but not all the residues contributing to the 'H' interaction for EX4 and GLP-1 were identical. Therefore, the non-identical amino acids could be contributing to the 'EX' interaction via a selective interaction with EX4 rather than GLP-1 with GLP-1R.

Accordingly, as an initial approach, the residues of rGLP-1R potentially contributing to the differential binding of EX4 were selected as following; Val30, Thr35, Val36, Trp39, Tyr69, Tyr88, Trp91, Glu127 and Glu128 (Figure 4-2). Each residue was subjected to mutation followed by pharmacological characterization. The rationale behind the selection of each residue will be introduced separately with the relevant results.

4.2 Methodological considerations

The general methods described in Chapter 2 were applied. The peptides used for binding analysis have been expanded to include GLP-1, EX4 and EX4(9-39). Each mutant receptor underwent both binding and activity analysis as described in Chapters 2 and 3.

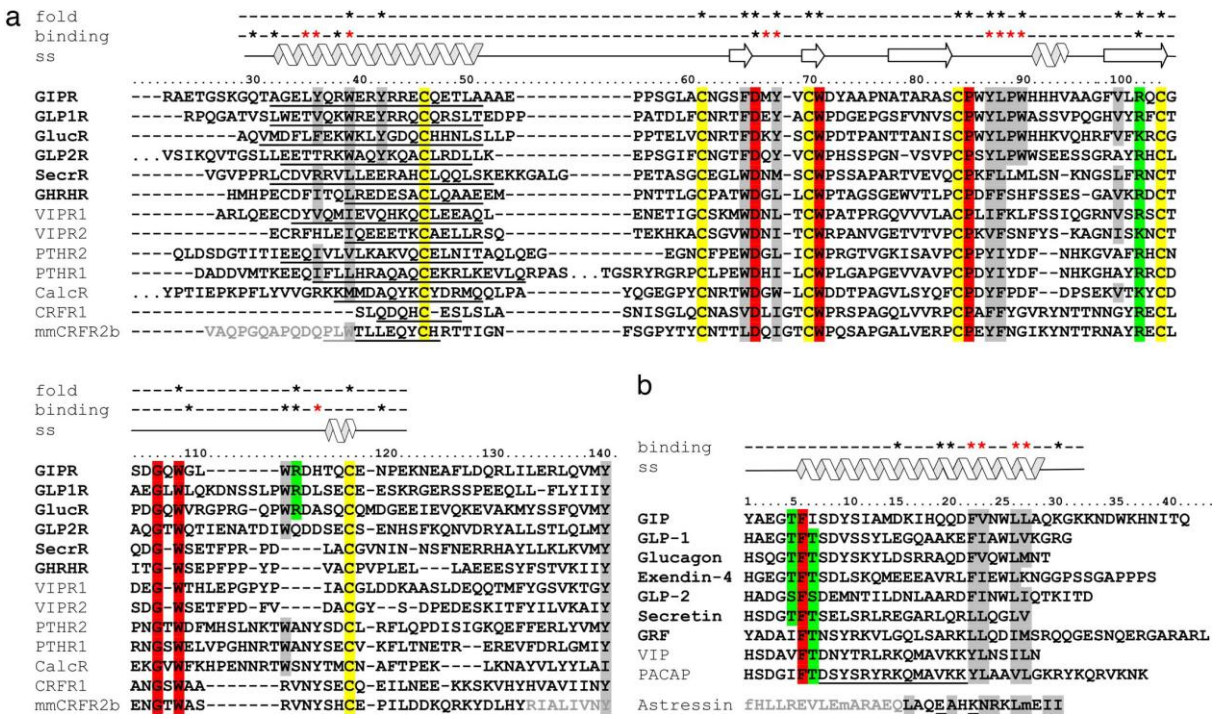

★ in 'fold' line for stabilizing residues
★ in 'binding' line for residues involved in hydrophobic interaction
---- Additional residues that are not shown
'ss' The secondary structure
■ Absolutely conserved residues
■ Less conserved residues (Basic) of receptors or ptential N-terminal helix-capping residues are marked in green,
■ Less conserved residues (Hydrophobic)
■ Conserved cysteins
U Underlined letters are amino acids of the predicted α helix of the receptor

Figure 4-1: Sequence alignment of the NTDs Family B GPCRs and their relevant ligands.
A: Hormone receptor NTDs with numbering according to GIPR; The names of the glucagon receptor family members are in bold. Residues missing from the construct of CRFR2β used for structure determination (Grace et al., 2007) are in gray. **B:** Sequence alignment of human peptide hormones with numbering according to GIP; the names of the ligands are in bold. PACAP residues forming α helix when bound to its receptor are underlined (Inooka et al., 2001). CRFR2β; f denotes DPhe12, m indicates norleucine residues 21 and 38, and underlined residues Glu30 and Lys33 are chemically linked through a lactam bridge. Residues not observed in the NMR structure are in gray (Parthier et al., 2007).

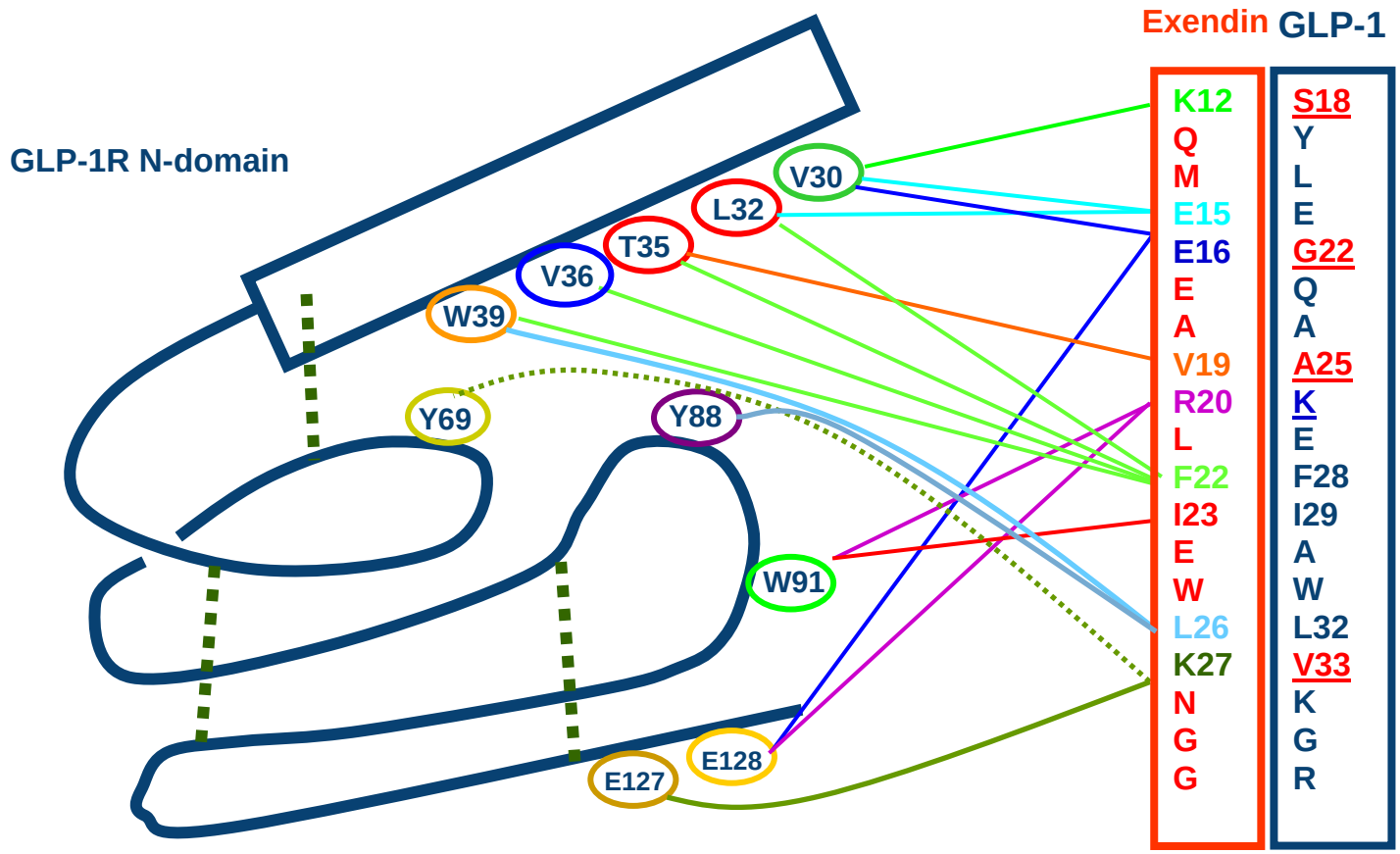

Figure 4-2: Cartoon model of the residues of the rGLP-1R-NTD that interact with GLP-1 and EX4.

The model shows the EX4 sequence in a red box, in which each amino acid is connected to the suggested interacting residue of the receptor by a colour matching line. GLP-1 is squared by a blue box; interacting residues that are different from corresponding ones in EX4 are underlined. Each mutated residue of the NTD is highlighted by coloured circles.

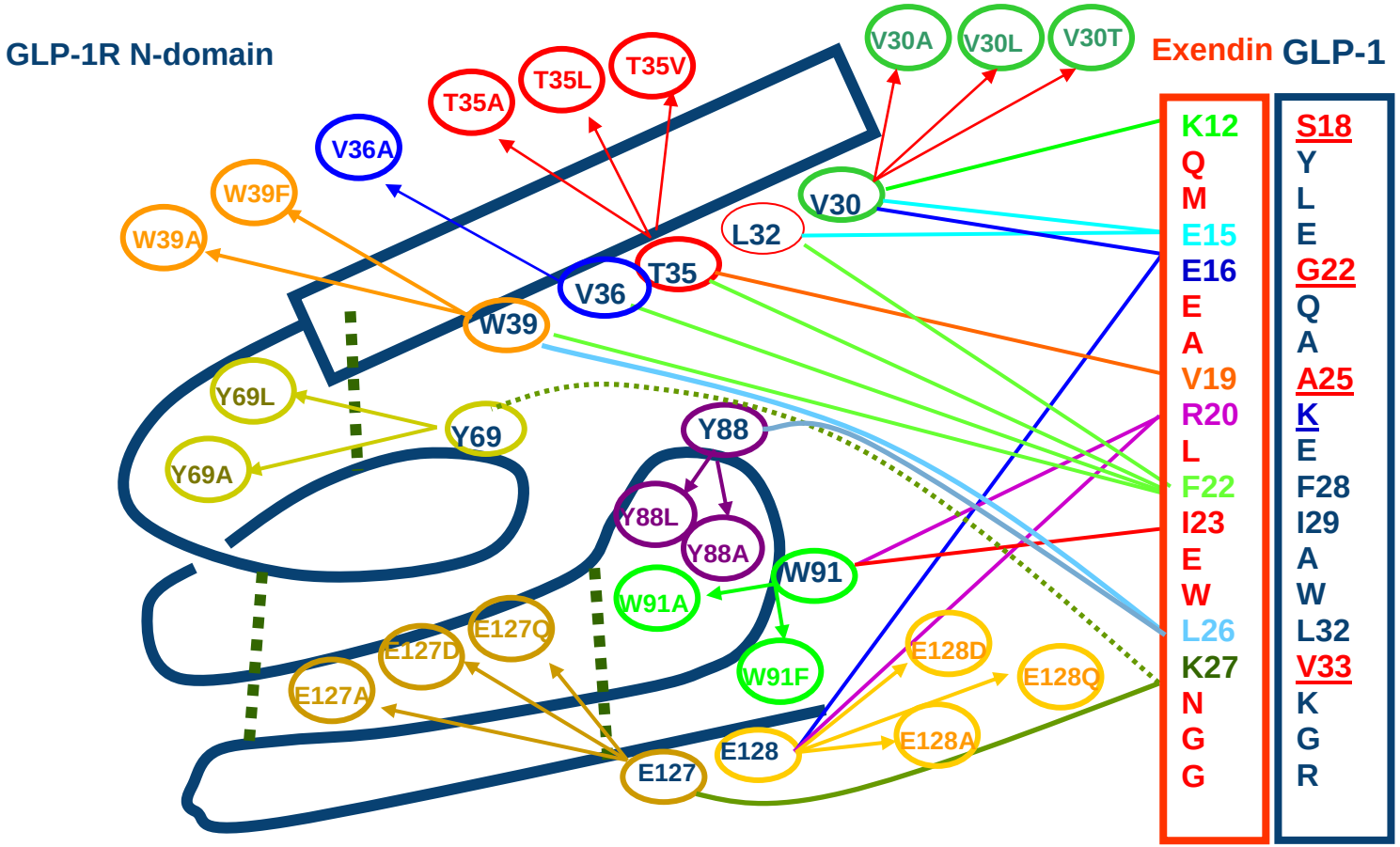

Figure 4-3: Cartoon model of the investigated mutants of the rGLP-1R-NTD with GLP-1 and EX4.

The figure is a repeated version of Figure 4-2 with the addition of the substituted amino acids for each residue. Each mutated residue of the NTD is highlighted by different coloured circles and connected to its same coloured and shaped substitutes by colour matching lines.

4.3 Results

4.3.1 Preparation of the mutants

The mutants were prepared using the same laboratory techniques mentioned under 2.1 and they were confirmed by sequencing and alignment. Figures 4-4 and 4-5 show the relevent sections of this sequencing

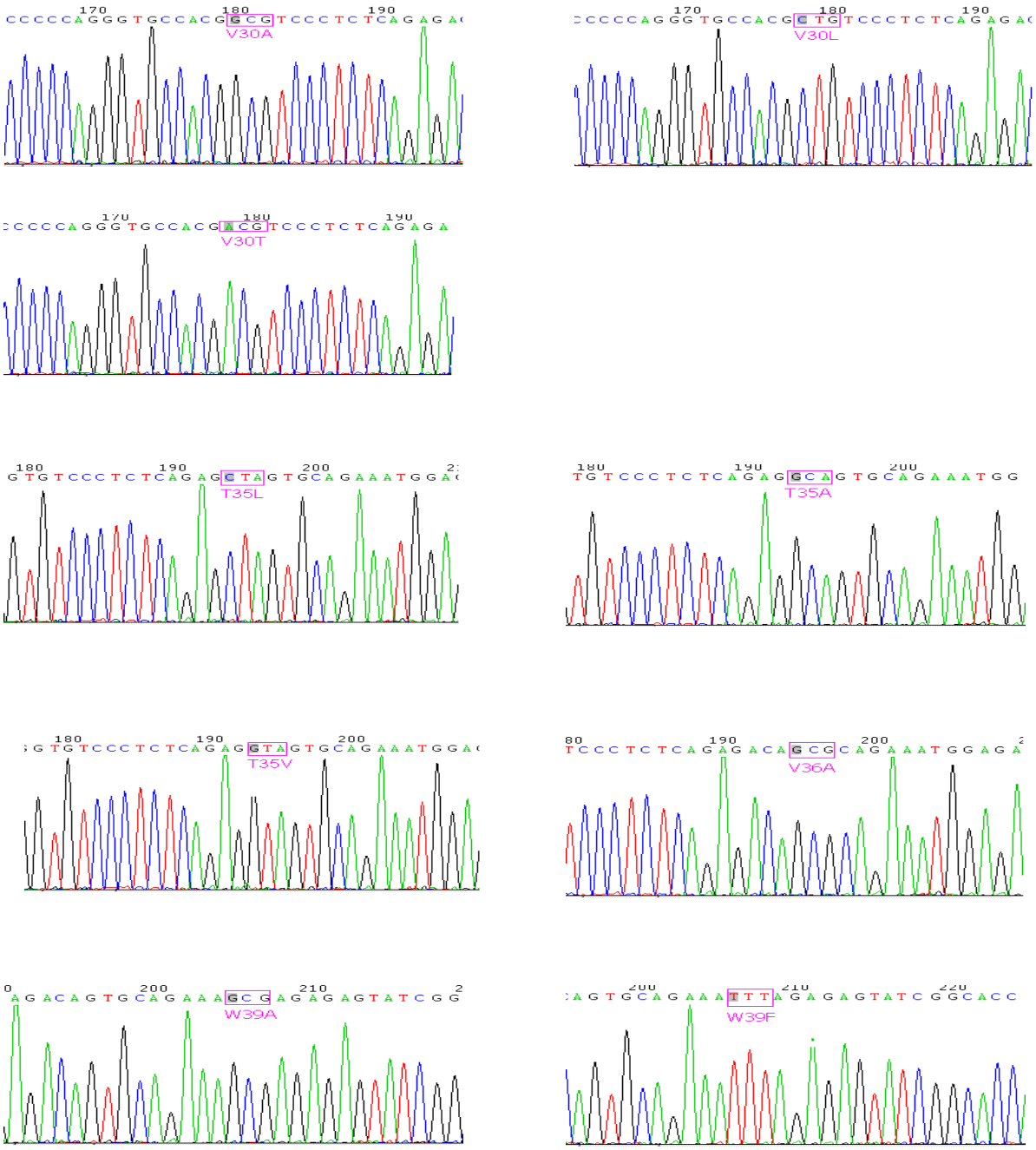

Figure 4-4: Sections of the nucleotide sequence of rGLP-1R$_{myc}$ single mutated receptors. Mutated codons are highlighted by pink squares.

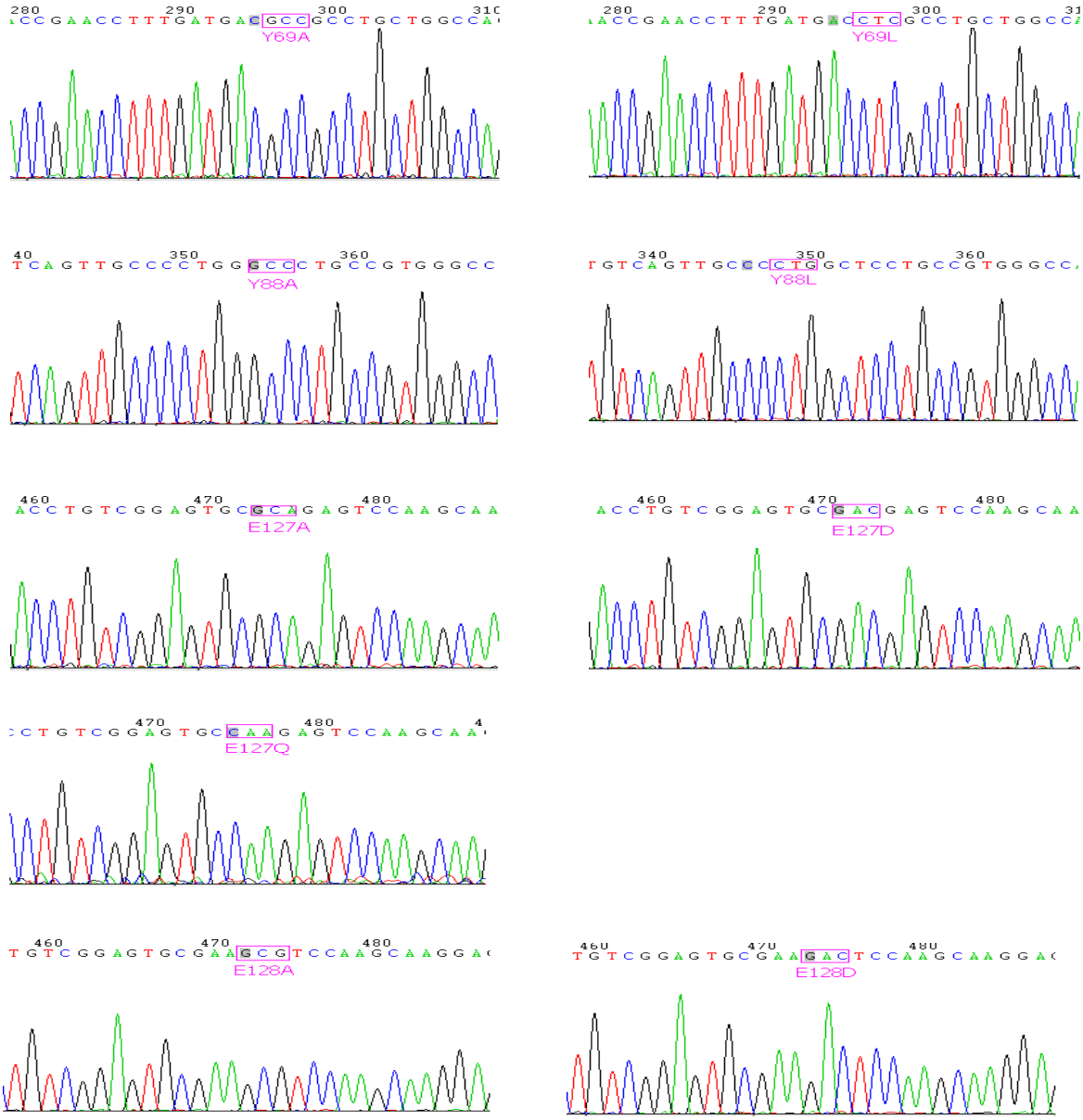

Figure 4-5: Sections of the nucleotide sequence of rGLP-1R$_{myc}$ single mutated receptors. Mutated codons are highlighted by pink squares.

4.3.2 Affinity and activity characterization

Stable cell lines were prepared as described in section 2.3 for each mutant receptor and then crude membrane preparations were prepared from these cells and subjected to both homologus radiolabelled competitive binding assays (using ^{125}I-GLP-1 against cold GLP-1) and heterologous competitive binding assays (using ^{125}I-GLP-1 against either EX4 or EX4(9-39)). In addition, LANCE cAMP assays were carried out using live cells expressing each mutant receptor. WT rGLP-1R$_{myc}$ membrane preparations and live cells were used as a control for each assay respectively. Although displayed in different tables below for reasons of clarity, the binding and cAMP data were generated over the same period for all mutants and therefore the same control WT data appears in all the tables. The work aimed to detect the impact of mutating these residue targets upon the differential GLP-1 and EX4 affinity and/or subsequent activity.

4.3.2.1 Effect of mutations at rGLP-1R-Val30

Valine is a branched, non-polar, neutral and hydrophobic amino acid. Interestingly, rGLP-1R-Val30 is located one residue from the beginning of the helical part of GLP-1R-NTD (Runge et al., 2008; Underwood et al., 2010). The GLP-1R-NTD crystal structure suggests that rGLP-1R-Val30 could interact with GLP-1 Ser12* and Glu15* and EX4 Lys12** and Glu15** respectively (Figure 4-2). Therefore, rGLP-1R-Val30 could play a role in the differential interaction of GLP-1 and EX4 and the receptor and its mutation may affect binding one or both of them. Hence, rGLP-1R-Val30 was mutated to the smaller Ala; similar volume, but neutral and polar, Thr; as well as the larger Leu. The affinity of each mutant was tested initially by radio-ligand competitive binding assays with full-length ligands GLP-1 and EX4, then with truncated EX4(9-39) to check its contribution to EX4 N-independent affinity. Interestingly, the mutants rGLP-1R-Val30Ala, rGLP-1R-

Val30Thr and rGLP-1R-Val30Leu reduced the affinity for GLP-1 by the same significant magnitude (Table 4-1, d= 9-13 fold, P < 0.01; Figure 4-6, A), while for rGLP-1R-Val30Ala and rGLP-1R-Val30Thr the changes to the affinity of EX4 were undetectable (Table 4-1, d< 5 fold and p>0.5) (Figure 4-5, B). However, rGLP-1R-Val30Leu showed a statistically significant reduction in EX4 affinity (d= 4.9 fold, p=0.005). In terms of fold difference, the affinity of EX4(9-39) was not affected by rGLP-1R-Val30Ala or rGLP-1R-Val30Leu mutations (Table 4-1, d< 5 folds and p>0.2) (Figure 4-6, C) but rGLP-1R-Val30Thr showed a slight but statistically significant reduction in its affinity (p<0.05) . Similarly, the mutants rGLP-1R-Val30Ala, rGLP-1R-Val30Thr and rGLP-1R-Val30Leu were also subjected to activity characterization by LANCE cAMP assay but showed activity similar to $rGLP\text{-}1R_{myc}$ (Figure 4-7, Table 4-2).

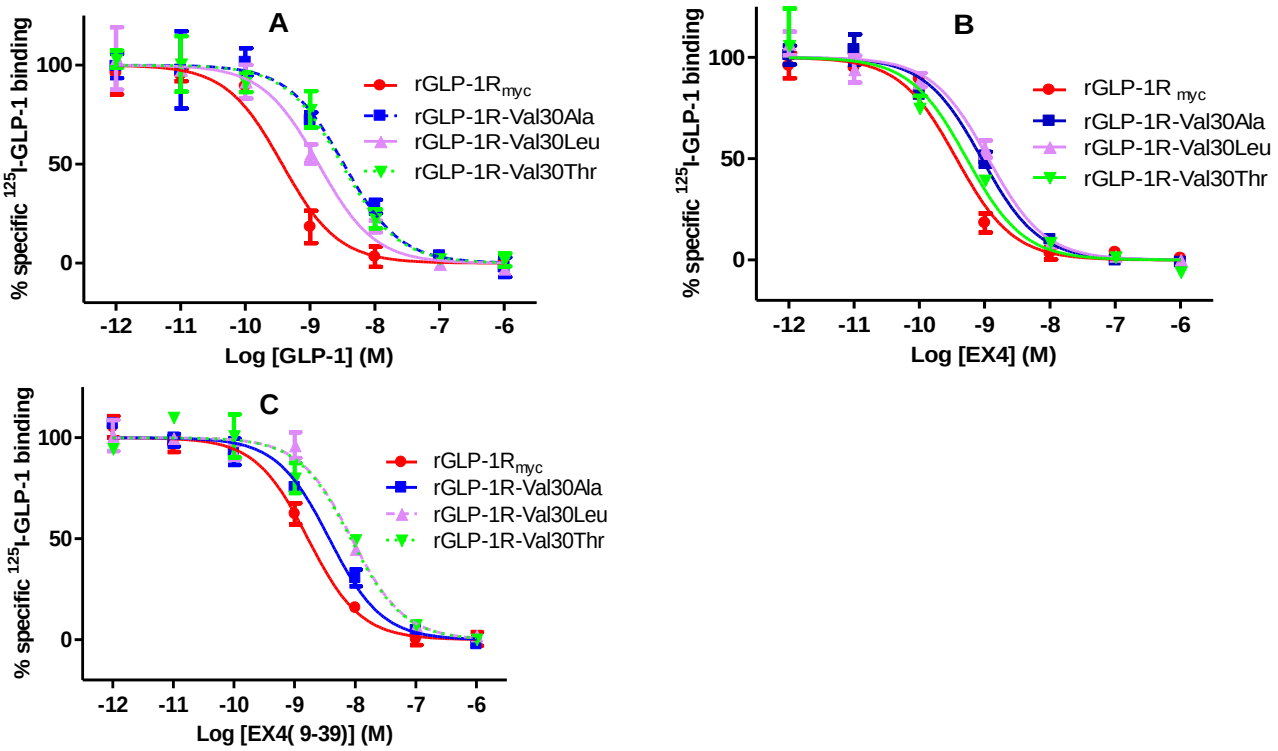

Figure 4-6: Competition-binding curves of GLP-1, EX4 and EX4(9-39) with receptors mutants of rGLP-1R-Val30.

^{125}I-GLP-1 competition-binding assays for rGLP-1R$_{myc}$ (●) and mutants rGLP-1R-Val30Ala (■), rGLP-1R-Val30Leu (▲) and rGLP-1R-Val30Thr (▼) with (A) GLP-1, (B) EX4 and (C) EX4(9-39). Mean pIC50 values are given in Table 4-1.

Table 4-1: pIC$_{50}$ values for ^{125}I-GLP-1 competition binding with GLP-1, EX4 and EX4(9-39) of rGLP-1R-Val30.

	GLP-1		EX4		EX4(9-39)	
	pIC50	**d**	**pIC50**	**d**	**pIC50**	**d**
rGLP-1Rmyc	9.60 ± 0.13		9.54 ± 0.05		8.46 ± 0.06	
rGLP-1R-Val30Ala	8.47 ± 0.14**	13.61	9.33 ± 0.17	1.60	8.43 ± 0.21	1.06
rGLP-1R-Val30Leu	8.63 ± 0.14**	9.20	8.85 ± 0.11**	4.92	8.26 ± 0.14	1.59
rGLP-1R-Val30Thr	8.64 ± 0.11**	9.06	9.39 ± 0.16	1.41	8.12 ± 0.10*	2.21

The data shows a reduction in GLP-1 affinity (about 10-fold) for the three ligands. A slight reduction, but nevertheless statistically significant, reduction was recorded for EX4 affinity at rGLP-1R-Val30Leu only. Similarly, a slight, but statistically significant, reduction was recorded in EX4 affinity for rGLP-1R-Val30Thr only.

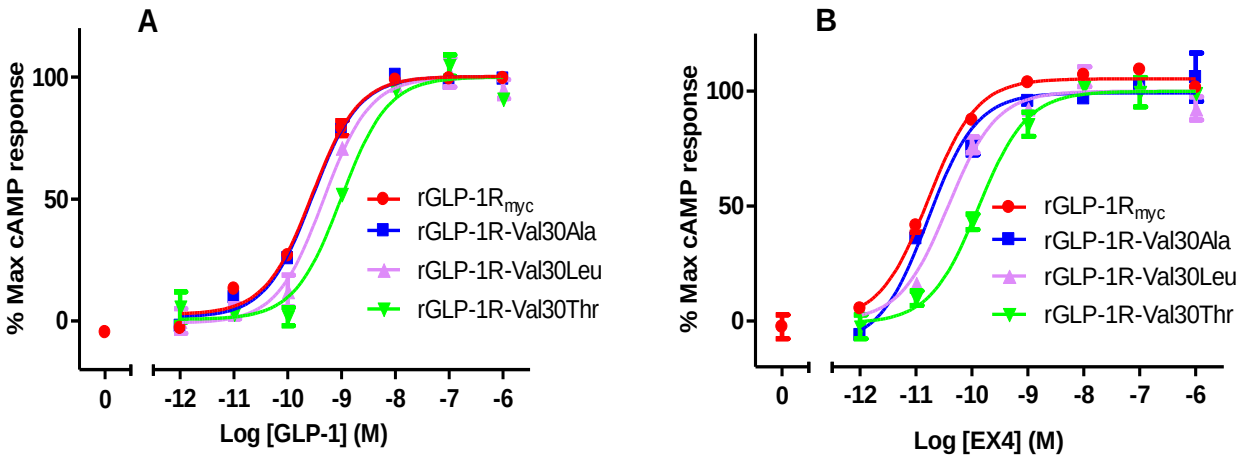

Figure 4-7: Dose response curves of rGLP-1R-Val30 mutants.

Dose response curves of rGLP-1R$_{myc}$ (●) mutants rGLP-1R-Val30Ala (■), rGLP-1R-Val30Leu (▲) and rGLP-1R-Val30Thr (▼) with (A) GLP-1 or (B) EX4. Mean pEC$_{50}$ values are given in Table 4-2.

Table 4-2: pEC$_{50}$ values for rGLP-1R-Val30 mutants stimulated by either GLP-1 or EX4.

	GLP-1		EX4	
	pEC$_{50}$	**d**	**pEC$_{50}$**	**d**
rGLP-1Rmyc	9.60 ± 0.06		10.74 ± 0.08	
rGLP-1R-Val30Ala	9.45 ± 0.07	1.43	10.38 ± 0.21	2.27
rGLP-1R-Val30Leu	9.38 ± 0.04	1.65	10.31 ± 0.18	2.67
rGLP-1R-Val30Thr	9.25 ± 0.12*	2. 24	10.09 ± 0.17*	4.42

The fold differences highlight the absence of any significant effect of these mutations on AC activation by either GLP-1 or EX4.

4.3.2.2 Effect of mutations at rGLP-1R-Thr35

Threonine is a polar and neutral amino acid. rGLP-1R-Thr35 is located within the helical part of the NTD of GLP-1R (Runge et al., 2008; Underwood et al., 2010) where it interacts with GLP-1 Ala25* and the highly conserved Phe28*, which correspond to EX4 Val19** and EX4 Phe22** respectively (Figures 4-2). So, rGLP-1R-Thr35 could have a differential interaction between GLP-1 and EX4 and, if so, its mutation should affect one of them. Consequently, rGLP-1R-Thr35 was mutated to the smaller Ala; similar volume, but non-polar, Val; as well as the bigger Leu. The binding affinity of each mutant was tested initially by radioligand competitive binding assay with full-length ligands GLP-1 and EX4, and with truncated EX4(9-39). No change in affinity for GLP-1, EX4 or EX4(9-39) was detected for rGLP-1R-Thr35Ala and rGLP-1R-Thr35Leu ($d < 5$ fold). However, a statistically significant reduction in affinity was recorded for rGLP-1R-Thr35Val using GLP-1 and EX4 (Figure 4-8, Table 4-3). In the same way, the cAMP produced in response to either GLP-1 or EX4, by HEK-293 cells stably expressing the rGLP-1R-Thr35 mutants, were assessed using the LANCE^{TM} cAMP assay, the data recorded revealed a statistically significant reduction ($p<0.001$, $d > 5$ fold) in the potency of GLP-1 at rGLP-1R-Thr35Leu and a slight reduction by rGLP-1R-Thr35Ala ($p<0.05$) while the others showed no significant changes ($d >$ 3-fold) compared to rGLP-1R$_{myc}$ (Figure 4-9, Table 4-4).

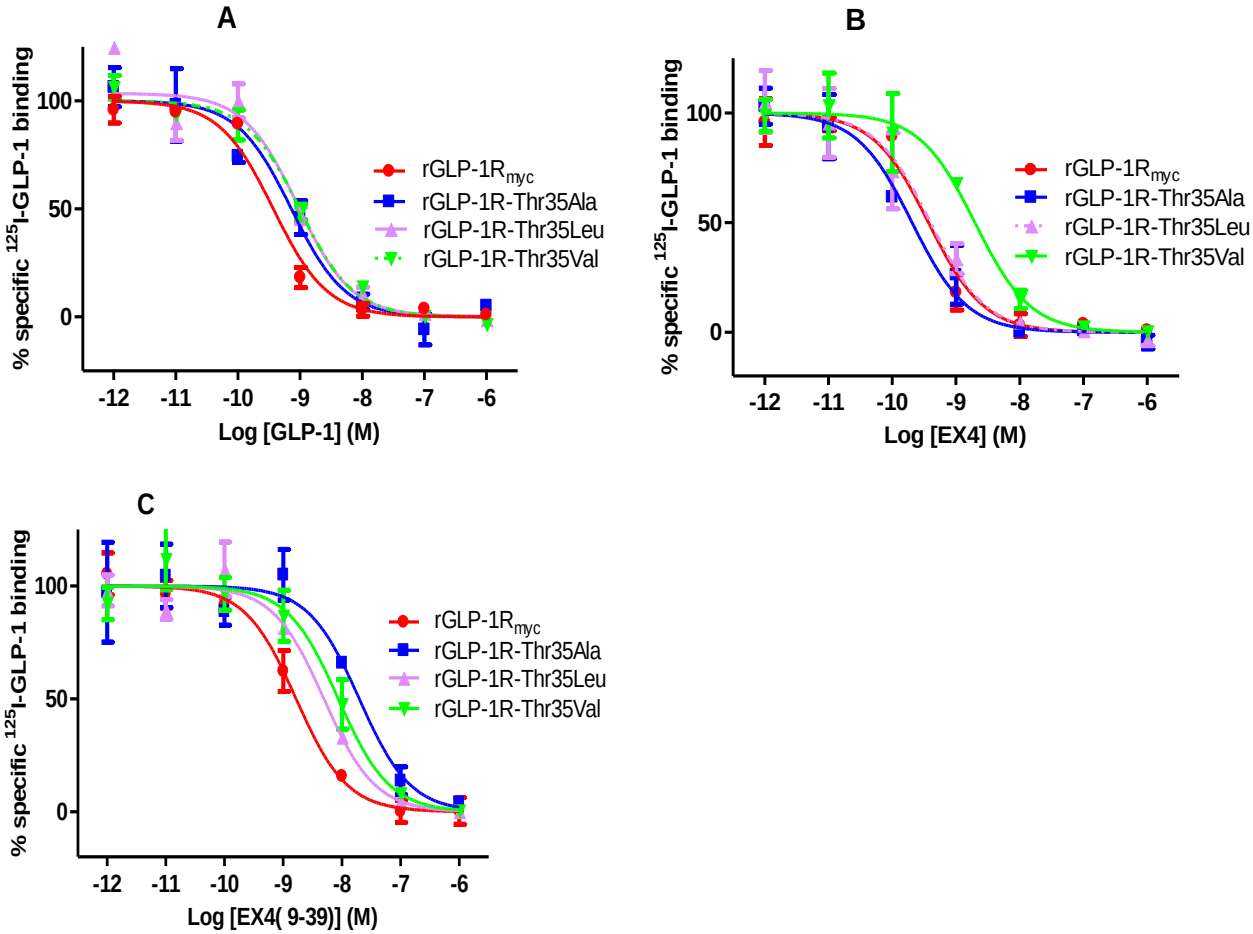

Figure 4-8: Competition-binding curves of GLP-1, EX4 and EX4(9-39) at the receptor mutants of rGLP-1R-Thr35.

^{125}I-GLP-1 competition-binding assays for rGLP-1R$_{myc}$ (●) and mutants rGLP-1- Thr35Ala (■), Thr35Leu (▲) and Thr35Val (▼) with (A) GLP-1, (B) EX4 and (C) EX4(9-39). Mean pIC$_{50}$ values are given in Table 4-3.

Table 4-3: pIC$_{50}$ values for ^{125}I-GLP-1 competition binding with GLP-1, EX4 and EX4(9-39) of rGLP-1R-Thr35 mutants.

	GLP-1		EX4		EX4(9-39)	
	pIC$_{50}$	**d**	**pIC$_{50}$**	**d**	**pIC$_{50}$**	**d**
rGLP-1R$_{myc}$	9.60 ± 0.13		9.54 ± 0.05		8.46 ± 0.06	
rGLP-1R-Thr35Ala	9.38 ± 0.12	1.66	9.55 ± 0.09	0.97	7.89 ± 0.13	3.72
rGLP-1R-Thr35Leu	9.36 ± 0.19	1.74	9.32 ± 0.13	1.65	8.54 ± 0.19	0.83
rGLP-1R-Thr35Val	8.99 ± 0.08*	4.06	8.78 ± 0.04*	6.64	8.21 ± 0.09	1.77

The data shows no change in affinity GLP-1, EX4 or EX4(9-39) due to mutations at rGLP-1R-Thr35Ala and rGLP-1R-Thr35Leu. Statistically reduction was recorded in affinity with rGLP-1R-Thr35Val for GLP-1 and EX4 only.

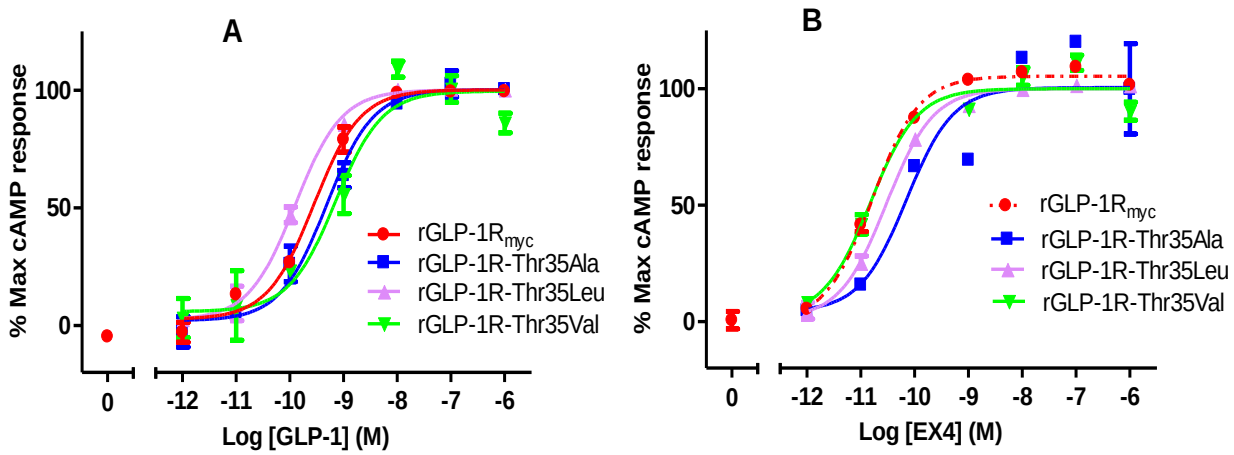

Figure 4-9: Dose response curves of the rGLP-1R-Thr35 mutants.

Dose response curves for rGLP-1R$_{myc}$ (●), mutants rGLP-1R-Thr35Ala (■), rGLP-1R-Thr35Leu (▲) and rGLP-1R-Thr35Val (▼) with (A) GLP-1, (B) EX4. Mean pEC$_{50}$ values are given in Table 4-4.

Table 4-4: pEC$_{50}$ values for the rGLP-1R-Thr35 mutants stimulated by either GLP-1 or EX4.

	GLP-1		EX4	
	pEC$_{50}$	**d**	**pEC$_{50}$**	**d**
rGLP-1R$_{myc}$	9.60 ± 0.06		10.74 ± 0.08	
rGLP-1R-Thr35Ala	9.39 ± 0.02*	1.63	10.62 ± 0.21	1.33
rGLP-1R-Thr35Leu	8.91 ± 0.06**	4.85	10.22 ± 0.19	3.28
rGLP-1R-Thr35Val	9.27 ± 0.12	2.12	10.70 ± 0.11	1.10

The data shows a statistically significant reduction (p=0.001, d > 5 fold) in the potency of GLP-1 at rGLP-1R-Thr35Leu and a slight but significant reduction at rGLP-1R-Thr35Ala (p<0.05). The others show no significant changes (< 3-fold) compared to rGLP-1R$_{myc}$.

4.3.2.3 Effect of mutations at rGLP-1R-Val36

Like rGLP-1R-Val30, rGLP-1R-Val36 is included in the receptor helical region and found to have hydrophobic interaction with the highly conserved GLP-1 Phe22* and EX4 Phe22**. rGLP-1R-Val36 was selected along with rGLP-1R-Trp39, rGLP-1R-Tyr88 and rGLP-1R-Trp91, although they interact with identical residues in both GLP-1 and EX4 (Figures 4-1 and 2), to make sure that the orientation of the 'H' region of the two ligands was similar. As a result, the data for affinity and activation properties indicated non-selective binding of GLP-1 and EX4 with wild-type-like activity (Figures 4-10 and 4-11). In contrast, reduced affinity was observed with EX4(9-39) (with about 10-fold decrease in affinity, Figure 4-10, Table 4-5, p=0.003).

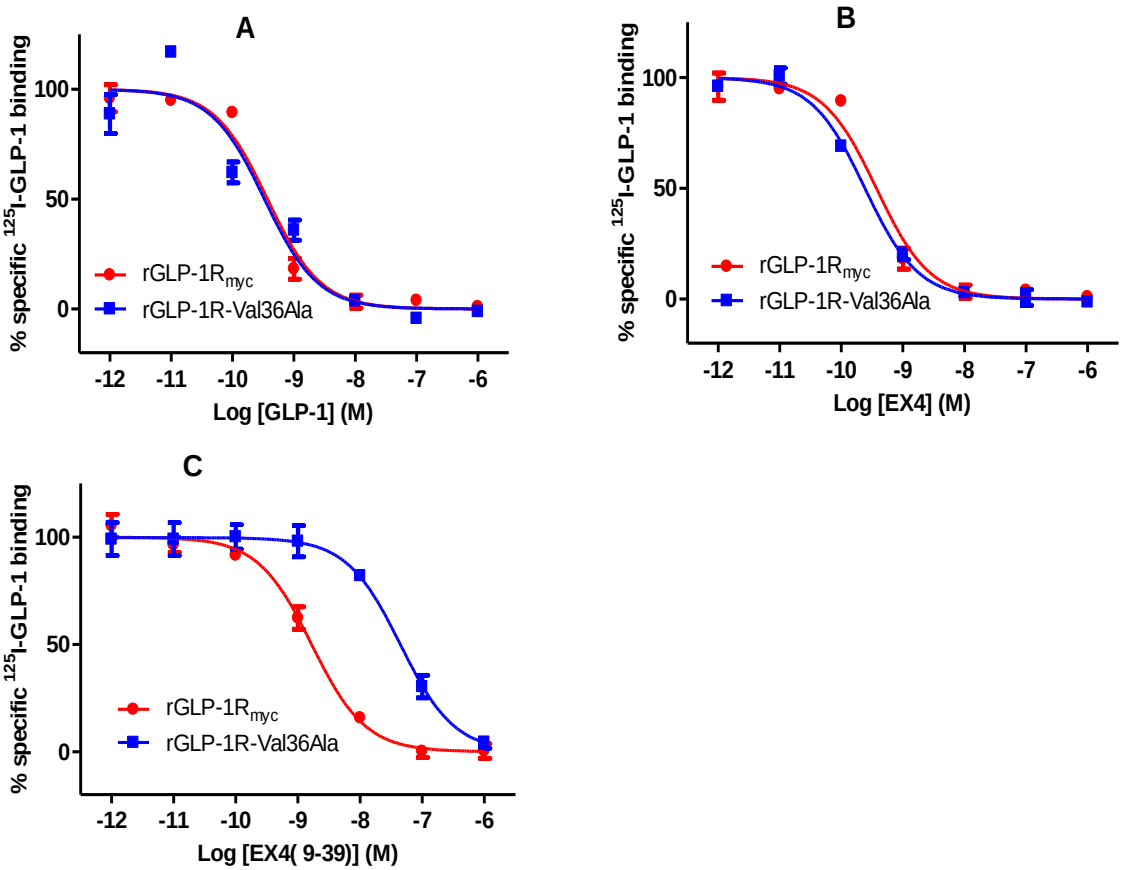

Figure 4-10: Competition-binding curves of GLP-1, EX4 and EX4(9-39) with the rGLP-1R-Val36.

^{125}I-GLP-1 competition-binding assays for rGLP-1R$_{myc}$ (●) and mutant rGLP-1R-Val36Ala (■) with (A) GLP-1, (B) EX4 and (C) EX4(9-39). Mean pIC$_{50}$ values are given in Table 4-5.

Table 4-5: pIC_{50} values for ^{125}I-GLP-1 competition-binding with GLP-1, EX4 and EX4(9-39) of rGLP-1R-Val36Ala.

	GLP-1		EX4		EX4(9-39)	
	pIC_{50}	d	pIC_{50}	d	pIC_{50}	d
$rGLP\text{-}1R_{myc}$	9.60 ± 0.13		9.54 ± 0.05		8.46 ± 0.06	
rGLP-1R-Val36Ala	9.53 ± 0.11	1.17	9.52 ± 0.05	1.04	7.46 ± 0.06**	9.94

The data show there was no change in GLP-1or EX4 binding affinity but a reduction in affinity for EX4(9-39), P<0.0001, due to mutation at position rGLP-1R-Val36Ala.

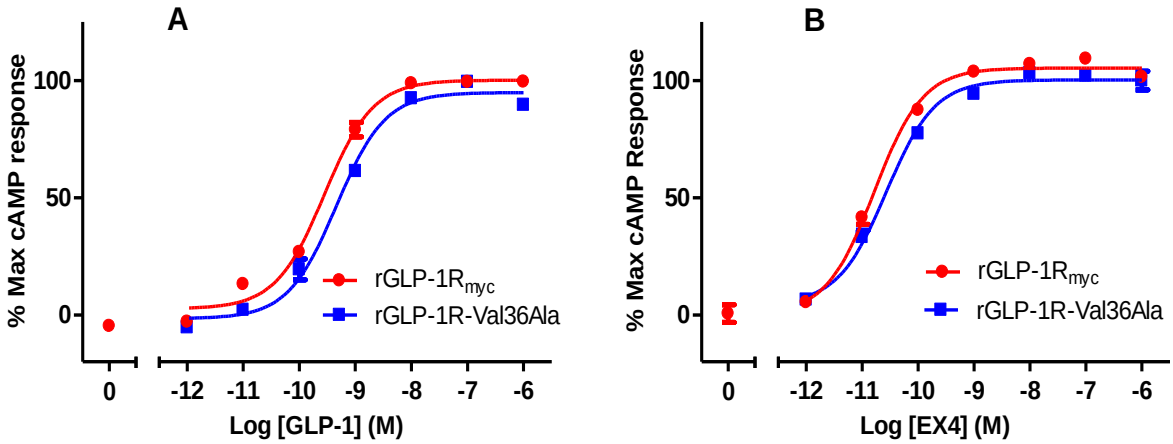

Figure 4-11: Dose response curves of rGLP-1R-Val36Ala.

Dose response curves for $rGLP\text{-}1R_{myc}$ (●) and mutant rGLP-1R-Val36Ala (■) stimulated by (A) GLP-1 or (B) EX4. Mean pEC_{50} values are given in Table 4-6.

Table 4-6: pEC_{50} values for the rGLP-1R-Val36Ala stimulated by either GLP-1 or EX4.

	GLP-1		EX4	
	pEC_{50}	d	pEC_{50}	d
$rGLP\text{-}1R_{myc}$	9.60 ± 0.06		10.74 ± 0.08	
rGLP-1R-Val36Ala	9.19 ± 0.20	2.57	10.56 ± 0.06	1.53

The fold differences highlight WT rGLP-1R like activity (d< 3-fold).

4.3.2.4 Effect of mutations at rGLP-1R-Trp39

rGLP-1R-Trp39 is located within the helix of NTD and is responsible, alongside Tyr42 and Phe66, as well as the adjacent disulphide bond (Cys-46–Cys-70), for holding the orientation of the N-terminal helix of NTD toward the core region of the NTD (Parthier et al., 2007). rGLP-1R-Trp39 is one of the residues that forms the hydrophobic binding cavity of EX4(9-39) (Figure 3-8) (Runge et al., 2008). Furthermore, a previous study reported that GLP-1 could not bind and activate receptors with mutations rGLP-1R-Trp39Ala or rGLP-1R-Trp39Phe (Van Eyll et al., 1996). So, rGLP-1R-Trp39Ala and rGLP-1R-Trp39Phe were tested here to investigate whether their mutation would affect EX4 in the same way. Radioligand competitive binding assays showed that the rGLP-1R-Trp39Ala and rGLP-1R-Trp39Phe mutants were unable to bind detectable levels of ^{125}I-GLP-1 (Figure 4-12). Surprisingly, rGLP-1R-Trp39Ala responded to activation by both of GLP-1 and EX4 (Figure 4-13) but with a significant reduction in potency (d= 18.94 and 18.07 for GLP-1 and EX4 respectively, $p<0.0004$). Flat activation curves in Figure 4-12 indicated that neither GLP-1 nor EX4 was able to activate rGLP-1R-Trp39 mutant receptor

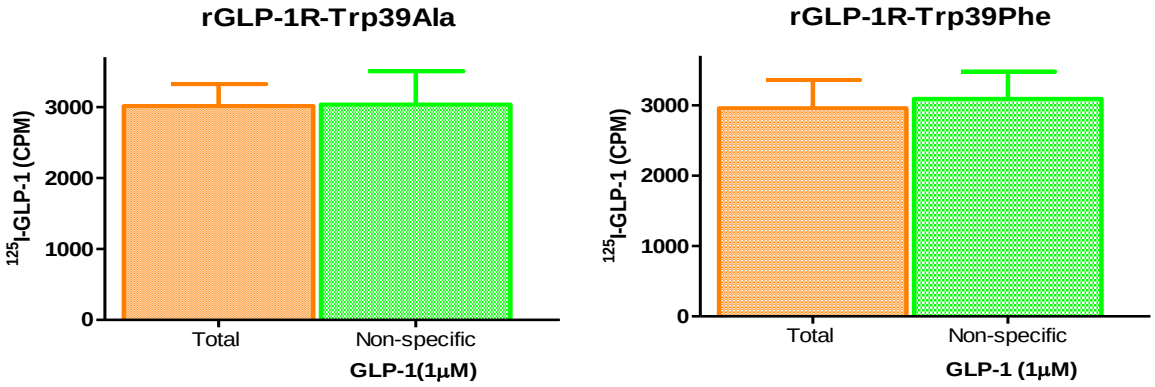

Figure 4-12: Homologous ^{125}I-GLP-1 ligand binding assay at mutants of rGLP-1R-Trp39.

'Total' refers to total binding using 50pM ^{125}I-GLP-1 alone while 'non-specific' refers to non-specific binding using 1µM GLP-1 versus 50 pM ^{125}I-GLP-1.The histogram reveals undetectable binding for the two mutants of rGLP-1R-Trp39.

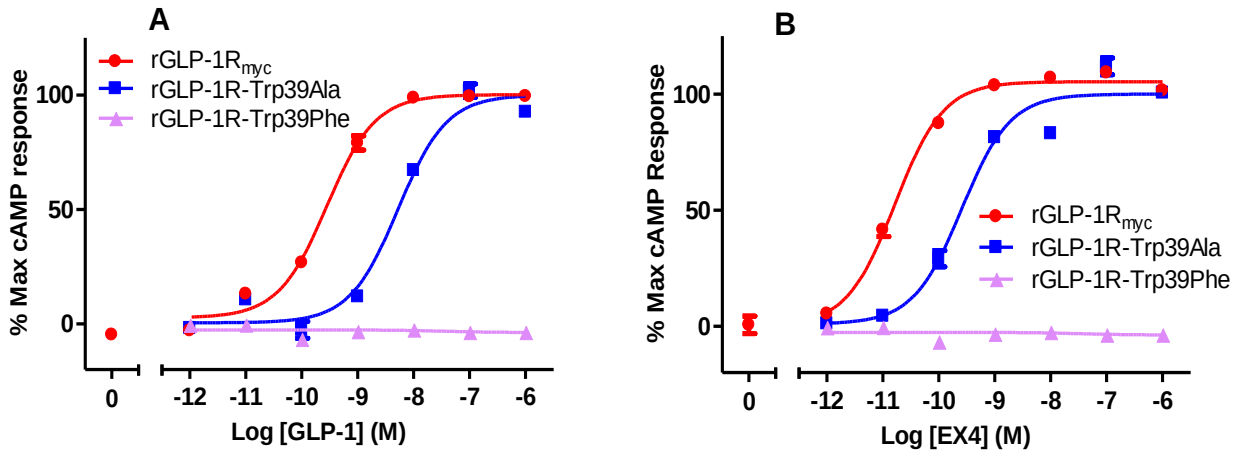

Figure 4-13: Dose response curves of the rGLP-1R-Trp39.

Dose response curves for rGLP-1R$_{myc}$ (●) versus mutants rGLP-1R-Trp39Ala (■) and rGLP-1R-Trp39Phe (▲). Mean pEC$_{50}$ values are given in Table 4-7.

Table 4-7: pEC$_{50}$ values for the rGLP-1R-Trp39 stimulated by either GLP-1 or EX4.

	GLP-1		EX4	
	pEC$_{50}$	**d**	**pEC$_{50}$**	**d**
rGLP-1R$_{myc}$	9.60 ± 0.06		10.74 ± 0.08	
rGLP-1R-Trp39Ala	8.32 ± 0.07	18.94**	9.48 ± 0.06	18.07**

The fold differences highlight significant, p<0.0004, reductions at the rGLP-1R-Trp39Ala mutant on both GLP-1 and EX4 potency.

4.3.2.5 Effect of mutations at rGLP-1R-Tyr69

rGLP-1R-Tyr69 is part of the hydrophobic ligand binding groove (Figure 3-8) (Runge et al., 2008; Underwood et al., 2010). The rGLP-1R-Tyr69 should interact with GLP-1 Val33* and EX4 Lys27**. Mutation of rGLP-1R-Tyr69 could therefore have differential effects on the binding GLP-1 and EX4. To test this hypothesis, rGLP-1R-Tyr69 was mutated to the smaller non-polar amino acid Ala and the hydrophobic amino acid Leu. The data gained after radioligand binding assay showed that both of the mutants were unable to bind 50 pM ^{125}I-GLP-1 (Figure 4-14) and consequently EX4 affinity could not be tested. Likewise, live cells expressing rGLP-1R-Tyr69Ala did not respond to activation by either GLP-1 or EX4. In contrast, the rGLP-1R-Tyr69Leu mutant was able to reach the maximal response, albeit with much lower potency compared to rGLP-1R$_{myc}$, as demonstrated by widely right-shifted curves in Figure 4-15 and pEC$_{50}$ in Table 4-8 (d = 58.79 and 117.49 for GLP-1 and EX4 respectively).

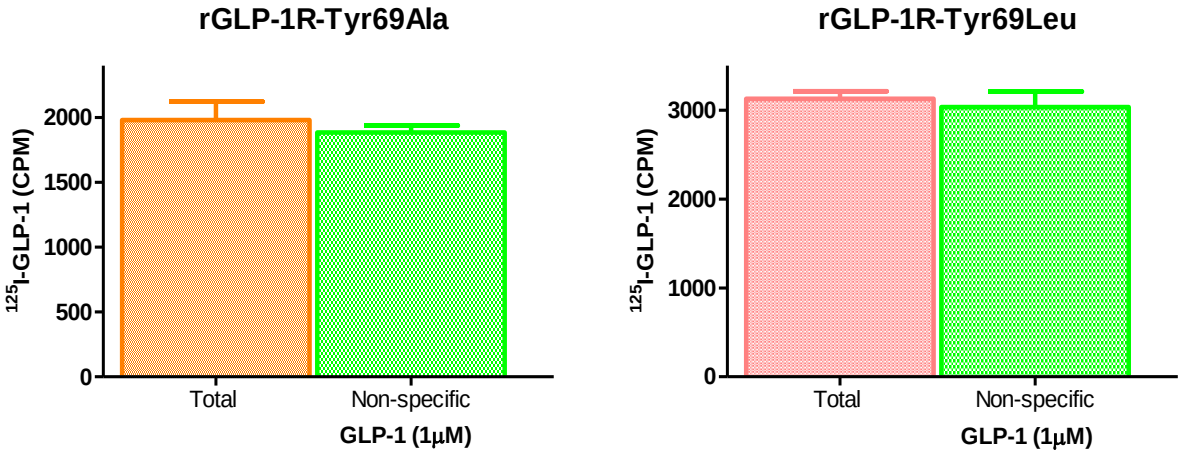

Figure 4-14: Homologous ^{125}I-GLP-1 ligand binding assay of mutants of rGLP-1R-Tyr69.

'Total' refers to total binding using 50pM ^{125}I-GLP-1 alone while 'non-specific' refers to non-specific binding using 1µM GLP-1 versus 50 pM ^{125}I-GLP-1.The histogram reveals undetectable binding for the two mutants of rGLP-1R-Tyr69.

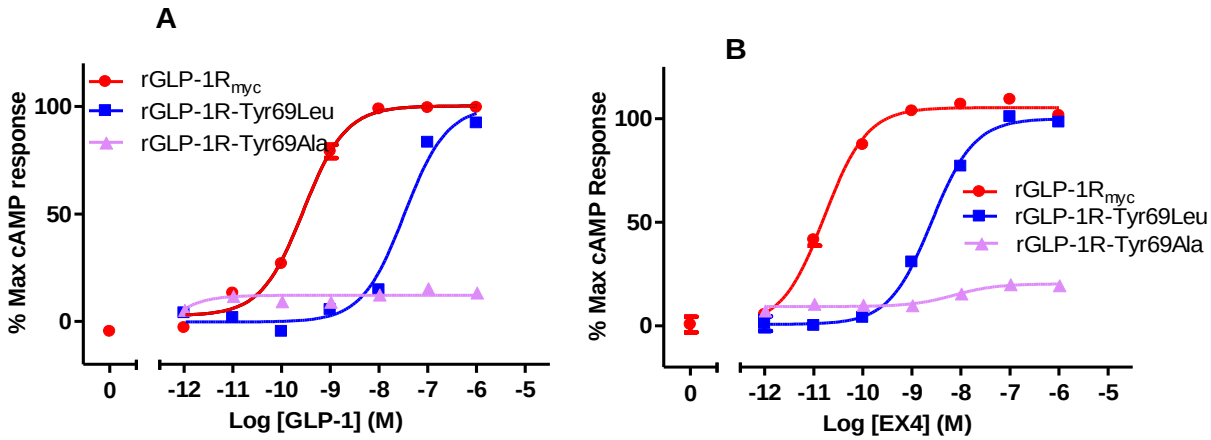

Figure 4-15: Dose response curves of the rGLP-1R-Tyr69 mutants.

Dose response curves for rGLP-1R (●) and mutant rGLP-1R-Tyr69Leu (■), rGLP-1R-Tyr69Ala (▲). Mean pEC_{50} values are given in Table 4-8.

Table 4-8: pEC_{50} values for the rGLP-1R-Tyr69L stimulated by either GLP-1 or EX4.

	GLP-1		EX4	
	pEC_{50}	**d**	**pEC_{50}**	**d**
$rGLP\text{-}1R_{myc}$	9.60 ± 0.06		10.74 ± 0.08	
rGLP-1R-Tyr69L	7.83 ± 0.19**	58.79	8.67 ± 0.17**	117.49

The data shows a significant reduction, $p<0.0006$, in GLP-1 and EX4 potency due to rGLP-1R-Tyr69Leu mutation.

4.3.2.6 Effect of mutations at rGLP-1R-Tyr88

Tyr88 is located within loop 2 of the hGLP-1R-NTD, where it shares in building the hydrophobic binding groove (Figure 1-17 and 3-8) (Runge et al., 2008; Underwood et al., 2010). According to the hGLP-1R-NTD crystal structure, rGLP-1R-Tyr88, like rGLP-1R-Trp39, interacts with Leu32* and Leu 26** in GLP-1 and EX4 respectively. Similar to rGLP-1R-Trp39, the rGLP-1R-Tyr88 mutation could interfere with ligand binding and/or activation. Similar effects on binding of either ligand confirm that the 'H' interaction of the two ligands is equivalent. To investigate this prediction, rGLP-1R-Tyr88 was mutated to give rGLP-1R-Tyr88Ala and rGLP-1R-Tyr88Leu. Both mutant receptors failed to bind 50 pM ^{125}I-GLP-1 and consequently EX4 binding affinity could not be tested (Figure 4-16). Furthermore, neither rGLP-1R-Tyr88Ala nor rGLP-1R-Tyr88Leu could be stimulated for cAMP production, failing to respond to either GLP-1 or EX4 (Figure 4-17).

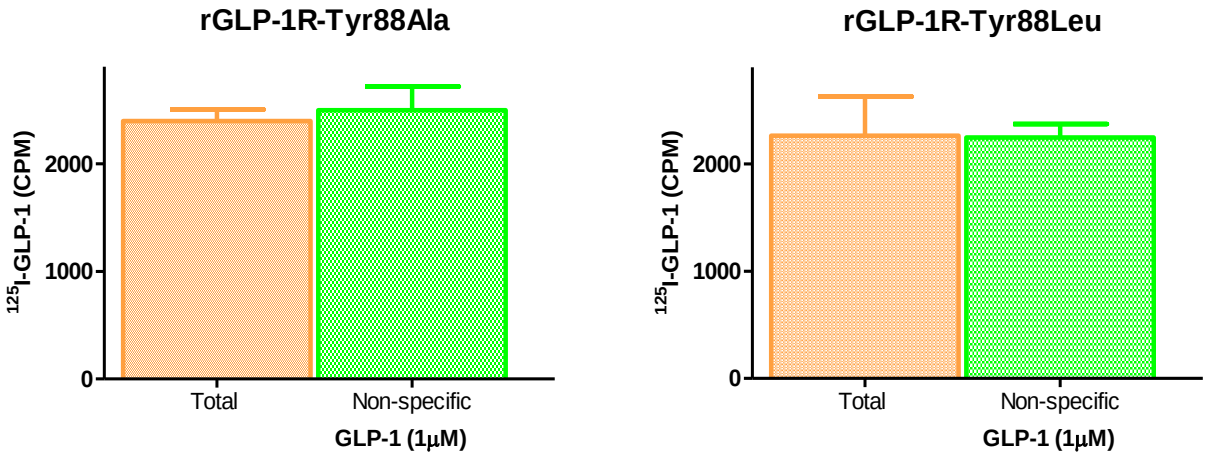

Figure 4-16: Homologous ^{125}I-GLP-1 ligand binding assay of mutants of rGLP-1R-Tyr88.

'Total' refers to total binding using 50 pM ^{125}I-GLP-1 alone while 'non-specific' refers to non-specific binding using 1μM GLP-1 versus 50 pM ^{125}I-GLP-1.The histogram reveals undetectable binding for the two mutants of rGLP-1R-Tyr88.

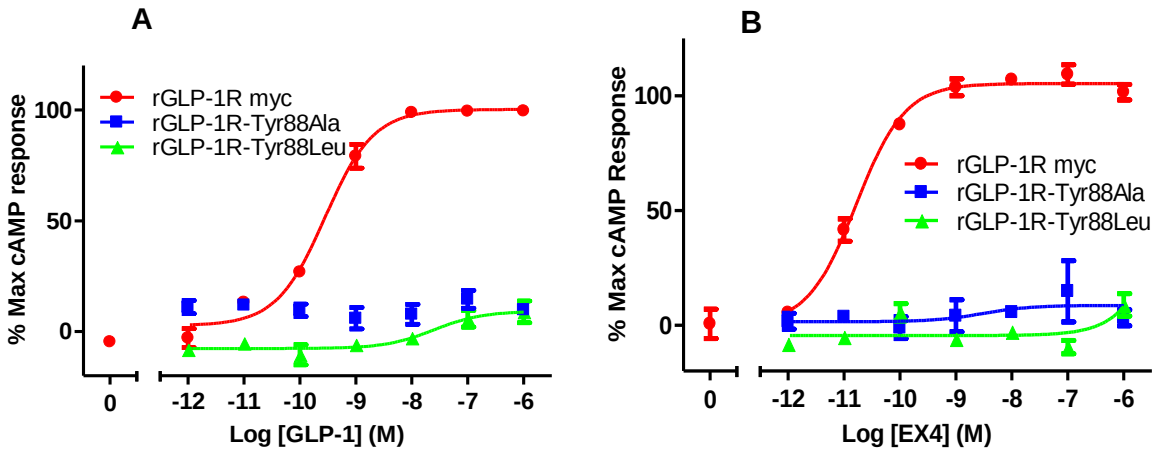

Figure 4-17: Dose response curves of rGLP-1R-Tyr88.

Dose response curves for rGLP-1R$_{myc}$ (●) and mutant rGLP-1R-Tyr88Ala (■) and rGLP-1R-Tyr88Leu (▲). Flat curves indicate undetectable activity of the mutant receptors.

4.3.2.7 Effect of mutations at rGLP-1R-Trp91

Trp91 is located adjacent to rGLP-1R-Tyr88 (Figure 1-17) (Runge et al., 2008, Underwood et al., 2010). It interacts with another conserved residue of the ligands, which is Ile 29* and 23** in GLP-1 and EX4 respectively. Accordingly, if there is no selective interaction with GLP-1 or EX4 it would be a further indication about the similarity of their 'H' interaction, already supported by the effect of mutations to Trp39, Tyr69 and Tyr88. To test this proposal, rGLP-1R-Trp91 was mutated to rGLP-1R-Trp91Ala and rGLP-1R-Trp91Phe and the mutant receptors subjected to radioligand binding analysis using ^{125}I-GLP-1 versus GLP-1; however, the two mutants failed to bind detectable levels of 50 pM ^{125}I-GLP-1 (Figure 4-18). Meanwhile, living cells expressing the rGLP-1R-Trp91Ala and rGLP-1R-Trp91Phe receptors were stimulated by either GLP-1 or EX4. Surprisingly, the potency of either GLP-1 or EX4 was only slightly lower at the rGLP-1R-Trp91Phe mutant compared with rGLP-1R$_{myc}$ (d= 5.31 and 3.96 for GLP-1 and EX4 respectively, $P < 0.05$, Table 4-9). Additionally, the rGLP-1R-Trp91Ala AC response reached the maximal value, although its potency was greatly reduced compared to rGLP-1R$_{myc}$ (Figure 4-19, Table 4-9).

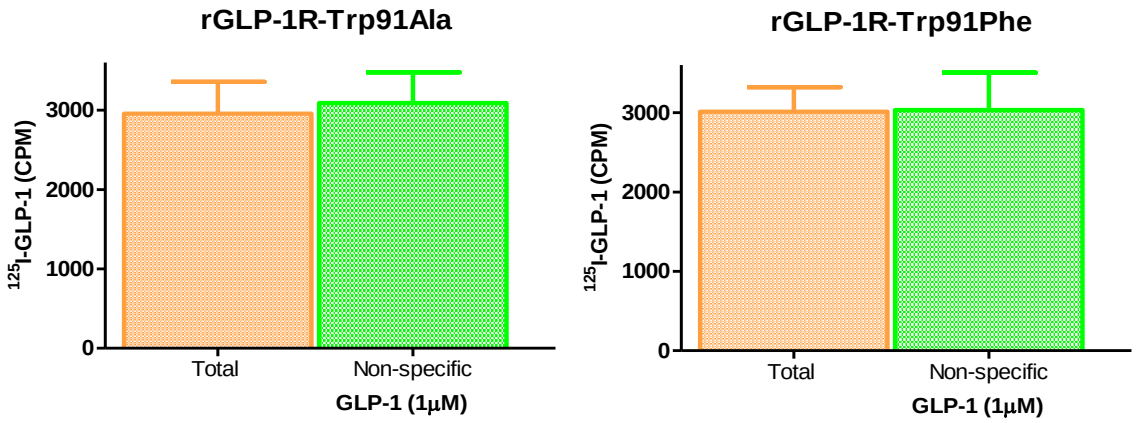

Figure 4-18: Homologous ^{125}I-GLP-1 ligand binding of mutations of the rGLP-1R-Trp91.

'Total' refers to total binding using 50 pM ^{125}I-GLP-1 alone while 'non-specific' refers to non-specific binding using 1µM GLP-1 versus 50 pM ^{125}I-GLP-1.The histogram reveals undetectable binding for the two mutants of rGLP-1R-Trp91.

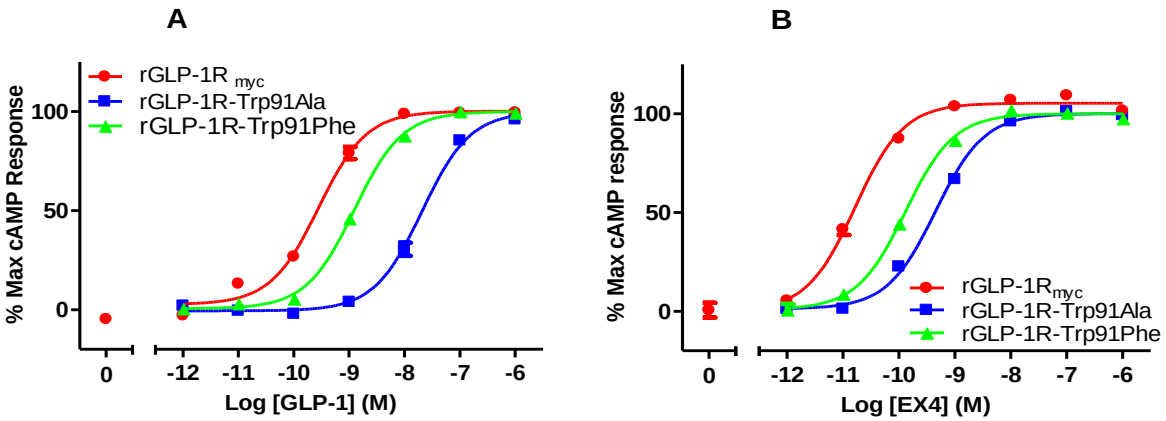

Figure 4-19: Dose response curves of mutants of the rGLP-1R-Trp91.

Dose response curves for rGLP-1R$_{myc}$ (●) and mutant rGLP-1R-Trp91Ala (■) and rGLP-1R-Trp91Phe (▲). Mean pEC$_{50}$ values are given in Table 4-9.

Table 4-9: pEC$_{50}$ values for the rGLP-1R-Trp91 mutants stimulated by either GLP-1 or EX4.

	GLP-1		EX-4	
	pEC$_{50}$	**d**	**pEC$_{50}$**	**d**
rGLP-1R$_{myc}$	9.60 ± 0.06		10.74 ± 0.08	
rGLP-1R-Trp91Ala	7.49 ± 0.10**	129.42	9.27 ± 0.06**	29.81
rGLP-1R-Trp91Phe	8.88 ± 0.14*	5.31	10.14 ± 0.19*	3.96

The fold differences highlight big reduction made by the effect of rGLP-1R-Trp91Ala mutation on either GLP-1 or EX4 potency.

4.3.2.8 Effect of mutations at rGLP-1R-Glu127

Underwood's crystal structure (Underwood et al., 2010) suggested that rGLP-1R-Glu127 interacts with EX4 Lys27** (Figure 1-17) but not with its corresponding GLP-1 residue Val33*. This distinction suggested a possible source of the 'EX' interaction. Accordingly, rGLP-1R-Glu127 was mutated to the smaller amino acid Ala, a negative side chain residue Asp and a neutral polar Gln. Membranes of the mutants were subjected to binding analysis using GLP-1, EX4 and EX4(9-39) versus ^{125}I-GLP-1. The data represented in Figure 4-20 and Table 4-10 show a slight reduction in the affinity of GLP-1 for both of the mutants (d < 5 fold, p<0.05). However, the rGLP-1R-Glu127Ala and rGLP-1R-Glu127Asp mutants displayed EX4 affinity not significantly different from that of rGLP-1R$_{myc}$. The affinity of rGLP-1R-Glu127Gln for EX4 was slightly reduced (d=3.5 fold p>0.1) while a great reduction in affinity was recorded for EX4(9-39) at rGLP-1R-Glu127Gln mutant (d= 18.95 fold, p < 0.01). The activity properties of the rGLP-1R-Glu127 mutant receptors were also analyzed by stimulation of the cells expressing them with either GLP-1 or EX4. According to the data represented by Figure 4-21 and Table 4-11, the rGLP-1R-Glu127 mutants showed similar responses to both EX4 and GLP-1 as the WT rGLP-1R.

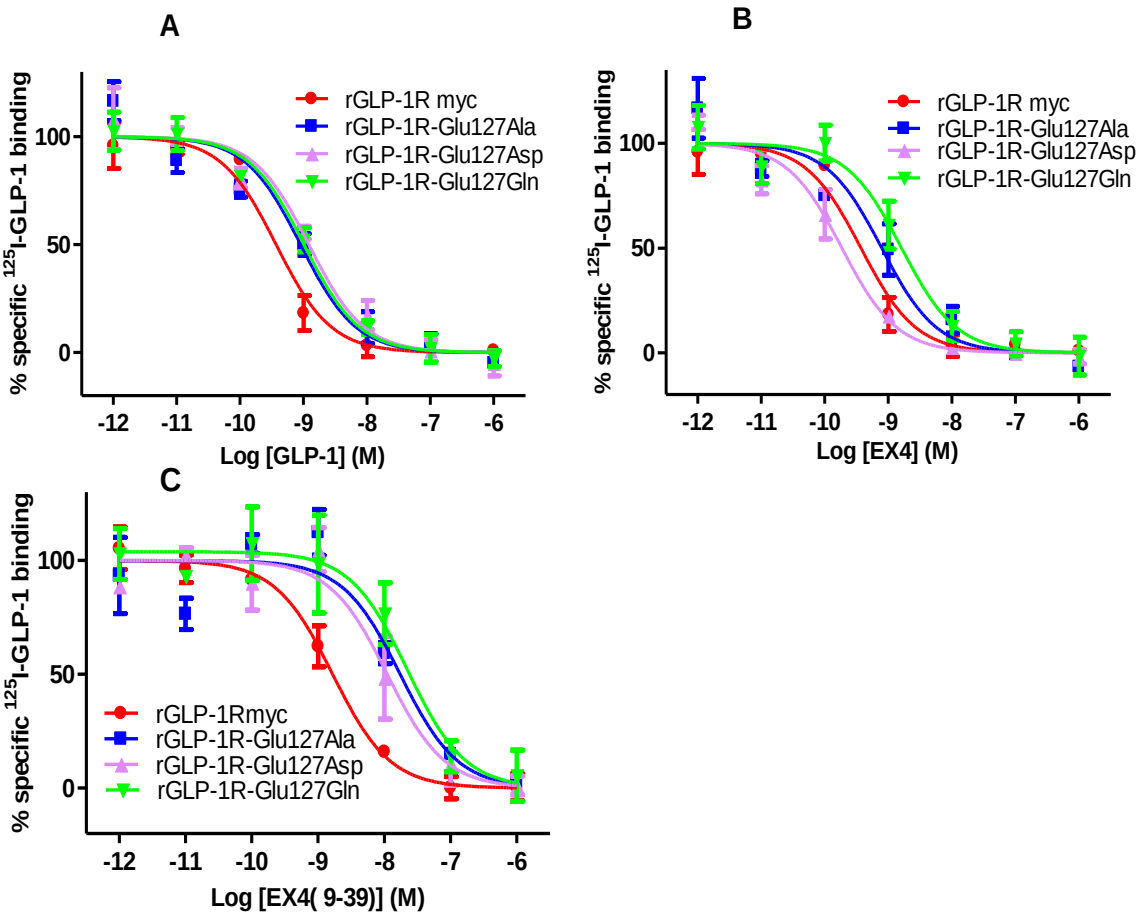

Figure 4-20: Competition-binding curves of GLP-1, EX4 and EX4(9-39) with receptors mutants of the rGLP-1R-Glu127.

^{125}I-GLP-1 competition binding assays for rGLP-1R$_{myc}$ (●) and mutants rGLP-1R-Glu127Ala (■), rGLP-1R-Glu127Asp (▲) and rGLP-1R-Glu127Gln (▼) with (A) GLP-1, (B) EX4 and (C) EX4(9-39). Mean pIC$_{50}$ values are given in Table 4-10.

Table 4-10: pIC$_{50}$ values for ^{125}I-GLP-1 competition binding with GLP-1, EX4 and EX4(9-39) of rGLP-1R-Glu127.

	GLP-1		EX4		EX4(9-39)	
	pIC50	**d**	**pIC50**	**d**	**pIC50**	**d**
rGLP-1R$_{myc}$	9.60 ± 0.13		9.54 ± 0.05		8.46 ± 0.06	
rGLP-1R-Glu127Ala	8.91 ± 0.10*	4.12	9.06 ± 0.19	3.05	7.80 ± 0.19	4.56
rGLP-1R-Glu127Asp	8.99 ± 0.09*	4.94	9.68 ± 0.03	0.73	7.90 ± 0.20	3.67
rGLP-1R-Glu127Gln	8.88 ± 0.07*	4.03	9.00 ± 0.13*	3.50	7.18 ± 0.15**	18.95

The data show there is a slight but statistically significant change in affinity for GLP-1 by both of the three mutants (d< 5 fold) while the same degree by rGLP-1R-Glu127Ala and rGLP-1R-Glu127Gln on affinity for EX4 (d< 4 fold). rGLP-1R-Glu127Gln showed a highly significant reduction, p<0.001, in affinity for EX4(9-39).

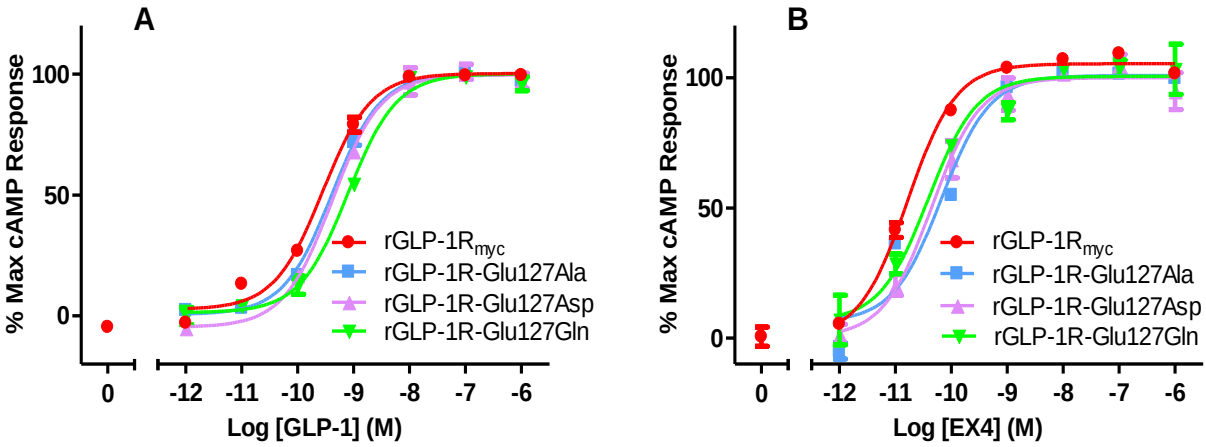

Figure 4-21: Dose response curves of the rGLP-1R-Glu127 mutants.

Dose response curves are for rGLP-1R$_{myc}$ (●) and mutants rGLP-1R-Glu127Ala (■), rGLP-1R-Glu127Asp (▲) and rGLP-1R-Glu127Gln (▼) with (A) GLP-1, (B) EX4. Mean pEC$_{50}$ values are given in Table 4-11.

Table 4-11: pEC$_{50}$ values for the rGLP-1R-Glu127 mutants stimulated by GLP-1 or EX4.

	GLP-1		EX-4	
	pEC$_{50}$	**d**	**pEC$_{50}$**	**d**
rGLP-1R$_{myc}$	9.60 ± 0.06		10.74 ± 0.08	
rGLP-1R-Glu127Ala	9.55 ± 0.10	1.12	10.62 ± 0.15	1.33
rGLP-1R-Glu127Asp	9.39 ± 0.05	1.61	10.41 ± 0.04	2.14
rGLP-1R-Glu127Gln	9.67 ± 0.28	0.86	10.61 ± 0.06	1.34

The data show WT rGLP-1R-like response

4.3.2.9 Effect of mutations at rGLP-1R-Glu128

rGLP-1R-Glu128 was selected and mutated according the same rationale as rGLP-1R-Glu127, since rGLP-1R-Glu128 was also suggested to interact with two non-identical amino acids Arg20** and Lys26* at comparable positions in EX4 and GLP-1 respectively (Figure 1-17). Hence, membranes derived from cells expressing rGLP-1R-Glu128 mutants were used to explore their binding with GLP-1, EX4 and EX4(9-39). According to data represented by Table 4-12 and Figure 4-22, the affinity of GLP-1 was slightly reduced by the rGLP-1R-Glu128Ala and rGLP-1R-Glu128Asp mutations (d= 5 fold, $p< 0.01$) but not by the rGLP-1R-Glu128Gln change (d=1.28, $p>0.1$). Affinity for EX4 was affected by almost the same degree, while none of the mutations could greatly affect the affinity for EX4(9-39). Meanwhile, HEK-293 cells expressing the rGLP-1R-Glu128 mutants were stimulated by either EX4 or GLP-1 to test the effect of mutations on the potency of the ligands but again none of the mutants showed changes greater than their effect on the affinity (Figure 4-22, Table 4-13). pEC_{50} values are not significantly different from those for WT rGLP-1R with either ligand.

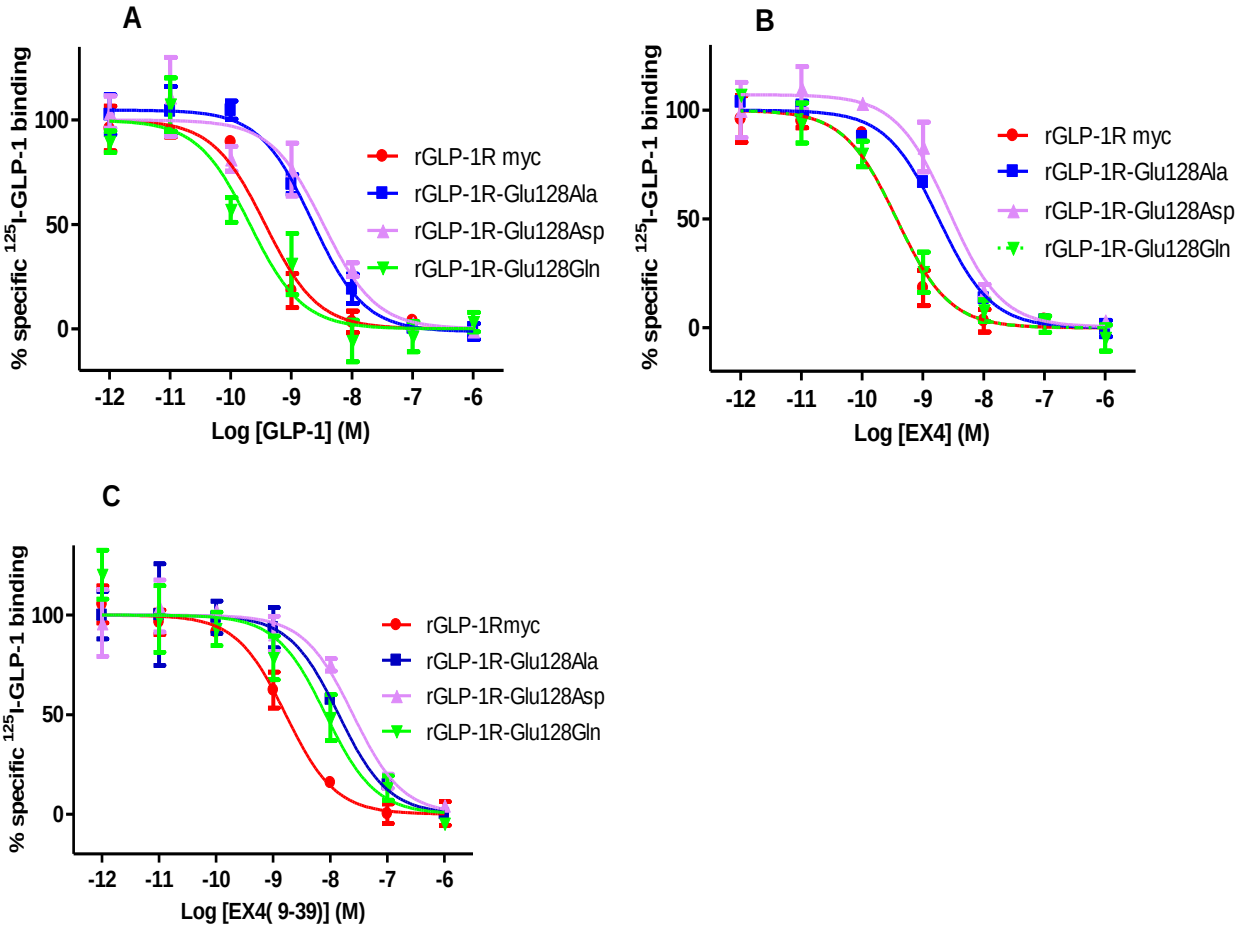

Figure 4-22: Competition-binding curves of GLP-1, EX4 and EX4(9-39) with receptors mutants of the rGLP-1R-Glu128.

^{125}I-GLP-1 competition-binding assays for rGLP-1R (●) and mutants rGLP-1R-Glu128Ala (■), rGLP-1R-Glu128Asp (▲) and rGLP-1R-Glu128Gln (▼) with (A) GLP-1, (B) EX4 and (C) EX4(9-39). Mean pIC_{50} values are given in Table 4-12.

Table 4-12: pIC_{50} values for ^{125}I-GLP-1 competition binding with GLP-1, EX4 and EX4(9-39) of rGLP-1R-Glu128.

	GLP-1		EX4		EX4(9-39)	
	pIC_{50}	d	pIC_{50}	d	pIC_{50}	d
$rGLP\text{-}1R_{myc}$	9.60 ± 0.13		9.54 ± 0.05		8.46 ± 0.06	
rGLP-1R-Glu128Ala	8.88 ± 0.17*	5.24	8.95 ± 0.12*	3.86	8.34 ± 0.25	1.33
rGLP-1R-Glu128Asp	8.90 ± 0.21*	5.04	8.65 ± 0.14**	7.75	7.94 ± 0.06*	3.32
rGLP-1R-Glu128Gln	9.49 ± 0.25	1.28	9.40 ± 0.03	1.39	8.27 ± 0.11	1.57

The data show nearly equal change in the affinity of GLP-1 or EX4 by rGLP-1R-Glu128Ala and rGLP-1R-Glu128Asp (d=5-7 fold) while slight but statistically significant in affinity of EX4 was recorded. There was no change in affinity of the three ligands due to mutations at position rGLP-1R-Glu128Gln.

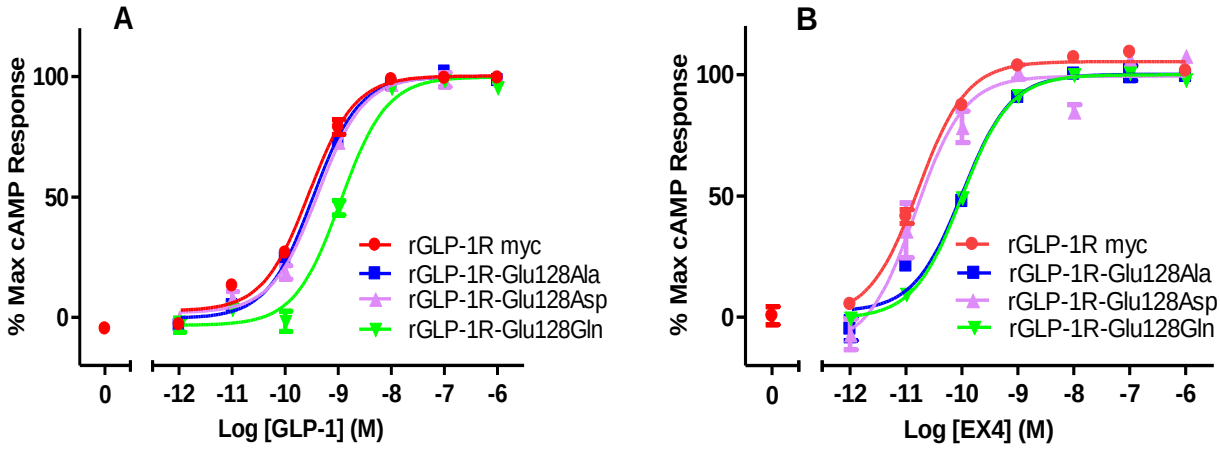

Figure 4-23: Dose response curves of the rGLP-1R-Glu128 mutants.

Dose response curves for rGLP-1R$_{myc}$ (●), mutants rGLP-1R-Glu128Ala (■), rGLP-1R-Glu128Asp (▲) and rGLP-1R-Glu128Gln (▼) with (A) GLP-1, (B) EX4. Mean pEC$_{50}$ values are given in Table 4-13.

Table 4-13: pEC$_{50}$ values for the rGLP-1R-Glu127 mutants stimulated by GLP-1 or EX4.

	GLP-1		EX4	
	pEC$_{50}$	**d**	**pEC$_{50}$**	**d**
rGLP-1R$_{myc}$	9.60 ± 0.06		10.74 ± 0.08	
rGLP-1R-Glu128Ala	9.84 ± 0.19	0.57	10.37 ± 0.20	2.36
rGLP-1R-Glu128Asp	9.36 ± 0.10	1.73	9.96 ± 0.19*	5.98
rGLP-1R-Glu128Gln	9.08 ± 0.20	3.29	10.01 ± 0.21*	5.37

The values highlight the absence of any effect on GLP-1 by rGLP-1R-Glu128Ala and Asp but a slight reduction by rGLP-1R-Glu128Gln, while rGLP-1R-Glu128Asp and Gln reduced EX4 potency significantly ($p < 0.05$).

4.4 Discussion

The failure of protein modelling to provide a reliable model with which to understand EX4's superior affinity directed this study toward other available sources of information. The crystal structure of the GIPR-NTD in complex with GIP became available in 2007 (Parthier et al., 2007), which allowed the planning of a mutagenesis study to characterise the 'EX' interaction. The crystal structures of hGLP-1R-NTD bound to EX4 (9-39) in one study, and to GLP-1 in another, were published after this mutagenesis project has been started (Runge et al., 2008, Underwood et al., 2010). In general, the two hGLP-1R structures showed a common binding mode for EX4 and GLP-1. Hence, the selected group of residues that were mutated, could still be used to identify the 'EX' interaction.

The crystal structure of the hGLP-1R-NTD showed that only segment Glu15**-Asn28** of EX4 is in contact with the NTD, although the ligand forms an α-helix from residues Leu10**-Asn28** (Runge et al., 2008). Similarly, the later crystal structure of GLP-1 bound to the hGLP-1R-NTD showed that GLP-1 forms an α-helix from Thr13*-Val33* with only Ala24*-Val33* contacting the NTD (Underwood et al., 2010).

Accordingly, Val30 should interact with Glu15** and Glu16** of EX4 and not GLP-1 and would be responsible for the differential affinity of EX4. However, the recorded results showed that mutation of this residue reduced GLP-1 affinity but had no effect on affinity of EX4 or EX4(9-39) suggesting that rGLP-1R-Val30 does not participate in the 'EX' interaction. Mutants with changes to rGLP-1R-Thr35 showed no reduction in affinity for either GLP-1 or EX4, although this position (according to Runge's crystal structure) should be part of the hydrophobic binding cavity and interact with the important Phe residue, which is conserved in GLP-1(Phe28*) and EX4 (Phe22**) respectively. Likewise, a mutant receptor

containing a substitution of rGLP-1R-Thr35 for Ala showed no discrimination between GLP-1 and EX4 (Underwood et al., 2010)

The results recorded for receptor with mutations at rGLP-1R-Val36, as well as rGLP-1R-Trp39, rGLP-1R-Tyr88 and rGLP-1R-Trp91, emphasised the identical interactions made by conserved residues in both EX4 and GLP-1 with the NTD, in an agreement with other reported observations (Underwood et al., 2010). Nevertheless, the observations enabled a ranking of the importance of each residue in that group. The unchanged ligand binding and activation characteristics at the rGLP-1R-Val36Ala compared to non-mutated rGLP-1R$_{myc,}$ indicated a non-essential interaction formed by this residue with either GLP-1 or EX4. The ineffective mutation of rGLP-1R-Val36 seemes consistent with mutagenesis work that accompanied the crystallization of the hGLP-1R-NTD bound to GLP-1 (Underwood et al., 2010). In contrast to rGLP-1R-Val36, rGLP-1R-Trp39 and rGLP-1R-Trp91 were important for ligand binding as their mutation strongly interfered with binding of GLP-1. The binding results are in agreement with previously published studies about the importance of tryptophans in the GLP-1R-NTD for GLP-1 binding (Van Eyll et al., 1996, Wilmen et al., 1997). The reduced activity recorded for some mutated receptors (rGLP-1R-Trp39Ala, rGLP-1R-Trp91Ala, and rGLP-1R-Trp91Phe mutants) could indicate normal expression of the mutated receptors but with an impaired function that is not ligand selective.

The same observations of undetectable binding and reduced activation were made with rGLP-1R-Tyr88, consistent with the description of EX4/NTD crystal structure in which rGLP-1R-Tyr88, rGLP-1R-Trp91 and rGLP-1R-Trp39 were included in the hydrophobic binding cavity with the ligand (Figures 1-17 and 3-8) (Runge et al., 2008).

Binding and activity analysis of rGLP-1R-Tyr69 mutants reinforced the view of a common 'H' interaction in EX4 and GLP-1. Moreover, despite binding to non-conserved GLP-1 Val33* and EX4 Lys27**, rGLP-1R-Tyr69 makes similar interactions with both, in addition to rGLP-1R-Leu123 (Runge et al., 2008). rGLP-1R-Tyr69 is involved in the structure of the hydrophobic binding cavity with the ligand (Figures 1-17 and 3-8) (Runge et al., 2008). Disruption of the hydrophic cavity by introduction of the mutations rGLP-1R-Tyr69Ala and rGLP-1R-Tyr69Leu would explain failure to bind either EX4 or GLP-1. Also, the absence of binding could be a consequence of disturbed receptor structure because rGLP-1R-Tyr69 interacts with the side chain and backbone of the absolutely conserved Asp67, stabilizing the turn between β1 and β2 (Runge et al., 2008). The observed failure to be selective for a particular ligand by rGLP-1R-Tyr69Leu could be due to increased hydrophobicity by Leu over Ala that was sufficient for detection of ligand activity but not for binding. Alternatively, the ligand affinity for the rGLP-1R-Tyr69Leu and rGLP-1R-Tyr69Ala is too weak to be detected by the applied method.

The crystal structure for the hGLP-1R-NTD (Runge et al., 2008) has disclosed more ligand interaction between the side chains of rGLP-1R-Glu127 and EX4 Lys27**. In contrast, this interaction is not possible for GLP-1 because the corresponding residue Val33* is unable to interact with rGLP-1R-Glu127, leading to loss of the water molecule observed with EX4 (Underwood et al., 2010). Consequently, rGLP-1R-Glu127 mutation should strongly contribute to differential binding of EX4 or GLP-1. Apart from significantly reduced affinity for EX4(9-39) by the rGLP-1R-Glu127Gln mutant, the other binding data appeared similar to WT controls for the tested ligands, limiting the importance of the rGLP-1R-Glu127 interaction to the short version of EX4. Likewise, none of the mutants influenced

the activity of either EX4 or GLP-1 similar to the observations of other workers (Underwood et al., 2010).

Although rGLP-1R-Glu128 should interact with two different residues GLP-1 Lys26* and EX4 Arg20**, rGLP-1R-Glu128 did not show discriminatory affinity between the three tested ligands. Furthermore, the non-selective decrease in binding to rGLP-1R-Glu128Ala and rGLP-1R-Glu128Asp, as well as negligible decrease for the rGLP-1R-Glu128Gln mutant, revealed the importance of the residue volume over its negative charge. In addition, the absence of differential affinity for GLP-1 or EX4 could be due to equal positive charge of GLP-1 Lys26* and EX4 Arg20** (Underwood et al., 2010). Consequently, the three mutants of rGLP-1R-Glu128 demonstrated a neutral effect upon either GLP-1 or EX4 stimulation, not significantly different from WT receptor with either ligand.

The data seem in agreement with other published studies, particularly regarding the non-binding mutants (Van Eyll et al., 1996, Wilmen et al., 1997). It could therefore be predicted that the orientation of the 'H' interaction for both EX4 and GLP-1 would be similar, since mutations of their non-conserved residues did not display highly differential affinity with the NTD of the target receptor.

In fact, even the decrease in affinity for EX4(9-39) shown by some mutants did not take affinity down to the level recorded for the C-terminal nine residues deficient EX4(9-30) or its equivalent length GLP-1(15-36) (pIC_{50} 6.3 and 6.8) (Al-Sabah and Donnelly, 2003a). Consequently, attention focused on the C-terminus of EX4. Since species differences of rGLP-1R have been excluded by focusing on conserved residues, it could also be useful if the species-different residues were investigated.

5 - Determining of 'EX' interaction based on hydrogen bond from Ser32**-EX4.

5.1 Introduction and strategy

As previously introduced, EX4 has an extra nine residues (31-39) that form its C-terminal extension, with no equivalent in GLP-1 (Figure 4-1) (Al-Sabah and Donnelly, 2003a). A previous binding analysis carried out by Donnelly's group using the rGLP-1R showed that the deletion of residues 31-39 of EX4 resulted in a 25-fold reduction in binding affinity to the rGLP-1R-NTD (Al-Sabah and Donnelly, 2003a). EX4 has a superior affinity over GLP-1 and can maintain high affinity with the expressed NTD even after deletion of up to 8 residues from its N-terminus (Lopez de Maturana et al., 2003). Al-Sabah and Donnelly proposed a model for the super-affinity of EX4 whereby it formed an 'EX' interaction between its C-terminal extension and the NTD.

In a hydrophobic environment, the C-terminus of EX4 has been shown to form part of a compact folding unit called a 'Trp-cage' (Neidigh et al., 2001). It was therefore speculated that the involvement of residues EX4(31-39) in forming the 'EX' interaction may be mediated via such a Trp-cage motif. However, more recent work has suggested that, although present in artificial mini-proteins designed from EX4 (Barua et al., 2008), the Trp-cage is unlikely to form in receptor-bound EX4 itself (Runge et al., 2008).

Furthermore, the involvement of residues EX4(31-39) in forming the 'EX' interaction has been questioned since a subsequent combination of pharmacological and biophysical approaches demonstrated that the removal of this C-terminal region had no effect upon binding to the hGLP-1R (Runge et al., 2007).

Taken together, the aim of the work described here was to investigate the reason for these apparent contradictions in the literature regarding the role of the C- terminal extension of EX4 in receptor binding. In doing so, the aim was to understand the peptide-receptor interaction further, such that the design of higher affinity analogues can be envisaged. Firstly it was hypothesised, and then was demonstrated, that the apparent contradictions were rooted in the species variability between receptors (rat and human GLP-1R cDNA were used in previous studies). The crystal structure of EX4(9-39) bound to the hGLP-1R-NTD was then used to locate potential species-specific interactions between GLP-1R and the C-terminal extension of EX4(9-39). In this way, an interaction between Glu68 in hGLP-1R (Asp in rGLP-1R) and Ser32** in EX4(9-39) was identified and further investigated via receptor mutagenesis and ligand modification, coupled with pharmacological characterisation. This work was carried out in parallel to some related work carried out by Dr Ros Mann in the lab of Dr Dan Donnelly at Leeds. All the cell lines expressing mutant hGLP-1Rs were made by Dr. Mann, as were those for rNT-TM1 and hNT-TM1. In addition, with the exception of the data shown in this chapter, all the competitive radioactive binding analysis using ^{125}I-EX4(9-39) were carried out by Dr. Mann. On the other hand, I made all the mutants of rGLP-1R and carried out all of the competitive radioactive binding assays using ^{125}I-GLP-1. While the ^{125}I-GLP-1 and ^{125}I-EX4(9-39) binding assays led to the same conclusions, only the latter were used in our publication (Mann et al., 2010b) in order to maintain consistency, since only ^{125}I-EX4(9-39) binds to rNT-TM1 and hNT-TM1. Additionally, Dr E. Paci kindly carried out the molecular dynamics simulation. Hence, while I was donated the cell lines for rNT-TM1, hNT-TM1, hGLP-1R and its mutants, I made all the rGLP-1R mutants and cell lines and I carried out all the cell culture and the binding assays.

5.2 Methodological considerations

5.2.1 Peptides

In order to perform a comparative study, a group of normal, modified, full-length and truncated EX4 and GLP-1 analogues have been used as shown in Figure 5-1.

```
GLP-1              HAEGTFTSDVSSYLEGQAAKEFIAWLVKGR
EX4(9-30)                  DLSKQMEEEAVRLFIEWLKNGG
EX4(9-39)                  DLSKQMEEEAVRLFIEWLKNGGPSSGAPPPS
Ala32-EX4(9-39)            DLSKQMEEEAVRLFIEWLKNGGPASGAPPPS
EX4                HGEGTFTSDLSKQMEEEAVRLFIEWLKNGGPSSGAPPPS
```

Figure 5-1: Alignment of the used peptides.

The exchanged amino acids are underlined.

5.2.2 Radiolabelled tracer

An alternative to ^{125}I-GLP-1, ^{125}I-EX4(9-39) was used as a tracer at the rat or human NTD anchored in the membrane by trans-membrane helix 1 (rNT-TM1 and hNT-TM1) because rNT-TM1 and hNT-TM1 have too low affinity for GLP-1 to be used as a tracer.

5.3 Results

5.3.1 Preparation of mutant receptor

The rGLP-1R-Asp68Glu mutant was prepared as stated in section 3.1 and was stably expressed in HEK-239 cells then their crude membrane preparations and live cells were used in affinity and AC activity assays respectively.

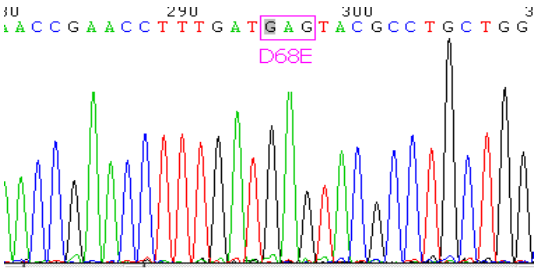

Figure 5-2: Sections of the nucleotide sequence of rGLP-1R-Asp68Glu mutant receptor cDNA.

The mutated codon is highlighted by a pink square.

5.3.2 Ligand binding analysis

5.3.2.1 Assessment of GLP-1 binding mutant receptors

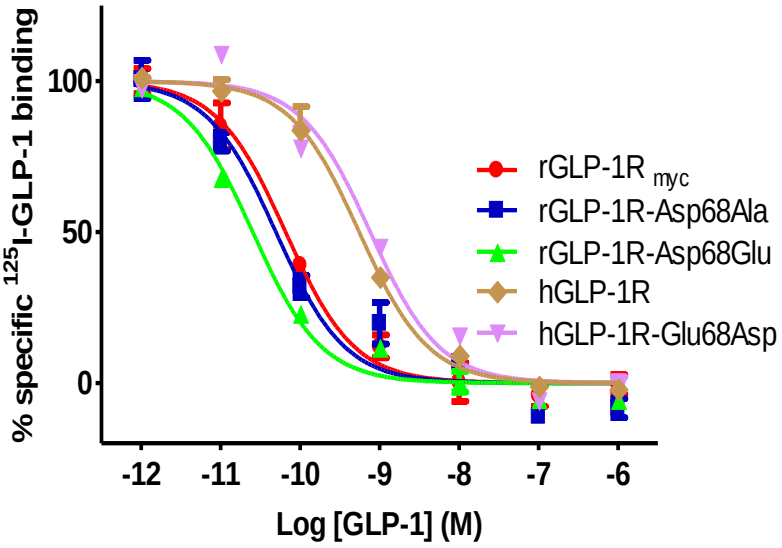

Figure 5-3: Competition radioligand binding assay with GLP-1 as a natural ligand for rat/human GLP-1R and Asp68/Glu68 mutant recceptors

Membranes prepared from HEK-293 cells expressing individually all receptors to be used for investigation were tested by radioactive competitive binding assay using natural ligand GLP-1 versus ^{125}I-GLP-1. Both WTs and their mutants showed normal binding function as reflected by normal ranges of pIC_{50} showed in Table 5-1.

Table 5-1: pIC_{50} values for ^{125}I-GLP-1 competition binding with GLP-1 as a naturalligand for rat/human GLP-1R and Asp68/Glu68 mutant recceptors

	rGLP-1R$_{myc}$	rGLP-1R-Asp68Glu	rGLP-1R-Asp68Ala	hGLP-1R	hGLP1R-Glu68Asp
GLP-1 pIC_{50}	9.51 ± 0.10	10.59 ± 0.03	10.22 ± 0.25	9.06 ± 0.12	8.92 ± 0.10

5.3.2.2 Species preference owing to single amino acid exchange rGLP-1RAsp68Glu

The importance of nine amino acid extension in EX4(9-39) and its involvement in ligand affinity discrimination by the rat and human rGLP-1R was tested by using ^{125}I-GLP-1 as a tracer to compete with either EX4(9-39), EX4(9-30) or Ala32-EX4(9-39) in membrane preparations of HEK-293 cells expressing either rat or human WT of receptors . Likewise, the two homologous mutants

hGLP-1RGlu68Asp and rGLP-1R-Asp68Glu were tested. The data obtained are represented in Figure 5-4 and Table 5-2. The WT rGLP-1R showed significantly reduced affinity for EX4(9-30) and Ala32-EX4(9-39) (11.67 and 9.21 fold respectively, $p<0.05$) compared to EX4(9-39). Crucially, the hGLP1R-Glu68Asp that 'mimicks' the rGLP-1R showed a similar decrease in affinity for EX4(9-30) and Ala32-EX4(9-39) (Tabl 5-2)

On the other hand, the three analogues of exendins looked to have the same affinity for hGLP-1R and for the 'human receptor mimicks' rGLP-1R-Asp68Glu (0.96 and 1.59 fold respectively $P>0.1$) (Table 5-2). Consistent with these observations, rGLP-1R-Asp68Ala showed no significant difference in affinity ($d> 5$ fold, $p> 0.1$) for the three-exendin forms (Figure 5-5).

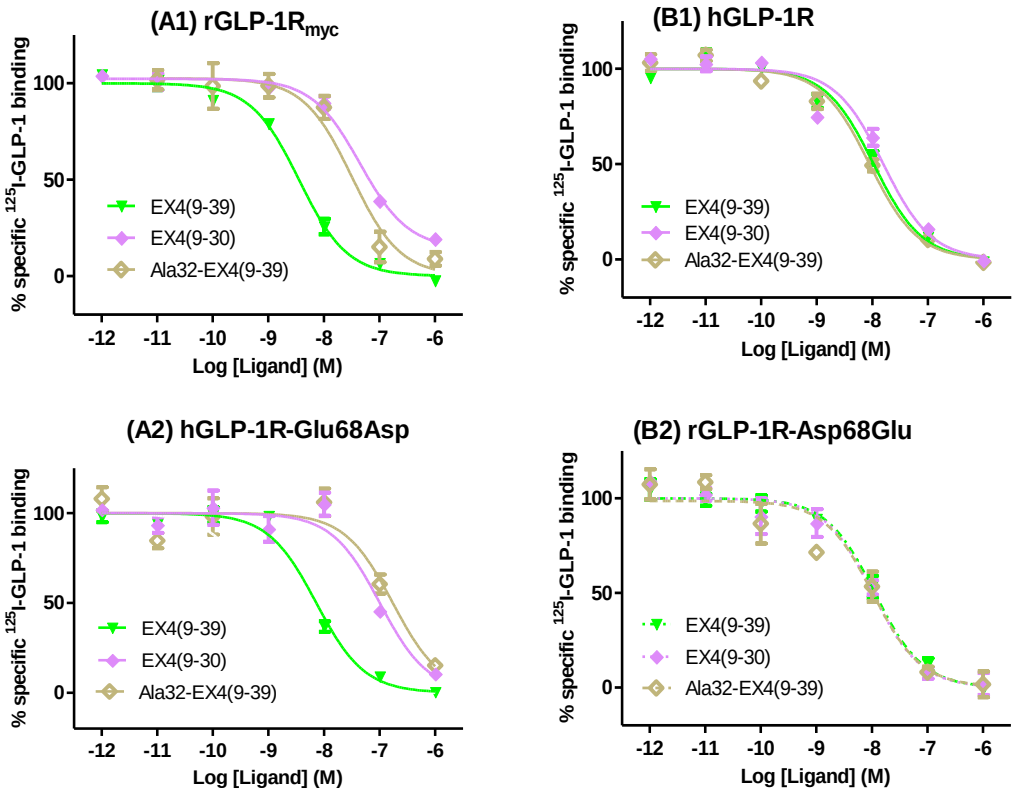

Figure 5-4: Competition binding curves showing species selectivity of EX4(9-39).

^{125}I-GLP-1 competition-binding assays were assessed in membrane preparation of HEK-293 cells expressing WT or mutated receptors with either deletion of 31-39 from EX4(9-39) (▼) as EX4(9-30) (♦) or substitution of Ser32 by Ala(◊). pIC_{50} values are given in Table 5-2.

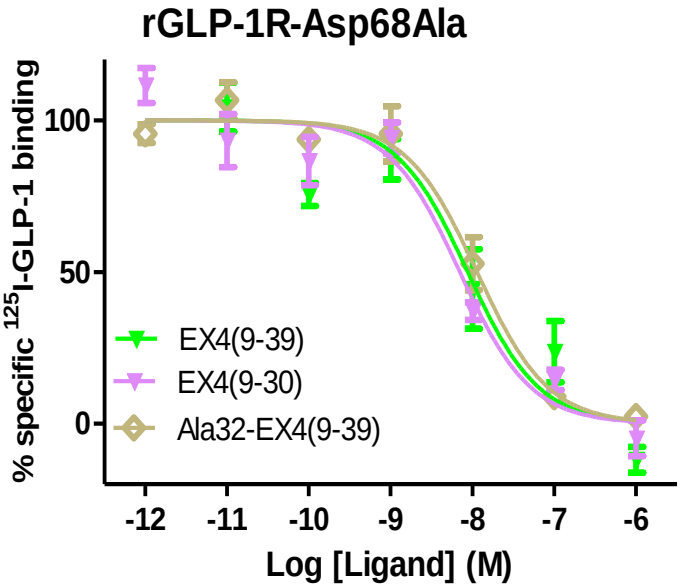

Figure 5-5: Competition binding curves of GLP-1, EX4 and EX4(9-39) with receptors mutants of the rGLP-1R-Asp68Ala.

^{125}I-GLP-1 competition-binding assays were assessed in membrane preparation of HEK-293 cells expressing rGLP-1R- Asp68Ala.

Table 5-2: pIC_{50} values for ^{125}I-GLP-1 competition binding with EX4(9-39), EX4(9-30) and Ala32-EX4(9-39) of rGLP-1R, rGLP-1R-Asp68Glu, rGLP-1R-Asp68Ala, hGLP-1R and hGLP1R-Glu68Asp .

	pIC_{50}				
	EX4(9-39)	**EX4(9-30)**	**Ala32-EX4(9-39)**	**d1**	**d2**
rGLP-1R	8.54 ± 0.14	7.47 ± 0.23*	7.58 ± 0.14*	11.76	9.21
rGLP-1R-Asp68Glu	7.99 ± 0.03	7.99 ± 0.04	7.90 ± 0.16	1.0	1.23
rGLP-1R-Asp68Ala	8.44 ± 0.19	7.99 ± 0.12	8.11 ± 0.05	2.82	2.15
hGLP-1R	8.01 ± 0.06	8.03 ± 0.13	7.81 ± 0 .21	0.96	1.59
hGLP1R-Glu68Asp	8.41 ± 0.18	7.57 ± 0.05*	7.41 ± 0.09*	6.37	13.75

Values represent mean pIC_{50} values ± s.e. for three independent competition binding assays using EX4(9-39), EX4(9-30) and Ala32-EX4(9-39) as the unlabelled ligands with ^{125}I-GLP-1 as the tracer. d1 refers to the fold-change in mean pIC_{50} values of EX4(9-30) relative to EX4(9-39), and d2 refers to the fold-change in mean pIC_{50} values of Ala32-EX4(9-39) relative to EX4(9-39). * $P < 0.05$, ** $P < 0.01$.

5.3.2.3 The rat or human receptor NTD anchored in the membrane with trans-membrane helix 1 (rNT-TM1 and hNT-TM1)

Receptors consisting of the NTD of either the rat or human receptor that were anchored in the membrane with trans-membrane helix 1 (rNT-TM1 and hNT-TM1) were also tested for sensitivity of their ligand binding to the removal of the C-terminal extension of EX4 (Figure 5-6 and Table 5-3). The data demonstrated the same effects observed with the full- length receptors (1.43 fold reduction in affinity at hNT-TM1 and 9.33 fold at rNT-TM1, $p<0.004$) indicating that residues 31-39 of EX4 interact with the rGLP-1R-NTD. Similarly, a slight difference between affinities for EX4 and EX4(1-32), as well as 7.9-fold ($p<0.004$) decrease by substituting Ser32Ala, revealed that Ser32 is also involved in this interaction. An alternative to ^{125}I-GLP-1, ^{125}I-EX4(9-39) was used as a tracer because those two receptors structures have too low affinity for GLP-1 for this to be used as a tracer.

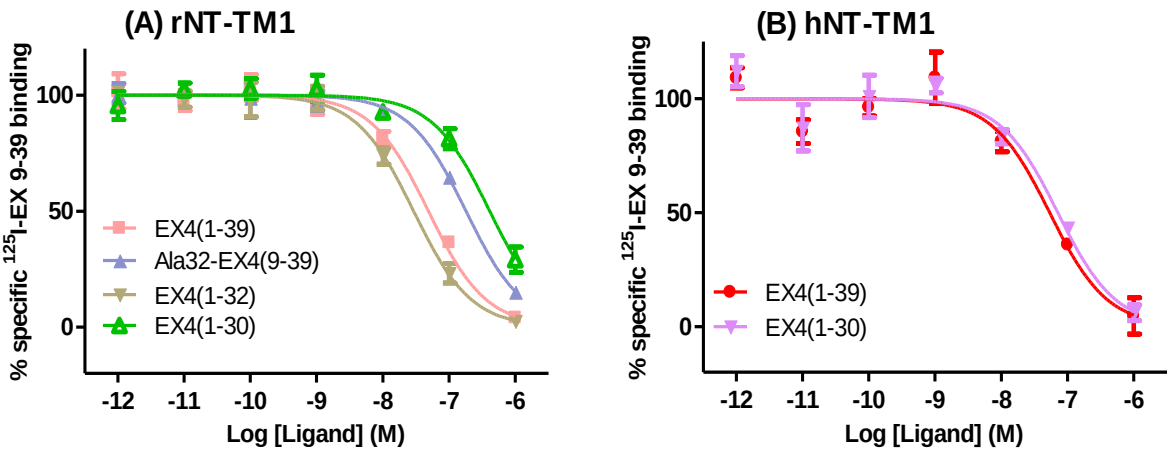

Figure 5-6: Competition binding curves of rNT-TM1, hNT-TM1.
Competitive radioligand binding experiments using ^{125}I-EX4(9-39) as a tracer and either EX4**,** EX4(1-32) with (A) rNT-TM1, (B) hNT-TM1. The receptors derived from rat are highly sensitive to the removal of the C-terminal extension of EX4 while those from human are not.

Table 5-3: pIC_{50} values for ^{125}I-EX4(9-39) competition-binding with rNT-TM1 and hNT-TM1 for EX4, EX4(1-32), Ala32-EX4(9-39) and EX4(1-30).

	rNT-TM1		hNT-TM1	
	pIC_{50}	**d**	**pIC_{50}**	**d**
EX4	7.57 ± 0.13		7.31 ± 0.05	
EX4(1-32)	7.42 ± 0.10	1.42	ND	
Ala32-EX4(9-39)	6.67 ± 0.08**	7.94	ND	
EX4(1-30)	6.60 ± 0.13**	9.33	7.02 ± 0.10	1.93

d refers to the fold-change in mean pIC_{50} values of EX4(1-32), Ala32-EX4(9-39) and EX4(1-30) relative to EX4. * $P < 0.05$, ** $P < 0.01$

5.3.2.4 Contribution of another rat-human homolog rGLP-1R-Ser33Trp

The residue hGLP-1R-Trp33 has been reported before as a main determinant in the interaction between hGLP-1R and its non-peptide antagonist T-0632 (Tibaduiza et al., 2001). Furthermore, the same study demonstrated that mutation of hGLP-1R-Trp33 to its rat homolog rGLP-1R-Ser33 (hGLP-1R-Trp33Ser) could prevent species selection by T-0632. Mutation of rGLP-1R-Ser33 to Trp was carried out to explore whether this change could prevent species preference for the EX4 C-terminus. Firstly, the molecular biology work was carried out as in section 3.1 and confirmation of the mutation sequence is shown in Figure 5-7.

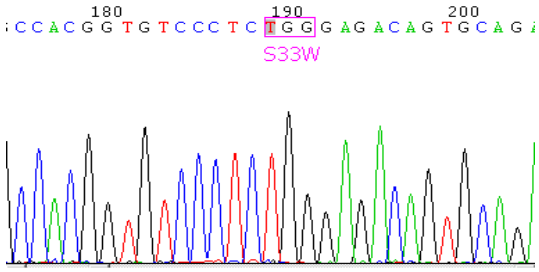

Figure 5-7: Nucleotide sequence of rGLP-1R-Ser33Trp mutant cDNA
Mutated codon is highlighted by pink rectangle.

Membranes prepared from HEK-293 expressing rGLP-1R-Ser33Trp were tested by competitive radioactive binding assay using GLP-1, EX4 and EX4(9-39) versus ^{125}I-GLP-1. The data are shown in Figure 5-8 and Table 5-4. In general the mutation caused some small but statistically significant decreas in affinity for all ligands (<5 fold) (Table 5-4).

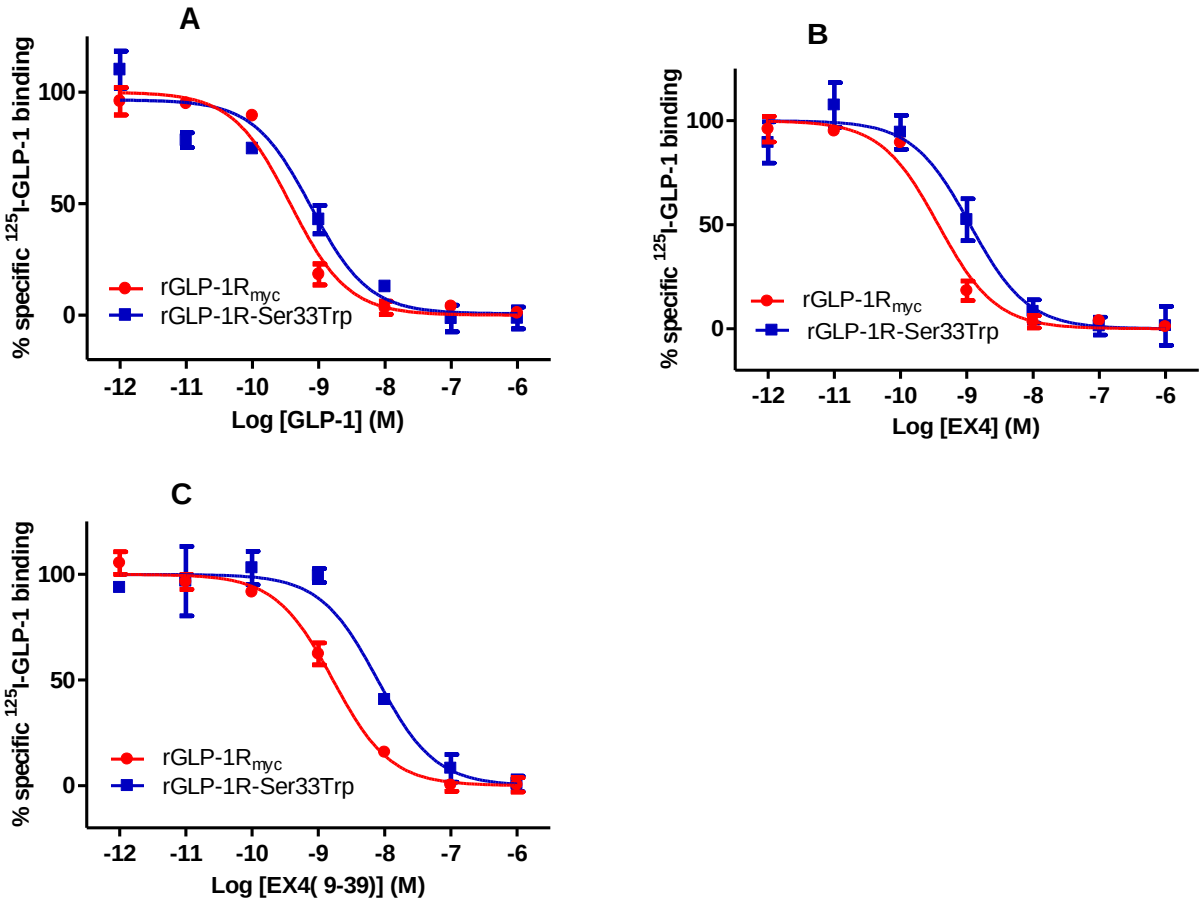

Figure 5-8: Competition-binding curves for GLP-1, EX4 and EX4(9-39) with the rGLP-1R-Ser33Trp.

^{125}I-GLP-1 competition-binding assays for rGLP-1R and mutant rGLP-1R-Ser33Trp with (A) GLP-1, (B) EX4 and (C) EX4(9-39). The curves represent pIC_{50} values from Table 5-4.

Table 5-4: pIC_{50} values for ^{125}I-GLP-1 competition binding with GLP-1, EX4 and EX4(9-39) for the rGLP-1R-Ser33Trp.

	GLP-1		EX4		EX4(9-39)	
	pIC_{50}	**d**	**pIC_{50}**	**d**	**pIC_{50}**	**d**
rGLP-1R$_{myc}$	9.60 ± 0.13		9.54 ± 0.05		8.46 ± 0.06	
rGLP-1R-Ser33Trp	8.98 ± 0.09**	4.21	9.05 ± 0.05**	3.12	7.91 ± 0.11*	3.59

The data shows reduction in affinity with GLP-1, EX4 or EX4(9-39) due to mutations at position rGLP-1R-Ser33Trp. * P < 0.05, ** P < 0.01.

In addition, the activity of the rGLP-1R-Ser33Trp mutant was tested by LANCE™ assay. The effect of the mutation on AC was similar to its effect on affinity; the mutation maintains its neutral effect similar to WT rGLP-1R (Figure 5-9 and Table 5-5).

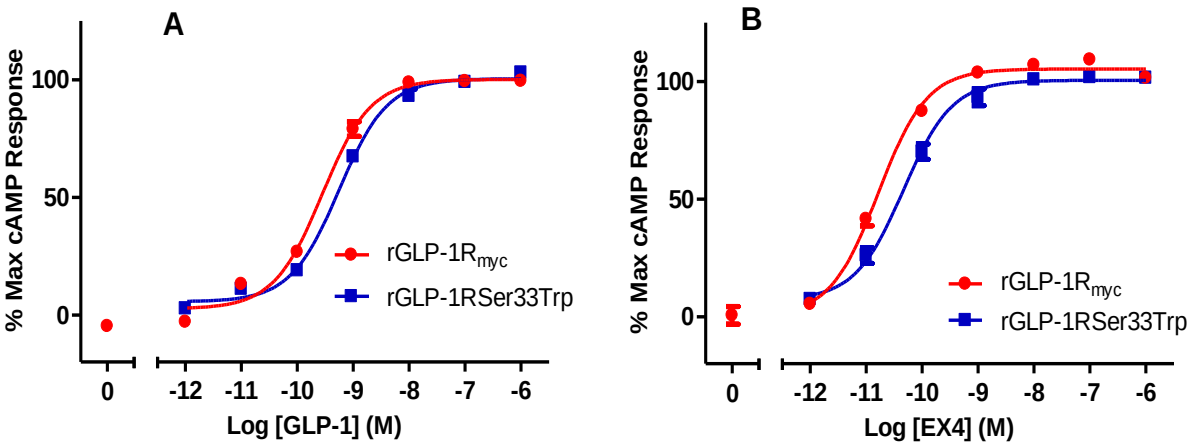

Figure 5-9: Dose response curves of the rGLP-1R-Ser33Trp.

Dose response curves for activation of rGLP-1R$_{myc}$(●) and its mutant at position rGLP-1R-Ser33Trp(■) by (A) GLP-1, (B) EX4. The curves represent pEC$_{50}$ values from Table 5-5.

Table 5-5: pEC$_{50}$ values for the rGLP-1R-Ser33Trp stimulated by GLP-1 or EX4.

	GLP-1		EX4	
	pEC$_{50}$	**d**	**pEC$_{50}$**	**d**
rGLP-1R$_{myc}$	9.60 ± 0.06		10.74 ± 0.08	
rGLP-1R-Ser33Trp	9.36 ± 0.07	1.72	10.58 ± 0.15	1.45

The fold differences highlight negligible reduction made by the effect of mutation on either GLP-1 or EX4 potency.

5.4 Discussion

As mentioned above, hGLP-1R-Trp33 has been reported before as a main determinant of species selection by T-0632 since hGLP-1R-Trp33Ser mutation eliminated this selection (Tibaduiza et al., 2001). In the same way, the reverse mutant, rGLP-1R-Ser33Trp was tested to explore whether rGLP-1R-Ser33 is involved in the species related difference in affinity for the EX4 C-terminus. The data described in this chapter showed that the rGLP-1R-Ser33Trp mutation led to slight but statistically significant decrease in the affinity for both ligands (d> 5 fold, $p<0.01$), which abrogates any role of rGLP-1R-Ser33 in species selective binding of the EX4 C-terminus residues. It is worth mentioning that hGLP-1R-Trp33Ser was tested for the same target in Donnelly's lab but the data showed WT values for rGLP-1R withr espct to affinity and activity. The crystal structure of hGLP-1-NTD bound to EX4(9-39) (Runge et al., 2008) revealed that hGLP-1R-Trp33 is in the opposite site of Trp39 and a short distance from the hydrophobic interaction with EX4(9-39) but is not involved either directly or indirectly in the ligand interaction. Consequently, rGLP-1R-Ser33Trp could slightly disturb the receptor structure that sub-optimizes the binding site of the ligand. Furthermore, T-0632 was found to reduce the potency of GLP-1 via a non-competitive mechanism (Tibaduiza et al., 2001). Accordingly, rGLP-1R-Ser33Trp had a neutral effect on the potency of both EX4 and GLP-1.

The work described in chapter 4 has revealed that the 'H' interaction by both EX4 and GLP-1 is similar. The mutagenesis approach based upon the crystal structure failed to determine the particular interaction that accounts for discriminatory binding of GLP-1 and EX4. Indeed, the data also abrogated the hypothesis that the enhanced affinity of EX4 at the isolated NTD is mainly due to the higher helical propensity of EX4 compared to GLP-1 (Runge et al., 2007).

However, the crystal structure showed just one interaction with the C-terminus of EX4, represented by a hydrogen bond between hGLP-1R-Glu68 and EX4 Ser32** (Runge et al., 2008). Interestingly, the only significant methodological difference between Donnelly's work and Runge's was that Donnelly's lab used rGLP-1R while Runge's used hGLP-1R. Surprisingly, in the previous part of the present study, all the mutated residues in the NTD were identical in both human and rat receptors. In contrast, hGLP-1R-Glu68 is the only residue different in the two receptor types described in the crystal structure as it is involved in binding Ser32**-EX4. It is noteworthy that position 68 in rGLP-1R is occupied by Asp instead of Glu.

Although the two amino acids are similar, the observations recorded by using different analogues of EX4 raise the possibility that different mechanism may underlie the binding of EX4 to either rGLP-1R or hGLP-1R. This study demonstrates that the N-independent affinity of EX4 for rGLP-1R-NTD is in large part dependent on a single residue within the NTD, which plays the primary role in ligand binding (Wilmen et al., 1997). Furthermore, the observations recorded for rNT-TM1 versus hNT-TM1 supported this hypothesis (Figure 5-6, Table 5-3) since the removal of Ser32** reduced significantly the affinity of rNT-TM1 for EX4(1-30) compared to EX4 but displayed no significant difference in affinity with hNT-TM1 .

The Ala32-EX4(9-39) peptide showed reduced affinity for rGLP-1R by a magnitude equal to the effect of deleting EX4 residues 31-39 (Table 5-2). The considerable selectivity of Ala32-EX4(9-39) for rGLP-1R versus hGLP-1R (despite the high degree of sequence identity between these two proteins (91%)) suggested according to crystal structure (Runge et al., 2008) that the contribution of selection by Ala32-EX4(9-39) could be restricted to the different residue at 68th position between the two receptor species in the binding site of EX4 C-terminus.

Although the crystal structure shows that Glu68 forms a hydrogen bond with Ser32** of the ligand, (Runge et al., 2008) implied that this assignment was tentative due to the increasing B-factors for the C-terminal end of the ligand. Indeed, molecular dynamic simulations demonstrated that this interaction was transient and unlikely to generate affinity (Figure 5-10 A-C) (Mann et al., 2010b). The present study confirmed this experimentally by the disruption of this interaction via the replacement of Ser32** with Ala in EX4(9–39), which had no effect on the affinity of the peptide at hGLP-1R (Table 5-2; Figure 5-5). On the other hand, the molecular dynamic simulations using the hGLP-1R mutant Glu68Asp bound with EX4(9–39) (Mann et al., 2010b) predicted a much more stable interaction via a hydrogen bond between the Asp68 side chain and the hydroxyl group of Ser32**. It would therefore be expected that the removal of the hydroxyl by mutation of Ser32** would manifest as a reduction in binding affinity and, once again, this was confirmed experimentally (Table 5-2; Figure 5-4). In fact, despite the subtle change at only one side chain, the Glu68Asp mutation at hGLP-1R conferred pharmacological selectivity that closely resembled that observed at rGLP-1R, presumably by enabling the 'EX' interaction to form.

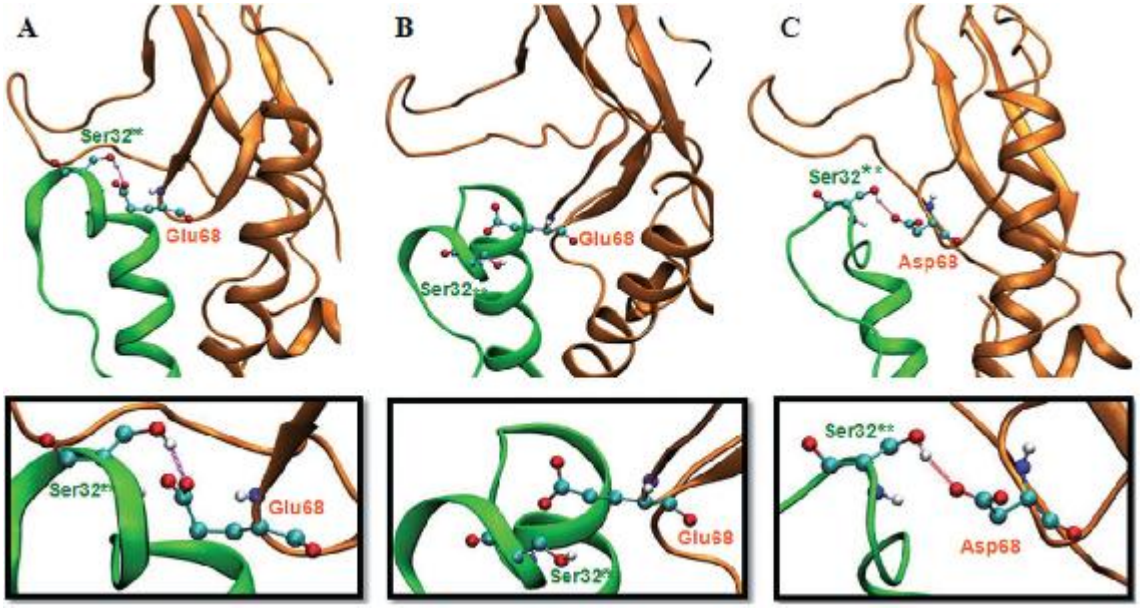

Figure 5-10: Molecular dynamics simulations.

Ribbon diagrams illustrating snapshots of the structure of EX4(9–39) bound to hGLP-1R taken from different points during molecular dynamics simulations. EX4(9–39) is shown in green, GLP-1R is shown in orange and the atoms of Ser32* of EX4(9–39) and Glu/Asp from GLP-1R are shown as ball and sticks coloured by atom type. Hydrogen bond formation between these groups is indicated (see boxed panels for close-up views). In the WT hGLP-1R, Ser32** and Glu spend a relatively short amount of time at a hydrogen bonding distance, [for example, (A)] while, instead, the majority of time is spent over 4 Å apart, [for example, (B)], a distance too great to allow a hydrogen bond. In hGLP-1R-Glu68Asp, Ser32** and Asp have a high probability of forming a distance ideal for hydrogen bond formation, for example (C) (Mann et al., 2010b).

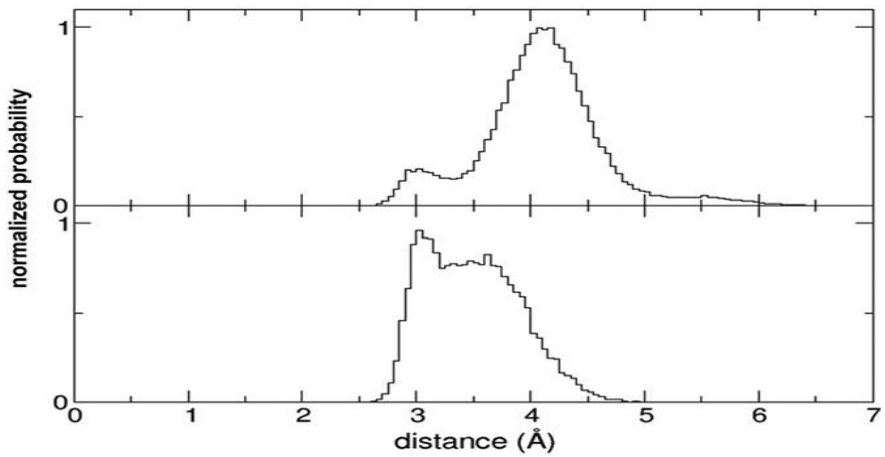

Figure 5-11: Histogram of molecular dynamics simulations.

Histogram chart showing calculations from molecular dynamics simulations. Histogram is showing the probability (normalized so that the integral between 0 and infinity is 1) that the side chain oxygen of Ser32** of EX4(9–39) and the closest side chain oxygen of Asp/Glu of GLP-1R are at a given distance. A peak at 3 Å indicates the atoms are at an ideal distance for hydrogen bond formation to occur. Upper panel: probabilities of distances between atoms of Ser32** in EX4(9–39) and Glu in GLP-1R. Lower panel: probabilities of distances between atoms of Ser32** in EX4(9–39) and Asp in GLP-1R (Mann et al., 2010b).

Taken together, it looked feasible to explore the importance of the residue underlying the species selectivity of EX4 C-terminus. To confirm the importance of the Asp68Ser32** interaction between rGLP-1R and EX4(9–39), this residue was mutated to either Glu or Ala. The Asp68Ala mutation would result in a side chain that cannot form hydrogen bond with Ser32**, and indeed this mutant receptor was insensitive to the removal of the serine hydroxyl of EX4(9–39) or the removal of residues 31–39 of EX4 (Table 5-2; Figure 5-4). Moreover, despite its theoretical ability to form an interaction resembling Asp68, the sensitivity of the Asp68Glu mutant to the removal of the Ser32** hydroxyl closely resembled that of the Asp68Ala mutant, indicating that no stable interaction between Glu and Ser32** was formed.

While the mutations at Asp68 abolished the selectivity between EX4(9–39) and Ala32–EX4(9–39), both mutants bound the peptides with higher affinity than expected, suggesting the possibility that conformational changes in the protein structure may enhance interactions with other regions of the peptide. While mutations often result in such unexpected observations, it has been found previously that the difference in the affinities of two very similar ligands at the same receptor is highly diagnostic for identifying ligand–receptor interactions (Mann et al., 2007, Pioszak et al., 2009). Taken with the data from the pharmacological assays and molecular dynamic simulation of hGLP-1R, it can be concluded that a glutamic acid side chain at residue 68 of hGLP-1R cannot form a stable hydrogen bond with Ser32** of the peptide ligand, and therefore does not contribute to the affinity of the peptide.

As the C-terminal extension of EX4 has been shown to form part of a Trp-cage motif in some environments (Neidigh et al., 2001), it is feasible that this structure could play a role in enhancing the affinity of the peptide at rGLP-1R. Trp-

cage formation is dependent upon a number of sequence-dependent features, one of which is the presence of the hydroxyl side chain of Ser33** which forms an intra-molecular hydrogen bond (Barua et al., 2008). In order to examine the putative role of the Trp-cage in enhancing the affinity of EX4(9–39), EX4 Ser33** was substituted with Ala, preventing the intra-molecular hydrogen bond and hence disrupting Trp-cage formation. However, this substitution had no effect upon the peptide's affinity for rGLP-1R (Mann et al., 2010b). Hence, it is clear that Donnelly and co-workers previous speculation was wrong, since neither the putative Trp cage motif nor the hydroxyl side chain of Ser33** is responsible for the observed affinity enhancement mediated by residues EX4(31–39). These data were supported by the molecular dynamics simulations where the Trp-cage motif included in the starting conformation was observed to unfold early in the simulation (Mann et al., 2010b).

Overall, the present study along with published work from the Donnelly's lab demonstrates a surprising observation showing that the large difference in affinity between GLP-1 and EX4 observed with the isolated hGLP-1R-NTD (Mann et al., 2010b) was almost absent when the membrane-tethered hNT-TM1 (Table 5-3, Figure 5-6). This similarity in binding affinity is in agreement with the binding data resulting from the mutagenic analysis of Runge's lab, which noted that EX4 makes only minor additional interactions with the hGLP-1R-NTD relative to GLP-1 (Underwood et al., 2010). However, the data appear to conflict with the binding data at the purified NTD, and therefore, in order to explain these apparently conflicting observations, an alternative modified peptide/receptor binding model has been proposed (Figure 5-12) (Mann et al., 2010b).

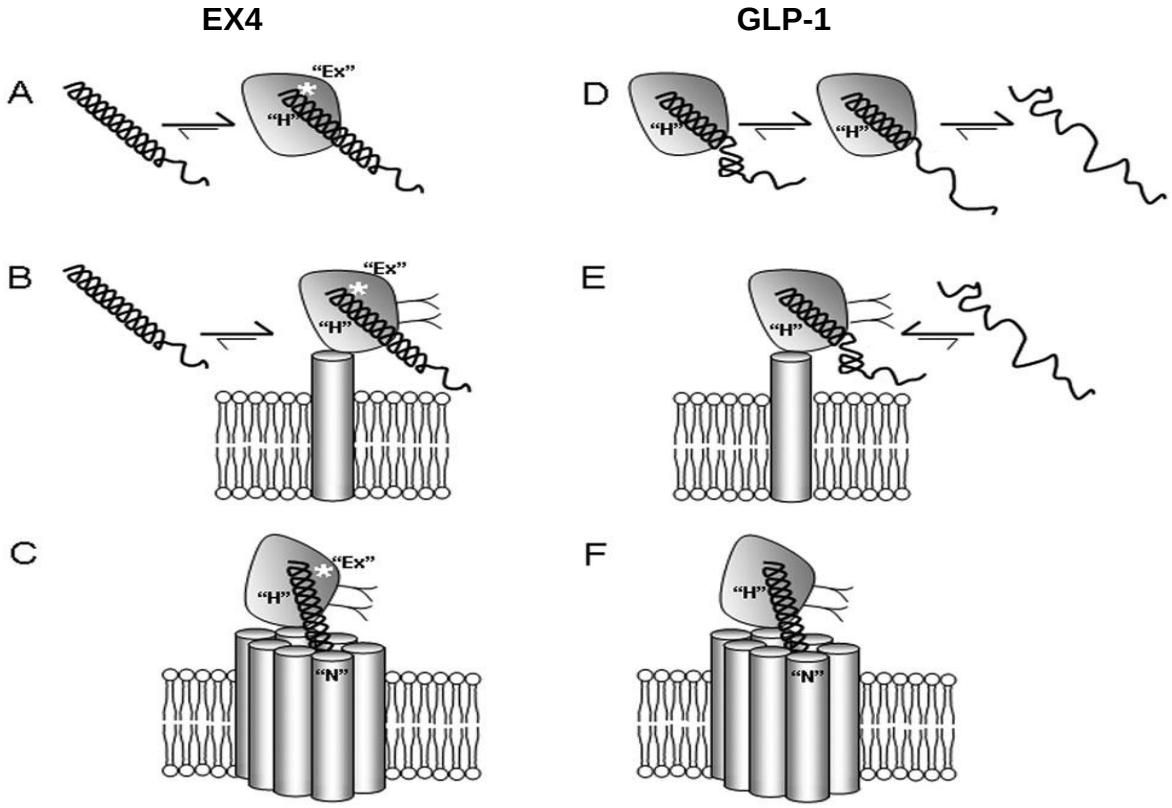

Figure 5-12: A model for the binding of EX4 and GLP-1.

Binding of EX4 (left panels, A–C) and GLP-1 (right panels, D–F) to either the fully isolated/soluble GLP-1R-NTD expressed in *Escherichia coli* (A, D), the isolated NTD tethered to the membrane, expressed in HEK-293 cells (NT-TM1, B and E) or the full-length receptor expressed in HEK-293 cells (C, F). The helical structure of the peptide ligands is critical for their high-affinity interaction with the NTD via the 'H' interaction. (A) A cartoon representation of the binding of EX4 (helix) with the isolated GLP-1R-NTD based on the crystal structure. The C-terminal half of the peptide interacts with the NTD, while the high helical propensity of EX4 enables its helical structure to remain intact, despite the absence of interactions with the N-terminal region of the ligand. However, the binding of GLP-1 with the isolated GLP-1R-NTD occurs with much lower affinity because the lower helical propensity of GLP-1, coupled with the absence of interactions with the N-terminal region of the ligand, results in the more frequent unwinding of the helix, loss of the 'H' interaction and consequent dissociation of the ligand (D). Hence, there is a large affinity difference between EX4 and GLP-1 at the isolated NTD (200- to 400-fold), which reflects the difference in helical propensity rather than the relative strength of the 'H' interaction. However, the two ligands bind with much more similar affinity to the isolated NTD tethered to the plasma membrane (B, E). It is speculated that this is due to the close proximity of the membrane, which stabilizes the N-terminal region of GLP-1, eliminating the difference in helical propensity, and thus enabling the C-terminal helix to remain intact and interact with the NTD. The addition of the core domain of the receptor (C, F) results in additional interactions with the N-terminal region of the ligands, the 'N' interaction, which is stronger for GLP-1 than for EX4. A third interaction, termed 'EX' (white asterisk), represents a specific interaction between Ser32** in the C-terminal region of EX4 and the GLP-1R-NTD (Mann et al., 2010b).

While the 200-fold difference in affinity between GLP-1 and EX4 at rGLP-1R is substantially reduced at rNT-TM1 (25-fold), there nevertheless still remained a significant difference between the affinities of the two peptides (Mann et al., 2010b). This observation has been described previously and has been explained by defining an extra 'EX' interaction between EX4 and the rGLP-1R-NTD, which was localized to the C-terminal extension of EX4 (asterisk in Figure 5-12; (Al-Sabah and Donnelly, 2003a). This 'EX' interaction also accounts for the ~30-fold difference between the affinities of EX4(9–39) and EX4(9–30) observed with both the isolated rNTD and rNT-TM1 (Table 2 in (Al-Sabah and Donnelly, 2003a).The modest affinity enhancement that EX4 attains over GLP-1 as a result of the 'EX' interaction with rGLP-1R is physiologically relevant and should not be confused with the larger affinity difference observed at the isolated NTD, which results from the low helical propensity of GLP-1 in this artificial receptor-binding environment.

6 - 'EX' interaction and truncated peptides

6.1 Introduction

6.1.1 Antagonist-agonist switching of peptide ligands at the GLP-1R

As previously introduced, the NTD of GLP-1R is critical for high ligand affinity, whereas the receptor core domain is essential for the activation of the receptor (Al-Sabah and Donnelly, 2003a, Lopez de Maturana et al., 2003). The proposed model for agonist-induced activation of Family B GPCRs, including GLP-1R, is a two-step mechanism in which the C-terminal half of the peptide hormone's α-helix binds to the NTD, while a second interaction between the N-terminal residues of the ligand and the core domain of the receptor leads to receptor activation (e.g. (Mann et al., 2010b). While the details of the first interaction are well understood via X-ray crystallography of the NTD (Underwood et al., 2010, Runge et al., 2008), the paucity of structural data for the core domain means that the understanding of the second interaction remains poor.

The X-ray structure of the isolated NTD of GLP-1R with EX4(9-39) showed that the N-terminal region of the peptide from Asp9** to Met14** does not interact with the NTD (Runge et al., 2008). Nevertheless, residues Leu10** to Met14** form part of a well-defined α-helix that continues to Asn28**, with the region between Glu15** and Asn28** interacting with a shallow binding site on the NTD. The C-terminal half of GLP-1 bound to GLP-1R also forms an α-helix from Ala24* to Val33*, which interacts with the isolated NTD in a manner that closely resembles that of EX4(9-39) (Underwood et al., 2010). However, while residues Thr13* to Glu21* adopt an α-helical conformation protruding from the NTD, the orientation of this N-terminal half of GLP-1 differs from that of the regular helix of EX4(9-39) since the helix in GLP-1 is kinked at Gly22 (Underwood et al., 2010).

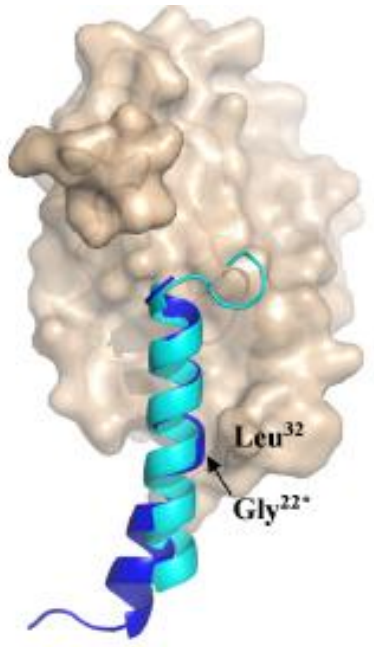

Figure 6-1: The kink at Gly22 of GLP-1.

Superposition of GLP-1R-NTD bound GLP-1 (blue) and EX4(9-39) (cyan). GLP-1 residue Gly22* denotes a kink in the α-helix, which is situated in close proximity to Leu32 of the NTD (Underwood et al., 2010).

The aim of the work described in this section was to explore the nature of the agonist/antagonist properties of truncated GLP-1 and EX4. While GLP-1 is rapidly cleaved *in vivo* after Ala2* to yield the low potency agonist GLP-1(9-36)amide (Elahi et al., 2008), EX4 is resistant to such degradation due to the substitution of residue 2 by Gly (Figure 1-4). Nevertheless, when the equivalent truncated version of EX4 was synthesised, it was found that EX4(3-39) acted as a high affinity antagonist (Montrose-Rafizadeh et al., 1997), suggesting the possibility that the two analogous peptides interact differently with the activation pocket in the receptor's core domain. Therefore, we set out to compare and contrast the properties of truncated GLP-1 and EX4 in order to understand the mechanisms that underlie their different efficacy and, in doing so, to understand further the nature of the receptor activation mechanism.

6.1.2 'EX' interaction and helical propensity of EX4 and GLP-1

Previous studies referred to the superior affinity of EX4 as being due to its stabilized helix (Runge et al., 2007), since EX4 has a strong helical area (EEEAVRL) in contrast to the corresponding kinked segment in GLP-1(EGQAAKE) (Montrose-Rafizadeh et al., 1997), which looks less helical due to the presence of Gly22* (Figure 6-2). The crystal structure of EX4/hGLP-1R-NTD suggested that, in addition to Arg20**/Glu128 interaction, the interaction of Arg20** with Glu16** and Glu17**, could stabilize the α-helical structure of EX4(9-39) (Runge et al., 2008). On the other hand, the kink of the α-helix around Gly22* suggested that the opposite charges of residues in the corresponding positions in GLP-1 interfere with the stabilization similar to EX4 (Underwood et al., 2010). Actually, this was just a theoretical prediction without supporting experimental data. Consequently, the aim of work in this section is to explore the exchange of residues of interest between GLP-1 and EX4. Accordingly, a modified version GLP-1(15-36) with the mid-section EGQAAKE of GLP-1 swapped with EEEAVRL of EX4 was made to give the peptide EX2G13. The modified EX2G13 is equivalent in length to GLP-1(15-36) but, if the hypotheses are correct, it should have a higher affinity than normal GLP-1(15-36). In the same way, Gly22* in GLP-1(15-36) was replaced by the corresponding residue in EX4, Glu16. The ligands were used for binding and activation assays with both rGLP-1R and hGLP-1R.

6.1.3 Possibility of improvement of EX4 pharmacological properties

In fact, based on the recorded affinity and activity data, attention has been given to what could improve the pharmacological properties of EX4. Connecting all the points together, the work above revealed that the main factor in maintaining EX4 N-independent affinity at rGLP-1R is the interaction between EX4 Ser32** and rGLP-1R-Asp68 via a hydrogen bond. Accordingly, the work was directed to

examine five synthetic EX4 peptides with Ser32** substituted by other hydrogen donor amino acids (Lys32-EX4, Arg32-EX4, His32-EX4, Asn32-EX4 and Gln32-EX4). All peptides were subjected to binding and activity analysis with either rGLP-$1R_{myc}$ or hGLP-1R to investigate whether any of them could show improved EX4 characters or species selection.

6.2 Methodological considerations

General methods were applied during molecular biology work and cell culturing as in Chapter 2. Competitive radioligand binding assays were carried out using ^{125}I-GLP-1 as a tracer and the various unlabelled ligands showed in Figure 6-2 as competitors. In LANCE cAMP assay, the number of stimulated cells was optimized at 4000 cells/well stimulated for 30 min at room temperature before the detection mix was added to each well and incubated at room temperature for 1hr.

```
GLP-1(7-36)        HAEGTFTSDVSSYLEGQAAKEFIAWLVKGR
GLP-1(15-36)               DVSSYLEGQAAKEFIAWLVKGR
EX2G13                     DVSSYLEEEAVRLFIAWLVKGR
Glu22-GLP-1(15-36)         DVSSYLEEQAAKEFIAWLVKGR
Gly16-Ex4(9-30)            DLSKQMEGEAVRLFIEWLKNGG
Ex4(9-30)                  DLSKQMEEEAVRLFIEWLKNGG
Gly16-Ex4(9-39)            DLSKQMEGEAVRLFIEWLKNGGPSSGAPPPS
Ex4(9-39)                  DLSKQMEEEAVRLFIEWLKNGGPSSGAPPPS
Gly16-Ex4          HGEGTFTSDLSKQMEGEAVRLFIEWLKNGGPSSGAPPPS
Ex4                HGEGTFTSDLSKQMEEEAVRLFIEWLKNGGPSSGAPPPS
                   |       |                     |        |
                   1       9                     30       39
```

Figure 6-3: Alignment of the synthetic ligands peptides.

The exchanged amino acids are underlined.

6.3 Results

6.3.1 Antagonist-agonist switching of peptide ligands at the GLP-1R

As expected from previous studies, the removal of the first eight residues from the N-terminus of GLP-1, to yield GLP-1(15-36), resulted in a substantial reduction in affinity at both rat GLP-1R (Figure 6-3, Table 6-1) (rGLP-1R; 1445-fold, P<0.0005) and human GLP-1R (hGLP-1R; 1318-fold, P<0.0005). The removal of the equivalent region of EX4, to yield EX4(9-39), resulted in a more modest reduction in affinity (83-fold at rGLP-1R, P<0.0005 and 46-fold at hGLP-1R, P<0.0003). Further truncation of EX4(9-39) at the C-terminus to yield EX4(9-30), the direct equivalent of GLP-1(15-36), resulted in a further 9-fold reduction in affinity at rGLP-1R (P<0.002) but no significant reduction at hGLP-1R (P<0.1) (Figure 6-3, Table 6-1).

The removal of the first eight N-terminal residues from GLP-1 also resulted in a large decrease in agonist potency with the EC_{50} for GLP-1(15-36) being >5000-fold at rGLP-1R and >12,000-fold higher at hGLP-1R compared with GLP-1 itself. Nevertheless, the truncated peptide was a partial agonist with an intrinsic maximal activity of 82.3 ± 3.9% (n=3) relative to GLP-1. In contrast, the first eight N-terminal residues of EX4 were essential for efficacy since both EX4(9-39) and EX4(9-30) displayed no intrinsic activity at either rGLP-1R or hGLP-1R (table 6-1; Figure 6-3).

Both NMR and X-ray crystallography have demonstrated that, relative to the regular α-helix observed for EX4, the α-helical region of GLP-1 is kinked due to presence of Gly at the 16th position of GLP-1 (Gly22*) which is Glu16** in EX4 (Neidigh et al., 2001, Underwood et al., 2010). In order to examine whether the efficacy of GLP-1(15-36) relative to its inactive analogue EX(9-30) was due to this kinked helix, Glu16** of EX4(9-30) was replaced with Gly. Gly16-EX4(9-30) was

indistinguishable from EX4(9-30) at hGLP-1R, displaying similar affinity and no detectable activity in the LANCE™ cAMP assays at concentrations up to 100 µM (Table 6-1; Figure 6-3B). However, despite only a modest reduction in affinity at rGLP-1R (4-fold, P > 0.02), Gly16-EX4(9-30) was a partial agonist with intrinsic activity and potency very similar to that of GLP-1(15-36) (Table 6-1; Figure 6-3A).

Surprisingly, the equivalent Glu16-Gly substitution in EX4(9-39), to yield Gly16-EX4(9-39), did not result in any detectable agonist activity at rGLP-1R, even with 100 µM of peptide. Since the nine residue C-terminal extension of EX4 interacts with the N-terminal domain of the receptor (Al-Sabah and Donnelly, 2003a, Runge et al., 2008, Mann et al., 2010b), it has been predicted that the NTD would be the source of the different functional properties observed between Gly16-EX(9-30) and Gly16-EX4(9-39) at rGLP-1R. Furthermore, the ability of Gly16-EX4(9-30) to activate rGLP-1R, but not hGLP-1R (Table 6-1) suggested that a difference within the primary structure of rGLP-1R and hGLP-1R may be responsible. Limiting the search to only those residues that interact with the C-terminal region of EX4(9-39), residue 68 (Asp68 in rGLP-1R; Glu-68 in hGLP1R) was identified as a candidate responsible for the different properties of rGLP-1R and hGLP-1R. Therefore, stable cell lines expressing the Asp/Glu substitutions in the receptors from both species (rGLP-1R-Asp68-Glu and hGLP-1R-Glu68-Asp) were used to assess the efficacy of the truncated GLP-1 and EX4 peptides. As shown in Table 6-2 and Figure 6-4, the side chain substitution at residue 68 had no effect upon the agonist properties of GLP-1(15-36). However, unlike WT rGLP-1R, the mutant rGLP-1R-Asp68-Glu receptor was no longer activated by Gly16-EX4(9-30) while, conversely, hGLP-1R-Glu68-Asp was activated by Gly16-EX4(9-30) which was inactive at WT hGLP-1R.

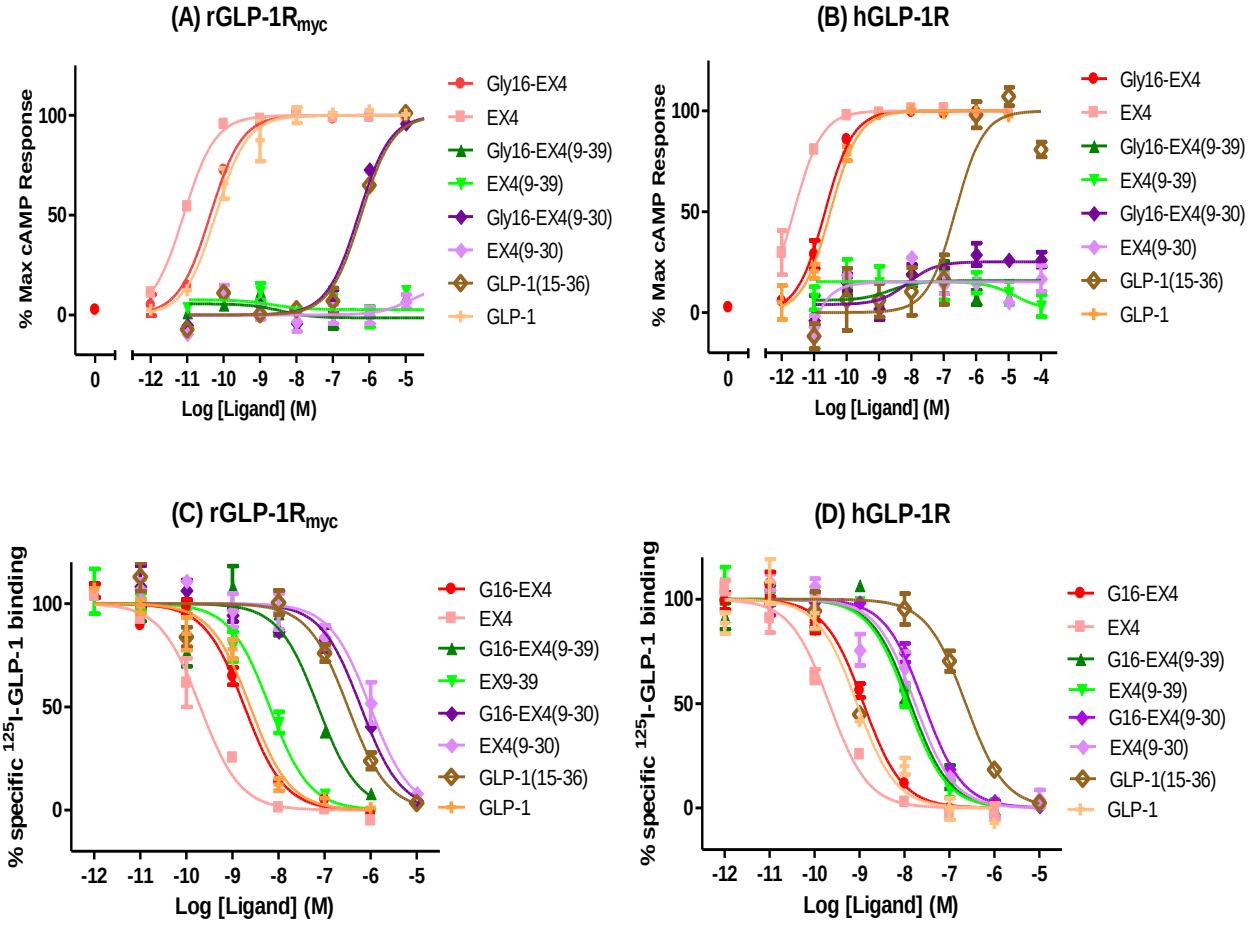

Figure 6-4: Pharmacological profile of Glu16Gly modified Exendins and with the rGLP-1R$_{myc}$ and the hGLP-1R.

A: Dose response curves of normal and modified exendins with the rGLP-1R$_{myc}$. As can be seen species selection still controls the effect of deletion of last 9 amino acids of exendin. Gly16-EX4(9-30)(♦) is converted to agonist. Although Gly16-EX4(9-30)(♦) has greatly reduced potency relative to EX4(■) and Gly16-EX4(●)(d1 is 48666) it was able to stimulate rGLP-1R$_{myc}$ unlike other short normal exendins EX4(9-39)(▼) and EX4(9-30)(♦), which were as usual antagonists. Moreover, Gly16-EX4(9-39)(▲) is surprisingly antagonist as well. Glu16Gly in Gly16-EX4(●) slightly reduced its potency (d1 is 3.95) **B:** at hGLP-1R, all ligands appeared with the same potency pattern as with rGLP-1R$_{myc}$ but maybe with different numbers except Gly16-EX4(9-30)(♦) was an antagonist indicating Gly16-EX4(9-30)(♦) has a species selective agonism toward rGLP-1R$_{myc.}$ **C:** competition-binding curves show the reduced affinity of the C-terminal truncated exendins at rGLP-1R regardless Glu16Gly substitution relative to EX4(9-39)(▼) and Gly16-EX4(9-39)(▲). **D:** at hGLP-1R: the curves showed that four truncated exendins has nearly equally reduced affinity relative to EX4(■). $pIC_{50\ and}$ pEC_{50} values are given in Table 6-1.

Table 6-1: pEC_{50} and pIC_{50} of the rGLP-1R and the hGLP-1R with extchanged 16th position EX4.

	rGLP-1R$_{myc}$		hGLP-1R	
	pEC50	**pIC50**	**pEC50**	**pIC50**
GLP-1	9.98 ± 0.19	9.20 ± 0.03	10.65 ± 0.08	9.33 ± 0.16
GLP-1(15-36)	6.28 ± 0.09**	6.04 ± 0.28**	6.56 ± 0.11**	6.21 ± 0.23**
Gly16-EX4(9-30)	6.27 ± 0.12	6.54 ± 0.15	ND	7.85 ± 0.15
EX4(9-30)	ND	7.14 ± 0.08**	ND	7.77 ± 0.01
Gly16-EX4(9-39)	ND	7.21 ± 0.05	ND	7.34 ± 0.09
EX4(9-39)	ND	8.10 ± 0.11**	ND	8.04 ± 0.13**
Gly16-EX4	10.33 ± 0.06	8.84 ± 0.16	10.72 ± 0.03	8.89 ± 0.02
EX4	10.93 ± 0.12	10.02 ± 0.14	11.56 ± 0.11	9.70 ± 0.02

Note pEC_{50} values of Gly16-EX4(9-30), ND means not determined.

Table 6-2: pEC_{50} and pIC_{50} of the hGLP-1R-like rGLP-1R-Asp68Glu and the rGLP-1R-like hGLP-1R Glu68Asp with extchanged 16th position EX4.

	rGLP-1R-Asp68Glu		hGLP-1R-Glu68Asp	
	pEC50	**pIC50**	**pEC50**	**pIC50**
Gly16-EX4(9-30)	ND	6.96 ± 0.09**	6.38 ± 0.13	6.38 ± 0.09**
EX4(9-30)	ND	7.57 ± 0.05	ND	7.49 ± 0.15**
Gly16-EX4(9-39)	ND	6.67 ± 0.04**	ND	7.57 ± 0.03**
EX4(9-39)	ND	7.80 ± 0.07	ND	8.66 ± 0.08
GLP-1(15-36)	6.23 ± 0.16	6.85 ± 0.17	6.45 ± 0.14	6.70 ± 0.19

Note pEC_{50} values of Gly16-EX4(9-30) compared to values in table 6-1.

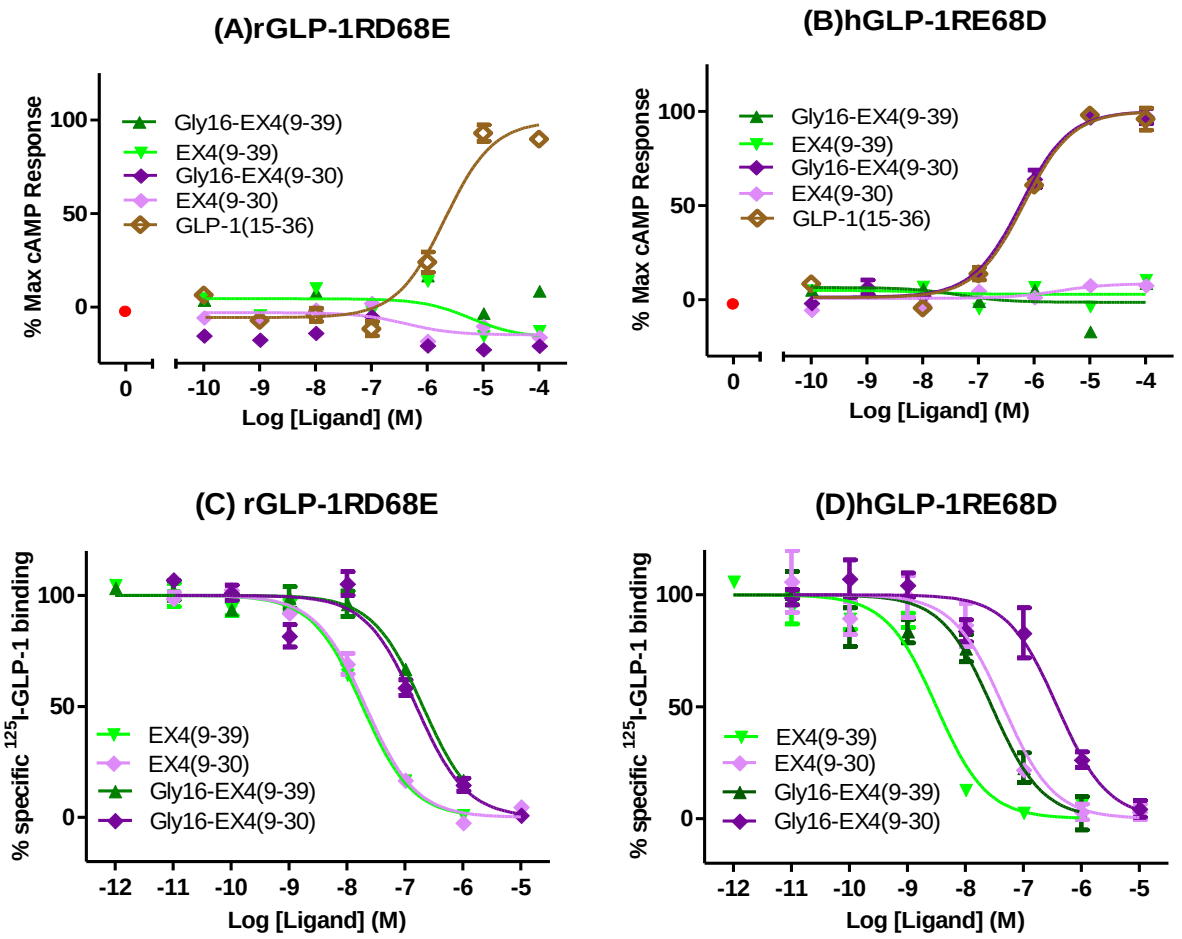

Figure 6-5: Dose response curves and competition binding curves of Glu16Gly-modified EX4 and GLP-1 with the hGLP-1R-like rGLP-1R-Asp68Glu and the rGLP-1R-like hGLP-1R Glu68Asp.

A: Dose response curves of normal and modified EX4 and GLP-1 with rGLP-1R-Asp68Glu, Gly16-EX4(9-30)(♦) lost its potency like other short normal exendins EX4(9-39)(▼) and EX4(9-30)(♦), as well as Gly16-EX4(9-39)(▲). **B**: at hGLP-1R-Glu68Asp, Gly16-EX4(9-30)(♦) regained its agonism while other exendins stayed with the same response. **C:** rGLP-1R-Asp68Glu showed lower affinity to less helical exendins as Gly16-EX4(9-30)(♦) and Gly16-EX4(9-39)(▲) with low helical stability looked have the same affinity and curves of both of them are shifted to right of curves of both EX4(9-39)(▼) and EX4(9-30)(♦). **D:** hGLP-1R-Glu68Asp regained the species selection based affinity of the Ex4 C-terminus as the affinity depended on the length of the ligand and not on its helical structure. Gly16-EX4(9-39)(▲) has higher affinity than Gly16-EX4(9-30)(♦) as well as EX4(9-39)(▼) has higher affinity than EX4(9-30)(♦). pIC_{50} and pEC_{50} values are given in Table 6-2.

6.3.2 'EX' interaction and helical propensity of EX4

As showed in the previous section, the removal of the first eight residues from the N-terminus of GLP-1, to yield GLP-1(15-36), resulted in a substantial reduction in affinity at both rat and human GLP-1R. Surprisingly, the insertion of the stabilizing residues of EX4 to yield EX2G13 failed to improve its affinity and showed typical affinity of normal GLP-1(15-36) (less than 4-fold change at both types of receptors, p> 0.1). On the other hand, compared to GLP-1(15-36), replacement of Gly22 only by Glu to yield Glu22-GLP-1(15-36) showed non-significant improvement in affinity at rGLP-1R (3.8 <fold, P>0.1) but a slightly significant improvement at hGLP-1R (9.65 fold, P<0.01) (Figure 6-6, Table 6-3).

Interestingly, EX2G12 was inactive at both types of receptors though Glu22-GLP-1(15-36) was active at both rat and human GLP-1R (Figure 6-6, Table 6-3) with high significant improved potency compared to GLP-1(15-36) (rGLP-1R: 14 fold, p<0.0003; hGLP-1R: 17 fold, p<0.003).

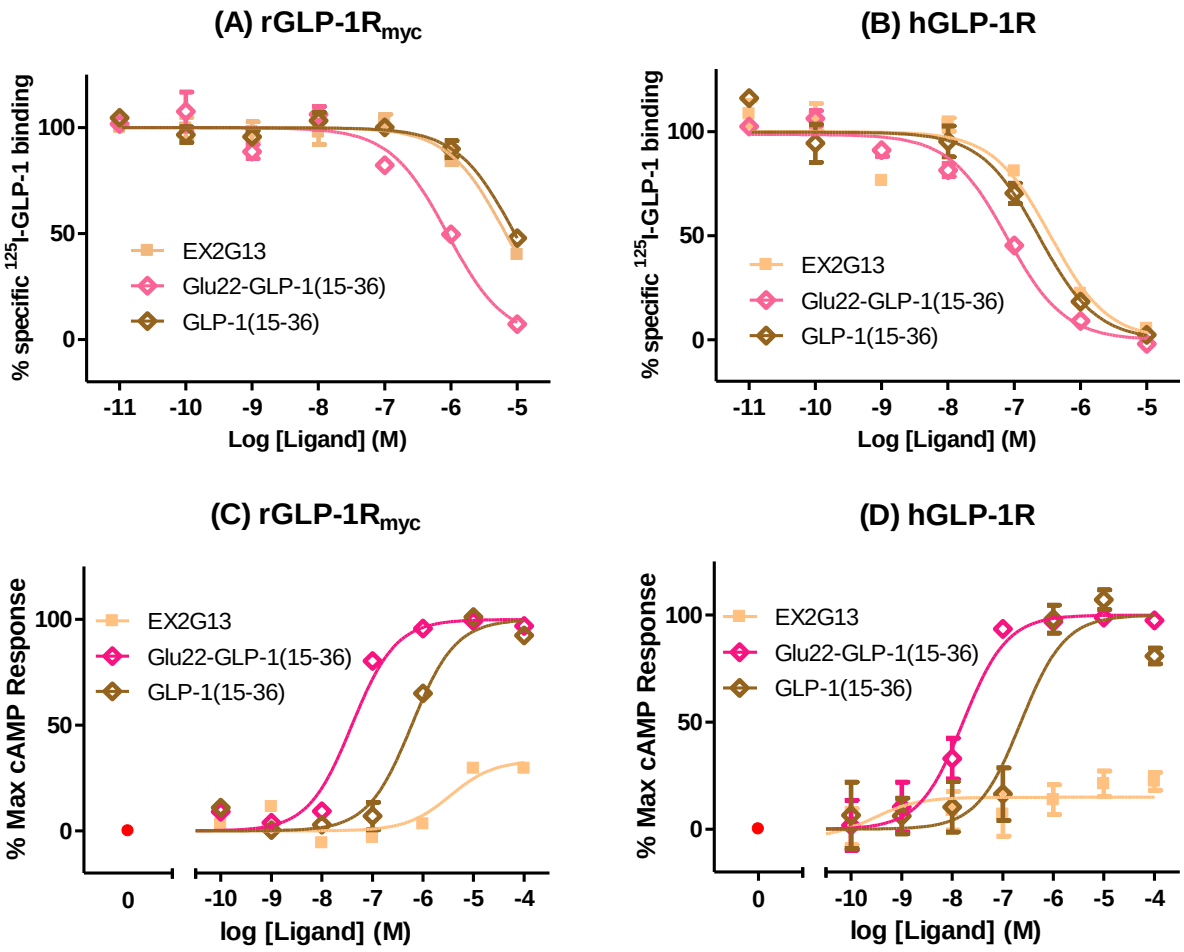

Figure 6-6: Dose response curves and competition-binding curves of EX2G13, E22-GLP-1(15-36) with the rGLP-1R and the hGLP-1R.

A and **B** show competition-binding assays were assessed using ^{125}I-GLP-1 versus Three equal length ligands GLP-1(15-36) (◊), Glu22-GLP-1(15-36) (◊) and EX2G13 (□) at membrane preparation of HEK-293 cells expressing WT receptors. **C** and **D** show the potency of the same ligand stimulated the HEK-293 live cells expressing the same receptors. $pIC_{50\ and}$ pEC_{50} values are given in Table 6-3.

Table 6-3: pEC_{50} and pIC_{50} of EX2G13, E22-GLP-1(15-36) and with GLP-1(15-36) the rGLP-1R and the hGLP-1R.

	rGLP-1R$_{myc}$		hGLP-1R	
	pEC_{50}	**pIC_{50}**	**pEC_{50}**	**pIC_{50}**
EX2G13	ND	6.24±0.22	ND	6.76±0.18
GLP-1(15-36)	6.28 ± 0.09**	6.04±0.28	6.56 ± 0.11**	6.21±0.23*
Glu22-GLP-1(15-36)	7.52 ± 0.06	6.60±0.09	7.72 ± 0.14	7.19±0.07

* P < 0.05, ** P < 0.01 compared to E22-GLP-1(15-36).

6.3.3 Possibility of improvement of EX4 pharmacological properties

Indeed, none of the modified EX4 peptides showed improved affinity or activity with either species receptors, as shown in Tables 6-4 and 6-5. Furthermore, mutations His32-EX4, Asn32-EX4 and Gln32-EX4 showed adverse effect reflected by statistically significant reductions in affinity at receptors of both types compared to normal EX4 (≈ 5-10 fold, P<0.01). The potency of the peptides was slightly better than their affinity but still lower than normal EX4 (d< 5 fold)

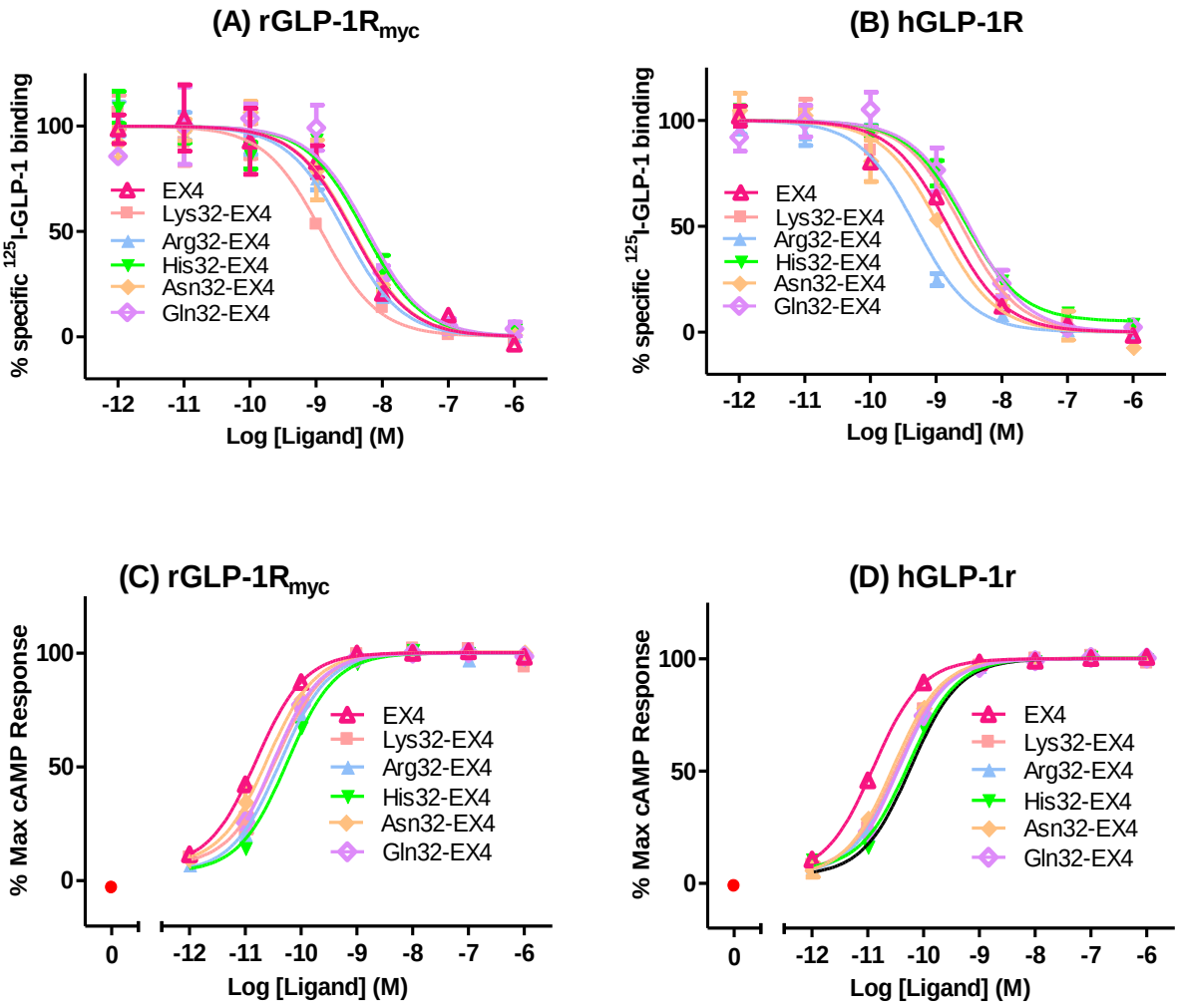

Figure 6-7: Dose response curves and competition-binding curves of Ser32-modified analogues of EX4 with the rGLP-1R and the hGLP-1R.

A and **B,** competition-binding curves of ^{125}I-GLP-1 and Ser32-modified analogues of EX4 with rGLP-1R or hGLP-1R. **C** and **D** show the potency of the same ligands stimulated the HEK-293 live cells expressing the same receptors. pIC_{50} and pEC_{50} values are given in Tables 6-4 and 6-5.

Table 6-4: pIC_{50} values of Ser32 modified analogues of EX4 with the rGLP-1R or the hGLP-1R.

	$rGLP\text{-}1R_{myc}$		hGLP-1R	
	pIC50	**d**	**pIC50**	**d**
EX4	9.34 ± 0.18		9.26 ± 0.10	
Lys32-EX4	8.78 ± 0.15	3.68	8.66 ± 0.08**	3.98
Arg32-EX4	8.78 ± 0.12	3.72	8.99 ± 0.18	1.85
His32-EX4	8.35 ± 0.05**	10.00	8.74 ± 0.13*	3.34
Asn32-EX4	8.44 ± 0.07**	8.15	8.70 ± 0.16*	3.63
Gln32-EX4	8.32 ± 0.10**	10.75	8.53 ± 0.06**	5.37

d is Fold difference was calculated compared to normal EX4. * P < 0.05, ** P < 0.01.

Table 6-5: pEC_{50} values of Ser32 modified analogues of EX4 with the rGLP-1R or the hGLP-1R.

	$rGLP\text{-}1R_{myc}$		hGLP-1R	
	pEC_{50}	**d1**	**pEC_{50}**	**d1**
EX4	10.80 ± 0.09		10.94 ± 0.03	
Lys32-EX4	10.47 ± 0.08	2.15	10.42 ± 0.10**	3.29
Arg32-EX4	10.63 ± 0.28	1.48	10.55 ± 0.24	2.44
His32-EX4	10.20 ± 0.06**	3.98**	10.15 ± 0.10**	6.17
Asn32-EX4	10.51 ± 0.13	1.93	10.48 ± 0.14*	2.91
Gln32-EX4	10.45 ± 0.08*	2.26*	10.39 ± 0.05**	3.52

d is Fold difference was calculated compared to normal EX4. * P < 0.05, ** P < 0.01

6.4 Discussion

6.4.1 Antagonist-agonist switching

The details of the 'H' interactions have been resolved by X-ray crystallography via the solving of the structure of the isolated hGLP-1R-NTD complexed with EX4 and GLP-1 (Runge et al., 2008, Underwood et al., 2010). However, although it is accepted that the N-terminal region of GLP-1 binds to the core domain of the receptor, the details of the 'N' interaction remain to be resolved. Some progress has been made; for example, several residues have been previously identified in the core domain (Lopez de Maturana and Donnelly, 2002, Al-Sabah and Donnelly, 2003b, Lopez de Maturana et al., 2004) which are required for maintaining the high affinity of full-length GLP-1 but not GLP-1(15-36), suggesting that they interact with the first eight residues of the peptide. Furthermore, this approach has recently been validated via a photo-cross-linking study which demonstrated a direct interaction between the extreme N-terminus of GLP-1 and Tyr-205 in the first extracellular loop (Chen et al., 2010).

While the 'H' interactions of EX4 and GLP-1 are largely equivalent (Mann et al., 2010b) their 'N' interactions are likely to differ since both X-ray crystallography and NMR analysis have shown that, while the helix of EX4 is regular, the helix of GLP-1 is kinked at Gly22* (Neidigh et al., 2001, Underwood et al., 2010). The result of the kink is that the N-terminal half of the helix is orientated differently with respect to its C-terminus, which is likely to result in a different interaction with the receptor's core domain and consequential differences in the nature of the 'N' interaction. Indeed, while the first eight residues of both GLP-1 and EX4 are critical for their efficacy at GLP-1R, the interaction between this region of EX4 and the core domain of the receptor comprises a substantially lower proportion of the peptide's affinity compared with GLP-1 (Table 1 in Al-Sabah and Donnelly, 2003a).

However, since both peptides are able to fully activate the receptor, this difference in the 'N' interaction only results in different contributions to affinity, suggesting that the efficacy-generating component of the peptides' interaction with the core domain is independent from the affinity-generating component. To account for this in the current work, the 'N' interaction is defined to account only for the affinity generated between the N-terminal region of the peptide and the core domain, while now defining an independent interaction, 'A', to describe the efficacy-generating interaction. Indeed, previous disruption of the affinity-generating component of the 'N' interaction in the core domain, via mutagenesis of Asp198 to Ala, did not result in loss of efficacy, suggesting that the 'A' interaction was not disrupted and therefore independent from 'N' (Lopez de Maturana and Donnelly, 2002). A pictorial description of the interactions between the agonists and GLP-1R is provided by Figure 6-8 which indicates equivalent H and 'A' interactions for both peptides but a reduced N interaction for EX4.

The N-terminal region of GLP-1 is critical for its high potency at both rGLP-1R and hGLP-1R since the removal of the first eight residues substantially reduces both its affinity (>1,300-fold) and potency (>5,000-fold) (Table 6-1). However, the observation that GLP-1(15-36) acts as a low-potency partial agonist demonstrated that much of the efficacy-generating properties still reside in the truncated peptide, further substantiating the independence of the 'N' and 'A' interactions. The observation that EX4(2-39) acts as an agonist while Glu9-EX4(2-39) acts as an antagonist (Montrose-Rafizadeh et al., 1997) may suggest that it is the Asp at the first position of GLP-1(15-36) that is critical for efficacy. Furthermore, the substitution of Asp-9 of GLP-1 with Ala resulted in 40-fold reduction in affinity but an almost complete loss of efficacy (Adelhorst et al., 1994). While GLP-1(15-36) could activate GLP-1R, its analogue EX4(9-30) displayed no detectable efficacy,

even at 100 µM. Therefore, despite the slightly higher affinity of EX4(9-30) compared with GLP-1(15-36), it appears that only GLP-1(15-36) is able to form the A interaction in the core domain (Figure 6-8).

Given this surprising observation, it was fascinating to discover that a single Glu to Gly residue substitution at position 16 of EX4(9-30) was able to confer agonist properties, such that Gly16-EX4(9-30) acted as a partial agonist at rGLP-1R with properties similar to GLP-1(15-36). While it is possible that Glu16 to Gly substitution results in a direct alteration between the interaction of this residue's side chain and the receptor's activation pocket, it is proposed that the Glu-16 to Gly substitution in EX4(9-30) enables the helix to bend in a similar manner to that observed in GLP-1, allowing its extreme N-terminus to interact with the activation pocket in the core domain and to form the 'A' interaction (Figure 6-8C (i)).

Despite the ability of Gly16-EX4(9-30) to activate rGLP-1R, this receptor could not be activated by Gly16-EX4(9-39). it has been shown previously that the nine residue C-terminal extension of EX4(9-39) interacts with the N-domain of rGLP-1 via a hydrogen bond between Asp68 of the receptor and Ser32** of the ligand (previous chapter). Therefore, the observation that this C-terminal extension prevented receptor activation was surprising since it would be expected to be distant from the activation pocket in the core domain. A second surprising observation was the absence of agonist activity for Gly16-EX4(9-30) at hGLP-1R, despite being a partial agonist at rGLP-1R. This suggested that a side chain within the human receptor was preventing the peptide from acting as an agonist. Although it was initially suspected that such a human-rat residue difference may be in close to the activation pocket within the receptor's core domain, the ability of the C-terminal extension of Gly16-EX4(9-39) to prevent activation of rGLP-1R suggested that a site on the NTD could be responsible. Hence the study targeted

residue 68 of GLP-1R, since this was the only residue which interacted with the C-terminal extension of EX4(9-39) and which also differed in the human and rat receptor sequences. The exchange of Asp68 for Glu in rGLP-1R abolished the agonist induced activity of Gly16-EX(9-30) but had no effect upon GLP-1(15-36). Furthermore, the exchange of Glu-68 for Asp in hGLP-1R enabled Gly16-EX(9-30) to act as a partial agonist with similar properties to GLP-1(15-36).

It was therefore clear that either (1) the presence of the C-terminal extension in the peptide, or (2) the presence of Glu at position 68 of the receptor, was sufficient to prevent Gly16-EX4(9-30) from acting as an agonist. The surprise was that the location of the ligand-receptor interaction that resulted in this disruption of activity involved the C-terminus of the ligand and the NTD of the receptor, a site that would be distant from the activation pocket in the receptor. It is proposed that the source of this disruption to agonist activity is an interaction between the C-terminal region of the peptide and the NTD which limits the mobility of the peptide within the binding site on the NTD and therefore prevents its N-terminus from interacting with the activation pocket on the core domain (Figure 6-8C (ii) and (iii)). Analysis of the X-ray structure of EX4(9-39) complexed with the isolated N-domain of hGLP-1R suggests that the longer side chain of Glu68 can interact with the extreme C-terminus of Gly16-EX4(9-30), whereas the shorter side chain of Asp68 cannot.

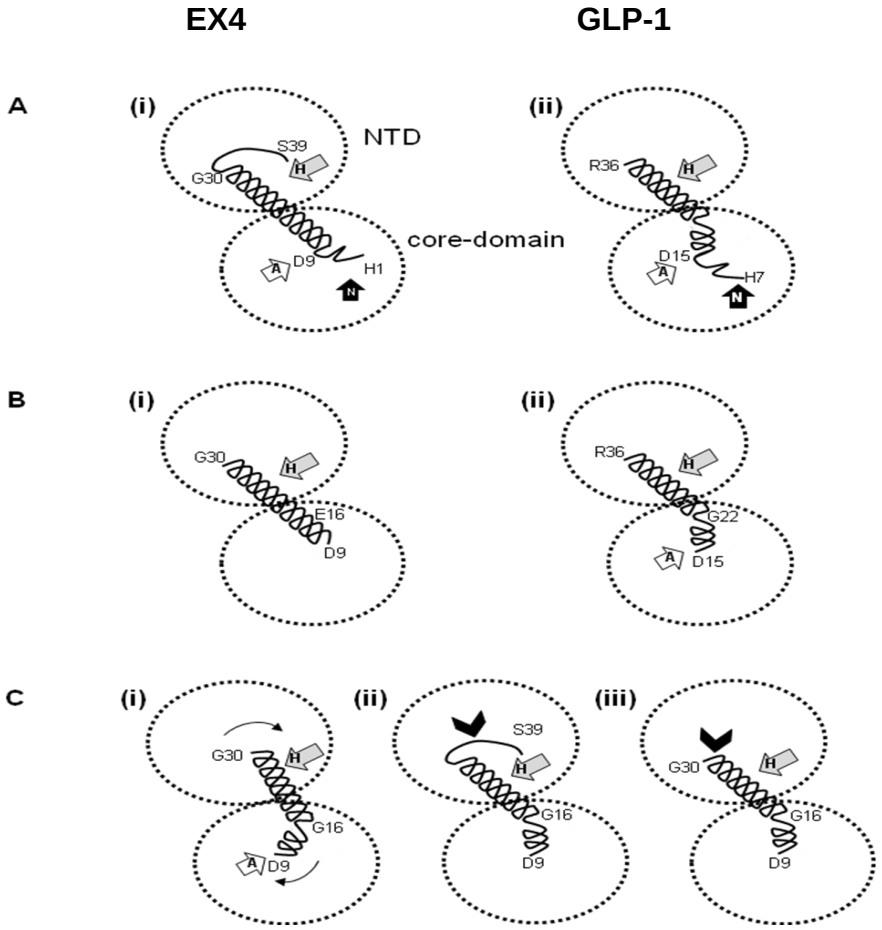

Figure 6-8: Cartoon representations of peptide-receptor interactions.

The two domains of the receptor are depicted as two dotted ovals, with the NTD on top of the core domain. The ligand is depicted by the solid line that includes a helix, with particular residue types displayed as their single-letter code and residue number. The helix of EX4 is shown as regular while that of GLP-1 is shown with a kink at Gly22: substitution of Glu-16 of truncated EX4 peptides with Gly is depicted with a kinked helix analogous to that of GLP-1. The three interactions between the ligand and receptor are shown by three arrows labelled either H (grey), N (black) or A (white). The 'H' interaction generates affinity between the NTD and the C-terminal half of the ligand; the 'N' interaction generates affinity between the N-terminal 8 residues of the peptide and the core domain of the receptor; the 'A' interaction generates receptor activity/efficacy via an interaction between the N-terminal region of the receptor and the core domain. EX4 makes all three interactions with the receptor (Ai) although its 'N' interaction is weaker than that of GLP-1, which also makes all three interactions (Aii). EX4(9-30) is only able to make the H interaction and therefore has lower affinity than EX4 and also possesses no efficacy (Bi). On the other hand, GLP-1(15-36) is able to activate the receptor since its bent helix can form the A interaction. However, the absence of the N interaction results in low affinity and potency for GLP-1(15-36). Gly-16-EX(9-30) acts as an agonist in a similar manner to GLP-1(15-36) (Ci). However, for Gly-16-EX4(9-39) (Cii), the presence of the C-terminal extension results in an interaction (black chevron) at the C-terminus which restricts the ability of the N-terminus to form the 'A' interaction. Likewise, an interaction (black chevron) between Glu-68 and the C-terminus of Gly-16-EX4(9-30) (Ciii) also restricts the ability of the N-terminus to form the 'A' interaction. The curved arrows in Ci indicate the increased mobility of the peptide within the binding site, enabled by the absence of a restrictive interaction at the C-terminus of Gly-16-EX(9-30).

Such an interaction could restrict the mobility of the C-terminal helix of the ligand within the binding site on the N-domain (Figure 6-8C (iii)). While the mobility of Gly16-EX(9-30) would be enabled by the absence of an interaction with the shorter side chain of Asp-68, the C-terminal extension of Gly16-EX(9-39) would result in a hydrogen bond between Asp-68 and the side chain of Ser32 on the ligand ((Mann et al., 2010b); Figure 6-8C(ii)). Therefore, agonist activity is prevented by the presence of either Glu68 in the receptor or the C-terminal extension in the ligand.

6.4.2 'EX' interaction and helical propensity of EX4

Consistent with previous observations, it was interesting to explore the exchange of the kinked helix region in GLP-1 with the corresponding highly helical segment of EX4. The sequence EEEAVRL of EX4 has been assumed to support the higher helicity of EX4 over the corresponding area of GLP-1 (EGQAAKE) which is interrupted and weakened by a kink at Gly22* (Montrose-Rafizadeh et al., 1997). Consequently, that observation has been taken as a support for the hypothesis that high helicity of EX4 is the main reason for its superior affinity (Runge et al., 2007). EX2G13, GLP-1(15-36) and Glu22-GLP-1(15-36) were used in binding assays to eliminate any effect of other parts (the N and C-termini) of the two ligands on the tested affinity or activation. EX2G13 and GLP-1(15-36) showed the same affinity without any species preference, emphasising the contribution of EX4 C-terminus over its helical propensity, discussed in Chapter 5.

However, Glu22-GLP-1(15-36) showed slightly enhanced affinity compared with the GLP-1(15-36) (Table 6-3; Figure 6-5). This observation would suggest that the effect, mediated via the helix occurs as a result of the Gly22Glu substitution alone. The introduced negative charge of Glu would together with Gln23*, support optimal positioning of Lys26*, the residue at the equivalent

position to (and with equivalent charge as Arg20**) in EX4, forming similar stabilising interaction of EX4 (Runge et al., 2008). However, the closer affinities of EX4(9-30), Gly16-EX4(9-30) and GLP-1(15-36) as well as Gly22-GLP-1(15-36) reduce the correlation of this interaction with the superior affinity of EX4. Alternatively, this stabilization would elongate the segment of GLP-1 that interacts with the helix of NTD, increasing the peptide affinity. The enhanced potency of Gly22-GLP-1(15-36) over GLP-1(15-36) could be explained by increased stabilization of the peptide helix that could optimize its position relative to the activation pocket of the receptors.

Unlike Gly22-GLP-1(15-36), EX2G13 induced no activity with either receptor form reflected by absence of cAMP production. The reasons may be related to the degree of peptide flexibility around this group of introduced EX4 residues. These observations raised the interest in these amino acids as an agonist/antagonist switching factor. Moreover, the important residue for the peptide activation, the 'A' interaction, might be hidden within this area.

6.4.3 The improvement of peptide affinity and activity at GLP-1R

The improvement of peptide affinity and activity at GLP-1R by the modification of the C-terminal end of the ligand has been observed in other studies. (Knudsen et al., 2000) have shown that the addition of a o-carboxyundecanoyl or o-carboxypentadecanoyl group at the C-terminus of a GLP-1 analogue can enhance activity 10-fold. (Hjorth et al., 1994) have also demonstrated that the replacement of the final three residues of glucagon (a 29-residue peptide) with the final four residues of GLP-1 results in a 169-fold improvement in affinity at GLP-1R. Furthermore, the 41000-fold selectivity of GLP-1R for GLP-1 over glucagon (Hjorth et al., 1994) is reduced to only a 50-fold difference when glucagon is extended by eight residues to give oxyntomodulin

(Dakin et al., 2001). Conversely, the replacement of the final four residues of GLP-1 with the final three residues of glucagon reduces affinity at GLP-1R by 475-fold (Hjorth et al., 1994). Hence, the interaction of the C-terminal region of the peptide ligand with the receptor is clearly important for affinity, and could be exploited in the design of modified ligands with increased activity. Since this study showed that rGLP-1R does interact with Ser32** while hGLP-1R does not; consequently, the work was encouraged to yield 'super EX4' with highest affinity and/or activity for either rGLP-1R or hGLP-1R by exchanging Ser32** into another hydrogen donor amino acid. These replacements led to affinity and activation properties similar to values with wild type receptor, or lower, indicating the indispensability Asp/Ser32** interaction.

7 - Summarising discussion and conclusion

7.1 Introduction

GLP-1 is an incretin hormone secreted by enteroendocrine L-cells in the intestinal mucosa in response to food intake. GLP-1 plays an important role in controling blood glucose homeostasis via a specific 7TM receptor that is expressed in peripheral tissues, as well as in the nervous system. The GLP-1R is a prototypical member of a Family B within the GPCR superfamily. Like other Family B receptors, the GLP-1R stimulates cAMP production as a second messenger of intracellular signalling cascades.

In vivo, stimulation of the GLP-1R by endogenous GLP-1 induces multiple interactive mechanisms, which together result in normalization of blood glucose levels. These mechanisms include receptor-mediated enhancement of glucose-induced insulin secretion from pancreatic β-cells, deceleration of gastric emptying with a delay in the gastrointestinal absorption of nutrients, inhibition of glucagon secretion, and inhibition of food intake.

Consistent with these physiological functions, it has been reported that an administration of exogenous GLP-1 provides an effective approach for the treatment of type two diabetes mellitus. However, this therapeutic strategy is hampered by serious challenges, such as the susceptibility of GLP-1 to rapid enzymatic inactivation and the need for frequent painful parenteral drug administration. To overcome these limitations, drug investigators have focused on the identification of alternative long acting GLP-1R agonists, potential drugs that would mimic the activity of the endogenous hormone.

EX4 is an agonist of GLP-1R with the same physiological similarities and differences of GLP-1. Consequently, synthetic EX4 has been licensed as a drug, exenatide (Byetta®) for the treatment of type 2 diabetes mellitus. EX4 has significantly greater affinity at the isolated GLP-1R-NTD, relative to GLP-1, but the mechanism underlying this property has been controversial.

Initial studies of the interaction between EX4 and rGLP-1R in Donnelly's group correlated this superior affinity with the extra nine amino acids at the C-terminus of EX4. The approach taken, therefore, was to determine a receptor contact for any of these amino acids and to investigate how this interaction mediates the receptor binding discrimination.

7.2 Computer based models

At the time of starting this work, there was only CRFR2β-NTD as an available NMR structure of a Family B GPCR-NTD, so other methods have to be recruited to explore the biomolecular interaction between ligand and receptor. Computer built models for EX4/NTD of the rGLP-1R complex have been designed in Donnelly's lab. These models identified a set of residues of the receptors that are suggested to be involved in the interaction with the C-terminus of EX4. The first part of this project was a practical work based on those models. Eventually, none of the models revealed a realistic description of the actual interaction. However, both binding and activity analysis indicated the importance of some of the selected residues for the interaction between ligand and receptor. This importance was elucidated in the light of latterly released Family B GPCR crystal structures.

7.3 'EX' interaction based on crystal structure

Later, the first crystal structure of Family B GPCR was published for GIPR in complex with GIP (Parthier et al., 2007). Shortly afterwords, the crystal structure of hGLP-1R-NTD bound to EX4(9-39) was published (Runge et al., 2008) followed by a GLP-1 bound one (Underwood et al., 2010). Other studies at the hGLP-1R disputed our group's conclusions and related EX4 superior affinity to the greater stability of the helical region of EX4 in relations to its counter part in GLP-1 (Runge et al., 2007). The crystal structure for hGLP-1R-NTD bound to EX4(9-39) supported by mutagenic analysis suggested only one subtle interaction of the C-terminus of EX4 with the NTD (Runge et al., 2008). Both of the crystal structures seemed consistent with the data recorded in the current study about the 'H' interaction of the ligand with the GLP-1R. Furthermore, the data appeared as a detailed scene of the equal affinity reported before in our group for the amino acids at positions (9-30) or the 'H' region in either EX4 or GLP-1. Accordingly, the interaction behind the superaffinity of EX4 would be beyond its 'H' interaction and is still to be allocated.

7.4 Determining of 'EX' interaction using crystal structure Ser32/Asp68 interaction

The crystal structure of the isolated hGLP-1R-NTD identified only one residue difference between rat and hGLP-1R, Glu68 in hGLP-1R while Asp68 in rGLP-1R that interacts with the C-terminal region of EX4 (via Ser32**). The data of the current study demonstrates that the reversely mutated receptor of both species binds the natural ligands, GLP-1 and EX4, with a similar affinity compared to the WT GLP-1R, suggesting that residue 68 does not affect either the N or H interaction of the ligand with the receptor, which is in agreement with our group's previous study (Al-Sabah and Donnelly, 2003a).

Two truncated forms of EX4, EX4(9-39) and EX4(9-30), were used so that any difference in affinity between EX4(9-39) and EX4(9-30) could be related to the interaction of the receptor with the extra 9 amino acids in the C-terminus of EX4(9-30). As demonstrated by previous studies with rGLP-1R (Al-Sabah and Donnelly, 2003a), the C-terminally truncated peptide displayed lower affinity. Since the human receptor has been reported to be unaffected by the same ligand truncation, Asp68 was selected as a potential target as it was (a) different in the human receptors, being Glu and (b) suggested to be in contact with Ser32** in the nine-residue C-terminal extension of EX4 (Runge et al., 2008).

While the binding analysis demonstrated superior affinity of EX4 (9-39) over EX4(9-30) to WT rGLP-1R, when Asp68 was mutated to glutamic acid (Asp68Glu) the difference in affinity disappeared. This strongly supports the notion that Asp68 is capable of enhancing EX4 affinity by interacting with the C-terminal extension of EX4. In order to demonstrate that the affinity-enhancing interaction between residue 68 and the C-terminal extension of EX4 occurs via the side chain of Ser32**, a peptide analogue of EX4(9-39) was synthesized with Ser-32 replaced by Ala. The binding properties of this peptide mimicked those of the fully truncated EX4(9-30) peptide, confirming Ser32** as the interaction site for Asp68.

7.5 Antagonist-agonist switching

The study demonstrated that GLP-1(15-36) acts as a partial agonist while the equivalent analogue EX4(9-30) shows no activity. However, the substitution of Glu16** for Gly in EX4(9-30) resulted in a peptide with agonist properties at rGLP-1R that are similar to those of GLP-1(15-36). The study proposed that Gly16** enables the helix of the ligand to kink in a similar manner to that observed in GLP-1, and that this enables its N-terminus to interact with the activation pocket in the core domain of the receptor. The activity of Gly16-EX4(9-30) at rGLP-1R is lost

when Asp-68 in the N-domain of the receptor is substituted by Glu, the equivalent residues in hGLP-1R. Indeed, Gly16-EX4(9-30) shows no activity at hGLP-1R but becomes a partial agonist when Glu68 is replaced by Asp, the equivalent residue in rGLP-1R. The study proposed that Glu-68, but not Asp68, is able to interact with the C-terminus of Gly16-EX4(9-30) by virtue of its longer side chain, with the result that the ligand's movement is restricted such that its N-terminus cannot interact with the activation pocket. Furthermore, Gly16-EX4(9-39) shows no activity at either rGLP-1R or hGLP-1R. The study proposed that the interaction between the C-terminal extension of Gly16-EX4(9-39) and the N-domain, restricts the mobility of the peptide and prevents the N-terminus from interacting with the activation pocket in the core domain. The work demonstrated the independence of the 'N' and 'A' interactions in the receptor core domain and also shows that interactions between the C-terminal helix and the NTD in Family B GPCRs can influence the efficacy-generating interactions between the ligand and the core domain.

Modified Gly16-EX4(9-39) and Gly16-EX4(9-30) underwent binding analysis by the same way. Interestingly, if the ligands were tested with rGLP-1R and its homolog hGLP-1R-Glu68Asp the C- terminus of the modified Gly16-EX4(9-39) could enhance its affinity over its truncated analogue Gly16-EX4(9-30). In contrast, if they tested with hGLP-1R and its homolog hGLP-1R-Asp68Glu the two ligands had equal affinity which is lower than that of normal EX4(9-39) and EX4(9-30) implying the dominance of the C-terminus interaction with rGLP-1R albeit the interrupted helix of EX4.

7.6 'EX' interaction and helical propensity of EX4 and GLP-1

To examine the reverse modification in Gly16-EX4(9-30) , initially both GLP-1(15-36), Glu22-GLP-1(15-36) and EX1G23 were subjected to binding analysis with the two species receptors. While GLP-1(15-36) and EX1G23 had non-selective equal affinities Glu22-GLP-1(15-36) showed enhanced affinity which is non-selective too. Gly16-EX4(9-30) at rGLP-1R, GLP-1(15-36) and Glu22-GLP-1(15-36) at human and rat GLP-1R were partial agonists in contrast to EX2G13 which was antagonist at both types of receptors indicating the importance of the middle sequence in both EX4 and GLP-1 agonist /antagonist switching but this sequence does not contribute to 'EX' interaction.

7.7 'Super' exendins

Understanding the mechanism underlying EX4 species selective interaction may lead research to design a higher affinity analogue of EX4 at the human receptor. Although it appears that Ser32** can only interact with rGLP-1R- Asp68 and not hGLP-1R-Glu68, it may yet be possible to make further analogues of EX4 with alternative substitutions at residue 32nd with enhanced affinity and potency at the hGLP-1R. Accordingly, a number of EX4 analogues were synthesized with replacement of Ser32** by hydrogen donors amino acids Arg, Lys, His, Asn and Gln. Results obtained via binding and activity analysis of those analogues were disappointing since all of the analogues showed equal or even lower affinity and potency. However, it could indicate that it is not just a direct interaction between Ser32** and Asp68 but could be extended to control further interactive interactions.

7.8 Conclusion

The present project employed more than one strategy in order to reveal the structural determinants of the ligand binding and functional activation of receptors. The approaches included the use of protein models, site directed mutagenesis and construction of chimeric and/or modified synthetic peptides as well as collaboration with another research group to carry out the molecular dynamics simulations. The work reports that EX4 and its modified analogues have specific pharmacological properties at rGLP-1R. Understanding the mechanisms underlying these characterisations provides a new insight into how peptide molecules can interact with Family B GPCRs.

7.9 Future work

The study showed a new separate interaction, 'A' interaction is necessary for potency of the peptide. Three peptides GLP-1 (15-36), Glu22-GLP-1(15-36) and Gly16-EX4(9-30) were partial agonists though they lack their N-termini. The observations indicated that the activation of the receptor is not an exclusive function of the N-terminus of the peptide. Furthermore, the activation of rGLP-1R rather than hGLP-1R by Gly16-EX4(9-30) was very interesting since this activity was controlled by a residue rGLP-1R-Asp68 in the NTD abrogating the former hypothesis that NTD is highly important for ligand binding. Thereby, the 'A' interaction has an independent mechanism that remains to be uncovered.

A future strategy could be planned for solving the 'A' interaction by adopting relevant modification of the target residues of GLP-1 and EX4 either by exchanging the equivalent positions or replacement with alanine. Comprehensive assignment of the receptor activity controlling interactions should have a crucial impact on the development of the affinity and activity properties of GLP-1 and EX4.

Moreover, understanding the mechanism behind the ‘A’ interaction would be the base for the design and discovery of new agonists for GLP-1R.

8 - Appendix

1. Luria-Bertani (LB) agar media

Tryptone:	(Oxoid)	(1%)	16 g
Yeast extract:	(Oxoid)	(0.5%)	10 g
NaCl:	(BDH)	(1%)	5 g
Agar:	(Oxoid)	(1.5%)	15 g

Deionized water: add to 1000 ml. Autoclaved and kept sealed until using
.

2. Luria-Bertani (LB) media

Tryptone:	(Oxoid)	(1%)	16 g
Yeast extract:	(Oxoid)	(0.5%)	10 g
NaCl:	(BDH)	(1%)	5 g

Deionized water: add to 1000 ml. Autoclaved and kept sealed until using

3. Ampicillin:

Stock solution: 50 mg/ml water
Working solution: 100 µg/ml media (1/500)

4. 2X YT media (Components per liter)

Tryptone:	(Oxoid)	(1.6%)	16 g
Yeast extract:	(Oxoid)	(1%)	10 g
NaCl:	(BDH)	(0.5%)	5 g

Deionized water: add to 1000ml

5. Lysis buffer

Glucose	(Sigma , FW:180.2)	(50 mM)
Tris-HCl (pH 8.0)	(Sigma)	(25 mM)
EDTA	(Sigma , FW:372.2)	(10 mM)

Deionized water: as required

6. 0.2 M NaOH / 1% SDS

NaOH	(Sigma)	(0.2M)
SDS	(Malford laboratories, FW:288.4)	(10%)

Deionized water: as required

7. TAE (50x Stock solution components per liter)

Tris base	(Malford laboratories, FW:121.1)	242 g
EDTA	(0.5 M)	
Glacial acetic acid	57.1 ml	

8. Ammonium Acetate

ammonium acetate	(Sigma , FW:77.08)	7.5 M	57.81 g
Deionized water	Up to 100 ml (pH 7.8)		

9. CM-10

DMEM	(Sigma)	500 ml
FBS	Lonza	10%
Penicillin		1 U/ml
streptomycin	(invitrogen)	0.1 µg/ml
L-Glutamine		2 mM

Stored at 2-8°C and pre-warmed to 37°C before use.

10. Cryo-preservation media

DMEM	45% (pre-warmed to 37°C before use)
FBS	45% (pre-warmed to 37°C before use)
DMSO	10%

11. HEPES binding buffer

HEPES	(Sigma)	50mM	11.9155 g
CaCl2	(Sigma)	1mM	147m g
MgCl2	(Sigma)	5mM	1.0166 g
BSA	(Sigma)	0.2%	
Deionized water:	1000ml, then filtered and stored at 4°C		

12. HEPES washing buffer

HEPES	(Sigma)	50 mM	11.9155 g
NaCl	(Sigma)	500 mM	28 g
BSA	(Sigma)	0.1%	
Deionized water:	1000 ml, then filtered and stored at 4°C		

13. TFB1 buffer (Components per litre of deionized water)

RbCl	(100 mM)	12.1 g
MnCl2	(50 mM)	(MnCl2·4H2O) 9.9 g
CH3COOK	(30 mM)	2.9 g
CaCl2	10 mM	1.1 g
Glycerol	15%	15 ml
Deionized water:	1000 ml. Adjust pH to 5.8 then sterilized by filtration and Stored at 2-8°C	

14. TFB2

MOPS	10 mM	2.1 g
RbCl	10 mM	1.2 g
CaCl2	75 mM	8.3 g
Glycerol Glycerol	15%	15 ml
Deionized water:	1000 ml	

Adjust pH to 6.8 with KOH then aliquot to 1 ml aliquots and stored at -20°C

15. Stimulation buffer

HBSS			500 ml
HEPES	(Sigma)	5 mM	0.6 g

pH to 7.4 then take 50 ml and add 0.1% BSA, valid for one week when stored at 4°C but discarded any time if it becomes turbid

16. Peptides

EX4, EX4(9–39) and GLP-1 were from Bachem (Saffron Walden,U.K.), while all other truncated peptide ligandswere custom synthesised by Genosphere Biotechnologies(Paris, France). ^{125}I-EX-4(9–39), labelled via Bolton–Hunter reagent at Lys-12, was purchased from NEN-Perkin-Elmer (Boston, MA, U.S.A.). ^{125}I-GLP-1(7-36), labelled via lactoperoxidase metod and was a gift from Norvo Nordisk A/S (Novo Allé, Denmark).

```
GLP-1(7-36)       HAEGTFTSDVSSYLEGQAAKEFIAWLVKGR
GLP-1(15-36)              DVSSYLEGQAAKEFIAWLVKGR
EX2G13                    DVSSYLEEEAVRLFIAWLVKGR
Glu22-GLP-1(15-36)        DVSSYLEEQAAKEFIAWLVKGR
Gly16-Ex4(9-30)           DLSKQMEGEAVRLFIEWLKNGG
Ex4(9-30)                 DLSKQMEEEAVRLFIEWLKNGG
Gly16-Ex4(9-39)           DLSKQMEGEAVRLFIEWLKNGGPSSGAPPPS
Ex4(9-39)                 DLSKQMEEEAVRLFIEWLKNGGPSSGAPPPS
Gly16-Ex4         HGEGTFTSDLSKQMEGEAVRLFIEWLKNGGPSSGAPPPS
Ex4               HGEGTFTSDLSKQMEEEAVRLFIEWLKNGGPSSGAPPPS
                  |       |                   |       |
                  1       9                   30      39
```

17. Sequences of primers used in PCR work used in site directed mutagenesis:

Primer Name	Sequence	Description
rGLP-1R-Val30Ala-For	5’CCAGGGTGCCACGGCGTCCCTCTCAGAG3’	Start at position Val30
rGLP-1R-Val30Ala-Rev	5’CTCTGAGAGGGACGCCGTGGCACCCTGG3’	Terminate at position Val30
rGLP-1R-Val30Leu-For	5’CCCCAGGGTGCCACGCTGTCCCTCTCAGAG3’	Start at position Val30
rGLP-1R-Val30Leu-Rev	5’CTCTGAGAGGGACAGCGTGGCACCCTGGGG3’	Terminate at position Val30
rGLP-1R-Val30Thr-For	5’CCCCAGGGTGCCACGACGTCCCTCTCAGAGAC3’	Start at position Val30
rGLP-1R-Val30Thr-Rev	5’GTCTCTGAGAGGGACGTCGTGGCACCCTGGGG3’	Terminate at position Val30
rGLP-1R-Ser33Trp-For	5'GGTGCCACGGTGTCCCTCTGGGAGACAGTGCAGAAATGG3'	Start at position Ser33
rGLP-1R-Ser33Trp-Rev	5'CCATTTCTGCACTGTCTCCCAGAGGGACACCGTGGCACC3'	Terminate at position Ser33
rGLP-1R-Thr35Ala-For	5’CGGTGTCCCTCTCAGAGGCAGTGCAGAAATGGAG3’	Start at position Thr35
rGLP-1R-Thr35Ala-Rev	5’CTCCATTTCTGCACTGCCTCTGAGAGGGACACCG3’	Terminate at position Thr35
rGLP-1R-Thr35Ile-For	5’GGTGTCCCTCTCAGAGATAGTGCAGAAATGGAGAG3’	Start at position Thr35
rGLP-1R-Thr35 Leu-Rev	5’CTCTCCATTTCTGCACTAGCTCTGAGAGGGACACC3’	Terminate at position Thr35
rGLP-1R-Thr35Val-For	5’CGGTGTCCCTCTCAGAGGTAGTGCAGAAATGGAGAG3’	Start at position Thr35
rGLP-1R-Thr35Val-Rev	5’CTCTCCATTTCTGCACTACCTCTGAGAGGGACACCG3’	Terminate at position Thr35
rGLP-1R-Val36Ala-For	5’GTGTCCCTCTCAGAGACAGCGCAGAAATGGAGAGAGTATC3’	Start at position Val36
rGLP-1R-Val36Ala-Rev	5’GATACTCTCTCCATTTCTGCGCTGTCTCTGAGAGGGACAC3’	Terminate at position Val36

Primer Name	Sequence	Description
rGLP-1R-Trp39Ala-For	5’CAGAGACAGTGCAGAAAGCGAGAGAGTATCGGCACC3’	Start at positionTrp39
rGLP-1RR-Trp39Ala-Rev	5’GGTGCCGATACTCTCTCGCTTTCTGCACTGTCTCTG3’	Terminate at positionTrp39
rGLP-1R-Trp39Phe-For	5’CTCAGAGACAGTGCAGAAATTTAGAGAGTATCGGCACCAGTGC3’	Start at positionTrp39
rGLP-1R-Trp39Phe-Rev	5’GCACTGGTGCCGATACTCTCTAAATTTCTGCACTGTCTCTGAG3’	Terminate at positionTrp39
rGLP-1R-Arg40Ala-For	5'CAGTGCAGAAATGGGCAGAGTATCGGCACC 3'	Start at position Arg40
rGLP-1R-Arg40Ala-Rev	5' GGTGCCGATACTCTGCCCATTTCTGCACTG 3'	Terminate at position Arg40
rGLP-1R-Y42Ala-For	5'GCAGAAATGGAGAGAGGCTCGGCACCAGTGCCAAC 3'	Start at position Tyr42
rGLP-1R-Tyr42Ala-Rev	5'GTTGGCACTGGTGCCGAGCCTCTCTCCATTTCTGC 3'	Terminate at position Tyr42
rGLP-1R-His44Ala-For	5'GGAGAGAGTATCGGGCGCAGTGCCAACGTTTC 3'	Start at position His44
rGLP-1R-His44Ala-Rev	5'GAAACGTTGGCACTGCGCCCGATACTCTCTCC 3'	Terminate at position His44
rGLP-1R-Phe66Ala-For	5'CTTCTGCAACCGAACCGCTGATGACTACGCCTG 3'	Start at position Phe66
rGLP-1R-Phe66Ala-Rev	5'CAGGCGTAGTCATCAGCGGTTCGGTTGCAGAAG 3'	Terminate at position Phe66
rGLP-1R-Asp68Ala-For	5'CGAACCTTTGATGCCTACGCCTGCTGG3'	Start at position Asp68
rGLP-1R-Asp68Ala-Rev	5'CCAGCAGGCGTAGGCATCAAAGGTTCG3'	Terminate at position Asp68
rGLP-1R-Asp68Glu-For	5'CAACCGAACCTTTGATGAGTACGCCTGCTGGCCAGATG3’	Start at position Asp68
rGLP-1R-Asp68Glu-Rev	5'CATCTGGCCAGCAGGCGTACTCATCAAAGGTTCGGTTG3'	Terminate at position Asp68

Primer Name	Sequence	Description
rGLP-1R-Tyr69Ala-For	5’CCGAACCTTTGATGACGCCGCCTGCTGGCCAGATG3’	Start at position Tyr69
rGLP-1R-Tyr69Ala-Rev	5’CATCTGGCCAGCAGGCGGCGTCATCAAAGGTTCGG3’	Terminate at position Tyr69
rGLP-1R-Tyr69Leu-For	5’CAACCGAACCTTTGATGACCTCGCCTGCTGGCCAGATGG3’	Start at position Tyr69
rGLP-1R-Tyr69Leu-Rev	5’CCATCTGGCCAGCAGGCGAGGTCATCAAAGGTTCGGTTG3’	Terminate at position Tyr69
rGLP-1R-Tyr88Ala-For	5’CAGTTGCCCCTGGGCCCTGCCGTGGGCC3’	Start at position Y88
rGLP-1R-Tyr88Ala-Rev	5’GGCCCACGGCAGGGCCCAGGGGCAACTG3’	Terminate at position Tyr88
rGLP-1R-Tyr88Leu-For	5’GTCAGTTGCCCCTGGCTCCTGCCGTGGGCCAG3’	Start at position Tyr88
rGLP-1R-Tyr88Leu-Rev	5’CTGGCCCACGGCAGGAGCCAGGGGCAACTGAC3’	Terminate at position Tyr88
rGLP-1R-Trp91Ala-For	5’CCCTGGTACCTGCCGGCGGCCAGTAGTGTGC3’	Start at positionTrp91
rGLP-1R-Trp91Ala-Rev	5’GCACACTACTGGCCGCCGGCAGGTACCAGGG3’	Terminate at positionTrp91
rGLP-1R-Trp91Phe-For	5’CCCTGGTACCTGCCGTTTGCCAGTAGTGTGCTCC3’	Start at positionTrp91
rGLP-1R-Trp91Phe-Rev	5’GGAGCACACTACTGGCAAACGGCAGGTACCAGGG3’	Terminate at positionTrp91
rGLP-1R-Ser94Ala-For	5'GTACCTGCCGTGGGCCAGTGCAGTGCTCCAAGGGCATGTG 3'	Start at position Ser94
rGLP-1R-Ser94Ala-Rev	5'ACATGCCCTTGGAGCACTGCACTGGCCCACGGCAGGTAC3'	Terminate at position Ser94
rGLP-1R-Val95Ala-For	5'GTGGGCCAGTAGTGCCCTCCAAGGGCATGTG3'	Start at position Val95
rGLP-1R-Val95Ala-Rev	5'CACATGCCCTTGGAGGGCACTACTGGCCCAC3'	Terminate at position Val95
rGLP-1R-Leu96Ala-For	5'GTGGGCCAGTAGTGTGGCACAAGGGCATGTGTACC3'	Start at position Leu96
rGLP-1R-Leu96Ala-Rev	5'GGTACACATGCCCTTGTGCCACACTACTGGCCCAC3'	Terminate at position Leu96

Primer Name	Sequence	Description
rGLP-1R-Gln97Ala-For	5'CCAGTAGTGTGCTCGCAGGGCATGTGTACC3'	Start at position Gln97
rGLP-1R-Gln97Ala-Rev	5'GGTACACATGCCCTGCGAGCACACTACTGG3'	Terminate at position Gln97
rGLP-1R-Gly98Ala-For	5'GTAGTGTGCTCCAAGCGCATGTGTACCGGTTC3'	Start at position Gly98
rGLP-1R-Gly98Ala-Rev	5'GAACCGGTACACATGCGCTTGGAGCACACTAC3'	Terminate at position Gly98
rGLP-1R-Glu107Ala-For	5'CCGGTTCTGCACGGCCGCAGGTATCTGGCTGCATAAG3'	Start at position Glu107
rGLP-1R- Glu 107Ala-Rev	5'CTTATGCAGCCAGATACCTGCGGCCGTGCAGAACCGG3'	Terminate at position Glu107
rGLP-1R-Ile109Ala-For	5'GTTCTGCACGGCCGAGGGTGCATGGCTGCATAAGGACAAC3'	Start at position Ile109
rGLP-1R-Ile109Ala-Rev	5'GTTGTCCTTATGCAGCCATGCACCCTCGGCCGTGCAGAAC3'	Terminate at position Ile109
rGLP-1R-Leu111Ala-For	5'GCCGAGGGTATCTGGGCGCATAAGGACAACTC3'	Start at position Leu111
rGLP-1R-Leu111Ala-Rev	5'GAGTTGTCCTTATGCGCCCAGATACCCTCGGC3'	Terminate at position Leu111
rGLP-1R-His112Ala-For	5'CGAGGGTATCTGGCTGGCTAAGGACAACTCCAG3'	Start at position His112
rGLP-1R-His112Ala-Rev	5'CTGGAGTTGTCCTTAGCCAGCCAGATACCCTCG3'	Terminate at position His112
rGLP-1R-Lys113Ala-For	5'GTATCTGGCTGCATGCGGACAACTCCAGCC3'	Start at position Lys113
rGLP-1R-Lys113Ala-Rev	5'GGCTGGAGTTGTCCGCATGCAGCCAGATAC3'	Terminate at position Lys113
rGLP-1R-Asp114Ala-For	5'CTGGCTGCATAAGGCAAACTCCAGCCTGCC3'	Start at position Asp114
rGLP-1R-Asp114Ala-Rev	5'GGCAGGCTGGAGTTTGCCTTATGCAGCCAG3'	Terminate at position Asp114
rGLP-1R-Asn115Ala-For	5'CTGGCTGCATAAGGACGCATCCAGCCTGCCCTGG3'	Start at position Asn115
rGLP-1R-Asn115Ala-Rev	5'CCAGGGCAGGCTGGATGCGTCCTTATGCAGCCAG3'	Terminate at position Asn115

Primer Name	Sequence	Description
rGLP-1R-Glu127Ala-For	5'GACCTGTCGGAGTGCGCAGAGTCCAAGCAAGGAG3'	Start at position Glu127
rGLP-1R-Glu127Ala-Rev	5'CTCCTTGCTTGGACTCTGCGCACTCCGACAGGTC3'	Terminate at position Glu127
rGLP-1R-Glu127Asp-For	5'CCTGTCGGAGTGCGACGAGTCCAAGCAAGG3'	Start at position Glu127
rGLP-1R-Glu127Asp-Rev	5'CCTTGCTTGGACTCGTCGCACTCCGACAGG3'	Terminate at position Glu127
rGLP-1R-Glu127Gln-For	5'GGACCTGTCGGAGTGCCAAGAGTCCAAGCAAG3'	Start at position Glu127
rGLP-1R-Glu127Gln-Rev	5'CTTGCTTGGACTCTTGGCACTCCGACAGGTCC3'	Terminate at position Glu127
rGLP-1R-Glu128Ala-For	5'CTGTCGGAGTGCGAAGCGTCCAAGCAAGGAGAG3'	Start at position Glu128
rGLP-1R-Glu128Ala-Rev	5'CTCTCCTTGCTTGGACGCTTCGCACTCCGACAG3'	Terminate at position Glu128
rGLP-1R-Glu128Asp-For	5'CCTGTCGGAGTGCGAAGACTCCAAGCAAGGAGAGAG3'	Start at position Glu128
rGLP-1R-Glu128Asp-Rev	5'CTCTCTCCTTGCTTGGAGTCTTCGCACTCCGACAGG3'	Terminate at position Glu128
rGLP-1R-Glu128Gln-For	5'CCTGTCGGAGTGCGAACAGTCCAAGCAAGGAG3'	Start at position Glu128
rGLP-1R-Glu128Gln-Rev	5'CTCCTTGCTTGGACTGTTCGCACTCCGACAGG3'	Terminate at position Glu128

18. List of suppliers

SUPPLIER	ADDRESS
Amersham-Biosciences UK Ltd.	Little Chalfont, Buckinghamshire, England
Bachem Ltd.	Saffron Walden, Essex,England
Beckman instruments, Inc.	Palo Alto, CA, USA
Becton Dickinson UK Ltd.	Oxford, England
Bio-Rad Laboratories Ltd.	Hemel Hempstead, Hertfordshire, England
Calbiochem	Nottingham, England
Fisher Scientific	Loughborough, Leistershire, England
Gibco-Invitrogen Ltd.	Paisley, Scotland
GraphPad Software Inc.	San Diego, CA, USA
Helena Biosciences Ltd.	Gateshead, Tyne& Wear, England
Invitrogen BV	Groningen, The Netherland
Jencons Scientific	Leighton Buzzard, Bedfordshire, England
MBI Fermentas	Sunderland, Tyne& Wear, England
Melford Laboratories Ltd.	Ipswich, Suffolk, England
New Brunswick Scientific	Edison, NJ, USA
New England Biolabs Inc. (NEB)	Hitchin, Hertfordshire, England
Oxoid Ltd.	Cambridge, England
Packard Instrument Co., Inc.	Pang Bourne, England
Perkin Elmer Life science Inc.	Boston, MA, USA
Qiagen Ltd.	Crawley, West Sussex, England
Sartorious AG	Goettingen, Germany.
Sigma-Aldrich Co. LTD	Poole, Dorset, England
Stratagene Europe	Amsterdam Zuidoost, The Netherland
VWR International LTD	Lutternworth, Leistershire, England
Wolf Laboratories LTD.	Oxford, England

References

ADELHORST, K., HEDEGAARD, B. B., KNUDSEN, L. B. & KIRK, O. 1994. Structure-activity studies of glucagon-like peptide-1. *J Biol Chem,* 269**,** 6275-8.

AL-SABAH, S. & DONNELLY, D. 2003a. A model for receptor-peptide binding at the glucagon-like peptide-1 (GLP-1) receptor through the analysis of truncated ligands and receptors. *Br J Pharmacol,* 140**,** 339-46.

AL-SABAH, S. & DONNELLY, D. 2003b. The positive charge at Lys-288 of the glucagon-like peptide-1 (GLP-1) receptor is important for binding the N-terminus of peptide agonists. *FEBS Lett,* 553**,** 342-6.

ALTSCHUL, S. F., MADDEN, T. L., SCHAFFER, A. A., ZHANG, J., ZHANG, Z., MILLER, W. & LIPMAN, D. J. 1997. Gapped BLAST and PSI-BLAST: a new generation of protein database search programs. *Nucleic Acids Res,* 25**,** 3389-402.

ANINI, Y. & BRUBAKER, P. L. 2003. Muscarinic receptors control glucagon-like peptide 1 secretion by human endocrine L cells. *Endocrinology,* 144**,** 3244-50.

ANINI, Y., HANSOTIA, T. & BRUBAKER, P. L. 2002. Muscarinic receptors control postprandial release of glucagon-like peptide-1: in vivo and in vitro studies in rats. *Endocrinology,* 143**,** 2420-6.

ATTWOOD, T. K. & FINDLAY, J. B. 1994. Fingerprinting G-protein-coupled receptors. *Protein Eng,* 7**,** 195-203.

BABENKO, A. P., GONZALEZ, G., AGUILAR-BRYAN, L. & BRYAN, J. 1998. Reconstituted human cardiac KATP channels: functional identity with the native channels from the sarcolemma of human ventricular cells. *Circ Res,* 83**,** 1132-43.

BAGGIO, L. L., HUANG, Q., BROWN, T. J. & DRUCKER, D. J. 2004. A recombinant human glucagon-like peptide (GLP)-1-albumin protein (albugon) mimics peptidergic activation of GLP-1 receptor-dependent pathways coupled with satiety, gastrointestinal motility, and glucose homeostasis. *Diabetes,* 53**,** 2492-500.

BAGGIO, L. L., HUANG, Q., CAO, X. & DRUCKER, D. J. 2008. An albumin-exendin-4 conjugate engages central and peripheral circuits regulating murine energy and glucose homeostasis. *Gastroenterology,* 134**,** 1137-47.

BALKAN, B. & LI, X. 2000. Portal GLP-1 administration in rats augments the insulin response to glucose via neuronal mechanisms. *Am J Physiol Regul Integr Comp Physiol,* 279**,** R1449-54.

BALKS, H. J., HOLST, J. J., VON ZUR MUHLEN, A. & BRABANT, G. 1997. Rapid oscillations in plasma glucagon-like peptide-1 (GLP-1) in humans: cholinergic control of GLP-1 secretion via muscarinic receptors. *J Clin Endocrinol Metab,* 82**,** 786-90.

BALLESTEROS, J. A. & WEINSTEIN, H. 1992. Analysis and refinement of criteria for predicting the structure and relative orientations of transmembranal helical domains. *Biophys J,* 62**,** 107-9.

BARUA, B., LIN, J. C., WILLIAMS, V. D., KUMMLER, P., NEIDIGH, J. W. & ANDERSEN, N. H. 2008. The Trp-cage: optimizing the stability of a globular miniprotein. *Protein Eng Des Sel,* 21**,** 171-85.

BAYLISS, W. M. & STARLING, E. H. 1902. The mechanism of pancreatic secretion. *J Physiol,* 28**,** 325-53.

BAZARSUREN, A., GRAUSCHOPF, U., WOZNY, M., REUSCH, D., HOFFMANN, E., SCHAEFER, W., PANZNER, S. & RUDOLPH, R. 2002. In vitro folding, functional characterization, and disulfide pattern of the extracellular domain of human GLP-1 receptor. *Biophys Chem,* 96**,** 305-18.

BEINBORN, M., WORRALL, C. I., MCBRIDE, E. W. & KOPIN, A. S. 2005. A human glucagon-like peptide-1 receptor polymorphism results in reduced agonist responsiveness. *Regul Pept,* 130**,** 1-6.

BELL, G. I., SANTERRE, R. F. & MULLENBACH, G. T. 1983. Hamster preproglucagon contains the sequence of glucagon and two related peptides. *Nature,* 302**,** 716-8.

BELL, P. M., HENRY, R. W., BUCHANAN, K. D. & ALBERTI, K. G. 1984. The effect of starvation on the gastro-entero-pancreatic hormonal and metabolic responses to exercise. (GEP hormones in starvation and exercise). *Diabete Metab,* 10**,** 194-8.

BERGWITZ, C., GARDELLA, T. J., FLANNERY, M. R., POTTS, J. T., JR., KRONENBERG, H. M., GOLDRING, S. R. & JUPPNER, H. 1996. Full activation of chimeric receptors by hybrids between parathyroid hormone and calcitonin. Evidence for a common pattern of ligand-receptor interaction. *J Biol Chem,* 271**,** 26469-72.

BIRNBAUMER, L., YATANI, A., VANDONGEN, A. M., GRAF, R., CODINA, J., OKABE, K., MATTERA, R. & BROWN, A. M. 1990. G protein coupling of receptors to ionic channels and other effector systems. *Br J Clin Pharmacol,* 30 Suppl 1**,** 13S-22S.

BRADY, P. A. & TERZIC, A. 1998. The sulfonylurea controversy: more questions from the heart. *J Am Coll Cardiol,* 31**,** 950-6.

BROWN, J. C. 1974. "Enterogastrone" and other new gut peptides. *Med Clin North Am,* 58**,** 1347-58.

BROWNLEE, M. 2003. A radical explanation for glucose-induced beta cell dysfunction. *J Clin Invest,* 112**,** 1788-90.

BRUBAKER, P. L. 2006. The glucagon-like peptides: pleiotropic regulators of nutrient homeostasis. *Ann N Y Acad Sci,* 1070**,** 10-26.

BUTEAU, J., EL-ASSAAD, W., RHODES, C. J., ROSENBERG, L., JOLY, E. & PRENTKI, M. 2004. Glucagon-like peptide-1 prevents beta cell glucolipotoxicity. *Diabetologia,* 47**,** 806-15.

BUTEAU, J., FOISY, S., JOLY, E. & PRENTKI, M. 2003. Glucagon-like peptide 1 induces pancreatic beta-cell proliferation via transactivation of the epidermal growth factor receptor. *Diabetes,* 52**,** 124-32.

CABRERA-VERA, T. M., VANHAUWE, J., THOMAS, T. O., MEDKOVA, M., PREININGER, A., MAZZONI, M. R. & HAMM, H. E. 2003. Insights into G protein structure, function, and regulation. *Endocr Rev,* 24**,** 765-81.

CARRUTHERS, C. J., UNSON, C. G., KIM, H. N. & SAKMAR, T. P. 1994. Synthesis and expression of a gene for the rat glucagon receptor. Replacement of an aspartic acid in the extracellular domain prevents glucagon binding. *J Biol Chem,* 269**,** 29321-8.

CAULFIELD, M. P., MCKEE, R. L., GOLDMAN, M. E., DUONG, L. T., FISHER, J. E., GAY, C. T., DEHAVEN, P. A., LEVY, J. J., ROUBINI, E., NUTT, R. F. & ET AL. 1990. The bovine renal parathyroid hormone (PTH) receptor has equal affinity for two different amino acid sequences: the receptor binding domains of PTH and PTH-related protein are located within the 14-34 region. *Endocrinology,* 127**,** 83-7.

CHEN, Q., PINON, D. I., MILLER, L. J. & DONG, M. 2010. Spatial approximations between residues 6 and 12 in the amino-terminal region of glucagon-like peptide 1 and its receptor: a region critical for biological activity. *J Biol Chem,* 285**,** 24508-18.

CHERRINGTON, A. D. 1999. Banting Lecture 1997. Control of glucose uptake and release by the liver in vivo. *Diabetes,* 48**,** 1198-214.

CLAING, A., LAPORTE, S. A., CARON, M. G. & LEFKOWITZ, R. J. 2002. Endocytosis of G protein-coupled receptors: roles of G protein-coupled receptor kinases and beta-arrestin proteins. *Prog Neurobiol,* 66**,** 61-79.

CLEATOR, I. G. & GOURLAY, R. H. 1975. Release of immunoreactive gastric inhibitory polypeptide (IR-GIP) by oral ingestion of food substances. *Am J Surg,* 130**,** 128-35.

COUVINEAU, A., GAUDIN, P., MAORET, J. J., ROUYER-FESSARD, C., NICOLE, P. & LABURTHE, M. 1995. Highly conserved aspartate 68, tryptophane 73 and glycine 109 in the N-terminal extracellular domain of the human VIP receptor are essential for its ability to bind VIP. *Biochem Biophys Res Commun,* 206**,** 246-52.

CREUTZFELDT, W. 1979. The incretin concept today. *Diabetologia,* 16**,** 75-85.

CUFF, J. A., CLAMP, M. E., SIDDIQUI, A. S., FINLAY, M. & BARTON, G. J. 1998. JPred: a consensus secondary structure prediction server. *Bioinformatics,* 14**,** 892-3.

DAKIN, C. L., GUNN, I., SMALL, C. J., EDWARDS, C. M., HAY, D. L., SMITH, D. M., GHATEI, M. A. & BLOOM, S. R. 2001. Oxyntomodulin inhibits food intake in the rat. *Endocrinology,* 142**,** 4244-50.

DAVIS, S. J., DAVIES, E. A., BARCLAY, A. N., DAENKE, S., BODIAN, D. L., JONES, E. Y., STUART, D. I., BUTTERS, T. D., DWEK, R. A. & VAN DER MERWE, P. A. 1995. Ligand binding by the immunoglobulin superfamily recognition molecule CD2 is glycosylation-independent. *J Biol Chem,* 270**,** 369-75.

DEACON, C. F., NAUCK, M. A., TOFT-NIELSEN, M., PRIDAL, L., WILLMS, B. & HOLST, J. J. 1995. Both subcutaneously and intravenously administered glucagon-like peptide I are rapidly degraded from the NH2-terminus in type II diabetic patients and in healthy subjects. *Diabetes,* 44**,** 1126-31.

DEACON, C. F., PRIDAL, L., KLARSKOV, L., OLESEN, M. & HOLST, J. J. 1996. Glucagon-like peptide 1 undergoes differential tissue-specific metabolism in the anesthetized pig. *Am J Physiol,* 271**,** E458-64.

DHANVANTARI, S., IZZO, A., JANSEN, E. & BRUBAKER, P. L. 2001. Coregulation of glucagon-like peptide-1 synthesis with proglucagon and prohormone convertase 1 gene expression in enteroendocrine GLUTag cells. *Endocrinology,* 142**,** 37-42.

DI PAOLO, E., VILARDAGA, J. P., PETRY, H., MOGUILEVSKY, N., BOLLEN, A., ROBBERECHT, P. & WAELBROECK, M. 1999. Role of charged amino acids conserved in the vasoactive intestinal polypeptide/secretin family of receptors on the secretin receptor functionality. *Peptides,* 20**,** 1187-93.

DILLON, J. S., TANIZAWA, Y., WHEELER, M. B., LENG, X. H., LIGON, B. B., RABIN, D. U., YOO-WARREN, H., PERMUTT, M. A. & BOYD, A. E., 3RD 1993. Cloning and functional expression of the human glucagon-like peptide-1 (GLP-1) receptor. *Endocrinology,* 133**,** 1907-10.

DING, X., SAXENA, N. K., LIN, S., GUPTA, N. A. & ANANIA, F. A. 2006. Exendin-4, a glucagon-like protein-1 (GLP-1) receptor agonist, reverses hepatic steatosis in ob/ob mice. *Hepatology,* 43**,** 173-81.

DONG, M., GAO, F., PINON, D. I. & MILLER, L. J. 2008. Insights into the structural basis of endogenous agonist activation of family B G protein-coupled receptors. *Mol Endocrinol,* 22**,** 1489-99.

DORN, A., RINNE, A., BERNSTEIN, H. G., ZIEGLER, M., HAHN, H. J. & RASANEN, O. 1983. The glucagon/glucagon-like immunoreactivities in neurons of the human brain. *Exp Clin Endocrinol,* 81**,** 24-32.

DOYLE, M. E. & EGAN, J. M. 2007. Mechanisms of action of glucagon-like peptide 1 in the pancreas. *Pharmacol Ther,* 113**,** 546-93.

DOYLE, M. E., THEODORAKIS, M. J., HOLLOWAY, H. W., BERNIER, M., GREIG, N. H. & EGAN, J. M. 2003. The importance of the nine-amino acid C-terminal sequence of exendin-4 for binding to the GLP-1 receptor and for biological activity. *Regul Pept,* 114**,** 153-8.

DREWS, J. 2000. Drug discovery: a historical perspective. *Science,* 287**,** 1960-4.

DRUCKER, D. J. 2006. The biology of incretin hormones. *Cell Metab,* 3**,** 153-65.

DRUCKER, D. J. 2007. Dipeptidyl peptidase-4 inhibition and the treatment of type 2 diabetes: preclinical biology and mechanisms of action. *Diabetes Care,* 30**,** 1335-43.

DRUCKER, D. J. & BRUBAKER, P. L. 1989. Proglucagon gene expression is regulated by a cyclic AMP-dependent pathway in rat intestine. *Proc Natl Acad Sci U S A,* 86**,** 3953-7.

DRUCKER, D. J., MOJSOV, S. & HABENER, J. F. 1986. Cell-specific post-translational processing of preproglucagon expressed from a metallothionein-glucagon fusion gene. *J Biol Chem,* 261**,** 9637-43.

DRUCKER, D. J., PHILIPPE, J., MOJSOV, S., CHICK, W. L. & HABENER, J. F. 1987. Glucagon-like peptide I stimulates insulin gene expression and increases cyclic AMP levels in a rat islet cell line. *Proc Natl Acad Sci U S A,* 84**,** 3434-8.

DUPRE, J. & BECK, J. C. 1966. Stimulation of release of insulin by an extract of intestinal mucosa. *Diabetes,* 15**,** 555-9.

DURING, M. J., CAO, L., ZUZGA, D. S., FRANCIS, J. S., FITZSIMONS, H. L., JIAO, X., BLAND, R. J., KLUGMANN, M., BANKS, W. A., DRUCKER, D. J. & HAILE, C. N. 2003. Glucagon-like peptide-1 receptor is involved in learning and neuroprotection. *Nat Med,* 9**,** 1173-9.

EBERT, R. & CREUTZFELDT, W. 1982. Influence of gastric inhibitory polypeptide antiserum on glucose-induced insulin secretion in rats. *Endocrinology,* 111**,** 1601-6.

EBERT, R., ILLMER, K. & CREUTZFELDT, W. 1979. Release of gastric inhibitory polypeptide (GIP) by intraduodenal acidification in rats and humans and abolishment of the incretin effect of acid by GIP-antiserum in rats. *Gastroenterology,* 76**,** 515-23.

EBERT, R., UNGER, H. & CREUTZFELDT, W. 1983. Preservation of incretin activity after removal of gastric inhibitory polypeptide (GIP) from rat gut extracts by immunoadsorption. *Diabetologia,* 24**,** 449-54.

EDWARDS, C. M., STANLEY, S. A., DAVIS, R., BRYNES, A. E., FROST, G. S., SEAL, L. J., GHATEI, M. A. & BLOOM, S. R. 2001. Exendin-4 reduces fasting and postprandial glucose and decreases energy intake in healthy volunteers. *Am J Physiol Endocrinol Metab,* 281**,** E155-61.

EGAN, J. M., CLOCQUET, A. R. & ELAHI, D. 2002. The insulinotropic effect of acute exendin-4 administered to humans: comparison of nondiabetic state to type 2 diabetes. *J Clin Endocrinol Metab,* 87**,** 1282-90.

EISSELE, R., GOKE, R., WILLEMER, S., HARTHUS, H. P., VERMEER, H., ARNOLD, R. & GOKE, B. 1992. Glucagon-like peptide-1 cells in the gastrointestinal tract and pancreas of rat, pig and man. *Eur J Clin Invest,* 22**,** 283-91.

ELAHI, D., EGAN, J. M., SHANNON, R. P., MENEILLY, G. S., KHATRI, A., HABENER, J. F. & ANDERSEN, D. K. 2008. GLP-1 (9-36) amide, cleavage product of GLP-1 (7-36) amide, is a glucoregulatory peptide. *Obesity (Silver Spring),* 16**,** 1501-9.

ELLIOTT, R. M., MORGAN, L. M., TREDGER, J. A., DEACON, S., WRIGHT, J. & MARKS, V. 1993. Glucagon-like peptide-1 (7-36)amide and glucose-dependent insulinotropic polypeptide secretion in response to nutrient ingestion in man: acute post-prandial and 24-h secretion patterns. *J Endocrinol,* 138**,** 159-66.

ENG, J., ANDREWS, P. C., KLEINMAN, W. A., SINGH, L. & RAUFMAN, J. P. 1990. Purification and structure of exendin-3, a new pancreatic secretagogue isolated from Heloderma horridum venom. *J Biol Chem,* 265**,** 20259-62.

ENG, J., KLEINMAN, W. A., SINGH, L., SINGH, G. & RAUFMAN, J. P. 1992. Isolation and characterization of exendin-4, an exendin-3 analogue, from Heloderma suspectum venom. Further evidence for an exendin receptor on dispersed acini from guinea pig pancreas. *J Biol Chem,* 267**,** 7402-5.

ESWAR, N., JOHN, B., MIRKOVIC, N., FISER, A., ILYIN, V. A., PIEPER, U., STUART, A. C., MARTI-RENOM, M. A., MADHUSUDHAN, M. S., YERKOVICH, B. & SALI, A. 2003. Tools for comparative protein structure modeling and analysis. *Nucleic Acids Res,* 31**,** 3375-80.

FARILLA, L., BULOTTA, A., HIRSHBERG, B., LI CALZI, S., KHOURY, N., NOUSHMEHR, H., BERTOLOTTO, C., DI MARIO, U., HARLAN, D. M. & PERFETTI, R. 2003. Glucagon-like peptide 1 inhibits cell apoptosis and improves glucose responsiveness of freshly isolated human islets. *Endocrinology,* 144**,** 5149-58.

FEHMANN, H. C. & HABENER, J. F. 1991. Functional receptors for the insulinotropic hormone glucagon-like peptide-I(7-37) on a somatostatin secreting cell line. *FEBS Lett,* 279**,** 335-40.

FEHMANN, H. C., JIANG, J., SCHWEINFURTH, J., DORSCH, K., WHEELER, M. B., BOYD, A. E., 3RD & GOKE, B. 1994. Ligand-specificity of the rat GLP-I receptor recombinantly expressed in Chinese hamster ovary (CHO-) cells. *Z Gastroenterol,* 32**,** 203-7.

FERGUSON, S. S. 2001. Evolving concepts in G protein-coupled receptor endocytosis: the role in receptor desensitization and signaling. *Pharmacol Rev,* 53**,** 1-24.

FREDRIKSSON, R., LAGERSTROM, M. C., LUNDIN, L. G. & SCHIOTH, H. B. 2003. The G-protein-coupled receptors in the human genome form five main families. Phylogenetic analysis, paralogon groups, and fingerprints. *Mol Pharmacol,* 63**,** 1256-72.

GALLWITZ, B., SCHMIDT, W. E., CONLON, J. M. & CREUTZFELDT, W. 1990. Glucagon-like peptide-1(7-36)amide: characterization of the domain responsible for binding to its receptor on rat insulinoma RINm5F cells. *J Mol Endocrinol,* 5**,** 33-9.

GALLWITZ, B., WITT, M., PAETZOLD, G., MORYS-WORTMANN, C., ZIMMERMANN, B., ECKART, K., FOLSCH, U. R. & SCHMIDT, W. E. 1994.

Structure/activity characterization of glucagon-like peptide-1. *Eur J Biochem,* 225**,** 1151-6.

GARBER, A., HENRY, R., RATNER, R., GARCIA-HERNANDEZ, P. A., RODRIGUEZ-PATTZI, H., OLVERA-ALVAREZ, I., HALE, P. M., ZDRAVKOVIC, M. & BODE, B. 2009. Liraglutide versus glimepiride monotherapy for type 2 diabetes (LEAD-3 Mono): a randomised, 52-week, phase III, double-blind, parallel-treatment trial. *Lancet,* 373**,** 473-81.

GAUDIN, P., COUVINEAU, A., MAORET, J. J., ROUYER-FESSARD, C. & LABURTHE, M. 1995. Mutational analysis of cysteine residues within the extracellular domains of the human vasoactive intestinal peptide (VIP) 1 receptor identifies seven mutants that are defective in VIP binding. *Biochem Biophys Res Commun,* 211**,** 901-8.

GEDULIN, B. R., NIKOULINA, S. E., SMITH, P. A., GEDULIN, G., NIELSEN, L. L., BARON, A. D., PARKES, D. G. & YOUNG, A. A. 2005. Exenatide (exendin-4) improves insulin sensitivity and {beta}-cell mass in insulin-resistant obese fa/fa Zucker rats independent of glycemia and body weight. *Endocrinology,* 146**,** 2069-76.

GEFEL, D., HENDRICK, G. K., MOJSOV, S., HABENER, J. & WEIR, G. C. 1990. Glucagon-like peptide-I analogs: effects on insulin secretion and adenosine 3',5'-monophosphate formation. *Endocrinology,* 126**,** 2164-8.

GELLING, R. W., WHEELER, M. B., XUE, J., GYOMOREY, S., NIAN, C., PEDERSON, R. A. & MCINTOSH, C. H. 1997. Localization of the domains involved in ligand binding and activation of the glucose-dependent insulinotropic polypeptide receptor. *Endocrinology,* 138**,** 2640-3.

GETHER, U. 2000. Uncovering molecular mechanisms involved in activation of G protein-coupled receptors. *Endocr Rev,* 21**,** 90-113.

GETHER, U., ASMAR, F., MEINILD, A. K. & RASMUSSEN, S. G. 2002. Structural basis for activation of G-protein-coupled receptors. *Pharmacol Toxicol,* 91**,** 304-12.

GHIGLIONE, M., UTTENTHAL, L. O., GEORGE, S. K. & BLOOM, S. R. 1984. How glucagon-like is glucagon-like peptide-1? *Diabetologia,* 27**,** 599-600.

GOKE, R. & CONLON, J. M. 1988. Receptors for glucagon-like peptide-1(7-36) amide on rat insulinoma-derived cells. *J Endocrinol,* 116**,** 357-62.

GOKE, R., FEHMANN, H. C., LINN, T., SCHMIDT, H., KRAUSE, M., ENG, J. & GOKE, B. 1993. Exendin-4 is a high potency agonist and truncated exendin-(9-39)-amide an antagonist at the glucagon-like peptide 1-(7-36)-amide receptor of insulin-secreting beta-cells. *J Biol Chem,* 268**,** 19650-5.

GOKE, R., JUST, R., LANKAT-BUTTGEREIT, B. & GOKE, B. 1994. Glycosylation of the GLP-1 receptor is a prerequisite for regular receptor function. *Peptides,* 15**,** 675-81.

GRACE, C. R., PERRIN, M. H., DIGRUCCIO, M. R., MILLER, C. L., RIVIER, J. E., VALE, W. W. & RIEK, R. 2004. NMR structure and peptide hormone binding site of the first extracellular domain of a type B1 G protein-coupled receptor. *Proc Natl Acad Sci U S A,* 101**,** 12836-41.

GRACE, C. R., PERRIN, M. H., GULYAS, J., DIGRUCCIO, M. R., CANTLE, J. P., RIVIER, J. E., VALE, W. W. & RIEK, R. 2007. Structure of the N-terminal domain of a type B1 G protein-coupled receptor in complex with a peptide ligand. *Proc Natl Acad Sci U S A,* 104**,** 4858-63.

GRACE, C. R., PERRIN, M. H., GULYAS, J., RIVIER, J. E., VALE, W. W. & RIEK, R. NMR structure of the first extracellular domain of corticotropin releasing

factor receptor 1 (ECD1-CRF-R1) complexed with a high affinity agonist. *J Biol Chem*.

GRAUSCHOPF, U., LILIE, H., HONOLD, K., WOZNY, M., REUSCH, D., ESSWEIN, A., SCHAFER, W., RUCKNAGEL, K. P. & RUDOLPH, R. 2000. The N-terminal fragment of human parathyroid hormone receptor 1 constitutes a hormone binding domain and reveals a distinct disulfide pattern. *Biochemistry,* 39**,** 8878-87.

GRAZIANO, M. P., HEY, P. J., BORKOWSKI, D., CHICCHI, G. G. & STRADER, C. D. 1993. Cloning and functional expression of a human glucagon-like peptide-1 receptor. *Biochem Biophys Res Commun,* 196**,** 141-6.

GRAZIANO, M. P., HEY, P. J. & STRADER, C. D. 1996. The amino terminal domain of the glucagon-like peptide-1 receptor is a critical determinant of subtype specificity. *Receptors Channels,* 4**,** 9-17.

GRIBBLE, F. M., WILLIAMS, L., SIMPSON, A. K. & REIMANN, F. 2003. A novel glucose-sensing mechanism contributing to glucagon-like peptide-1 secretion from the GLUTag cell line. *Diabetes,* 52**,** 1147-54.

GRIMELIUS, L., CAPELLA, C., BUFFA, R., POLAK, J. M., PEARSE, A. G. & SOLCIA, E. 1976. Cytochemical and ultrastructural differentiation of enteroglucagon and pancreatic-type glucagon cells of the gastrointestinal tract. *Virchows Arch B Cell Pathol,* 20**,** 217-28.

GROMADA, J., ANKER, C., BOKVIST, K., KNUDSEN, L. B. & WAHL, P. 1998. Glucagon-like peptide-1 receptor expression in Xenopus oocytes stimulates inositol trisphosphate-dependent intracellular Ca2+ mobilization. *FEBS Lett,* 425**,** 277-80.

GROS, L., DEMIRPENCE, E., JARROUSSE, C., KERVRAN, A. & BATAILLE, D. 1992. Characterization of binding sites for oxyntomodulin on a somatostatin-secreting cell line (RIN T3). *Endocrinology,* 130**,** 1263-70.

GUTZWILLER, J. P., DEGEN, L., HEUSS, L. & BEGLINGER, C. 2004. Glucagon-like peptide 1 (GLP-1) and eating. *Physiol Behav,* 82**,** 17-9.

HANSEN, L., DEACON, C. F., ORSKOV, C. & HOLST, J. J. 1999. Glucagon-like peptide-1-(7-36)amide is transformed to glucagon-like peptide-1-(9-36)amide by dipeptidyl peptidase IV in the capillaries supplying the L cells of the porcine intestine. *Endocrinology,* 140**,** 5356-63.

HARETER, A., HOFFMANN, E., BODE, H. P., GOKE, B. & GOKE, R. 1997. The positive charge of the imidazole side chain of histidine7 is crucial for GLP-1 action. *Endocr J,* 44**,** 701-5.

HARMAR, A. J. 2001. Family-B G-protein-coupled receptors. *Genome Biol,* 2**,** REVIEWS3013.

HE, Y. L., WANG, Y., BULLOCK, J. M., DEACON, C. F., HOLST, J. J., DUNNING, B. E., LIGUEROS-SAYLAN, M. & FOLEY, J. E. 2007. Pharmacodynamics of vildagliptin in patients with type 2 diabetes during OGTT. *J Clin Pharmacol,* 47**,** 633-41.

HEINRICH, G., GROS, P. & HABENER, J. F. 1984. Glucagon gene sequence. Four of six exons encode separate functional domains of rat pre-proglucagon. *J Biol Chem,* 259**,** 14082-7.

HELLER, R. S., KIEFFER, T. J. & HABENER, J. F. 1996. Point mutations in the first and third intracellular loops of the glucagon-like peptide-1 receptor alter intracellular signaling. *Biochem Biophys Res Commun,* 223**,** 624-32.

HELLER, R. S., KIEFFER, T. J. & HABENER, J. F. 1997. Insulinotropic glucagon-like peptide I receptor expression in glucagon-producing alpha-cells of the rat endocrine pancreas. *Diabetes,* 46**,** 785-91.

HENDERSON, R., BALDWIN, J. M., CESKA, T. A., ZEMLIN, F., BECKMANN, E. & DOWNING, K. H. 1990. Model for the structure of bacteriorhodopsin based on high-resolution electron cryo-microscopy. *J Mol Biol,* 213**,** 899-929.

HERMAN, G. A., BERGMAN, A., LIU, F., STEVENS, C., WANG, A. Q., ZENG, W., CHEN, L., SNYDER, K., HILLIARD, D., TANEN, M., TANAKA, W., MEEHAN, A. G., LASSETER, K., DILZER, S., BLUM, R. & WAGNER, J. A. 2006. Pharmacokinetics and pharmacodynamic effects of the oral DPP-4 inhibitor sitagliptin in middle-aged obese subjects. *J Clin Pharmacol,* 46**,** 876-86.

HERMANS, M. P., VAN YPERSELE DE STRIHOU, M., KETELSLEGERS, J. M., SQUIFFLET, J. P. & BUYSSCHAERT, M. 1995. Fasting and postprandial plasma glucose and peripheral insulin levels in insulin-dependent diabetes mellitus and non-insulin-dependent diabetes mellitus subjects during continuous intraperitoneal versus subcutaneous insulin delivery. *Transplant Proc,* 27**,** 3329-30.

HERRMANN-RINKE, C., MCGREGOR, G. P. & GOKE, B. 2000. Calcitonin gene-related peptide potently stimulates glucagon-like peptide-1 release in the isolated perfused rat ileum. *Peptides,* 21**,** 431-7.

HIRASAWA, A., TSUMAYA, K., AWAJI, T., KATSUMA, S., ADACHI, T., YAMADA, M., SUGIMOTO, Y., MIYAZAKI, S. & TSUJIMOTO, G. 2005. Free fatty acids regulate gut incretin glucagon-like peptide-1 secretion through GPR120. *Nat Med,* 11**,** 90-4.

HJORTH, S. A., ADELHORST, K., PEDERSEN, B. B., KIRK, O. & SCHWARTZ, T. W. 1994. Glucagon and glucagon-like peptide 1: selective receptor recognition via distinct peptide epitopes. *J Biol Chem,* 269**,** 30121-4.

HO, M. K. C. & WONG, Y. H. 2002. G protein structure diversity *In:* EDS.PANGALOS, M. N. & DAVIES, C. H. (eds.) *Understanding G protein-coupled receptors and their role in the CNS*

Oxford University Press.

HOARE, S. R. 2005. Mechanisms of peptide and nonpeptide ligand binding to Class B G-protein-coupled receptors. *Drug Discov Today,* 10**,** 417-27.

HOGAN, P., DALL, T. & NIKOLOV, P. 2003. Economic costs of diabetes in the US in 2002. *Diabetes Care,* 26**,** 917-32.

HOLST, J. J., ORSKOV, C., NIELSEN, O. V. & SCHWARTZ, T. W. 1987. Truncated glucagon-like peptide I, an insulin-releasing hormone from the distal gut. *FEBS Lett,* 211**,** 169-74.

HOLTMANN, M. H., HADAC, E. M. & MILLER, L. J. 1995. Critical contributions of amino-terminal extracellular domains in agonist binding and activation of secretin and vasoactive intestinal polypeptide receptors. Studies of chimeric receptors. *J Biol Chem,* 270**,** 14394-8.

HOLZ, G. G. T., KUHTREIBER, W. M. & HABENER, J. F. 1993. Pancreatic beta-cells are rendered glucose-competent by the insulinotropic hormone glucagon-like peptide-1(7-37). *Nature,* 361**,** 362-5.

HOOSEIN, N. M. & GURD, R. S. 1984. Human glucagon-like peptides 1 and 2 activate rat brain adenylate cyclase. *FEBS Lett,* 178**,** 83-6.

HOPKINS, A. M., LI, D., MRSNY, R. J., WALSH, S. V. & NUSRAT, A. 2000. Modulation of tight junction function by G protein-coupled events. *Adv Drug Deliv Rev,* 41**,** 329-40.

HUPE-SODMANN, K., MCGREGOR, G. P., BRIDENBAUGH, R., GOKE, R., GOKE, B., THOLE, H., ZIMMERMANN, B. & VOIGT, K. 1995.

Characterisation of the processing by human neutral endopeptidase 24.11 of GLP-1(7-36) amide and comparison of the substrate specificity of the enzyme for other glucagon-like peptides. *Regul Pept,* 58**,** 149-56.

IISMAA, T. P., BIDEN, T. J., & SHINE, 1995. G Protein-Coupled Receptors. *New York: Springer-Verlag.***,** 1 – 181.

INOOKA, H., OHTAKI, T., KITAHARA, O., IKEGAMI, T., ENDO, S., KITADA, C., OGI, K., ONDA, H., FUJINO, M. & SHIRAKAWA, M. 2001. Conformation of a peptide ligand bound to its G-protein coupled receptor. *Nat Struct Biol,* 8**,** 161-5.

ISHIHARA, T., NAKAMURA, S., KAZIRO, Y., TAKAHASHI, T., TAKAHASHI, K. & NAGATA, S. 1991. Molecular cloning and expression of a cDNA encoding the secretin receptor. *Embo J,* 10**,** 1635-41.

JOVANOVIC, L. & GONDOS, B. 1999. Type 2 diabetes: the epidemic of the new millennium. *Ann Clin Lab Sci,* 29**,** 33-42.

JOY, S. V., RODGERS, P. T. & SCATES, A. C. 2005. Incretin mimetics as emerging treatments for type 2 diabetes. *Ann Pharmacother,* 39**,** 110-8.

KAISER, N., LEIBOWITZ, G. & NESHER, R. 2003. Glucotoxicity and beta-cell failure in type 2 diabetes mellitus. *J Pediatr Endocrinol Metab,* 16**,** 5-22.

KALLIOMAA, A. 2005. A homology model of extracellular N-terminal domain of glucagon-like peptide-1 receptor and hypotheses for 3D complexes with its peptide agonist. *Master thesis,The University of Leeds, Faculty of Biological Sciences*.

KAMITANI, S. & SAKATA, T. 2001. Glycosylation of human CRLR at Asn123 is required for ligand binding and signaling. *Biochim Biophys Acta,* 1539**,** 131-9.

KENDALL, D. M. 2005. Review: insulin monotherapy and insulin combined with oral hypoglycemic agents provide similar glycemic control. *ACP J Club,* 142**,** 62-3.

KIEFFER, T. J. & HABENER, J. F. 1999. The glucagon-like peptides. *Endocr Rev,* 20**,** 876-913.

KIEFFER, T. J., HELLER, R. S., UNSON, C. G., WEIR, G. C. & HABENER, J. F. 1996. Distribution of glucagon receptors on hormone-specific endocrine cells of rat pancreatic islets. *Endocrinology,* 137**,** 5119-25.

KIEFFER, T. J., MCINTOSH, C. H. & PEDERSON, R. A. 1995. Degradation of glucose-dependent insulinotropic polypeptide and truncated glucagon-like peptide 1 in vitro and in vivo by dipeptidyl peptidase IV. *Endocrinology,* 136**,** 3585-96.

KLABUNDE, T. & HESSLER, G. 2002. Drug design strategies for targeting G-protein-coupled receptors. *Chembiochem,* 3**,** 928-44.

KLINGER, S., POUSSIN, C., DEBRIL, M. B., DOLCI, W., HALBAN, P. A. & THORENS, B. 2008. Increasing GLP-1-induced beta-cell proliferation by silencing the negative regulators of signaling cAMP response element modulator-alpha and DUSP14. *Diabetes,* 57**,** 584-93.

KNAUF, C., CANI, P. D., PERRIN, C., IGLESIAS, M. A., MAURY, J. F., BERNARD, E., BENHAMED, F., GREMEAUX, T., DRUCKER, D. J., KAHN, C. R., GIRARD, J., TANTI, J. F., DELZENNE, N. M., POSTIC, C. & BURCELIN, R. 2005. Brain glucagon-like peptide-1 increases insulin secretion and muscle insulin resistance to favor hepatic glycogen storage. *J Clin Invest,* 115**,** 3554-63.

KNUDSEN, L. B. & PRIDAL, L. 1996. Glucagon-like peptide-1-(9-36) amide is a major metabolite of glucagon-like peptide-1-(7-36) amide after in vivo

administration to dogs, and it acts as an antagonist on the pancreatic receptor. *Eur J Pharmacol,* 318**,** 429-35.

KNUDSEN, S. M., TAMS, J. W. & FAHRENKRUG, J. 2000. Role of second extracellular loop in the function of human vasoactive intestinal polypeptide/pituitary adenylate cyclase activating polypeptide receptor 1 (hVPAC1R). *J Mol Neurosci,* 14**,** 137-46.

KOLAKOWSKI, L. F., JR. 1994. GCRDb: a G-protein-coupled receptor database. *Receptors Channels,* 2**,** 1-7.

KOLTERMAN, O. G., BUSE, J. B., FINEMAN, M. S., GAINES, E., HEINTZ, S., BICSAK, T. A., TAYLOR, K., KIM, D., AISPORNA, M., WANG, Y. & BARON, A. D. 2003. Synthetic exendin-4 (exenatide) significantly reduces postprandial and fasting plasma glucose in subjects with type 2 diabetes. *J Clin Endocrinol Metab,* 88**,** 3082-9.

KREYMANN, B., WILLIAMS, G., GHATEI, M. A. & BLOOM, S. R. 1987. Glucagon-like peptide-1 7-36: a physiological incretin in man. *Lancet,* 2**,** 1300-4.

KRISTIANSEN, K. 2004. Molecular mechanisms of ligand binding, signaling, and regulation within the superfamily of G-protein-coupled receptors: molecular modeling and mutagenesis approaches to receptor structure and function. *Pharmacol Ther,* 103**,** 21-80.

LA BARRE J & STILL, E. U. 1930. Studies on the physiology of secretin. *AmJ Physiol,* 91**,** 649-653.

LARSEN, P. J., TANG-CHRISTENSEN, M., HOLST, J. J. & ORSKOV, C. 1997. Distribution of glucagon-like peptide-1 and other preproglucagon-derived peptides in the rat hypothalamus and brainstem. *Neuroscience,* 77**,** 257-70.

LAURITSEN, K. B., MOODY, A. J., CHRISTENSEN, K. C. & LINDKAER JENSEN, S. 1980. Gastric inhibitory polypeptide (GIP) and insulin release after small-bowel resection in man. *Scand J Gastroenterol,* 15**,** 833-40.

LEE, C., GARDELLA, T. J., ABOU-SAMRA, A. B., NUSSBAUM, S. R., SEGRE, G. V., POTTS, J. T., JR., KRONENBERG, H. M. & JUPPNER, H. 1994. Role of the extracellular regions of the parathyroid hormone (PTH)/PTH-related peptide receptor in hormone binding. *Endocrinology,* 135**,** 1488-95.

LEHLE, L. & SCHWARZ, R. T. 1976. Formation of dolichol monophosphate 2-deoxy-D-glucose and its interference with the glycosylation of mannoproteins in yeast. *Eur J Biochem,* 67**,** 239-45.

LOPEZ DE MATURANA, R. & DONNELLY, D. 2002. The glucagon-like peptide-1 receptor binding site for the N-terminus of GLP-1 requires polarity at Asp198 rather than negative charge. *FEBS Lett,* 530**,** 244-8.

LOPEZ DE MATURANA, R., TREECE-BIRCH, J., ABIDI, F., FINDLAY, J. B. & DONNELLY, D. 2004. Met-204 and Tyr-205 are together important for binding GLP-1 receptor agonists but not their N-terminally truncated analogues. *Protein Pept Lett,* 11**,** 15-22.

LOPEZ DE MATURANA, R., WILLSHAW, A., KUNTZSCH, A., RUDOLPH, R. & DONNELLY, D. 2003. The isolated N-terminal domain of the glucagon-like peptide-1 (GLP-1) receptor binds exendin peptides with much higher affinity than GLP-1. *J Biol Chem,* 278**,** 10195-200.

LOPEZ, L. C., FRAZIER, M. L., SU, C. J., KUMAR, A. & SAUNDERS, G. F. 1983. Mammalian pancreatic preproglucagon contains three glucagon-related peptides. *Proc Natl Acad Sci U S A,* 80**,** 5485-9.

LUCK, M. D., CARTER, P. H. & GARDELLA, T. J. 1999. The (1-14) fragment of parathyroid hormone (PTH) activates intact and amino-terminally truncated PTH-1 receptors. *Mol Endocrinol,* 13**,** 670-80.

LUND, P. K., GOODMAN, R. H., DEE, P. C. & HABENER, J. F. 1982. Pancreatic preproglucagon cDNA contains two glucagon-related coding sequences arranged in tandem. *Proc Natl Acad Sci U S A,* 79**,** 345-9.

LUND, P. K., GOODMAN, R. H. & HABENER, J. F. 1981. Intestinal glucagon mRNA identified by hybridization to a cloned islet cDNA encoding a precursor. *Biochem Biophys Res Commun,* 100**,** 1659-66.

LUND, P. K., GOODMAN, R. H., MONTMINY, M. R., DEE, P. C. & HABENER, J. F. 1983. Anglerfish islet pre-proglucagon II. Nucleotide and corresponding amino acid sequence of the cDNA. *J Biol Chem,* 258**,** 3280-4.

MANN, R., NASR, N., HADDEN, D., SINFIELD, J., ABIDI, F., AL-SABAH, S., DE MATURANA, R. L., TREECE-BIRCH, J., WILLSHAW, A. & DONNELLY, D. 2007. Peptide binding at the GLP-1 receptor. *Biochem Soc Trans,* 35**,** 713-6.

MANN, R. J., AL-SABAH, S., DE MATURANA, R. L., SINFIELD, J. K. & DONNELLY, D. 2010a. Functional coupling of Cys-226 and Cys-296 in the glucagon-like peptide-1 (GLP-1) receptor indicates a disulfide bond that is close to the activation pocket. *Peptides,* 31**,** 2289-93.

MANN, R. J., NASR, N. E., SINFIELD, J. K., PACI, E. & DONNELLY, D. 2010b. The major determinant of exendin-4/glucagon-like peptide 1 differential affinity at the rat glucagon-like peptide 1 receptor N-terminal domain is a hydrogen bond from SER-32 of exendin-4. *Br J Pharmacol,* 160**,** 1973-84.

MARGUET, D., BAGGIO, L., KOBAYASHI, T., BERNARD, A. M., PIERRES, M., NIELSEN, P. F., RIBEL, U., WATANABE, T., DRUCKER, D. J. & WAGTMANN, N. 2000. Enhanced insulin secretion and improved glucose tolerance in mice lacking CD26. *Proc Natl Acad Sci U S A,* 97**,** 6874-9.

MARIN, E. P., KRISHNA, A. G., ZVYAGA, T. A., ISELE, J., SIEBERT, F. & SAKMAR, T. P. 2000. The amino terminus of the fourth cytoplasmic loop of rhodopsin modulates rhodopsin-transducin interaction. *J Biol Chem,* 275**,** 1930-6.

MATHI, S. K., CHAN, Y., LI, X. & WHEELER, M. B. 1997. Scanning of the glucagon-like peptide-1 receptor localizes G protein-activating determinants primarily to the N terminus of the third intracellular loop. *Mol Endocrinol,* 11**,** 424-32.

MATSCHINSKY, F. M. 2002. Regulation of pancreatic beta-cell glucokinase: from basics to therapeutics. *Diabetes,* 51 Suppl 3**,** S394-404.

MCDONALD, T. J., GHATEI, M. A., BLOOM, S. R., ADRIAN, T. E., MOCHIZUKI, T., YANAIHARA, C. & YANAIHARA, N. 1983. Dose-response comparisons of canine plasma gastroenteropancreatic hormone responses to bombesin and the porcine gastrin-releasing peptide (GRP). *Regul Pept,* 5**,** 125-37.

MEIER, J. J. & NAUCK, M. A. 2005. Glucagon-like peptide 1(GLP-1) in biology and pathology. *Diabetes Metab Res Rev,* 21**,** 91-117.

MEIER, J. J., NAUCK, M. A., KRANZ, D., HOLST, J. J., DEACON, C. F., GAECKLER, D., SCHMIDT, W. E. & GALLWITZ, B. 2004. Secretion, degradation, and elimination of glucagon-like peptide 1 and gastric inhibitory polypeptide in patients with chronic renal insufficiency and healthy control subjects. *Diabetes,* 53**,** 654-62.

MENTLEIN, R. 1999. Dipeptidyl-peptidase IV (CD26)--role in the inactivation of regulatory peptides. *Regul Pept,* 85**,** 9-24.

MEYER, C., WOERLE, H. J., DOSTOU, J. M., WELLE, S. L. & GERICH, J. E. 2004. Abnormal renal, hepatic, and muscle glucose metabolism following

glucose ingestion in type 2 diabetes. *Am J Physiol Endocrinol Metab,* 287**,** E1049-56.

MOJSOV, S. 1992. Structural requirements for biological activity of glucagon-like peptide-I. *Int J Pept Protein Res,* 40**,** 333-43.

MOJSOV, S., HEINRICH, G., WILSON, I. B., RAVAZZOLA, M., ORCI, L. & HABENER, J. F. 1986. Preproglucagon gene expression in pancreas and intestine diversifies at the level of post-translational processing. *J Biol Chem,* 261**,** 11880-9.

MOJSOV, S., KOPCZYNSKI, M. G. & HABENER, J. F. 1990. Both amidated and nonamidated forms of glucagon-like peptide I are synthesized in the rat intestine and the pancreas. *J Biol Chem,* 265**,** 8001-8.

MOJSOV, S., WEIR, G. C. & HABENER, J. F. 1987. Insulinotropin: glucagon-like peptide I (7-37) co-encoded in the glucagon gene is a potent stimulator of insulin release in the perfused rat pancreas. *J Clin Invest,* 79**,** 616-9.

MONTROSE-RAFIZADEH, C., YANG, H., RODGERS, B. D., BEDAY, A., PRITCHETTE, L. A. & ENG, J. 1997. High potency antagonists of the pancreatic glucagon-like peptide-1 receptor. *J Biol Chem,* 272**,** 21201-6.

MOORE, B. 1906. On the treatment of Diabetus mellitus by acid extract of Duodenal Mucous Membrane. *Biochem J,* 1**,** 28-38.

MURAGE, E. N., BEINBORN, M. & AHN, J. M. 2008. Search for alpha-helical propensity in the receptor-bound conformation of glucagon-like peptide-1. *Bioorg Med Chem*.

NABHAN, C., XIONG, Y., XIE, L. Y. & ABOU-SAMRA, A. B. 1995. The alternatively spliced type II corticotropin-releasing factor receptor, stably expressed in LLCPK-1 cells, is not well coupled to the G protein(s). *Biochem Biophys Res Commun,* 212**,** 1015-21.

NAGELL, C. F., WETTERGREN, A., ORSKOV, C. & HOLST, J. J. 2006. Inhibitory effect of GLP-1 on gastric motility persists after vagal deafferentation in pigs. *Scand J Gastroenterol,* 41**,** 667-72.

NAUCK, M. A., HOLST, J. J. & WILLMS, B. 1997. Glucagon-like peptide 1 and its potential in the treatment of non-insulin-dependent diabetes mellitus. *Horm Metab Res,* 29**,** 411-6.

NEIDIGH, J. W., FESINMEYER, R. M., PRICKETT, K. S. & ANDERSEN, N. H. 2001. Exendin-4 and glucagon-like-peptide-1: NMR structural comparisons in the solution and micelle-associated states. *Biochemistry,* 40**,** 13188-200.

NIKOLAIDIS, L. A., MANKAD, S., SOKOS, G. G., MISKE, G., SHAH, A., ELAHI, D. & SHANNON, R. P. 2004. Effects of glucagon-like peptide-1 in patients with acute myocardial infarction and left ventricular dysfunction after successful reperfusion. *Circulation,* 109**,** 962-5.

NUCK, R., PAUL, C., WIELAND, B., HEIDRICH, C., GEILEN, C. C. & REUTTER, W. 1993. Comparative study of high-mannose-type oligosaccharides in membrane glycoproteins of rat hepatocytes and different rat hepatoma cell lines. *Eur J Biochem,* 216**,** 215-21.

NUSSENZVEIG, D. R., THAW, C. N. & GERSHENGORN, M. C. 1994. Inhibition of inositol phosphate second messenger formation by intracellular loop one of a human calcitonin receptor. Expression and mutational analysis of synthetic receptor genes. *J Biol Chem,* 269**,** 28123-9.

NYSTROM, T., GUTNIAK, M. K., ZHANG, Q., ZHANG, F., HOLST, J. J., AHREN, B. & SJOHOLM, A. 2004. Effects of glucagon-like peptide-1 on endothelial function in type 2 diabetes patients with stable coronary artery disease. *Am J Physiol Endocrinol Metab,* 287**,** E1209-15.

OHNEDA, A., OHNEDA, K., OHNEDA, M., KOIZUMI, F., OHASHI, S., KAWAI, K. & SUZUKI, S. 1991. The structure-function relationship of GLP-1 related peptides in the endocrine function of the canine pancreas. *Tohoku J Exp Med,* 165**,** 209-21.

ORSKOV, C., RABENHOJ, L., WETTERGREN, A., KOFOD, H. & HOLST, J. J. 1994. Tissue and plasma concentrations of amidated and glycine-extended glucagon-like peptide I in humans. *Diabetes,* 43**,** 535-9.

PALCZEWSKI, K., KUMASAKA, T., HORI, T., BEHNKE, C. A., MOTOSHIMA, H., FOX, B. A., LE TRONG, I., TELLER, D. C., OKADA, T., STENKAMP, R. E., YAMAMOTO, M. & MIYANO, M. 2000. Crystal structure of rhodopsin: A G protein-coupled receptor. *Science,* 289**,** 739-45.

PANG, R. T., NG, S. S., CHENG, C. H., HOLTMANN, M. H., MILLER, L. J. & CHOW, B. K. 1999. Role of N-linked glycosylation on the function and expression of the human secretin receptor. *Endocrinology,* 140**,** 5102-11.

PARKER, J. C., ANDREWS, K. M., RESCEK, D. M., MASSEFSKI, W., JR., ANDREWS, G. C., CONTILLO, L. G., STEVENSON, R. W., SINGLETON, D. H. & SULESKE, R. T. 1998. Structure-function analysis of a series of glucagon-like peptide-1 analogs. *J Pept Res,* 52**,** 398-409.

PARKES, D. G., PITTNER, R., JODKA, C., SMITH, P. & YOUNG, A. 2001. Insulinotropic actions of exendin-4 and glucagon-like peptide-1 in vivo and in vitro. *Metabolism,* 50**,** 583-9.

PARTHIER, C., KLEINSCHMIDT, M., NEUMANN, P., RUDOLPH, R., MANHART, S., SCHLENZIG, D., FANGHANEL, J., RAHFELD, J. U., DEMUTH, H. U. & STUBBS, M. T. 2007. Crystal structure of the incretin-bound extracellular domain of a G protein-coupled receptor. *Proc Natl Acad Sci U S A,* 104**,** 13942-7.

PARTHIER, C., REEDTZ-RUNGE, S., RUDOLPH, R. & STUBBS, M. T. 2009. Passing the baton in class B GPCRs: peptide hormone activation via helix induction? *Trends Biochem Sci,* 34**,** 303-10.

PFEIFER, M. A., HALTER, J. B., BEARD, J. C. & PORTE, D., JR. 1981. Differential effects of tolbutamide on first and second phase insulin secretion in noninsulin-dependent diabetes mellitus. *J Clin Endocrinol Metab,* 53**,** 1256-62.

PIERCE, K. L., PREMONT, R. T. & LEFKOWITZ, R. J. 2002. Seven-transmembrane receptors. *Nat Rev Mol Cell Biol,* 3**,** 639-50.

PIOSZAK, A. A., PARKER, N. R., GARDELLA, T. J. & XU, H. E. 2009. Structural basis for parathyroid hormone-related protein binding to the parathyroid hormone receptor and design of conformation-selective peptides. *J Biol Chem,* 284**,** 28382-91.

PIOSZAK, A. A., PARKER, N. R., SUINO-POWELL, K. & XU, H. E. 2008. Molecular recognition of corticotropin-releasing factor by its G-protein-coupled receptor CRFR1. *J Biol Chem,* 283**,** 32900-12.

PIOSZAK, A. A. & XU, H. E. 2008. Molecular recognition of parathyroid hormone by its G protein-coupled receptor. *Proc Natl Acad Sci U S A,* 105**,** 5034-9.

PISEGNA, J. R. & WANK, S. A. 1996. Cloning and characterization of the signal transduction of four splice variants of the human pituitary adenylate cyclase activating polypeptide receptor. Evidence for dual coupling to adenylate cyclase and phospholipase C. *J Biol Chem,* 271**,** 17267-74.

PLAMBOECK, A., HOLST, J. J., CARR, R. D. & DEACON, C. F. 2005. Neutral endopeptidase 24.11 and dipeptidyl peptidase IV are both mediators of the

degradation of glucagon-like peptide 1 in the anaesthetised pig. *Diabetologia,* 48**,** 1882-90.

POITOUT, V. & ROBERTSON, R. P. 2002. Minireview: Secondary beta-cell failure in type 2 diabetes--a convergence of glucotoxicity and lipotoxicity. *Endocrinology,* 143**,** 339-42.

POLAK, J. A. & BLOOM, S. R. 1982. Localization of regulatory peptides in the gut. *Br Med Bull,* 38**,** 303-7.

PRIGEON, R. L., QUDDUSI, S., PATY, B. & D'ALESSIO, D. A. 2003. Suppression of glucose production by GLP-1 independent of islet hormones: a novel extrapancreatic effect. *Am J Physiol Endocrinol Metab,* 285**,** E701-7.

QIAN, F., MATHIAS, N., MOENCH, P., CHI, C., DESIKAN, S., HUSSAIN, M. & SMITH, R. L. 2009. Pulmonary delivery of a GLP-1 receptor agonist, BMS-686117. *Int J Pharm,* 366**,** 218-20.

RAUFMAN, J. P., SINGH, L. & ENG, J. 1991. Exendin-3, a novel peptide from Heloderma horridum venom, interacts with vasoactive intestinal peptide receptors and a newly described receptor on dispersed acini from guinea pig pancreas. Description of exendin-3(9-39) amide, a specific exendin receptor antagonist. *J Biol Chem,* 266**,** 2897-902.

REIMANN, F. & GRIBBLE, F. M. 2002. Glucose-sensing in glucagon-like peptide-1-secreting cells. *Diabetes,* 51**,** 2757-63.

RENDELL, M., ROSS, D. A., DREW, H. M. & ZARRIELLO, J. 1981. Endogenous insulin secretion measured by C-peptide in maturity-onset diabetes controllable by diet alone. *Arch Intern Med,* 141**,** 1617-22.

ROBERGE, J. N. & BRUBAKER, P. L. 1991. Secretion of proglucagon-derived peptides in response to intestinal luminal nutrients. *Endocrinology,* 128**,** 3169-74.

ROCCA, A. S. & BRUBAKER, P. L. 1999. Role of the vagus nerve in mediating proximal nutrient-induced glucagon-like peptide-1 secretion. *Endocrinology,* 140**,** 1687-94.

ROSS, S. A. & DUPRE, J. 1978. Effects of ingestion of triglyceride or galactose on secretion of gastric inhibitory polypeptide and on responses to intravenous glucose in normal and diabetic subjects. *Diabetes,* 27**,** 327-33.

RUIZ-GRANDE, C., ALARCON, C., MERIDA, E. & VALVERDE, I. 1992. Lipolytic action of glucagon-like peptides in isolated rat adipocytes. *Peptides,* 13**,** 13-6.

RUNGE, S., SCHIMMER, S., OSCHMANN, J., SCHIODT, C. B., KNUDSEN, S. M., JEPPESEN, C. B., MADSEN, K., LAU, J., THOGERSEN, H. & RUDOLPH, R. 2007. Differential structural properties of GLP-1 and exendin-4 determine their relative affinity for the GLP-1 receptor N-terminal extracellular domain. *Biochemistry,* 46**,** 5830-40.

RUNGE, S., THOGERSEN, H., MADSEN, K., LAU, J. & RUDOLPH, R. 2008. Crystal structure of the ligand-bound glucagon-like peptide-1 receptor extracellular domain. *J Biol Chem,* 283**,** 11340-7.

RUNGE, S., WULFF, B. S., MADSEN, K., BRAUNER-OSBORNE, H. & KNUDSEN, L. B. 2003. Different domains of the glucagon and glucagon-like peptide-1 receptors provide the critical determinants of ligand selectivity. *Br J Pharmacol,* 138**,** 787-94.

RUSSO, F., ROMEO, G., GUCCIONE, S. & DE BLASI, A. 1991. Pyrimido[5,4-b]indole derivatives. 1. A new class of potent and selective alpha 1 adrenoceptor ligands. *J Med Chem,* 34**,** 1850-4.

SAIFIA, S., CHEVRIER, A. M., BOSSHARD, A., CUBER, J. C., CHAYVIALLE, J. A. & ABELLO, J. 1998. Galanin inhibits glucagon-like peptide-1 secretion through pertussis toxin-sensitive G protein and ATP-dependent potassium channels in rat ileal L-cells. *J Endocrinol,* 157**,** 33-41.

SALAPATEK, A. M., MACDONALD, P. E., GAISANO, H. Y. & WHEELER, M. B. 1999. Mutations to the third cytoplasmic domain of the glucagon-like peptide 1 (GLP-1) receptor can functionally uncouple GLP-1-stimulated insulin secretion in HIT-T15 cells. *Mol Endocrinol,* 13**,** 1305-17.

SALI, A. & BLUNDELL, T. L. 1993. Comparative protein modelling by satisfaction of spatial restraints. *J Mol Biol,* 234**,** 779-815.

SALTIEL, A. R. 2001. New perspectives into the molecular pathogenesis and treatment of type 2 diabetes. *Cell,* 104**,** 517-29.

SAYDAH, S. H., GEISS, L. S., TIERNEY, E., BENJAMIN, S. M., ENGELGAU, M. & BRANCATI, F. 2004. Review of the performance of methods to identify diabetes cases among vital statistics, administrative, and survey data. *Ann Epidemiol,* 14**,** 507-16.

SCHMIDT, W. E., SIEGEL, E. G. & CREUTZFELDT, W. 1985. Glucagon-like peptide-1 but not glucagon-like peptide-2 stimulates insulin release from isolated rat pancreatic islets. *Diabetologia,* 28**,** 704-7.

SEGRE, G. V. & GOLDRING, S. R. 1993. Receptors for secretin, calcitonin, parathyroid hormone (PTH)/PTH-related peptide, vasoactive intestinal peptide, glucagonlike peptide 1, growth hormone-releasing hormone, and glucagon belong to a newly discovered G-protein-linked receptor family. *Trends Endocrinol Metab,* 4**,** 309-14.

SHAH, U. 2009. GPR119 agonists: a promising new approach for the treatment of type 2 diabetes and related metabolic disorders. *Curr Opin Drug Discov Devel,* 12**,** 519-32.

SIEGEL, E. G., GALLWITZ, B., SCHARF, G., MENTLEIN, R., MORYS-WORTMANN, C., FOLSCH, U. R., SCHREZENMEIR, J., DRESCHER, K. & SCHMIDT, W. E. 1999. Biological activity of GLP-1-analogues with N-terminal modifications. *Regul Pept,* 79**,** 93-102.

SIMONSEN, L., HOLST, J. J. & DEACON, C. F. 2006. Exendin-4, but not glucagon-like peptide-1, is cleared exclusively by glomerular filtration in anaesthetised pigs. *Diabetologia,* 49**,** 706-12.

SINFIELD, J. K. 2005. *The role of the extracellular face of the*
Glucagon-like peptide-1 receptor in ligand binding and activation. Ph D Ph D, University of Leeds.

STOFFEL, M., ESPINOSA, R., 3RD, LE BEAU, M. M. & BELL, G. I. 1993. Human glucagon-like peptide-1 receptor gene. Localization to chromosome band 6p21 by fluorescence in situ hybridization and linkage of a highly polymorphic simple tandem repeat DNA polymorphism to other markers on chromosome 6. *Diabetes,* 42**,** 1215-8.

STOFFERS, D. A., KIEFFER, T. J., HUSSAIN, M. A., DRUCKER, D. J., BONNER-WEIR, S., HABENER, J. F. & EGAN, J. M. 2000. Insulinotropic glucagon-like peptide 1 agonists stimulate expression of homeodomain protein IDX-1 and increase islet size in mouse pancreas. *Diabetes,* 49**,** 741-8.

STROOP, S. D., KUESTNER, R. E., SERWOLD, T. F., CHEN, L. & MOORE, E. E. 1995. Chimeric human calcitonin and glucagon receptors reveal two dissociable calcitonin interaction sites. *Biochemistry,* 34**,** 1050-7.

SU, H., HE, M., LI, H., LIU, Q., WANG, J., WANG, Y., GAO, W., ZHOU, L., LIAO, J., YOUNG, A. A. & WANG, M. W. 2008. Boc5, a non-peptidic glucagon-like

Peptide-1 receptor agonist, invokes sustained glycemic control and weight loss in diabetic mice. *PLoS ONE,* 3**,** e2892.

SUGA, A., HIRANO, T., KAGEYAMA, H., OSAKA, T., NAMBA, Y., TSUJI, M., MIURA, M., ADACHI, M. & INOUE, S. 2000. Effects of fructose and glucose on plasma leptin, insulin, and insulin resistance in lean and VMH-lesioned obese rats. *Am J Physiol Endocrinol Metab,* 278**,** E677-83.

SUN, C., SONG, D., DAVIS-TABER, R. A., BARRETT, L. W., SCOTT, V. E., RICHARDSON, P. L., PEREDA-LOPEZ, A., UCHIC, M. E., SOLOMON, L. R., LAKE, M. R., WALTER, K. A., HAJDUK, P. J. & OLEJNICZAK, E. T. 2007. Solution structure and mutational analysis of pituitary adenylate cyclase-activating polypeptide binding to the extracellular domain of PAC1-RS. *Proc Natl Acad Sci U S A,* 104**,** 7875-80.

SUZUKI, S., KAWAI, K., OHASHI, S., MUKAI, H. & YAMASHITA, K. 1989. Comparison of the effects of various C-terminal and N-terminal fragment peptides of glucagon-like peptide-1 on insulin and glucagon release from the isolated perfused rat pancreas. *Endocrinology,* 125**,** 3109-14.

SYME, C. A., ZHANG, L. & BISELLO, A. 2006. Caveolin-1 regulates cellular trafficking and function of the glucagon-like Peptide 1 receptor. *Mol Endocrinol,* 20**,** 3400-11.

SZAYNA, M., DOYLE, M. E., BETKEY, J. A., HOLLOWAY, H. W., SPENCER, R. G., GREIG, N. H. & EGAN, J. M. 2000. Exendin-4 decelerates food intake, weight gain, and fat deposition in Zucker rats. *Endocrinology,* 141**,** 1936-41.

TAKAHASHI, H., MANAKA, H., SUDA, K., FUKASE, N., SEKIKAWA, A., EGUCHI, H., TOMINAGA, M. & SASAKI, H. 1991. Hyperglycaemia but not hyperinsulinaemia prevents the secretion of glucagon-like peptide-1 (7-36 amide) stimulated by fat ingestion. *Scand J Clin Lab Invest,* 51**,** 499-507.

TAKHAR, S., GYOMOREY, S., SU, R. C., MATHI, S. K., LI, X. & WHEELER, M. B. 1996. The third cytoplasmic domain of the GLP-1[7-36 amide] receptor is required for coupling to the adenylyl cyclase system. *Endocrinology,* 137**,** 2175-8.

TAN, Y. V., COUVINEAU, A., MURAIL, S., CERAUDO, E., NEUMANN, J. M., LACAPERE, J. J. & LABURTHE, M. 2006. Peptide agonist docking in the N-terminal ectodomain of a class II G protein-coupled receptor, the VPAC1 receptor. Photoaffinity, NMR, and molecular modeling. *J Biol Chem,* 281**,** 12792-8.

TANIZAWA, Y., RIGGS, A. C., ELBEIN, S. C., WHELAN, A., DONIS-KELLER, H. & PERMUTT, M. A. 1994. Human glucagon-like peptide-1 receptor gene in NIDDM. Identification and use of simple sequence repeat polymorphisms in genetic analysis. *Diabetes,* 43**,** 752-7.

TER HAAR, E., KOTH, C. M., ABDUL-MANAN, N., SWENSON, L., COLL, J. T., LIPPKE, J. A., LEPRE, C. A., GARCIA-GUZMAN, M. & MOORE, J. M. 2010. Crystal structure of the ectodomain complex of the CGRP receptor, a class-B GPCR, reveals the site of drug antagonism. *Structure,* 18**,** 1083-93.

THEODORAKIS, M. J., CARLSON, O., MICHOPOULOS, S., DOYLE, M. E., JUHASZOVA, M., PETRAKI, K. & EGAN, J. M. 2006. Human duodenal enteroendocrine cells: source of both incretin peptides, GLP-1 and GIP. *Am J Physiol Endocrinol Metab,* 290**,** E550-9.

THOMPSON, J. D., HIGGINS, D. G. & GIBSON, T. J. 1994. CLUSTAL W: improving the sensitivity of progressive multiple sequence alignment through sequence weighting, position-specific gap penalties and weight matrix choice. *Nucleic Acids Res,* 22**,** 4673-80.

THORENS, B. 1992. Expression cloning of the pancreatic beta cell receptor for the gluco-incretin hormone glucagon-like peptide 1. *Proc Natl Acad Sci U S A,* 89**,** 8641-5.

THORENS, B., PORRET, A., BUHLER, L., DENG, S. P., MOREL, P. & WIDMANN, C. 1993. Cloning and functional expression of the human islet GLP-1 receptor. Demonstration that exendin-4 is an agonist and exendin-(9-39) an antagonist of the receptor. *Diabetes,* 42**,** 1678-82.

THORNTON, K. & GORENSTEIN, D. G. 1994. Structure of glucagon-like peptide (7-36) amide in a dodecylphosphocholine micelle as determined by 2D NMR. *Biochemistry,* 33**,** 3532-9.

THUM, A., HUPE-SODMANN, K., GOKE, R., VOIGT, K., GOKE, B. & MCGREGOR, G. P. 2002. Endoproteolysis by isolated membrane peptidases reveal metabolic stability of glucagon-like peptide-1 analogs, exendins-3 and -4. *Exp Clin Endocrinol Diabetes,* 110**,** 113-8.

TIBADUIZA, E. C., CHEN, C. & BEINBORN, M. 2001. A small molecule ligand of the glucagon-like peptide 1 receptor targets its amino-terminal hormone binding domain. *J Biol Chem,* 276**,** 37787-93.

TOKUYAMA, Y., MATSUI, K., EGASHIRA, T., NOZAKI, O., ISHIZUKA, T. & KANATSUKA, A. 2004. Five missense mutations in glucagon-like peptide 1 receptor gene in Japanese population. *Diabetes Res Clin Pract,* 66**,** 63-9.

TOURREL, C., BAILBE, D., LACORNE, M., MEILE, M. J., KERGOAT, M. & PORTHA, B. 2002. Persistent improvement of type 2 diabetes in the Goto-Kakizaki rat model by expansion of the beta-cell mass during the prediabetic period with glucagon-like peptide-1 or exendin-4. *Diabetes,* 51**,** 1443-52.

TURK, J., GROSS, R. W. & RAMANADHAM, S. 1993. Amplification of insulin secretion by lipid messengers. *Diabetes,* 42**,** 367-74.

TURTON, M. D., O'SHEA, D., GUNN, I., BEAK, S. A., EDWARDS, C. M., MEERAN, K., CHOI, S. J., TAYLOR, G. M., HEATH, M. M., LAMBERT, P. D., WILDING, J. P., SMITH, D. M., GHATEI, M. A., HERBERT, J. & BLOOM, S. R. 1996. A role for glucagon-like peptide-1 in the central regulation of feeding. *Nature,* 379**,** 69-72.

UNDERWOOD, C. R., GARIBAY, P., KNUDSEN, L. B., HASTRUP, S., PETERS, G. H., RUDOLPH, R. & REEDTZ-RUNGE, S. 2010. Crystal structure of glucagon-like peptide-1 in complex with the extracellular domain of the glucagon-like peptide-1 receptor. *J Biol Chem,* 285**,** 723-30.

UNGER, R. H. & EISENTRAUT, A. M. 1969. Entero-insular axis. *Arch Intern Med,* 123**,** 261-6.

UNGER, R. H., OHNEDA, A., VALVERDE, I., EISENTRAUT, A. M. & EXTON, J. 1968. Characterization of the responses of circulating glucagon-like immunoreactivity to intraduodenal and intravenous administration of glucose. *J Clin Invest,* 47**,** 48-65.

VAAG, A. A., HOLST, J. J., VOLUND, A. & BECK-NIELSEN, H. B. 1996. Gut incretin hormones in identical twins discordant for non-insulin-dependent diabetes mellitus (NIDDM)--evidence for decreased glucagon-like peptide 1 secretion during oral glucose ingestion in NIDDM twins. *Eur J Endocrinol,* 135**,** 425-32.

VAN EYLL, B., GOKE, B., WILMEN, A. & GOKE, R. 1996. Exchange of W39 by A within the N-terminal extracellular domain of the GLP-1 receptor results in a loss of receptor function. *Peptides,* 17**,** 565-70.

VAZQUEZ, P., RONCERO, I., BLAZQUEZ, E. & ALVAREZ, E. 2005a. The cytoplasmic domain close to the transmembrane region of the glucagon-like peptide-1 receptor contains sequence elements that regulate agonist-dependent internalisation. *J Endocrinol,* 186**,** 221-31.

VAZQUEZ, P., RONCERO, I., BLAZQUEZ, E. & ALVAREZ, E. 2005b. Substitution of the cysteine 438 residue in the cytoplasmic tail of the glucagon-like peptide-1 receptor alters signal transduction activity. *J Endocrinol,* 185**,** 35-44.

VENEMAN, T. F., TACK, C. J. & VAN HAEFTEN, T. W. 1998. The newly developed sulfonylurea glimepiride: a new ingredient, an old recipe. *Neth J Med,* 52**,** 179-86.

VILARDAGA, J. P., DI PAOLO, E., BIALEK, C., DE NEEF, P., WAELBROECK, M., BOLLEN, A. & ROBBERECHT, P. 1997. Mutational analysis of extracellular cysteine residues of rat secretin receptor shows that disulfide bridges are essential for receptor function. *Eur J Biochem,* 246**,** 173-80.

VILLANUEVA-PENACARRILLO, M. L., MARQUEZ, L., GONZALEZ, N., DIAZ-MIGUEL, M. & VALVERDE, I. 2001. Effect of GLP-1 on lipid metabolism in human adipocytes. *Horm Metab Res,* 33**,** 73-7.

VILSBOLL, T. 2009. Liraglutide: a new treatment for type 2 diabetes. *Drugs Today (Barc),* 45**,** 101-13.

VILSBOLL, T., AGERSO, H., KRARUP, T. & HOLST, J. J. 2003. Similar elimination rates of glucagon-like peptide-1 in obese type 2 diabetic patients and healthy subjects. *J Clin Endocrinol Metab,* 88**,** 220-4.

WANG, H., IEZZI, M., THEANDER, S., ANTINOZZI, P. A., GAUTHIER, B. R., HALBAN, P. A. & WOLLHEIM, C. B. 2005. Suppression of Pdx-1 perturbs proinsulin processing, insulin secretion and GLP-1 signalling in INS-1 cells. *Diabetologia,* 48**,** 720-31.

WANG, Q. & BRUBAKER, P. L. 2002. Glucagon-like peptide-1 treatment delays the onset of diabetes in 8 week-old db/db mice. *Diabetologia,* 45**,** 1263-73.

WANG, X., CAHILL, C. M., PINEYRO, M. A., ZHOU, J., DOYLE, M. E. & EGAN, J. M. 1999. Glucagon-like peptide-1 regulates the beta cell transcription factor, PDX-1, in insulinoma cells. *Endocrinology,* 140**,** 4904-7.

WATANABE, Y., KAWAI, K., OHASHI, S., YOKOTA, C., SUZUKI, S. & YAMASHITA, K. 1994. Structure-activity relationships of glucagon-like peptide-1(7-36)amide: insulinotropic activities in perfused rat pancreases, and receptor binding and cyclic AMP production in RINm5F cells. *J Endocrinol,* 140**,** 45-52.

WIDER, M. D., MATSUYAMA, T., DUNBAR, J. C. & FOA, P. P. 1976. Elevated gut glucagon-like immunoreactive material in human and experimental diabetes and its suppression by somatostatin. *Metabolism,* 25**,** 1487-9.

WIDMANN, C., DOLCI, W. & THORENS, B. 1995. Agonist-induced internalization and recycling of the glucagon-like peptide-1 receptor in transfected fibroblasts and in insulinomas. *Biochem J,* 310 (Pt 1)**,** 203-14.

WIDMANN, C., DOLCI, W. & THORENS, B. 1996a. Desensitization and phosphorylation of the glucagon-like peptide-1 (GLP-1) receptor by GLP-1 and 4-phorbol 12-myristate 13-acetate. *Mol Endocrinol,* 10**,** 62-75.

WIDMANN, C., DOLCI, W. & THORENS, B. 1996b. Heterologous desensitization of the glucagon-like peptide-1 receptor by phorbol esters requires phosphorylation of the cytoplasmic tail at four different sites. *J Biol Chem,* 271**,** 19957-63.

WIDMANN, C., DOLCI, W. & THORENS, B. 1997. Internalization and homologous desensitization of the GLP-1 receptor depend on phosphorylation of the receptor carboxyl tail at the same three sites. *Mol Endocrinol,* 11**,** 1094-102.

WILLMS, B., WERNER, J., HOLST, J. J., ORSKOV, C., CREUTZFELDT, W. & NAUCK, M. A. 1996. Gastric emptying, glucose responses, and insulin secretion after a liquid test meal: effects of exogenous glucagon-like peptide-1 (GLP-1)-(7-36) amide in type 2 (noninsulin-dependent) diabetic patients. *J Clin Endocrinol Metab,* 81**,** 327-32.

WILMEN, A., GOKE, B. & GOKE, R. 1996. The isolated N-terminal extracellular domain of the glucagon-like peptide-1 (GLP)-1 receptor has intrinsic binding activity. *FEBS Lett,* 398**,** 43-7.

WILMEN, A., VAN EYLL, B., GOKE, B. & GOKE, R. 1997. Five out of six tryptophan residues in the N-terminal extracellular domain of the rat GLP-1 receptor are essential for its ability to bind GLP-1. *Peptides,* 18**,** 301-5.

XIAO, Q., GIGUERE, J., PARISIEN, M., JENG, W., ST-PIERRE, S. A., BRUBAKER, P. L. & WHEELER, M. B. 2001. Biological activities of glucagon-like peptide-1 analogues in vitro and in vivo. *Biochemistry,* 40**,** 2860-9.

XIAO, Q., JENG, W. & WHEELER, M. B. 2000. Characterization of glucagon-like peptide-1 receptor-binding determinants. *J Mol Endocrinol,* 25**,** 321-35.

XU, G., STOFFERS, D. A., HABENER, J. F. & BONNER-WEIR, S. 1999. Exendin-4 stimulates both beta-cell replication and neogenesis, resulting in increased beta-cell mass and improved glucose tolerance in diabetic rats. *Diabetes,* 48**,** 2270-6.

YAGI, T., NISHI, S., HINATA, S., MURAKAMI, M. & YOSHIMI, T. 1996. A population association study of four candidate genes (hexokinase II, glucagon-like peptide-1 receptor, fatty acid binding protein-2, and apolipoprotein C-II) with type 2 diabetes and impaired glucose tolerance in Japanese subjects. *Diabet Med,* 13**,** 902-7.

YALOW, R. S., ROSE, H. G. & BAUMAN, W. A. 1988. Hyperinsulinemia. *Am J Med,* 85**,** 22-30.

YOKOSHIKI, H., SUNAGAWA, M., SEKI, T. & SPERELAKIS, N. 1998. ATP-sensitive K+ channels in pancreatic, cardiac, and vascular smooth muscle cells. *Am J Physiol,* 274**,** C25-37.

YOUNG, A. 2002. glucagon like peptide -1, Exendin and insulin sensitivity. *In: Hansen B, Shafrir E, editors. Insulin resistance and Insulin resistance syndrome. New york: Harwood Academic.***,** 235-62.

YU, M., MORENO, C., HOAGLAND, K. M., DAHLY, A., DITTER, K., MISTRY, M. & ROMAN, R. J. 2003. Antihypertensive effect of glucagon-like peptide 1 in Dahl salt-sensitive rats. *J Hypertens,* 21**,** 1125-35.

YUSTA, B., BAGGIO, L. L., ESTALL, J. L., KOEHLER, J. A., HOLLAND, D. P., LI, H., PIPELEERS, D., LING, Z. & DRUCKER, D. J. 2006. GLP-1 receptor activation improves beta cell function and survival following induction of endoplasmic reticulum stress. *Cell Metab,* 4**,** 391-406.

ZHANG, R., CAI, H., FATIMA, N., BUCZKO, E. & DUFAU, M. L. 1995. Functional glycosylation sites of the rat luteinizing hormone receptor required for ligand binding. *J Biol Chem,* 270**,** 21722-8.

ZHANG, Y., COOK, J. T., HATTERSLEY, A. T., FIRTH, R., SAKER, P. J., WARREN-PERRY, M., STOFFEL, M. & TURNER, R. C. 1994. Non-linkage of the glucagon-like peptide 1 receptor gene with maturity onset diabetes of the young. *Diabetologia,* 37**,** 721-4.

ZHAO, T., PARIKH, P., BHASHYAM, S., BOLUKOGLU, H., POORNIMA, I., SHEN, Y. T. & SHANNON, R. P. 2006. Direct effects of glucagon-like peptide-1 on myocardial contractility and glucose uptake in normal and postischemic isolated rat hearts. *J Pharmacol Exp Ther,* 317**,** 1106-13.

ZHOU, A. T., ASSIL, I. & ABOU-SAMRA, A. B. 2000. Role of asparagine-linked oligosaccharides in the function of the rat PTH/PTHrP receptor. *Biochemistry,* 39**,** 6514-20.

ZUNZ, E. & LABARRE, J. 1929. Contributions a l'etude des variations physiologiques de la secretion interne du pancreas: realations entre les secretions externe et interne du pancreas. Arch Int Physiol Biochim, 31, 20-44.